

UC San Diego

UC San Diego Electronic Theses and Dissertations

Title

Coordination and competition in optimal dispatch: distributed algorithms, saddle-point dynamics, and iterative bidding

Permalink

<https://escholarship.org/uc/item/6wq2x16c>

Author

Cherukuri, Ashish Kumar

Publication Date

2017

Peer reviewed|Thesis/dissertation

UNIVERSITY OF CALIFORNIA, SAN DIEGO

**Coordination and competition in optimal dispatch: distributed
algorithms, saddle-point dynamics, and iterative bidding**

A dissertation submitted in partial satisfaction of the
requirements for the degree
Doctor of Philosophy

in

Engineering Sciences (Mechanical Engineering)

by

Ashish Kumar Cherukuri

Committee in charge:

Professor Jorge Cortés, Chair
Professor William Helton
Professor Tara Javidi
Professor Miroslav Krstić
Professor Sonia Martinez

2017

Copyright
Ashish Kumar Cherukuri, 2017
All rights reserved.

The dissertation of Ashish Kumar Cherukuri is approved,
and it is acceptable in quality and form for publication
on microfilm and electronically:

Chair

University of California, San Diego

2017

DEDICATION

To my parents.

TABLE OF CONTENTS

	Signature Page	iii
	Dedication	iv
	Table of Contents	v
	List of Figures	viii
	List of Tables	x
	Acknowledgements	xi
	Vita	xvi
	Abstract of the Dissertation	xviii
Chapter 1	Introduction	1
	1.1 Literature review	4
	1.1.1 Distributed economic dispatch	4
	1.1.2 Saddle-point dynamics	6
	1.1.3 Competition in electricity markets	8
	1.2 Contributions	10
	1.2.1 Distributed economic dispatch	10
	1.2.2 Saddle-point dynamics	12
	1.2.3 Iterative bidding in electricity markets	15
	1.3 Organization	16
Chapter 2	Preliminaries	18
	2.1 Notation	18
	2.2 Graph theory	20
	2.3 Nonsmooth analysis and proximal calculus	21
	2.4 Saddle points and convex-concave functions	22
	2.5 Constrained optimization and exact penalty functions	24
	2.6 Dynamical systems	27
	2.6.1 Discontinuous dynamical systems	27
	2.6.2 Projected dynamical systems	28
	2.6.3 Differential inclusions	29
	2.7 Dynamic average consensus	30
	2.8 Input-to-state stability	30

Chapter 3	Anytime distributed dynamics for ED problem	32
	3.1 Problem statement	32
	3.2 Distributed algorithmic solution to the relaxed economic dispatch problem	34
	3.3 Distributed algorithmic solution to the economic dispatch problem	39
	3.3.1 Exact penalty function formulation	39
	3.3.2 Laplacian-nonsmooth-gradient dynamics	42
	3.4 Algorithm initialization and robustness against generator addition and deletion	45
	3.4.1 Algorithm rationale and informal description	46
	3.4.2 The GET CAPACITY strategy	47
	3.4.3 Algorithm: FEASIBLY ALLOCATE	49
	3.5 Simulations	52
Chapter 4	Robust distributed dynamics for ED problem	57
	4.1 Problem statement	57
	4.2 Robust centralized algorithmic solution	59
	4.3 Robust distributed algorithmic solution	63
	4.3.1 Convergence analysis	65
	4.3.2 Robustness analysis	72
	4.4 Simulations in a IEEE 118 bus system	76
	4.5 Refined LaSalle Invariance Principle for differential inclusions	80
Chapter 5	Robust distributed dynamics for DEDS problem	85
	5.1 Problem statement	85
	5.2 Distributed algorithmic solution	88
	5.3 Simulations	100
Chapter 6	Asymptotic convergence of saddle-point dynamics	103
	6.1 Problem statement	103
	6.2 Convergence analysis for convex-concave saddle functions	104
	6.2.1 Stability under strict convexity-concavity	104
	6.2.2 Stability under convexity-linearity or linearity-concavity	106
	6.2.3 Stability under strong quasiconvexity-quasiconcavity	110
	6.3 Convergence analysis for general saddle functions	113
	6.4 Auxiliary results	126

Chapter 7	Asymptotic convergence of primal-dual dynamics	136
	7.1 Problem statement	136
	7.2 Convergence analysis of primal-dual dynamics	141
Chapter 8	Role of convexity in saddle-point dynamics	150
	8.1 Problem statement	150
	8.2 Local properties of the saddle function imply global convergence	152
	8.3 Lyapunov function for constrained convex optimization problems	159
	8.4 ISS and self-triggered implementation of the saddle-point dynamics	167
	8.4.1 Input-to-state stability	168
	8.4.2 Self-triggered implementation	174
	8.5 Auxiliary results	181
Chapter 9	Iterative bidding in markets	187
	9.1 Problem statement	187
	9.2 Existence and uniqueness of efficient Nash equilibrium .	191
	9.3 The BID ADJUSTMENT ALGORITHM and its convergence properties	195
	9.3.1 BID ADJUSTMENT ALGORITHM	195
	9.3.2 Convergence analysis	197
	9.4 Robustness of the BID ADJUSTMENT ALGORITHM . .	205
	9.4.1 Robustness to disturbances	205
	9.4.2 Robustness to deviation in bid update	210
	9.4.3 Robustness to collusion	214
	9.5 Simulations	217
Chapter 10	Conclusions	223
	10.1 Future research directions	225
	10.1.1 Short-term plan	225
	10.1.2 Long-term plan	226
Bibliography	227

LIST OF FIGURES

Figure 1.1:	Hierarchical network architecture to facilitate power dispatch in the future grid.	3
Figure 3.1:	Evolution of the power allocation (a) and the network cost (b) under the Laplacian-nonsmooth-gradient dynamics in the IEEE 118 bus test case.	53
Figure 3.2:	Illustration of the DETERMINE FEASIBLE ALLOCATION strategy for a 6 generator network.	54
Figure 3.3:	Evolution of the power allocation and the network cost under the Laplacian-nonsmooth-gradient dynamics for a 6 generator network.	56
Figure 4.1:	Evolution of the power allocation, the total cost, and the total mismatch between generation and load under the $\text{dac}+\text{L}\partial$ dynamics and the ratio-consensus algorithm.	77
Figure 4.2:	Performance of the $\text{dac}+\text{L}\partial$ dynamics for the IEEE 118 bus system under time-varying load and generator addition and deletion.	78
Figure 4.3:	Evolution of the total power generation for the IEEE 118 bus example under the $\text{dac}+\text{L}\partial$ dynamics depicting the input-to-state stability property.	80
Figure 4.4:	Illustration showing various elements involved in the proof of Proposition 4.5.1	82
Figure 5.1:	Illustration of the execution of $\text{dac}+(\text{L}\partial, \partial)$ dynamics for a network of 10 generators.	101
Figure 5.2:	Plots showing the solution of the DEDS problem for 10 generators.	102
Figure 6.1:	Illustration of a trajectory of the saddle-point dynamics for the augmented Lagrangian \tilde{L} in (6.6).	110
Figure 6.2:	Illustration of a trajectory of the saddle-point dynamics for F given in (6.10).	113
Figure 6.3:	Illustration of a trajectory of the saddle-point dynamics for the Lagrangian of the constrained optimization problem (6.14).	118
Figure 6.4:	Illustration of a trajectory of the saddle-point dynamics for the function defined in (6.16)	122
Figure 6.5:	Illustration of a trajectory of the saddle-point dynamics for the function $F(x, z) = xz^2$	125
Figure 6.6:	Illustration of a trajectory of the vector field f defined in (6.41).	135
Figure 7.1:	An illustration depicting the vector field (7.5).	140

Figure 8.1:	Execution of the projected saddle-point dynamics (8.1) starting from $(1.7256, 0.1793, 2.4696, 0.3532)$ for Example 8.2.4.	158
Figure 8.2:	Plots illustrating the ISS property of the saddle-point dynamics.	175
Figure 8.3:	Illustration of the self-triggered saddle-point dynamics defined by (8.27) with the triggering criterium (8.29).	181
Figure 8.4:	Comparison between the self-triggered saddle-point dynamics and a first-order Euler discretization of the saddle-point dynamics with two different stepsize rules.	182
Figure 9.1:	Network layout of the modified IEEE 9-bus test case.	218
Figure 9.2:	Execution of the BID ADJUSTMENT ALGORITHM for the modified IEEE 9-bus test case in Figure 9.1.	219
Figure 9.3:	Execution of the BID ADJUSTMENT ALGORITHM under different stepsize selection for the example of Figure 9.2.	220
Figure 9.4:	Execution of the BID ADJUSTMENT ALGORITHM for the example considered in Figure 9.2 with generators 1, 3, and 5 forming a collusion.	221

LIST OF TABLES

Table 3.1:	Coefficients of the quadratic cost function $f_i(P_i) = a_i + b_i P_i + c_i P_i^2$ and lower P_i^m and upper P_i^M generation limits for each unit i .	55
Table 4.1:	Definition of the digraphs \mathcal{G} , $\hat{\mathcal{G}}$, $\hat{\mathcal{G}}_{\setminus\{4,11,25,45\}}$, and $\hat{\mathcal{G}}_{\setminus\{4,25,27\}}$. . .	77
Table 5.1:	Cost coefficients (a_i, b_i, c_i) and bounds $P_i^M, P_i^m, R_i^l, R_i^u$. The cost function of i is $f_i(P_i) = a_i + b_i P_i + c_i P_i^2$	100

ACKNOWLEDGEMENTS

To the greatest extent, this thesis was possible due to the efforts of my PhD supervisor Prof. Jorge Cortés and for that, I am highly indebted to him. Jorge, the fact that you meet every student every week and that you read and edit every single word that your student writes is incredible. This level of commitment towards mentoring is unmatched. The numerous hours we have spent solving things have been both fun and educative. When I came to UCSD, I was naive enough to think that I knew what research is. Over the years, I understood my weaknesses and improved. But during this entire period you have treated me as a peer; listening to whatever I said, never being dismissive and always being constructive. This helped a lot. Your constant encouragement and push has made my time in UCSD productive. Your passion and commitment towards research is contagious and I can only hope to continue in the future with this enthusiasm. Overall, thank you for everything.

A special thanks goes to my thesis committee: Prof. Sonia Martínez, Prof. Tara Javidi, Prof. Miroslav Krstić, and Prof. William Helton for taking out time and providing me with suggestions and criticisms.

During the past five years I have been fortunate enough to have fruitful collaborations outside UCSD. I am grateful to Alejandro Dominguez-García for giving me the opportunity to visit University of Illinois, Urbana-Champaign; spending time and energy in teaching me power systems; and giving me research advice wherever necessary. To Enrique Mallada, thank you for the fun discussions we had analyzing the rich behavior of the saddle-point dynamics. To Sairaj Dhople, Vijay Gupta, John Simpson-Porco, and Vaibhav Srivastava, at some point or the other, we have worked or planned to work on a problem together but could not bring things to fruition. However, experience is what matters the most and I thank you for that. I sincerely hope to continue collaborating with you in the future.

To Bahman Ghahsifard, more than a collaborator, you are that friend, philosopher, and guide who influenced me professionally the most in the past five years after Jorge. I have bugged you at various occasions, asking for advice over

silly things and ranting about petty anxieties. You absorbed it all and gave your honest opinion and advice. Thank you. I am sure we will continue to collaborate in the future.

My time at UCSD would not have been pleasant without friends and family here in San Diego. I am grateful for all their support and care. Looking back, the fun time I had with them is what I remember, not the times that I spent alone in my office. A special appreciation goes to all the group-mates that I had over the years. The discussions during our Friday meetings, the lunch sessions thereafter, the SoCal workshop trips, the fun time in conferences, . . . the list is long. Thank you for all these wonderful memories.

To the lunch/coffee-gang, Pedro, Federico, Andres, Eduardo, Aamodh, Mike, the time spent with you guys often came as the much needed break during the day. The discussions lightened my day and brought excitement into the otherwise monotonous PhD life. Mainly Eduardo, your positive attitude is uplifting. You listened patiently to all my frustrations and calmed me down when I was going crazy. As a true friend, you have helped me selflessly over all these years. Thank you.

I cannot explain in words the gratitude I feel towards all the teachers who have mentored me over the years. To Mr. Mandal, Mr. Satakopan, Prof. Srinivas Veeravalli, Prof. Sudipto Mukherjee, Prof. Debasish Chatterjee, Prof. John Lygeros, Prof. Jason Schweinsberg, and Prof. Jorge Cortés, your thoughts have shaped mine; your work ethic has inspired me; and your presence, in general, has made me feel secure and confident in what I was doing. Although implicit, your contribution towards this thesis is no less than the effort I have put in.

To Debasish Chatterjee, without your constant encouragement and unquestionable belief in my abilities, I would never have applied for a PhD program. You are my fallback option in a crisis, my last line of defense. It is reassuring to have a friend and a mentor like you. Thank you.

Above all, I express my deepest sense of gratitude towards my parents. You have sacrificed a lot of your happiness to buy some for me. You have taught me the value of education and you have made me what I am today. Only lately I have

understood what unconditional love means, or so I think. I dare not belittle your role in my life by thanking you. I dedicate this thesis to you and you own this work as much as I do.

Last but not the least, I thank my wife Manasa for being there with me through the thick and thin of it. Manasa, you brought the much needed stability and balance in my life. You made me realize that there is much more to life than just work and that work only never defines the worth of a person. I cannot imagine how I would have survived the past five years alone without you. Words defy me at this point. Simply, thank you for everything.

This research was possible because of the generous support of the following grants: US National Science Foundation (NSF) Award CMMI-1300272 and Award EECS-1307176; and ARPA-e Cooperative Agreement DE-AR0000695.

Chapter 3 is taken, in part, from the work [CC15c] published as “Distributed generator coordination for initialization and anytime optimization in economic dispatch” by A. Cherukuri and J. Cortés, in the IEEE Transaction on Control of Network Systems, 2015, as well as [CMC14] where it appears as “Distributed, anytime optimization in power-generator networks for economic dispatch” by A. Cherukuri, S. Martínez, and J. Cortés in the proceedings of the 2014 American Control Conference. The dissertation author was the primary investigator and author of these papers.

Chapter 4 is taken, in part, from the work [CC16d] published as “Initialization-free distributed coordination for economic dispatch under varying loads and generator commitment” by A. Cherukuri and J. Cortés, in Automatica, 2016, as well as [CC14] where it appears as “Distributed coordination for economic dispatch with varying load and generator commitment” by A. Cherukuri and J. Cortés in the proceedings of the 2014 Annual Allerton Conference on Communication, Control, and Computing. The dissertation author was the primary investigator and author of these papers.

Chapter 5 is taken, in part, from the work [CC18] submitted as “Distributed coordination of DERs with storage for dynamic economic dispatch” by A. Cherukuri and J. Cortés, to the IEEE Transactions on Automatic Control, as

well as [CC15b] where it appears as “Distributed dynamic economic dispatch of power generators with storage” by A. Cherukuri and J. Cortés in the proceedings of the 2015 IEEE Conference on Decision and Control. The dissertation author was the primary investigator and author of these papers.

Chapter 6 is taken, in part, from the work [CGC17] published as “Saddle-point dynamics: conditions for asymptotic stability of saddle points” by A. Cherukuri, B. Ghahesifard, and J. Cortés, in SIAM Journal on Control and Optimization, as well as [CC15a] where it appears as “Asymptotic stability of saddle points under the saddle-point dynamics” by A. Cherukuri and J. Cortés in the proceedings of the 2015 American Control Conference. The dissertation author was the primary investigator and author of these papers.

Chapter 7 is taken, in part, from the work [CMC16] published as “Asymptotic convergence of primal-dual dynamics” by A. Cherukuri, E. Mallada, and J. Cortés, in Systems and Control Letters, as well as [CMC15] where it appears as “Convergence of Caratheodory solutions for primal-dual dynamics in constrained concave optimization” by A. Cherukuri, E. Mallada, and J. Cortés in the proceedings of the 2015 SIAM Conference on Control and its Applications. The dissertation author was the primary investigator and author of these papers.

Chapter 8 is taken, in part, from the work [CMLC16a] submitted as “The role of convexity in saddle-point dynamics: Lyapunov function and robustness” by A. Cherukuri, E. Mallada, S. Low, and J. Cortés, to the IEEE Transactions on Automatic Control, as well as [CMLC16b] where it appears as “The role of strong convexity-concavity in the convergence and robustness of the saddle-point dynamics” by A. Cherukuri, E. Mallada, S. Low, and J. Cortés in the proceedings of the 2016 Annual Allerton Conference on Communication, Control, and Computing. The dissertation author was the primary investigator and author of these papers.

Chapter 9 is taken, in part, from the work [CC17b] submitted as “Iterative bidding in electricity markets: rationality and robustness” by A. Cherukuri and J. Cortés, to the IEEE Transactions on Control of Network Systems, as well as [CC16a] where it appears as “Decentralized Nash equilibrium learning by strategic generators for economic dispatch” by A. Cherukuri and J. Cortés in the pro-

ceedings of the 2016 American Control Conference and as [CC17a] where it is going to appear as “Decentralized Nash equilibrium seeking by strategic generators for DC optimal power flow” by A. Cherukuri and J. Cortés in the proceedings of the 2017 Conference on Information Sciences and Systems. The dissertation author was the primary investigator and author of these papers.

VITA

2008	Bachelor of Technology in Mechanical Engineering, Indian Institute of Technology, Delhi
2010	Master of Science in Mechanical and Process Engineering, ETH Zürich
2017	Doctor of Philosophy in Engineering Science (Mechanical Engineering), University of California, San Diego

PUBLICATIONS

Journal publications:

- A. Cherukuri and J. Cortés. Iterative bidding in electricity markets: rationality and robustness. *IEEE Transactions on Control of Network Systems*, 2017. Submitted
- A. Cherukuri, E. Mallada, S. Low, and J. Cortés. The role of convexity in saddle-point dynamics: Lyapunov function and robustness. *IEEE Transactions on Automatic Control*, 2016. Submitted
- A. Cherukuri and J. Cortés. Distributed coordination of DERs with storage for dynamic economic dispatch. *IEEE Transactions on Automatic Control*, 63(3), 2018. To appear
- A. Cherukuri, B. Ghahsifard, and J. Cortés. Saddle-point dynamics: conditions for asymptotic stability of saddle points. *SIAM Journal on Control and Optimization*, 55(1):486–511, 2017
- A. Cherukuri, E. Mallada, and J. Cortés. Asymptotic convergence of primal-dual dynamics. *Systems & Control Letters*, 87:10–15, 2016
- A. Cherukuri and J. Cortés. Initialization-free distributed coordination for economic dispatch under varying loads and generator commitment. *Automatica*, 74:183–193, 2016
- A. Cherukuri and J. Cortés. Distributed generator coordination for initialization and anytime optimization in economic dispatch. *IEEE Transactions on Control of Network Systems*, 2(3):226–237, 2015

Conference proceedings:

- A. Cherukuri and J. Cortés. Decentralized Nash equilibrium seeking by strategic generators for DC optimal power flow. In *Annual Conference on Information Systems and Sciences*, Baltimore, MD, March 2017. Electronic proceedings

- A. Cherukuri, A. D. Domínguez-García, and J. Cortés. Distributed coordination of power generators for a linearized optimal power flow problem. In *American Control Conference*, pages 3962–3967, Seattle, WA, May 2017
- A. Cherukuri and J. Cortés. Distributed algorithms for convex network optimization under non-sparse equality constraints. In *Allerton Conf. on Communications, Control and Computing*, pages 452–459, Monticello, IL, September 2016
- A. Cherukuri, E. Mallada, S. Low, and J. Cortés. The role of strong convexity-concavity in the convergence and robustness of the saddle-point dynamics. In *Allerton Conf. on Communications, Control and Computing*, pages 504–510, Monticello, IL, September 2016
- A. Cherukuri and J. Cortés. Decentralized Nash equilibrium learning by strategic generators for economic dispatch. In *American Control Conference*, pages 1082–1087, Boston, MA, July 2016
- A. Cherukuri and J. Cortés. Distributed dynamic economic dispatch of power generators with storage. In *IEEE Conf. on Decision and Control*, pages 2365–2370, Osaka, Japan, 2015
- A. Cherukuri, E. Mallada, and J. Cortés. Convergence of Caratheodory solutions for primal-dual dynamics in constrained concave optimization. *SIAM Conference on Control and Its Applications*, pages 290–296, July 2015
- A. Cherukuri and J. Cortés. Asymptotic stability of saddle points under the saddle-point dynamics. In *American Control Conference*, pages 2020–2025, Chicago, IL, July 2015
- A. Cherukuri and J. Cortés. Distributed coordination for economic dispatch with varying load and generator commitment. In *Allerton Conf. on Communications, Control and Computing*, pages 475–482, Monticello, IL, October 2014
- A. Cherukuri, S. Martínez, and J. Cortés. Distributed, anytime optimization in power-generator networks for economic dispatch. In *American Control Conference*, pages 172–177, Portland, OR, 2014
- A. Cherukuri, D. Chatterjee, P. Hokayem, and J. Lygeros. Stochastic receding horizon control: stability results. In *IFAC World Congress*, pages 150–155, Milan, Italy, July 2011
- Z. Nagy, S. Miyashita, S. Muntwyler, A. Cherukuri, J. J. Abbott, R. Pfeifer, and B. J. Nelson. Morphology detection for magnetically self-assembled modular robots. In *IEEE/RSJ Int. Conf. on Intelligent Robots & Systems*, pages 5281–5286, St. Louis, MO, USA, October 2009

ABSTRACT OF THE DISSERTATION

Coordination and competition in optimal dispatch: distributed algorithms, saddle-point dynamics, and iterative bidding

by

Ashish Kumar Cherukuri

Doctor of Philosophy in Engineering Sciences (Mechanical Engineering)

University of California, San Diego, 2017

Professor Jorge Cortés, Chair

The share of renewable energy generation in meeting our electricity needs is growing by the day. A majority of these renewables have small generation capacity and they are geographically distributed. It is for this reason that they are often termed as distributed energy resources (DERs). In addition to the capacity constraint, DERs' generation is highly variable and uncertain. The current electricity grid, on the other hand, was designed for centralized bulk generation. Therefore, regulating authorities like the Independent System Operator (ISO) or the Regional Transmission Organization (RTO) find it quite challenging to seamlessly integrate these DERs into the current grid, without affecting the quality of service to consumers. As one of the measures of tackling this issue, regulating

authorities envision a hierarchical architecture where, at the lower layer, different sets of distributed energy resources (DERs) coordinate their response under an aggregator and, at the upper layer, the ISO interacts (through a market) with the aggregators to solve the optimal dispatch problem. In this scenario, aggregators function as virtual, large-capacity generators. While the DERs under one aggregator can cooperate among themselves, the aggregators compete with each other in the market. Given this context, this thesis designs and analyzes coordination among DERs and competition among aggregators.

Specifically, the thesis can be divided into three parts. The first part focuses on the static and the dynamic optimal dispatch problems, where the aim for a set of DERs is to plan their generation so as to meet a particular load, minimize the total cost of generation, and respect individual constraints. For these optimization problems we design a suite of Laplacian-gradient based distributed algorithmic solutions and study their performance. The second part studies the asymptotic convergence and robustness properties of the saddle-point dynamics. This dynamics serves as the backbone of numerous distributed algorithms for network constrained optimization problems, including the dispatch problem. Finally, the third part investigates an electricity market designed for optimal dispatch among the aggregators. We design and analyze an iterative bid update scheme for the aggregators, discussing the advantages of this scheme using rationality and robustness arguments.

Chapter 1

Introduction

Traditional electricity grid was designed for the case where few bulk generators produce power at certain location; transmission lines carry that power over long distances at high voltage; and distribution system distributes this power to end-users by stepping down the voltage to a nominal value. In the past decade, and more so in the future, environmental concerns have fueled technological advancements in renewable energy sources and their share in total power generation has only increased. These renewables, unlike the bulk generators, have small capacity with uncertain and variable generation and are geographically distributed – the reason why they are commonly referred to as distributed energy resources (DERs). Since the grid was designed for bulk generation, integrating DERs into it while ensuring secure, reliable, and cost-effective power provision is a major challenge that the central regulating authorities like the Independent System Operator (ISO) or the Regional Transmission Organization (RTO) are concerned with.

One of the main ingredients of grid operation is the planning of generation based on the predicted load. This planning occurs at various stages. First, the generation levels at every hour of the next day is decided for the available generators. This planning is termed as the day-ahead dispatch. Then, this planned generation is adjusted every 15 minutes while the day progresses. This is commonly referred to as the economic dispatch or the optimal dispatch. Even at this level, the generation and load are not exactly same at all times, at which point, lower-level, primary and secondary controllers adjust the power at a faster time

scale to maintain the balance between generation and load. In this thesis our focus will be on the higher-level of planning, that is, the day-ahead dispatch and the optimal dispatch.

After the deregulation of the power generation, the well-established way for carrying out optimal dispatch has been through a market clearing. Here, generators bid into a market regulated by the ISO and based on the clearing done by the ISO, each generator gets a signal for the amount of generation requested. ISO operates various markets: day-ahead dispatch, real-time dispatch, regulation services, etc. For the dispatch markets, clearing is done by the ISO based on minimizing the payments made to the generators and ensuring secure and reliable power provision. Thus, the market clearing process is essentially finding the solution of a constrained optimization problem. Since traditionally there were few generators involved in power provision, solving this optimization problem was not too difficult. But renewables are more in number with low capacity and uncertain and volatile generation. This in turn makes the market clearing a very large stochastic optimization problem which is very difficult to solve. In order to handle this problem, the California ISO has recently proposed a hierarchical dispatch model [CAI15], shown in Figure 1.1. In this architecture, the distributed energy resource providers (DERPs), also known as aggregators, work as virtual power providers. Each of them either owns or has contracts with a group of DERs. DERPs compete with each other to provide power in the day-ahead and spot markets based on the number and variety of DERs available to each of them. On getting a load-demand signal from the market outcome, these DERPs then try to find a cost-effective way of meeting this load while coordinating among the DERs. Therefore, in the top-level of the hierarchy DERPs compete with each other and at the bottom-level DERs try to coordinate with each other. Since the number of DERs and DERPs is going to be big, *there is a need to devise efficient and scalable coordination and competition for this network to ensure reliable and cost-efficient power supply*. This is the central theme of this thesis.

The thesis can be divided into three parts. The first part (Chapter 3, Chapter 4, and Chapter 5) focusses on the static and the dynamic optimal dis-

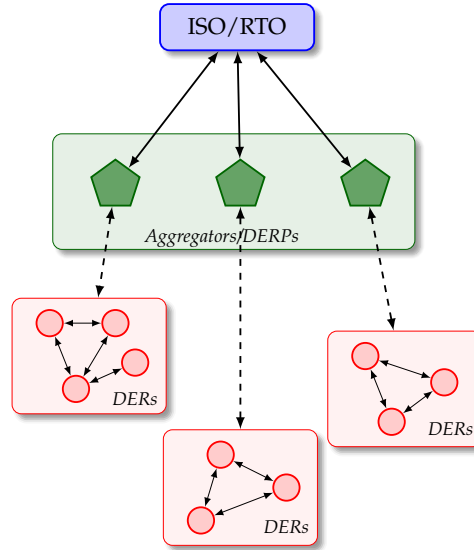


Figure 1.1: Hierarchical network architecture to facilitate power dispatch in the future grid.

patch problems for the DERs. Here, the aim for a set of DERs is to plan their generation so as to meet a particular load requested by an aggregator, minimize the total cost of generation, and respect individual constraints. For these optimization problems we design a suit of Laplacian-gradient based distributed algorithmic solutions and study their performance. The second part (Chapter 6, Chapter 7, and Chapter 8) studies the asymptotic convergence and robustness properties of the saddle-point dynamics. This dynamics serves as the backbone of numerous distributed algorithms for network constrained optimization problems, including the dispatch problem. Finally, the third part (Chapter 9) investigates an electricity market designed for optimal dispatch among the aggregators. We design and analyze an iterative bid update scheme for the aggregators, discussing the advantages of this scheme using rationality and robustness arguments.

1.1 Literature review

1.1.1 Distributed economic dispatch

The (static) ED problem has been traditionally solved in a centralized manner, see e.g. [CR90] and references therein. Given the expected high density of distributed energy resources (DERs) in the future electricity grid [Far10], the nature of the solution methodologies to the ED problem has shifted to distributed ones. While there exists a broad variety in the assumptions made, a majority of these works rely on the specific form of the solutions of the optimization problem and propose consensus-based algorithms. Many works consider convex, quadratic cost functions for the power generators and perform consensus over their incremental costs under undirected [ZC12, KH12] or directed [DGCH12, BDL⁺14] communication topologies. The work [LCA⁺12] considers linear cost functions and focuses on the design of a heterogeneous network architecture for faster convergence of the consensus scheme. Some works consider general convex cost functions, like we do in this thesis, but either do not consider capacity constraints on the generators [MDC12], assume the initial power allocation to meet the total load [PQP14], or require feedback on the power mismatch from the shift in frequency due to primary droop control [ZLW⁺14]. Along with load and capacity constraints, [BDL⁺14, LV14] consider transmission losses, and [BDN⁺14] additionally take into account valve-point loading effects and prohibited operating zones. However, these constraints make the problem nonconvex and prevent these works from obtaining theoretical guarantees on the algorithm convergence properties. In [DGH12], the authors propose best-response dynamics for a potential-game formulation of the nonconvex ED problem, but the implementation requires all-to-all communication among the generators. [XB06, JJ09] introduce distributed methods to solve resource allocation problem very similar to the ED problem, but without taking into account individual agent constraints. Instead, these are incorporated in the formulation of [SKJ12], but the proposed algorithm arrives at suboptimal solutions of the optimization problem. Our work is also related with the literature on distributed optimal frequency control in power networks [ZTLL14, MZL, LZC16]

dealing with primary and secondary control (tightly connected with the physical network and its dynamics over short time horizons), while we focus here on tertiary control (which allows for longer time horizons and more flexibility in planning). Regarding the information on the total load, there is a wide variety in the scenarios considered: in [DGCH12] a few randomly selected generators have this knowledge, in [ZYC11, KH12, LCA⁺12, BDL⁺14, LV14] each generator knows the load demand at the bus it is connected to and algorithms are devised to aggregate this information. None of the approaches mentioned above study scenarios where the set of generator units varies over time, which normally results in violations of the load requirements. The iterative algorithms in [DGH11] solve asymptotically the problem of finding a feasible (not necessarily optimal) power allocation for the ED problem. The algorithmic solutions that we provide in this thesis either find a feasible allocation in finite time or asymptotically track a time-varying load signal. Hence, these algorithms can handle unit addition and deletion.

As argued in [XE10, IXJ11], the dynamic version of the ED problem, termed dynamic economic dispatch (DED), results in better grid control as it optimally plans generation across a time horizon, specifically taking into account ramp limits and variability of renewable sources. A majority of solution methods to the DED problem are again centralized [XE10] with recent works employing model predictive control (MPC)-based algorithms [IXJ11, XZE11]. The work [LWZ⁺13] proposes a Lagrangian relaxation method to solve the DED problem, but the implementation requires a central coordinator that communicates with all generators. MPC methods have also been employed in [HMMD13] for the dynamic economic dispatch with storage (DEDS) problem, which adds storage units to the DED problem to lower the total cost and smooth out the generation profile across time. The stochastic version of the DEDS problem adds uncertainty in demand and generation by renewables. Algorithmic solutions for this problem emphasize on breaking down the complexity to speed up convergence for large-scale problems and include stochastic MPC [ZH14], dual decomposition [ZGG13], and optimal condition decomposition [SRK15] methods. The work [ZKG16] proposes an ADMM-based algorithm to solve a variation of the DEDS problem where optimal electrical ve-

hicle charging is the goal. The above-mentioned methods for the DEDS problem are either centralized or need a central coordinator. On the other hand, [KCLB13] proposes an ADMM-based distributed algorithm to find the optimizer of a general time-coupled dispatch problem. In comparison, the algorithm proposed in this thesis (see Chapter 5) is robust to load variations and intermittent generator commitment.

Our work on distributed solutions for dispatch problems is also related to the emerging body of research on distributed optimization, see e.g., [ZM12, NOP10, JRJ09] and references therein. In this class of problems, each agent in the network maintains, communicates, and updates an estimate of the complete solution vector. This is a major difference with respect to our setting, where each unit optimizes over and communicates its own local variable, and these variables are tied in together through a global constraint.

1.1.2 Saddle-point dynamics

In constrained optimization problems, the pioneering works [AHU58, Kos56] popularized the use of the primal-dual dynamics to arrive at the saddle points of the Lagrangian. This class of primal-dual dynamics is often alternatively termed as the saddle-point dynamics. For inequality constrained problems, this dynamics is modified with a projection operator on the dual variables to preserve their non-negativity. This results into a dynamical system with discontinuous right-hand side. Therefore, to analyze the asymptotic properties of the trajectory of this dynamics, the standard Lyapunov or LaSalle-based stability results for nonlinear systems, see e.g. [Kha02], are not directly applicable. This observation is at the basis of the direct approach to establish convergence taken in [AHU58], where the evolution of the distance of the solution of the primal-dual dynamics to an arbitrary primal-dual optimizer is approximated using power series expansions and its monotonic evolution is concluded by analyzing the local behavior around a saddle point of the terms in the series. Various instances of this argument are also combined to provide a global convergence result. Instead, [FP10] takes an indirect approach to establish asymptotic convergence based on the use of classical notions

such as invariant sets and LaSalle functions. This work models the primal-dual dynamics as a hybrid automaton, as defined in [LJS⁺03], and employs a LaSalle Invariance Principle to establish the asymptotic convergence of the solutions. This approach to establish convergence is appealing because of its conceptual simplicity and the versatility of Lyapunov-like methods in characterizing other properties of the dynamics. However, the hybrid automaton that corresponds to the primal-dual dynamics is in general not continuous, thereby not satisfying a key requirement of the invariance principle stated in [LJS⁺03]. In Chapter 7, we give an example that illustrates this point. Subsequently, we provide an alternative proof strategy to arrive at the same convergence results of [FP10] using the tools of projected dynamical systems [NZ96].

In the context of distributed control and multi-agent systems, an important motivation to study saddle-point dynamics comes from network optimization problems where the objective function is an aggregate of each agents' local objective function and the constraints are given by a set of conditions that are locally computable at the agent level. Because of this structure, the saddle-point dynamics of the Lagrangian for such problems is inherently amenable to distributed implementation. This observation explains the emerging body of work that, from this perspective, looks at problems in distributed convex optimization [WE11, GC14, DE14], distributed linear programming [RC15], and applications to power networks [ME13, ZP14, ZTLL14], wireless systems [CLCD07, FP10, CL12, FP14], and bargaining problems [RC16]. The work [KP87] shows an interesting application of the saddle-point dynamics to find a common Lyapunov function for a linear differential inclusion. In game theory, it is natural to study the convergence properties of saddle-point dynamics to find the Nash equilibria of two-person zero-sum games [BO82, GC13, RBS16]. A majority of these works assume the function whose saddle points are sought to be convex-concave in its arguments. Our focus in Chapter 6 is on the asymptotic stability of the min-max saddle points under the saddle-point dynamics for a wider class of functions, and without any nonnegativity-preserving projection on individual variables. We explicitly allow for the possibility of a continuum of saddle points, instead of isolated ones, and

wherever feasible, on establishing convergence of the trajectories to a point in the set. The issue of asymptotic convergence, even in the case of standard gradient systems, is a delicate one when equilibria are a continuum [AK06]. In such scenarios, convergence to a point might not be guaranteed, see e.g., the counter example in [PdM82]. Our results in Chapter 6 are complementary to those in [HL14], which focus on the characterization of the asymptotic behavior of the saddle-point dynamics when trajectories do not converge to saddle points and instead show oscillatory behaviour.

Most of the results mentioned in the previous paragraphs regarding convergence of saddle-point dynamics rely on global strict convexity-concavity of the function for which the dynamics is written. The results in Chapter 8 relaxes this assumption and thereby generalizes these results. Specifically, we show that global convergence of the projected saddle-point dynamics can be guaranteed under local strong convexity-concavity assumptions. Furthermore, if traditional assumptions do hold, then a stronger notion of convergence, that also implies robustness, is guaranteed: if strong convexity-concavity holds globally, the dynamics admits a Lyapunov function and in the absence of projection, the dynamics is ISS, admitting an ISS Lyapunov function. In the context of distributed optimization, the recent work [NC16] employs a (strict) Lyapunov function approach to ensure asymptotic convergence of saddle-point-like dynamics.

1.1.3 Competition in electricity markets

The study of competition in electricity markets is a classical topic [Sto02, KS04]. Extensively studied models are supply function, Bertrand (price) and Cournot (capacity) bidding, see [JT11, TJ13, CBW16], respectively, and references therein. These studies analyze the properties of the game that different bidding models result into by determining the existence of the Nash equilibrium of the game and estimating its efficiency. Some works [LS05, HR07, BCKS10, NP10], on the other hand, propose iterative algorithms for the players that compute the Nash equilibrium of the game. However, these algorithms either require generators to have some information about other generators (cost functions or bids) or assume

that the demand of each generator is a continuous function of the bids. Our work does not make any such assumptions, which also rules out the possibility of using various other Nash equilibrium learning algorithms, such as best-response [BGJ10], fictitious play [FL98], and extremum seeking [FKB12, SJS12]. In a related set of works [WGMM12, SCA16], decentralized generation planning is achieved by assuming the generators to be price-takers and designing iterative schemes based on dual-decomposition [PC07]. In our work, however, we consider a strategic scenario where generators bid into the market and are hence price-setters. The work [FD16] proposes an iterative auction algorithm for a market where both generators and consumers are strategic but does not provide convergence guarantees for the generated bid sequences. The paper [PG16], closer in spirit to our work, proposes an iterative method for the generators to find the Nash equilibrium assuming they do not have any information about each other. At each iteration, the generators send to the ISO the gradient of their cost functions at a certain generation value and the ISO then adjusts these generation values so that social welfare is maximized. An important difference between this setup and ours is that the market clearing strategy in there elucidates truthful bidding of gradient information by the generators.

The electricity market game considered in Chapter 9 belongs to the broader class of multi-leader-single-follower games [LM10, PF05]. The Nash equilibria of such games can be thought of as optimizers of mathematical programs with equilibrium constraints (MPEC) [LPR96], that are traditionally solved in a centralized manner [FDM05]. The work [ZL14] provides a distributed method to find the equilibria of an MPEC problem but requires the follower’s (the ISO in our case) optimization to have a unique solution for each action of the leaders (the generators). This is in general not the case for electricity markets. The results of Chapter 9 broadly relates to the recent developments in the area of “learning in games”, see e.g., [HMC15, LSET16], and references therein. Learning mechanisms proposed in there do not apply directly to the electricity market setting as they do not consider network constraints for allocation of goods.

1.2 Contributions

1.2.1 Distributed economic dispatch

We start in Chapter 3 with the formulation of the (static) ED problem for a group of generator units that communicate over an arbitrary weight-balanced, strongly connected digraph. The optimization problem is convex as the individual cost functions are smooth and convex, the load satisfaction is a linear constraint, and the individual generators' capacities prescribe convex inequality constraints. Our formulation is a simplification of the ED problem in its full generality, which in practice may have additional constraints that make it nonconvex. However, our developments show that obtaining a provably correct algorithmic solution for the formulation here of the ED problem given the performance requirements (distributed, convergent irrespective of initial condition, able to handle time-varying loads, and robust to intermittent power generation) is challenging.

The contributions of Chapter 3 are threefold. The first contribution pertains to the relaxed economic dispatch (rED) problem, which is the ED problem without bounds on the individual generators' capacity. We introduce the distributed Laplacian-gradient dynamics, establish its exponential convergence to the set of solutions of the rED problem, and characterize the associated rate. As a by-product of our analysis, we establish the anytime nature of this algorithm and its convergence under jointly strongly connected communication topologies. Our second contribution concerns the ED problem. We use a nonsmooth exact penalty function to transform the problem, which has generators' capacity bounds, into an equivalent optimization with no such constraints. The resulting formulation resembles the rED problem, and this leads us to the design of the distributed Laplacian-nonsmooth-gradient dynamics. This algorithm provably converges to the solutions of the ED problem, and is also anytime and robust to switching communication topologies that remain strongly connected. Our third contribution deals with the distributed allocation of the load to the network of generators while respecting the capacity bounds. We propose the three-phase strategy DETERMINE FEASIBLE ALLOCATION, that only involves message passing between generator units over a

spanning tree. The first phase maintains a spanning tree over the units present in the network, the second phase determines the capacity of each subtree to allocate additional power, and the third phase allocates power to each individual unit, respecting the constraints, to meet the overall load. Our algorithm terminates in finite time and can be used for the initialization of the Laplacian-nonsmooth-gradient dynamics and to handle scenarios with power imbalances caused by the addition or deletion of generators.

Chapter 4 builds and generalizes the results of Chapter 3. Our first contribution is the design of a centralized algorithm, termed “load mismatch + Laplacian-nonsmooth-gradient” dynamics, that solves the ED problem starting from any initial power allocation. This strategy has two components: one component seeks to optimize the network generation cost while keeping constant the total power generated; the other component is a feedback correction term driven by the error between the desired total load and the network generation. This latter term is responsible for ensuring that the algorithm trajectories asymptotically satisfy the load satisfaction constraint irrespective of the initial power allocation. These observations set the basis for our second contribution, which is the synthesis of a distributed coordination algorithm, termed “dynamic average consensus + Laplacian-nonsmooth-gradient” dynamics, with the same convergence guarantees. Our design consists of two coupled dynamical systems: a dynamic average consensus algorithm to estimate the mismatch between generation and desired load in a distributed fashion and distributed Laplacian-nonsmooth-gradient that employ these estimates to dynamically allocate the unit generation levels. Our third contribution is the development of a refined version of the LaSalle Invariance Principle for differential inclusions. Our final contribution is the formal characterization of the robustness properties of the distributed algorithm. Building on the observation that the mismatch dynamics between network generation and total load are exponentially convergent and input-to-state stable, we establish the algorithm ability to track time-varying loads and its robustness in scenarios with intermittent power generation.

Chapter 5 gives the formulation of the DEDS problem for a group of DERs

communicating over a weight-balanced strongly connected digraph. The decision variables are the power to be injected into the grid and power to be sent to storage by each DER at each time slot. Using exact penalty functions, we reformulate the problem as an equivalent optimization with equality constraints but without inequality ones. The structure of the modified problem guides our main contribution of this chapter: the design of the provably-correct distributed strategy termed “dynamic average consensus (dac) + Laplacian nonsmooth gradient ($L\partial$) + nonsmooth gradient (∂)” dynamics to solve the DEDS problem starting from any initial condition. As in “dynamic average consensus + Laplacian-nonsmooth-gradient” dynamics, the algorithm consists of two interconnected systems. A first block allows DERs to track, using dac, the mismatch between the current total power injected and the load for each time slot of the planning horizon. A second block has two components, one that minimizes the total cost while keeping the total injection constant (using Laplacian-nonsmooth-gradient dynamics on injection variables and nonsmooth-gradient dynamics on storage variables) and an error-correcting component that uses the mismatch signal estimated by the first block to adjust, exponentially fast, the total injection towards the load at each time slot.

1.2.2 Saddle-point dynamics

We start in Chapter 6 with the definition of the saddle-point dynamics for continuously differentiable functions of two (vector) variables, which we term saddle functions. The saddle-point dynamics consists of gradient descent of the saddle function in the first variable and gradient ascent in the second variable. The aim of Chapter 6 is to characterize the asymptotic convergence properties of the saddle-point dynamics to the set of min-max saddle points of the saddle function. Assuming this set is nonempty, our contributions can be understood as a catalog of complementary conditions on the saddle function that guarantee that the trajectories of the saddle-point dynamics are proved to converge to the set of saddle points, and possibly to a point in the set. We broadly divide our results in two categories, one in which the saddle function has convexity-concavity properties and the other in which it does not. For the first category, our starting

result considers saddle functions that are locally convex-concave on the set of saddle points. We show that asymptotic stability of the set of saddle points is guaranteed if either the convexity or concavity properties are strict, and convergence is pointwise. Furthermore, motivated by equality constrained optimization problems, our second result shows that the same conclusions on convergence hold for functions that depend linearly on one of its arguments if the strictness requirement is dropped. For the third and last result in this category, we relax the convexity-concavity requirement and establish asymptotic convergence for strongly jointly quasiconvex-quasiconcave saddle functions. Moving on to the second category of scenarios, where functions lack convexity-concavity properties, our first condition is based on linearization. We consider piecewise twice continuously differentiable saddle-point dynamics and provide conditions on the eigenvalues of the limit points of Jacobian matrices of the saddle function at the saddle points that ensure local asymptotic stability of a manifold of saddle points. Our convergence analysis is based on a general result of independent interest on the stability of a manifold of equilibria for piecewise smooth vector fields that we state and prove using ideas from center manifold theory. The next two results are motivated by the observation that saddle functions exist in the second category that do not satisfy the linearization hypotheses and yet have convergent dynamics. In one result, we justify convergence by studying the variation of the function and its Hessian along the proximal normal directions to the set of saddle points. Specifically, we assume polynomial bounds for these variations and derive an appropriate relationship between these bounds that ensures asymptotic convergence. In the other result, we assume the saddle function to be linear in one variable and indefinite in another, where the indefinite part satisfies some appropriate regularity conditions. When discussing each of the above scenarios, we extend the conditions to obtain global convergence wherever feasible. Various examples throughout the chapter justify the complementary character of the hypotheses in our results.

Chapter 7 studies the projected saddle-point dynamics (also termed as the primal-dual dynamics). This dynamics has a discontinuous right-hand side. We first show using the help of an example that the proof of convergence provided in the

literature [FP10] is not rigorous. Based on this observation, the main contribution of Chapter 7 is a novel proof strategy. We show that the primal-dual dynamics is a particular case of a projected dynamical system and, using results from [NZ96], we establish that Caratheodory solutions exist, are unique, and are continuous with respect to the initial condition. Using these properties, we show that the omega-limit set of any solution of the primal-dual dynamics is invariant under the dynamics. Finally, we employ the invariance principle for Caratheodory solutions of discontinuous dynamical systems from [BC06] to show that the primal-dual optimizers are globally asymptotically stable under the primal-dual dynamics and that each solution of the dynamics converges to an optimizer.

Chapter 8 defines the projected saddle-point dynamics for a differentiable convex-concave saddle function. The dynamics has three components: gradient descent, projected gradient ascent, and gradient ascent of the saddle function, where each gradient is with respect to a subset of the arguments of the function. This unified formulation encompasses all forms of the saddle-point dynamics discussed in the previous paragraphs. Our contributions of this chapter are fivefold that shed light on the effect that the convexity-concavity of the saddle function has on the convergence attributes of the projected saddle-point dynamics. Our first contribution is a novel characterization of the omega-limit set of the trajectories of the projected saddle-point dynamics in terms of the diagonal Hessian blocks of the saddle function. To this end, we use the distance to a saddle point as a LaSalle function, express the Lie derivative of this function in terms of the Hessian blocks, and show it is nonpositive using second-order properties of the saddle function. Building on this characterization, our second contribution establishes global asymptotic convergence of the projected saddle-point dynamics to a saddle point assuming only local strong convexity-concavity of the saddle function. Our third contribution identifies a novel Lyapunov function for the projected saddle-point dynamics for the case when strong convexity-concavity holds globally and the saddle function can be written as the Lagrangian of a constrained optimization problem. This discontinuous Lyapunov function can be interpreted as multiple continuously differentiable Lyapunov functions, one for each set in a particular partition of the

domain determined by the projection operator of the dynamics. Interestingly, the identified Lyapunov function is the sum of two previously known and independently considered LaSalle functions. When the saddle function takes the form of the Lagrangian of an equality constrained optimization, then no projection is present. In such scenarios, if the saddle function satisfies global strong convexity-concavity, our fourth contribution establishes input-to-state stability (ISS) of the dynamics with respect to the saddle point by providing an ISS Lyapunov function. Our fifth contribution uses this function to design an opportunistic state-triggered implementation of the saddle-point dynamics. We show that the trajectories of this discrete-time system converge asymptotically to the saddle points and that executions are Zeno-free, i.e., that the difference between any two consecutive triggering times is lower bounded by a common positive quantity.

1.2.3 Iterative bidding in electricity markets

We start in Chapter 9 with the definition of an inelastic electricity market where the ISO seeks to find the production levels that solve the DC optimal power flow (DC-OPF) problem for a group of strategic generators which do not share their cost functions. Consequently, the ISO cannot solve the DC-OPF problem by itself. However, each generator submits a bid to the ISO specifying the price per unit of electricity at which the generator is willing to provide power. Given these bids, the ISO decides how much production to allocate to each generator so that the cost of generation is minimized, the loads are met, and the network flow constraints are satisfied. The resulting Bertrand competition model defines the game among the generators, where the actions are the bids and the payoffs are the profits. We define the concept of the efficient Nash equilibrium, that is, the Nash equilibrium at which the generators are willing to produce the amount that corresponds to the optimizer of the DC-OPF problem. Our first contribution in this chapter gives two set of conditions that ensure existence and uniqueness, respectively, of an efficient Nash equilibrium for the inelastic electricity market game. Our second contribution is the design of the BID ADJUSTMENT ALGORITHM along with its correctness analysis. This algorithm can be understood as

“learning via repeated play”, where generators are “myopically selfish”, changing their bid at each iteration with the aim of maximizing their own payoff. Along the execution, the only information available to the generators is their bid and the amount of generation that the ISO request from them. In particular, generators are not aware of the number of other generators, their costs, bids, or payoffs. We show that this decentralized iterative scheme is guaranteed to take the bids of the generators to any neighborhood of the unique efficient Nash equilibrium provided the stepsizes are chosen appropriately. Further, we establish that the convergence rate is linear. Our third contribution analyzes the robustness properties of the BID ADJUSTMENT ALGORITHM. Specifically, we establish that the convergence is not affected by affine disturbances, thus showing that deviations in stepsizes by the generators can be handled gracefully. Additionally, we show that there is no incentive for any individual generator to deviate from the algorithm by using an alternative bid update scheme. Finally, we also show that, if at each generator bus there is at least one generator running the BID ADJUSTMENT ALGORITHM, then there is no incentive for other generators connected to the network to not follow the algorithm, i.e., this adjustment scheme becomes a rational choice for all generators. These properties provide a sound justification for why the group generators would adopt this iterative bid adjustment scheme to solve the DC-OPF problem.

1.3 Organization

Chapter 2 collects the notation and some preliminaries used throughout this thesis. Chapter 3 introduces the problem of economic dispatch and proposes an anytime distributed algorithm for solving it. Chapter 4 provides a robust, initialization-free, distributed algorithm for the economic dispatch problem. Consequently, these algorithms are leveraged upon in Chapter 5 to design a distributed algorithm for the dynamic economic dispatch problem with storages. Chapter 6 studies the asymptotic properties of the saddle-point dynamics. Chapter 7 analyzes the convergence properties of the primal-dual dynamics using the concepts

of projected dynamical systems. Chapter 8 gives a Lyapunov function for the saddle-point dynamics and analyzes the input-to-state properties of the dynamics using this tool. Chapter 9 defines an electricity market setup and investigates the properties of an iterative bid adjustment scheme. Finally, Chapter 10 summarizes our contributions and outlines important future research directions.

Chapter 2

Preliminaries

This section introduces basic concepts and preliminaries from graph theory, nonsmooth analysis, proximal calculus, saddle points, constrained optimization, and dynamical systems. We begin with some notational conventions.

2.1 Notation

Let \mathbb{R} , $\mathbb{R}_{\geq 0}$, $\mathbb{R}_{\leq 0}$, $\mathbb{R}_{> 0}$, $\mathbb{Z}_{\geq 0}$, and $\mathbb{Z}_{\geq 1}$ be the set of real, nonnegative real, nonpositive real, positive real, nonnegative integer, and positive integer numbers, respectively. The 2- and ∞ -norms on \mathbb{R}^n and their respective induced norms on $\mathbb{R}^{n \times n}$ are denoted with $\|\cdot\|$ and $\|\cdot\|_{\infty}$, respectively. Let $B_{\delta}(x) = \{y \in \mathbb{R}^n \mid \|y-x\| < \delta\}$ be the open ball centered at $x \in \mathbb{R}^n$ with radius $\delta > 0$. The notation $[n]$ stands for the set $\{1, \dots, n\}$. For a set D , its cardinality is represented by $|D|$. For a set $\mathcal{S} \subset \mathbb{R}^n$, its interior, closure, and boundary are denoted by $\text{int}(\mathcal{S})$, $\text{cl}(\mathcal{S})$, and $\text{bd}(\mathcal{S})$, respectively. The distance of a point $x \in \mathbb{R}^n$ to the set $\mathcal{S} \subset \mathbb{R}^n$ in 2-norm is $\|x\|_{\mathcal{S}} = \inf_{y \in \mathcal{S}} \|x - y\|$. The projection of x onto a closed set \mathcal{S} is defined as the set $\text{proj}_{\mathcal{S}}(x) = \{y \in \mathcal{S} \mid \|x - y\| = \|x\|_{\mathcal{S}}\}$. When \mathcal{S} is also convex, $\text{proj}_{\mathcal{S}}(x)$ is a singleton for any $x \in \mathbb{R}^n$. For $x \in \mathbb{R}^n$, $x_i \in \mathbb{R}$ denotes its i -th component. Given vectors $x, y \in \mathbb{R}^n$, $x \leq y$ if and only if $x_i \leq y_i$ for all $i \in [n]$. For $x \in \mathbb{R}^n$ and $y \in \mathbb{R}^m$, $(x; y) \in \mathbb{R}^{n+m}$ denotes its concatenation. Let $\mathbf{0}_n = (0, \dots, 0) \in \mathbb{R}^n$, $\mathbf{1}_n = (1, \dots, 1) \in \mathbb{R}^n$, and $I_n \in \mathbb{R}^{n \times n}$ be the identity matrix.

Denote $[u]^+ = \max\{0, u\}$ for $u \in \mathbb{R}$. For scalars $a, b \in \mathbb{R}$, the operator $[a]_b^+$ is

$$[a]_b^+ = \begin{cases} a, & \text{if } b > 0, \\ \max\{0, a\}, & \text{if } b = 0. \end{cases}$$

For vectors $a, b \in \mathbb{R}^n$, $[a]_b^+$ denotes the vector whose i -th component is $[a_i]_{b_i}^+$, $i \in [n]$. For $r \in \mathbb{R}$, let $\mathcal{H}_r = \{x \in \mathbb{R}^n \mid \mathbf{1}_n^\top x = r\}$. For $\mathfrak{h} > 0$, $y \in \mathbb{R}^{n\mathfrak{h}}$ and $k \in [\mathfrak{h}]$, $y^{(k)} \in \mathbb{R}^n$ contains the $nk - n + 1$ to nk components of y (and so $y = (y^{(1)}; y^{(2)}; \dots; y^{(\mathfrak{h})})$). We use the notation \mathcal{C}^k for a function being $k \in \mathbb{Z}_{\geq 1}$ times continuously differentiable. For a real-valued function $V : \mathbb{R}^n \rightarrow \mathbb{R}$ and $\alpha > 0$, we denote the sublevel set of V by $V^{-1}(\leq \alpha) = \{x \in \mathbb{R}^n \mid V(x) \leq \alpha\}$. Given two sets X and Y , a set-valued map $f : X \rightrightarrows Y$ associates to each point in X a subset of Y . Given a set-valued map $f : \mathbb{R}^n \rightrightarrows \mathbb{R}^m$ and a matrix $A \in \mathbb{R}^{p \times m}$, their composition $h = Af : \mathbb{R}^n \rightrightarrows \mathbb{R}^p$ is the set-valued map defined by $h(x) = \{z \in \mathbb{R}^p \mid z = Ay \text{ with } y \in f(x)\}$. For a matrix $A \in \mathbb{R}^{n \times n}$, we use $A \succeq 0$, $A \succ 0$, $A \preceq 0$, and $A \prec 0$ to denote that A is positive semidefinite, positive definite, negative semidefinite, and negative definite, respectively. The eigenvalues of A are $\lambda_i(A)$ for $i \in [n]$. For a symmetric matrix $A \in \mathbb{R}^{n \times n}$, $\lambda_{\min}(A)$ and $\lambda_{\max}(A)$ denote the minimum and maximum eigenvalue of A . The range and null spaces of A are denoted by $\text{range}(A)$ and $\text{null}(A)$, respectively. The Kronecker product of $A \in \mathbb{R}^{n \times m}$ and $B \in \mathbb{R}^{p \times q}$ is $A \otimes B \in \mathbb{R}^{np \times mq}$. Given two sets $\mathcal{A}_1, \mathcal{A}_2 \subset \mathbb{R}^n$, we let $\mathcal{A}_1 + \mathcal{A}_2 = \{x + y \mid x \in \mathcal{A}_1, y \in \mathcal{A}_2\}$.

A set $\mathcal{S} \subset \mathbb{R}^n$ is *path connected* if for any two points $a, b \in \mathcal{S}$ there exists a continuous map $\gamma : [0, 1] \rightarrow \mathcal{S}$ such that $\gamma(0) = a$ and $\gamma(1) = b$. A set $\mathcal{S}_c \subset \mathcal{S} \subset \mathbb{R}^n$ is an *isolated path connected component* of \mathcal{S} if it is path connected and there exists an open neighborhood \mathcal{U} of \mathcal{S}_c in \mathbb{R}^n such that $\mathcal{U} \cap \mathcal{S} = \mathcal{S}_c$.

For a real-valued function $F : \mathbb{R}^n \times \mathbb{R}^m \rightarrow \mathbb{R}$, $(x, y) \mapsto F(x, y)$, we denote by $\nabla_x F$ and $\nabla_y F$ the column vector of partial derivatives of F with respect to the first and second arguments, respectively. Higher-order derivatives follow the convention $\nabla_{xy} F = \frac{\partial^2 F}{\partial x \partial y}$, $\nabla_{xx} F = \frac{\partial^2 F}{\partial x^2}$, and so on. The restriction of $f : \mathbb{R}^n \rightarrow \mathbb{R}^m$ to a subset $\mathcal{S} \subset \mathbb{R}^n$ is denoted by $f|_{\mathcal{S}}$. The Jacobian of a \mathcal{C}^1 map $f : \mathbb{R}^n \rightarrow \mathbb{R}^m$ at $x \in \mathbb{R}^n$ is denoted by $Df(x) \in \mathbb{R}^{m \times n}$. Finally, a vector field $f : \mathbb{R}^n \rightarrow \mathbb{R}^n$ is said

to be *piecewise \mathcal{C}^2* if it is continuous and there exists

- a finite collection of disjoint open sets $\mathcal{D}_1, \dots, \mathcal{D}_m \subset \mathbb{R}^n$, referred to as *patches*, whose closure covers \mathbb{R}^n , that is, $\mathbb{R}^n = \cup_{i=1}^m \text{cl}(\mathcal{D}_i)$, and
- a finite collection of \mathcal{C}^2 functions $\{f_i : \mathcal{D}_i^e \rightarrow \mathbb{R}^n\}_{i=1}^m$ where, for each $i \in [m]$, \mathcal{D}_i^e is open with $\text{cl}(\mathcal{D}_i) \subset \mathcal{D}_i^e$, such that $f_{|\text{cl}(\mathcal{D}_i)}$ and f_i take the same values over $\text{cl}(\mathcal{D}_i)$.

2.2 Graph theory

We present here notions from algebraic graph theory [BCM09]. A *directed graph* (or *digraph*) is a pair $\mathcal{G} = (\mathcal{V}, \mathcal{E})$, with \mathcal{V} the vertex set and $\mathcal{E} \subseteq \mathcal{V} \times \mathcal{V}$ the edge set. A path is a sequence of vertices connected by edges. A digraph is *strongly connected* if there is a path between any pair of vertices. The sets of out- and in-neighbors of v_i are, respectively, $\mathcal{N}_{v_i}^+ = \{v_j \in \mathcal{V} \mid (v_i, v_j) \in \mathcal{E}\}$ and $\mathcal{N}_{v_i}^- = \{v_j \in \mathcal{V} \mid (v_j, v_i) \in \mathcal{E}\}$. A *weighted digraph* $\mathcal{G} = (\mathcal{V}, \mathcal{E}, \mathbf{A})$ is composed of a digraph $(\mathcal{V}, \mathcal{E})$ and an *adjacency matrix* $\mathbf{A} \in \mathbb{R}_{\geq 0}^{n \times n}$ with $a_{ij} > 0$ if and only if $(v_i, v_j) \in \mathcal{E}$. The weighted out- and in-degree of v_i are, respectively, $d^{\text{out}}(v_i) = \sum_{j=1}^n a_{ij}$ and $d^{\text{in}}(v_i) = \sum_{j=1}^n a_{ji}$. The *Laplacian* matrix is $\mathbf{L} = \mathbf{D}_{\text{out}} - \mathbf{A}$, where \mathbf{D}_{out} is the diagonal matrix with $(\mathbf{D}_{\text{out}})_{ii} = d^{\text{out}}(v_i)$, for $i \in \{1, \dots, n\}$. Note that $\mathbf{L}\mathbf{1}_n = 0$. If \mathcal{G} is strongly connected, then 0 is a simple eigenvalue of \mathbf{L} . \mathcal{G} is undirected if $\mathbf{L} = \mathbf{L}^\top$. \mathcal{G} is *weight-balanced* if $d^{\text{out}}(v) = d^{\text{in}}(v)$, for all $v \in \mathcal{V}$ if and only if $\mathbf{1}_n^\top \mathbf{L} = 0$ if and only if $\mathbf{L}_s = (\mathbf{L} + \mathbf{L}^\top)/2 \geq 0$. An undirected graph is weight-balanced. If \mathcal{G} is weight-balanced and strongly connected, then 0 is a simple eigenvalue of \mathbf{L}_s , and

$$x^\top \mathbf{L}_s x \geq \lambda_2(\mathbf{L}_s) \left\| x - \frac{1}{n} (\mathbf{1}_n^\top x) \mathbf{1}_n \right\|^2, \quad \forall x \in \mathbb{R}^n, \quad (2.1)$$

with $\lambda_2(\mathbf{L}_s)$ the smallest non-zero eigenvalue of \mathbf{L}_s .

2.3 Nonsmooth analysis and proximal calculus

We introduce notions from nonsmooth analysis following [Cor08]. A map $f : \mathbb{R}^n \rightarrow \mathbb{R}^m$ is *locally Lipschitz* at $x \in \mathbb{R}^n$ if there exist $\delta_x, L_x > 0$ such that $\|f(y_1) - f(y_2)\| \leq L_x \|y_1 - y_2\|$ for any $y_1, y_2 \in B_{\delta_x}(x)$. If f is locally Lipschitz at every $x \in \mathcal{K} \subset \mathbb{R}^n$, then we simply say that f is locally Lipschitz on \mathcal{K} . The map f is *Lipschitz* on $\mathcal{K} \subset \mathbb{R}^n$ if there exists a constant $L > 0$ such that $\|f(x) - f(y)\| \leq L \|x - y\|$ for any $x, y \in \mathcal{K}$. Note that if f is locally Lipschitz on \mathbb{R}^n , then it is Lipschitz on every compact set $\mathcal{K} \subset \mathbb{R}^n$. The map f is *locally bounded* if for each $x \in \mathbb{R}^n$ there exist constants $M_x, \epsilon_x > 0$ such that $\|f(y)\| \leq M_x$ for all $y \in B_{\epsilon_x}(x)$. The *right directional derivative* of f at x in the direction $v \in \mathbb{R}^n$ is

$$f'(x; v) = \lim_{h \rightarrow 0^+} \frac{f(x + hv) - f(x)}{h},$$

when this limit exists. The *generalized directional derivative* of f at x in the direction $v \in \mathbb{R}^n$ is defined as

$$f^o(x; v) = \limsup_{y \rightarrow x, h \rightarrow 0^+} \frac{f(y + hv) - f(y)}{h}.$$

A function $f : \mathbb{R}^n \rightarrow \mathbb{R}$ is *regular* at $x \in \mathbb{R}^n$ if, for all $v \in \mathbb{R}^n$, the right and generalized directional derivatives of f at x in the direction of v coincide. Continuously differentiable and convex functions are both regular. A set-valued map $\mathcal{H} : \mathbb{R}^n \rightrightarrows \mathbb{R}^n$ is *upper semicontinuous* at $x \in \mathbb{R}^n$ if, for all $\epsilon \in (0, \infty)$, there exists $\delta \in (0, \infty)$ such that $\mathcal{H}(y) \subset \mathcal{H}(x) + B_\epsilon(0)$ for all $y \in B_\delta(x)$. Also, \mathcal{H} is *locally bounded* at $x \in \mathbb{R}^n$ if there exist $\epsilon, \delta \in (0, \infty)$ such that $\|z\| \leq \epsilon$ for all $z \in \mathcal{H}(y)$ and $y \in B_\delta(x)$. \mathcal{H} is locally bounded if it is so at each point in \mathbb{R}^n . Given a locally Lipschitz function $f : \mathbb{R}^n \rightarrow \mathbb{R}$, let Ω_f be the set (of measure zero) of points where f is not differentiable. The *generalized gradient* of f , denoted as $\partial f : \mathbb{R}^n \rightrightarrows \mathbb{R}^n$, is

$$\partial f(x) = \text{co}\left\{ \lim_{i \rightarrow \infty} \nabla f(x_i) \mid x_i \rightarrow x, x_i \notin S \cup \Omega_f \right\},$$

where co denotes convex hull and $S \subset \mathbb{R}^n$ is any set of measure zero. The set-valued map ∂f is locally bounded, upper semicontinuous, and takes non-empty,

compact, and convex values. A *critical point* $x \in \mathbb{R}^n$ of f satisfies $0 \in \partial f(x)$. For a locally Lipschitz $f : \mathbb{R}^n \times \mathbb{R}^m \rightarrow \mathbb{R}$, $(x, y) \mapsto f(x, y)$, the partial generalized gradient with respect to x and y are $\partial_x f$ and $\partial_y f$, respectively.

Next we present notions on proximal calculus following [CLSW98]. Given a closed set $\mathcal{E} \subset \mathbb{R}^n$ and a point $x \in \mathbb{R}^n \setminus \mathcal{E}$, the distance from x to \mathcal{E} is,

$$d_{\mathcal{E}}(x) = \min_{y \in \mathcal{E}} \|x - y\|. \quad (2.2)$$

We let $\text{proj}_{\mathcal{E}}(x)$ denote the set of points in \mathcal{E} that are closest to x , i.e., $\text{proj}_{\mathcal{E}}(x) = \{y \in \mathcal{E} \mid \|x - y\| = d_{\mathcal{E}}(x)\} \subset \mathcal{E}$. For $y \in \text{proj}_{\mathcal{E}}(x)$, the vector $x - y$ is a *proximal normal direction* to \mathcal{E} at y and any nonnegative multiple $\zeta = t(x - y)$, $t \geq 0$ is called a *proximal normal* (P -normal) to \mathcal{E} at y . The distance function $d_{\mathcal{E}}$ might not be differentiable in general (unless \mathcal{E} is convex), but is globally Lipschitz and regular [CLSW98, p. 23]. In the case of the square of the distance function, one can compute [CLSW98, p. 99] the generalized gradient as,

$$\partial d_{\mathcal{E}}^2(x) = \text{co}\{2(x - y) \mid y \in \text{proj}_{\mathcal{E}}(x)\}. \quad (2.3)$$

2.4 Saddle points and convex-concave functions

Here we review notions of convexity, concavity, and saddle points from [BV09]. A function $f : \mathcal{X} \rightarrow \mathbb{R}$ is *convex* if

$$f(\lambda x + (1 - \lambda)x') \leq \lambda f(x) + (1 - \lambda)f(x'),$$

for all $x, x' \in \mathcal{X}$ (where \mathcal{X} is a convex domain) and all $\lambda \in [0, 1]$. A convex differentiable f satisfies the following *first-order convexity condition*

$$f(x') \geq f(x) + (x' - x)^{\top} \nabla f(x),$$

for all $x, x' \in \mathcal{X}$. A \mathcal{C}^2 function f is *locally strongly convex* at $x \in \mathcal{X}$ if f is convex and $\nabla^2 f(x) \succeq mI$ for some $m > 0$. Moreover, a \mathcal{C}^2 function f is *strongly convex* if $\nabla^2 f(x) \succeq mI$ for all $x \in \mathcal{X}$ for some $m > 0$. A function $f : \mathcal{X} \rightarrow \mathbb{R}$

is *concave*, *locally strongly concave*, or *strongly concave* if $-f$ is convex, locally strongly convex, or strongly convex, respectively. Following [Jov96], a function f is *strongly quasiconvex* with parameter $s > 0$ over a convex set $\mathcal{D} \subset \mathcal{X}$ if for all $x, x' \in \mathcal{D}$ and all $\lambda \in [0, 1]$ we have,

$$\max\{f(x), f(x')\} - f(\lambda x + (1 - \lambda)x') \geq s\lambda(1 - \lambda)\|x - x'\|^2.$$

A function f is *strongly quasiconcave* with parameter $s > 0$ over the set \mathcal{D} if $-f$ is strongly quasiconvex with parameter s over \mathcal{D} .

A function $F : \mathcal{X} \times \mathcal{Y} \rightarrow \mathbb{R}$ is *locally convex-concave* at a point $(\tilde{x}, \tilde{y}) \in \mathcal{X} \times \mathcal{Y}$ if there exists an open neighborhood \mathcal{U} of (\tilde{x}, \tilde{y}) such that for all $(\bar{x}, \bar{y}) \in \mathcal{U}$, the functions $x \mapsto F(x, \bar{y})$ and $y \mapsto F(\bar{x}, y)$ are convex over $\mathcal{U} \cap (\mathcal{X} \times \{\bar{y}\})$ and concave over $\mathcal{U} \cap (\{\bar{x}\} \times \mathcal{Y})$, respectively. If in addition, either $x \mapsto F(x, \tilde{y})$ is strictly convex in an open neighborhood of \tilde{x} , or $y \mapsto F(\tilde{x}, y)$ is strictly concave in an open neighborhood of \tilde{y} , then F is *locally strictly convex-concave* at (\tilde{x}, \tilde{y}) . F is locally (resp. locally strictly) convex-concave on a set $\mathcal{S} \subset \mathcal{X} \times \mathcal{Y}$ if it is so at each point in \mathcal{S} . F is (*globally*) *convex-concave* if in the local definition $\mathcal{U} = \mathcal{X} \times \mathcal{Y}$. When the space $\mathcal{X} \times \mathcal{Y}$ is clear from the context, we refer to this property as F being convex-concave in (x, y) . Finally, F is *globally strictly convex-concave* if it is convex-concave and for any $(\bar{x}, \bar{y}) \in \mathcal{X} \times \mathcal{Y}$, either $x \mapsto F(x, \bar{y})$ is strictly convex or $y \mapsto F(\bar{x}, y)$ is strictly concave. Note that this notion is different than saying that F is *both* strictly convex and strictly concave. The function F is *locally jointly strongly quasiconvex-quasiconcave* at a point $(\tilde{x}, \tilde{y}) \in \mathcal{X} \times \mathcal{Y}$ if there exist $s > 0$ and an open neighborhood \mathcal{U} of (\tilde{x}, \tilde{y}) such that for all $(\bar{x}, \bar{y}) \in \mathcal{U}$, the function $x \mapsto F(x, \bar{y})$ is strongly quasiconvex with parameter s over $\mathcal{U} \cap (\mathcal{X} \times \{\bar{y}\})$ and the function $y \mapsto F(\bar{x}, y)$ is strongly quasiconvex with parameter s over $\mathcal{U} \cap (\{\bar{x}\} \times \mathcal{Y})$. F is locally jointly strongly quasiconvex-quasiconcave on a set $\mathcal{S} \subset \mathcal{X} \times \mathcal{Y}$ if it is so at each point in \mathcal{S} . F is *globally jointly strongly quasiconvex-quasiconcave* if in the local definition $\mathcal{U} = \mathcal{X} \times \mathcal{Y}$. A \mathcal{C}^2 function F is *locally strongly convex-concave* at a point (x, y) if it is convex-concave and either $\nabla_{xx}F(x, y) \succeq mI$ or $\nabla_{yy}F(x, y) \preceq -mI$ for some $m > 0$. Finally, F is *globally strongly convex-concave* if it is convex-concave and either $x \mapsto F(x, y)$ is strongly convex for all $y \in \mathcal{Y}$ or

$y \mapsto F(x, y)$ is strongly concave for all $x \in \mathcal{X}$.

A point $(x_*, y_*) \in \mathcal{X} \times \mathcal{Y}$ is a *local min-max saddle point* of a \mathcal{C}^1 function $F : \mathcal{X} \times \mathcal{Y} \rightarrow \mathbb{R}$ if there exist open neighborhoods $\mathcal{U}_{x_*} \subset \mathcal{X}$ of x_* and $\mathcal{U}_{y_*} \subset \mathcal{Y}$ of y_* such that

$$F(x_*, y) \leq F(x_*, y_*) \leq F(x, y_*), \quad (2.4)$$

for all $y \in \mathcal{U}_{y_*}$ and $x \in \mathcal{U}_{x_*}$. The point (x_*, y_*) is a *global min-max saddle point* of F if $\mathcal{U}_{x_*} = \mathcal{X}$ and $\mathcal{U}_{y_*} = \mathcal{Y}$. Min-max saddle points are a particular case of the more general notion of saddle points. We focus here on min-max saddle points motivated by problems in constrained optimization and zero-sum games, whose solutions correspond to min-max saddle points. With a slight abuse of terminology, throughout this treatise we refer to the local min-max saddle points simply as saddle points. We denote by $\text{Saddle}(F)$ the set of saddle points of F . From (2.4), for $(x_*, y_*) \in \text{Saddle}(F)$, the point $x_* \in \mathcal{X}$ (resp. $y_* \in \mathcal{Y}$) is a local minimizer (resp. local maximizer) of the map $x \mapsto F(x, y_*)$ (resp. $y \mapsto F(x_*, y)$). The set of saddle points of a convex-concave function F is convex. Each saddle point is a critical point of F , that is, $\nabla_x F(x_*, y_*) = 0$ and $\nabla_y F(x_*, y_*) = 0$. Additionally, if F is \mathcal{C}^2 , then $\nabla_{xx} F(x_*, y_*) \preceq 0$ and $\nabla_{yy} F(x_*, y_*) \succeq 0$. Also, if $\nabla_{xx} F(x_*, y_*) \prec 0$ and $\nabla_{yy} F(x_*, y_*) \succ 0$, then the inequalities in (2.4) are strict.

2.5 Constrained optimization and exact penalty functions

We introduce some notions on constrained optimization and exact penalty functions following [BV09, Ber75]. Consider

$$\text{minimize } f(x), \quad (2.5a)$$

$$\text{subject to } g(x) \leq \mathbf{0}_m, \quad h(x) = \mathbf{0}_p, \quad (2.5b)$$

where $f : \mathbb{R}^n \rightarrow \mathbb{R}$, $g : \mathbb{R}^n \rightarrow \mathbb{R}^m$, and $h : \mathbb{R}^n \rightarrow \mathbb{R}^p$, with $p \leq n$, are continuously differentiable. The *refined Slater condition* is satisfied by (2.5) if there exists $x \in \mathbb{R}^n$ such that $h(x) = \mathbf{0}_p$, $g(x) \leq \mathbf{0}_m$, and $g_j(x) < 0$ for all nonaffine functions g_j . The optimization (2.5) is convex if f and g are convex and h is affine. For convex optimization problems, the refined Slater condition implies that strong duality holds. A point $x \in \mathbb{R}^n$ is a Karush-Kuhn-Tucker (KKT) point of (2.5) if there exist Lagrange multipliers $\lambda \in \mathbb{R}_{\geq 0}^m$, $\nu \in \mathbb{R}^p$ such that

$$\begin{aligned} g(x) &\leq \mathbf{0}_m, \quad h(x) = \mathbf{0}_p, \quad \lambda^\top g(x) = 0, \\ \nabla f(x) + \sum_{j=1}^m \lambda_j \nabla g_j(x) + \sum_{k=1}^p \nu_k \nabla h_k(x) &= \mathbf{0}_n. \end{aligned}$$

If the optimization (2.5) is convex and strong duality holds, then a point is a solution of (2.5) if and only if it is a KKT point. The problem (2.5) satisfies the *strong Slater condition* with $\rho \in \mathbb{R}_{>0}$ and $x^\rho \in \mathbb{R}^n$ if $g(x^\rho) \leq -\rho \mathbf{1}_m$ and $h(x^\rho) = \mathbf{0}_p$. Under this condition, the following result provides a bound on a Lagrange multiplier corresponding to any primal-dual optimizer.

Lemma 2.5.1. (*Bound on Lagrange multiplier [HUL93, Remark 2.3.3]*): *If (2.5) satisfies the strong Slater condition with parameter $\rho \in \mathbb{R}_{>0}$ and feasible point $x^\rho \in \mathbb{R}^n$, then any primal-dual optimizer (x, λ, ν) of (2.5) satisfies*

$$\|\lambda\|_\infty \leq \frac{f(x^\rho) - f(x)}{\rho}.$$

Next, in the presence of inequality constraints in (2.5), we are interested in using exact penalty function methods to eliminate them while keeping the equality constraints. Following [Ber75], consider the nonsmooth exact penalty function $f^\epsilon : \mathbb{R}^n \rightarrow \mathbb{R}$,

$$f^\epsilon(x) = f(x) + \frac{1}{\epsilon} \sum_{j=1}^m [g_j(x)]^+$$

with $\epsilon > 0$, and define the minimization problem

$$\text{minimize } f^\epsilon(x), \tag{2.6a}$$

$$\text{subject to } h(x) = \mathbf{0}_p. \tag{2.6b}$$

Note that, if f is convex, then f^ϵ is convex (given that $t \mapsto \frac{1}{\epsilon}[t]^+$ is convex). Therefore, if the problem (2.5) is convex, then the problem (2.6) is convex as well. The following result, see e.g. [Ber75, Proposition 1], identifies conditions under which the solutions of the optimization problems (2.5) and (2.6) coincide.

Proposition 2.5.2. (*Equivalence between (2.5) and (2.6)*): *Assume that the problem (2.5) is convex, has nonempty and compact solution set, and satisfies the refined Slater condition. Then, (2.5) and (2.6) have exactly the same solutions if $\frac{1}{\epsilon} > \|\lambda\|_\infty$, for some Lagrange multiplier $\lambda \in \mathbb{R}_{\geq 0}^m$ of the problem (2.5).*

Note that a Lagrange multiplier for (2.5) exists because the refined Slater condition holds, and hence every solution is a KKT point. The next result characterizes the solutions of a class of optimization problems. The proof is straightforward.

Lemma 2.5.3. (*Solution form for a class of constrained optimization problems*): *Consider the problem*

$$\text{minimize } \sum_{i=1}^n f_i(x_i), \tag{2.7a}$$

$$\text{subject to } \mathbf{1}_n^\top x = x_l, \tag{2.7b}$$

where $\{f_i : \mathbb{R} \rightarrow \mathbb{R}\}_{i=1}^n$ are continuous, locally Lipschitz, and convex. Let $f : \mathbb{R}^n \rightarrow \mathbb{R}^n$, $f(x) = (f_1(x_1), \dots, f_n(x_n))$. A point x^* is a solution of (2.7) if and only if there exists $\mu \in \mathbb{R}$ such that

$$\mu \mathbf{1}_n \in \partial f(x^*) \quad \text{and} \quad \mathbf{1}_n^\top x^* = x_l. \tag{2.8}$$

2.6 Dynamical systems

We gather here some useful tools that aid in the analysis of dynamical systems studied in this thesis. These tools include basic notions of discontinuous dynamical systems and differential inclusions [BC06, NZ96, Cor08] and specific results on dynamic average consensus [KCM15b] and input-to-state stability [LSW95].

2.6.1 Discontinuous dynamical systems

Let $f : \mathbb{R}^n \rightarrow \mathbb{R}^n$ be Lebesgue measurable and locally bounded and consider the differential equation

$$\dot{x} = f(x). \quad (2.9)$$

A map $\gamma : [0, T) \rightarrow \mathbb{R}^n$ is a (*Caratheodory*) *solution* of (2.9) on the interval $[0, T)$ if it is absolutely continuous on $[0, T)$ and satisfies $\dot{\gamma}(t) = f(\gamma(t))$ almost everywhere in $[0, T)$. The words *solution* and *trajectory* are used interchangeably for any system. A set $\mathcal{S} \subset \mathbb{R}^n$ is *invariant* under (2.9) if every solution starting from any point in \mathcal{S} remains in \mathcal{S} . For a solution γ of (2.9) defined on the time interval $[0, \infty)$, the *omega-limit* set $\Omega(\gamma)$ is defined by

$$\Omega(\gamma) = \{y \in \mathbb{R}^n \mid \exists \{t_k\}_{k=1}^{\infty} \subset [0, \infty) \text{ with } \lim_{k \rightarrow \infty} t_k = \infty \text{ and } \lim_{k \rightarrow \infty} \gamma(t_k) = y\}.$$

If the solution γ is bounded, then $\Omega(\gamma) \neq \emptyset$ by the Bolzano-Weierstrass theorem [Lan93, p. 33]. These notions allow us to characterize the asymptotic convergence properties of the solutions of (2.9) via invariance principles. Given a continuously differentiable function $V : \mathbb{R}^n \rightarrow \mathbb{R}$, the *Lie derivative of V along (2.9)* at $x \in \mathbb{R}^n$ is $\mathcal{L}_f V(x) = \nabla V(x)^\top f(x)$. The next result is a simplified version of [BC06, Proposition 3] which will be of use in our later chapters.

Proposition 2.6.1. (*Invariance principle for discontinuous Caratheodory systems*): *Let $\mathcal{S} \subset \mathbb{R}^n$ be compact and invariant. Assume that, for each point $x_0 \in \mathcal{S}$, there exists a unique solution of (2.9) starting at x_0 and that its omega-limit set is invariant too. Let $V : \mathbb{R}^n \rightarrow \mathbb{R}$ be a continuously differentiable map such that $\mathcal{L}_f V(x) \leq 0$ for all $x \in \mathcal{S}$. Then, any solution of (2.9) starting at \mathcal{S} converges to*

the largest invariant set in $\text{cl}(\{x \in \mathcal{S} \mid \mathcal{L}_f V(x) = 0\})$.

2.6.2 Projected dynamical systems

Projected dynamical systems are a particular class of discontinuous dynamical systems. Let $\mathcal{K} \subset \mathbb{R}^n$ be a closed convex set. Given a point $y \in \mathbb{R}^n$, the (point) projection of y onto \mathcal{K} is $\text{proj}_{\mathcal{K}}(y) = \text{argmin}_{z \in \mathcal{K}} \|z - y\|$. The set $\text{proj}_{\mathcal{K}}(y)$ is a singleton and the map $\text{proj}_{\mathcal{K}}$ is Lipschitz on \mathbb{R}^n with constant $L = 1$ [Cla83, Proposition 2.4.1]. Given $x \in \mathcal{K}$ and $v \in \mathbb{R}^n$, the (vector) projection of v at x with respect to \mathcal{K} is

$$\Pi_{\mathcal{K}}(x, v) = \lim_{\delta \rightarrow 0^+} \frac{\text{proj}_{\mathcal{K}}(x + \delta v) - x}{\delta}.$$

Given a vector field $f : \mathbb{R}^n \rightarrow \mathbb{R}^n$ and a closed convex polyhedron $\mathcal{K} \subset \mathbb{R}^n$, the associated projected dynamical system is

$$\dot{x} = \Pi_{\mathcal{K}}(x, f(x)), \quad x(0) \in \mathcal{K}. \quad (2.10)$$

Note that at any point x in the interior of \mathcal{K} , we have $\Pi_{\mathcal{K}}(x, f(x)) = f(x)$. At any boundary point of \mathcal{K} , the projection operator restricts the flow of the vector field f such that the solutions of (2.10) remain in \mathcal{K} . Therefore, in general, (2.10) is a discontinuous dynamical system. The next result summarizes conditions under which the (Caratheodory) solutions of the projected system (2.10) exist, are unique, and continuous with respect to the initial condition.

Proposition 2.6.2. *(Existence, uniqueness, and continuity with respect to the initial condition [NZ96, Theorem 2.5]): Let $f : \mathbb{R}^n \rightarrow \mathbb{R}^n$ be Lipschitz on a closed convex polyhedron $\mathcal{K} \subset \mathbb{R}^n$. Then,*

- (i) *(existence and uniqueness): for any $x_0 \in \mathcal{K}$, there exists a unique solution $t \mapsto x(t)$ of the projected system (2.10) with $x(0) = x_0$ defined over the domain $[0, \infty)$,*
- (ii) *(continuity with respect to the initial condition): given a sequence of points $\{x_k\}_{k=1}^{\infty} \subset \mathcal{K}$ with $\lim_{k \rightarrow \infty} x_k = x$, the sequence of solutions $\{t \mapsto \gamma_k(t)\}_{k=1}^{\infty}$*

of (2.10) with $\gamma_k(0) = x_k$ for all k , converge to the solution $t \mapsto \gamma(t)$ of (2.10) with $\gamma(0) = x$ uniformly on every compact set of $[0, \infty)$.

2.6.3 Differential inclusions

A differential inclusion on \mathbb{R}^n is

$$\dot{x} \in \mathcal{H}(x), \tag{2.11}$$

where $\mathcal{H} : \mathbb{R}^n \rightrightarrows \mathbb{R}^n$ is a set-valued map. A (*Caratheodory*) *solution* of (2.11) on $[0, T] \subset \mathbb{R}$ is an absolutely continuous map $x : [0, T] \rightarrow \mathbb{R}^n$ that satisfies (2.11) for almost all $t \in [0, T]$. If \mathcal{H} is locally bounded, upper semicontinuous, and takes non-empty, compact, and convex values, then existence of solutions is guaranteed. The set of equilibria of (2.11) is $\text{Eq}(\mathcal{H}) = \{x \in \mathbb{R}^n \mid 0 \in \mathcal{H}(x)\}$. A set $S \subset \mathbb{R}^n$ is *weakly (resp., strongly) positively invariant* under (2.11) if, for each $x \in S$, at least a solution (resp., all solutions) starting from x is (resp., are) entirely contained in S . For dynamics with uniqueness of solution, both notions coincide and are referred as *positively invariant*.

Given a locally Lipschitz function $f : \mathbb{R}^n \rightarrow \mathbb{R}$, the *set-valued Lie derivative* $\mathcal{L}_{\mathcal{H}}f : \mathbb{R}^n \rightrightarrows \mathbb{R}$ of f with respect to (2.11) is

$$\mathcal{L}_{\mathcal{H}}f(x) = \{a \in \mathbb{R} \mid \exists v \in \mathcal{H}(x) \text{ such that } \zeta^\top v = a \text{ for all } \zeta \in \partial f(x)\}.$$

For a trajectory $t \mapsto \varphi(t)$, $\varphi(0) \in \mathbb{R}^n$ of (2.11), the evolution of f along it satisfies

$$\frac{d}{dt}f(\varphi(t)) \in \mathcal{L}_{\mathcal{H}}f(\varphi(t))$$

for almost all $t \geq 0$. Next, we characterize the asymptotic properties of (2.11).

Theorem 2.6.3. (*LaSalle Invariance Principle for differential inclusions*): *Let $\mathcal{H} : \mathbb{R}^n \rightrightarrows \mathbb{R}^n$ be locally bounded, upper semicontinuous, with non-empty, compact, and convex values. Let $f : \mathbb{R}^n \rightarrow \mathbb{R}$ be locally Lipschitz and regular. If $S \subset \mathbb{R}^n$ is compact and strongly invariant under (2.11) and $\max \mathcal{L}_{\mathcal{H}}f(x) \leq 0$ for all $x \in S$, then the solutions of (2.11) starting at S converge to the largest weakly invariant*

set M contained in $S \cap \{x \in \mathbb{R}^n \mid 0 \in \mathcal{L}_{\mathcal{H}}f(x)\}$. Moreover, if the set M is finite, then the limit of each solution exists and is an element of M .

In Section 4.5 we develop a novel refinement of the LaSalle Invariance Principle for differential inclusions which is suitable for the analysis of the coordination algorithms presented in Chapter 4.

2.7 Dynamic average consensus

Here, we introduce notions on dynamic average consensus following [KCM15b]. Consider $n \in \mathbb{Z}_{\geq 1}$ agents communicating over a strongly connected, weight-balanced digraph \mathcal{G} whose Laplacian is denoted as L . Each agent is associated with a state $x_i \in \mathbb{R}$ and an input signal $t \mapsto u_i(t) \subset \mathbb{R}$ that is measurable and locally essentially bounded. The aim is to provide distributed dynamics such that the state of each agent $x_i(t)$ tracks the average signal $\frac{1}{n} \sum_{i=1}^n u_i(t)$ asymptotically. This can be achieved via the dynamics $X_{\text{dac}} : \mathbb{R}^{2n} \rightarrow \mathbb{R}^{2n}$,

$$\begin{aligned}\dot{x} &= -\alpha x - \beta Lx - v + \nu u, \\ \dot{v} &= \alpha \beta Lx,\end{aligned}$$

where $\alpha, \beta, \nu > 0$ are design parameters and $v \in \mathbb{R}^n$ is an auxiliary state. If the initial condition satisfies $\mathbf{1}_n^\top v(0) = 0$ and the time-derivatives of the input signals are bounded, then one can show, cf. [KCM15b, Corollary 4.1], that the error signal $t \mapsto |x_i(t) - \frac{1}{n} \sum_{i=1}^n u_i(t)|$ is ultimately bounded for each $i \in [n]$. Moreover, this error vanishes if the input signal converges to a constant value.

2.8 Input-to-state stability

Here, we review the notion of input-to-state stability (ISS) following [LSW95]. A function $\alpha : \mathbb{R}_{\geq 0} \rightarrow \mathbb{R}_{\geq 0}$ is class \mathcal{K} if it is continuous, strictly increasing, and $\alpha(0) = 0$. The set of unbounded class \mathcal{K} functions are called \mathcal{K}_∞ functions. A function $\beta : \mathbb{R}_{\geq 0} \times \mathbb{R}_{\geq 0} \rightarrow \mathbb{R}_{\geq 0}$ is class \mathcal{KL} if for any $t \in \mathbb{R}_{\geq 0}$,

$x \mapsto \beta(x, t)$ is class \mathcal{K} and for any $x \in \mathbb{R}_{\geq 0}$, $t \mapsto \beta(x, t)$ is continuous, decreasing with $\beta(x, t) \rightarrow 0$ as $t \rightarrow \infty$. Consider a system

$$\dot{x} = f(x, u), \quad (2.13)$$

where $x \in \mathbb{R}^n$ is the state, $u : \mathbb{R}_{\geq 0} \rightarrow \mathbb{R}^m$ is the input that is measurable and locally essentially bounded, and $f : \mathbb{R}^n \times \mathbb{R}^m \rightarrow \mathbb{R}^n$ is locally Lipschitz. Assume that starting from any point in \mathbb{R}^n , the trajectory of (2.13) is defined on $\mathbb{R}_{\geq 0}$ for any given control. Let $\text{Eq}(f) \subset \mathbb{R}^n$ be the set of equilibria of the unforced system. Then, the system (2.13) is *input-to-state stable* (ISS) with respect to $\text{Eq}(f)$ if there exists $\beta \in \mathcal{KL}$ and $\gamma \in \mathcal{K}$ such that each trajectory $t \mapsto x(t)$ of (2.13) satisfies

$$\|x(t)\|_{\text{Eq}(f)} \leq \beta(\|x(0)\|_{\text{Eq}(f)}, t) + \gamma(\|u\|_{\infty})$$

for all $t \geq 0$, where $\|u\|_{\infty} = \text{ess sup}_{t \geq 0} \|u(t)\|$ is the essential supremum (see [Lan93, p. 185] for the definition) of u . This notion captures the graceful degradation of the asymptotic convergence properties of the unforced system as the size of the disturbance input grows. One convenient way of showing ISS is by finding an ISS-Lyapunov function. An *ISS-Lyapunov function* with respect to the set $\text{Eq}(f)$ for system (2.13) is a differentiable function $V : \mathbb{R}^n \rightarrow \mathbb{R}_{\geq 0}$ such that

- (i) there exist $\alpha_1, \alpha_2 \in \mathcal{K}_{\infty}$ such that for all $x \in \mathbb{R}^n$,

$$\alpha_1(\|x\|_{\text{Eq}(f)}) \leq V(x) \leq \alpha_2(\|x\|_{\text{Eq}(f)}); \quad (2.14)$$

- (ii) there exists a continuous, positive definite function $\alpha_3 : \mathbb{R}_{\geq 0} \rightarrow \mathbb{R}_{\geq 0}$ and $\gamma \in \mathcal{K}_{\infty}$ such that

$$\nabla V(x)^{\top} f(x, v) \leq -\alpha_3(\|x\|_{\text{Eq}(f)}) \quad (2.15)$$

for all $x \in \mathbb{R}^n$, $v \in \mathbb{R}^m$ for which $\|x\|_{\text{Eq}(f)} \geq \gamma(\|v\|)$.

Proposition 2.8.1. (*ISS-Lyapunov function implies ISS*): *If (2.13) admits an ISS-Lyapunov function, then it is ISS.*

Chapter 3

Anytime distributed dynamics for ED problem

In this chapter, we introduce the economic dispatch (ED) problem where a group of generators with generation costs described by smooth, convex functions seek to determine generation levels that respect individual constraints, meet a specified load, and minimize the total generation cost. Our aim will be to design distributed algorithms that asymptotically converge to the solutions of the ED problem, are *anytime*, i.e., generate executions that are feasible at any time and have monotonically decreasing cost, and handle unit addition and deletion.

3.1 Problem statement

Consider a network of $n \in \mathbb{Z}_{\geq 1}$ power generator units whose communication topology is represented by a strongly connected and weight-balanced digraph $\mathcal{G} = (\mathcal{V}, \mathcal{E}, \mathbf{A})$. Each generator corresponds to a vertex and an edge (i, j) represents the capability of unit j to transmit information to unit i . The power generated by unit i is $P_i \in \mathbb{R}$. Each generator $i \in [n]$ has a cost function $f_i : \mathbb{R} \rightarrow \mathbb{R}_{\geq 0}$, assumed to be convex and continuously differentiable. The total cost incurred by the network

with the power allocation $P = (P_1, \dots, P_n) \in \mathbb{R}^n$ is given by $f : \mathbb{R}^n \rightarrow \mathbb{R}_{\geq 0}$ as

$$f(P) = \sum_{i=1}^n f_i(P_i).$$

The function f is also convex and continuously differentiable. The generators must meet a total power load $P_l \in \mathbb{R}_{>0}$, i.e., $\sum_{i=1}^n P_i = P_l$, while at the same time minimizing the total cost $f(P)$. We assume that at least one generator knows the total load. Each generator has upper and lower limits on the power it can produce, $P_i^m \leq P_i \leq P_i^M$ for $i \in [n]$. We neglect any transmission losses and any constraints on the amount of power flow along transmission lines. Formally, the economic dispatch (ED) problem is

$$\text{minimize } f(P), \tag{3.1a}$$

$$\text{subject to } \mathbf{1}_n^\top P = P_l, \tag{3.1b}$$

$$P^m \leq P \leq P^M. \tag{3.1c}$$

We refer to (3.1b) as the *load condition* and to (3.1c) as the *box constraints*. We let $\mathcal{F}_{\text{ED}} = \{P \in \mathbb{R}^n \mid P^m \leq P \leq P^M \text{ and } \mathbf{1}_n^\top P = P_l\}$ denote the feasibility set of (3.1). Since \mathcal{F}_{ED} is compact, the set of solutions of (3.1) is compact. Moreover, since the constraints (3.1b) and (3.1c) are affine, feasibility of the ED problem implies that the refined Slater condition is satisfied and strong duality holds. Note that $P^M \in \mathcal{F}_{\text{ED}}$ implies \mathcal{F}_{ED} is a singleton set, i.e., $\mathcal{F}_{\text{ED}} = \{P^M\}$. Similarly $P^m \in \mathcal{F}_{\text{ED}}$ implies $\mathcal{F}_{\text{ED}} = \{P^m\}$. Without loss of generality, we assume that P^M and P^m are not feasible points.

A simpler version of this problem is the relaxed economic dispatch (rED) problem, where the total cost is optimized with the load condition but without the box constraints. Formally,

$$\text{minimize } f(P), \tag{3.2a}$$

$$\text{subject to } \mathbf{1}_n^\top P = P_l. \tag{3.2b}$$

We let $\mathcal{F}_{\text{rED}} = \{P \in \mathbb{R}^n \mid \mathbf{1}_n^\top P = P_l\}$ denote the feasibility set of (3.2). Our objective is to design distributed procedures that allow the network to solve the ED problem. In Section 3.2 we present an algorithmic solution to the rED problem and then build on it in Section 3.3 to solve the ED problem.

Remark 3.1.1. (*Power system implications*): In the power system literature, the cost function of a generator is usually quadratic and convex, and generator capacities have minimum and maximum bounds, see e.g. [Gai03]. In our algorithm design, we assume that (1) generators exchange information about the cost function or its gradient with their neighbors, and (2) one or more generators know the value of the total load. Both assumptions are reasonable in numerous scenarios. Regarding (1), generators can be categorized in families where each family’s cost function is defined by a finite number of parameters. Hence, neighboring units only need to communicate their category and parameters. Regarding (2), we have in mind hierarchical dispatch scenarios where a higher-level planner assigns loads to each microgrid, consisting of a group of generators, and communicates it to a unit in each group, see [LP04]. At the lower level, each microgrid executes our algorithms to arrive at an optimum dispatch allocation. •

3.2 Distributed algorithmic solution to the relaxed economic dispatch problem

Here we introduce a distributed algorithm to solve the rED problem (3.2). Consider the Laplacian-gradient dynamics

$$\dot{P} = -\mathbf{L}\nabla f(P), \tag{3.3}$$

where \mathbf{L} is the Laplacian of \mathcal{G} . This dynamics is distributed in the sense that each generator only requires information from its out-neighbors. Specifically, if each generator knows the cost function of its neighbors, then they interchange messages that contain their respective power levels. Else, if such knowledge is not available, (3.3) can be executed by neighboring generators exchanging their

respective gradient information.

Theorem 3.2.1. (*Convergence of the Laplacian-gradient dynamics*): Consider the rED problem (3.2) with $f : \mathbb{R}^n \rightarrow \mathbb{R}_{\geq 0}$ radially unbounded. Then, the feasible set \mathcal{F}_{rED} is positively invariant under the dynamics (3.3) and all trajectories starting from \mathcal{F}_{rED} converge to the set of solutions of (3.2).

Proof. We use the shorthand notation $X_{\text{L-g}} : \mathbb{R}^n \rightarrow \mathbb{R}^n$ to refer to (3.3). We first establish that the total power generated by the network is conserved,

$$\mathcal{L}_{X_{\text{L-g}}}(\mathbf{1}_n^\top P) = \mathbf{1}_n^\top X_{\text{L-g}}(P) = -(\mathbf{1}_n^\top \mathbf{L}) \nabla f(P) = 0, \quad (3.4)$$

where we have used that \mathcal{G} is weight-balanced in the last equality. As a consequence, \mathcal{F}_{rED} is positively invariant under (3.3). Next, we show that f is monotonically nonincreasing,

$$\mathcal{L}_{X_{\text{L-g}}}f(P) = -\nabla f(P)^\top \mathbf{L}_s \nabla f(P) \leq 0, \quad (3.5)$$

where we have used that \mathcal{G} is weight-balanced in the inequality. Given $P_0 \in \mathbb{R}^n$, let

$$f^{-1}(\leq f(P_0)) = \{P \in \mathbb{R}^n \mid f(P) \leq f(P_0)\}.$$

Note that this sublevel set is closed, and since f is radially unbounded, bounded. Then, the set $\mathcal{W}_{P_0} = f^{-1}(\leq f(P_0)) \cap \mathcal{F}_{\text{rED}}$ is closed, bounded, and from (3.4) and (3.5), positively invariant. The application of the LaSalle Invariance Principle, cf. Theorem 2.6.3, implies that the trajectories starting in \mathcal{W}_{P_0} converge to the largest invariant set M contained in $\{P \in \mathcal{W}_{P_0} \mid \mathcal{L}_{X_{\text{L-g}}}f(P) = 0\}$. From (3.5) and the fact that \mathcal{G} is weight-balanced and strongly connected, we deduce that $\mathcal{L}_{X_{\text{L-g}}}f(P) = 0$ implies $\nabla f(P) \in \text{span}\{\mathbf{1}_n\}$, and hence $P \in \text{Eq}(X_{\text{L-g}})$. Since $\mathbf{1}_n^\top P_0 = P_l$ by hypothesis, we conclude that $M = \text{Eq}(X_{\text{L-g}}) \cap \mathcal{F}_{\text{rED}}$, which precisely corresponds to the set of solutions of (3.2), cf. Lemma 2.5.3. \square

Remark 3.2.2. (*Initialization of (3.3)*): To solve the rED problem, the Laplacian-gradient dynamics (3.3) requires an initial condition satisfying the load constraints. Such initialization can be performed in various ways. If each unit knows P_l and n ,

then the network can start from $(P_l/n)\mathbf{1}_n$. If only one unit knows P_l , it can start from P_l while the others start from 0. \bullet

The proof of Theorem 3.2.1 reveals that the load condition is satisfied at all times and the total cost is monotonically decreasing until convergence. Both facts imply that (3.3) is *anytime*, i.e., its trajectories are feasible solutions at any time before convergence, and they become better as time elapses.

Proposition 3.2.3. (*Convergence rate of the Laplacian-gradient dynamics*): Under the hypotheses of Theorem 3.2.1, further assume that there exist $k, K \in \mathbb{R}_{>0}$ such that $kI_n \preceq \nabla^2 f(P) \preceq KI_n$ for $P \in \mathbb{R}^n$. Then, the dynamics (3.3) converges to the unique solution of (3.2) exponentially fast with rate greater than or equal to $k\lambda_2(\mathbf{L}_s)$.

Proof. Uniqueness of the solution to (3.2) follows from noting that strong convexity implies strict convexity. Let $P^{\text{opt}} \in \mathbb{R}^n$ denote the unique optimizer and let $V : \mathcal{F}_{\text{RED}} \subset \mathbb{R}^n \rightarrow \mathbb{R}$, $V(P) = f(P) - f(P^{\text{opt}})$. Note that $V(P) \geq 0$, and $V(P) = 0$ if and only if $P = P^{\text{opt}}$. From (3.5),

$$\mathcal{L}_{X_{\mathbf{L}-g}} V(P) \leq -\lambda_2(\mathbf{L}_s) \left\| \nabla f(P) - \frac{1}{n} (\mathbf{1}_n^\top \nabla f(P)) \mathbf{1}_n \right\|^2,$$

where we have used (2.1). For convenience, let $e(P) = \nabla f(P) - \frac{1}{n} (\mathbf{1}_n^\top \nabla f(P)) \mathbf{1}_n$. Using the fact that f is strongly convex, for $P, P' \in \mathcal{F}_{\text{RED}}$, we have

$$f(P') \geq f(P) + e(P)^\top (P' - P) + \frac{k}{2} \|P' - P\|^2. \quad (3.6)$$

For fixed P , the minimum of the right-hand side is $f(P) - \frac{1}{2k} \|e(P)\|^2$, and hence $f(P') \geq f(P) - \frac{1}{2k} \|e(P)\|^2$. In particular, for $P' = P^{\text{opt}}$, this yields $V(P) \leq \frac{1}{2k} \|e(P)\|^2$. Combining this with the bound on $\mathcal{L}_{X_{\mathbf{L}-g}} V$ above, we get

$$\mathcal{L}_{X_{\mathbf{L}-g}} V(P) \leq -2k\lambda_2(\mathbf{L}_s)V(P),$$

which implies that, along any trajectory $t \mapsto P(t)$ of (3.3), one has $V(P(t)) \leq V(P(0))e^{-2k\lambda_2(\mathbf{L}_s)t}$. Our next objective is to relate the magnitude of V at P with

$\|P - P^{\text{opt}}\|$. From $\nabla^2 f(P) \preceq KI_n$, one has $f(P') \leq f(P) + \nabla f(P)^\top (P' - P) + \frac{K}{2}\|P' - P\|_2^2$. Minimizing both sides over $P' \in \mathcal{F}_{\text{TED}}$,

$$V(P) \geq \frac{1}{2K}\|e(P)\|^2. \quad (3.7)$$

Having established the relation between $V(P)$ and $\|e(P)\|$, our final step consists of establishing the relation between the magnitudes of $e(P)$ and $P - P^{\text{opt}}$. Using (3.6) for $P' = P^{\text{opt}}$, one has

$$\begin{aligned} f(P^{\text{opt}}) &\geq f(P) + e(P)^\top (P^{\text{opt}} - P) + \frac{k}{2}\|P^{\text{opt}} - P\|^2 \\ &\geq f(P) - \|e(P)\|\|P^{\text{opt}} - P\| + \frac{k}{2}\|P^{\text{opt}} - P\|^2. \end{aligned}$$

Since $f(P^{\text{opt}}) \leq f(P)$ for any $P \in \mathcal{F}_{\text{TED}}$, we get $\|P - P^{\text{opt}}\|_2 \leq \frac{2}{k}\|e(P)\|_2$. Combining this with (3.7), we get

$$\|P - P^{\text{opt}}\|_2^2 \leq \frac{8}{k^2}KV(P). \quad (3.8)$$

To obtain an upper bound, we use the fact that f is convex, and hence $f(P^{\text{opt}}) \geq f(P) + \nabla f(P)^\top (P^{\text{opt}} - P)$. Rearranging,

$$V(P) \leq \nabla f(P)^\top (P - P^{\text{opt}}) = e(P)^\top (P - P^{\text{opt}})$$

implying $V(P)^2 \leq \|e(P)\|^2\|P - P^{\text{opt}}\|^2$. Using (3.7), we get

$$V(P) \leq 2K\|P - P^{\text{opt}}\|^2. \quad (3.9)$$

Finally, along any trajectory $t \mapsto P(t)$, using (3.8) and (3.9) with $P = P(0)$, we obtain $\|P(t) - P^{\text{opt}}\|^2 \leq \frac{16K^2}{k^2}\|P(0) - P^{\text{opt}}\|^2 e^{-2k\lambda_2(L_s)t}$, as claimed. \square

Proposition 3.2.3 opens up the possibility of selecting the edge weights of the communication digraph \mathcal{G} to maximize the rate of convergence of the Laplacian-gradient dynamics (3.3).

Remark 3.2.4. (*Comparison with the center-free algorithm*): The work [XB06]

proposes the center-free algorithm to solve the rED problem (termed there optimal resource allocation problem). This algorithm essentially corresponds to a discrete-time implementation of the Laplacian-gradient dynamics (3.3). The convergence analysis of the center-free algorithm relies on two assumptions. First, $\nabla^2 f$ needs to be globally upper and lower bounded (in particular, this implies that f is strongly convex). Second, the Laplacian must satisfy a linear matrix inequality that constrains the choice of weights. In contrast, no such conditions are required here to establish the convergence of (3.3). In addition, the guaranteed rate of convergence of the center-free algorithm vanishes once the upper bound on $\nabla^2 f$ reaches a certain finite value for a fixed weight assignment unlike the one obtained in Proposition 3.2.3 for (3.3). •

We next characterize the convergence of (3.3) when the topology is switching under a weaker form of connectivity.

Proposition 3.2.5. *(Convergence of the Laplacian-gradient dynamics under switching topology): Let Ξ_n be the set of weight-balanced digraphs over n vertices. Denote the communication digraph of the group of units at time t by $\mathcal{G}(t)$. Let $t \mapsto \mathcal{G}(t) \in \Xi_n$ be piecewise constant and assume there exists an infinite sequence of contiguous, nonempty, uniformly bounded time intervals over which the union of communication graphs is strongly connected. Then, the dynamics*

$$\dot{P} = -\mathbf{L}(\mathcal{G}(t))\nabla f(P), \quad (3.10)$$

starting from an initial power allocation P_0 satisfying $\mathbf{1}_n^\top P_0 = P_l$ converges to the set of solutions of (3.2).

The proof is similar to that of Theorem 3.2.1 using that (i) the load condition is preserved along (3.10), (ii) f is a common Lyapunov function, and (iii) infinite switching implies convergence to the invariant set characterized by $\nabla f \in \text{span}\{\mathbf{1}_n\}$, the set of solutions of the rED problem.

3.3 Distributed algorithmic solution to the economic dispatch problem

Here we propose a distributed algorithm to solve the ED problem. We first develop an alternative formulation of this problem without inequality constraints using an exact penalty function approach. This allows us to synthesize our distributed dynamics mimicking the algorithm design of Section 3.2.

3.3.1 Exact penalty function formulation

We first show that, unlike the rED problem, there might be no network-wide agreement on the gradients of the local objective functions at the solutions of the ED problem.

Lemma 3.3.1. (Solution form for the ED problem): *For any solution P^{opt} of the ED problem (3.1), there exist $\nu \in \mathbb{R}$, $\lambda^m, \lambda^M \in \mathbb{R}_{\geq 0}^n$ with $\|\lambda^m\|_\infty, \|\lambda^M\|_\infty, 2|\nu| \leq 2 \max_{P \in \mathcal{F}_{\text{ED}}} \|\nabla f(P)\|_\infty$ such that*

$$\nabla f_i(P_i^{\text{opt}}) = \begin{cases} -\nu + \lambda_i^m & \text{if } P_i^{\text{opt}} = P_i^m, \\ -\nu & \text{if } P_i^m < P_i^{\text{opt}} < P_i^M, \\ -\nu - \lambda_i^M & \text{if } P_i^{\text{opt}} = P_i^M. \end{cases}$$

Proof. The Lagrangian for the ED problem (3.1) is $L(P, \lambda^m, \lambda^M, \nu) = f(P) + (\lambda^m)^\top (P^m - P) + (\lambda^M)^\top (P - P^M) + \nu(\mathbf{1}_n^\top P - P_l)$. A point P^{opt} is a solution of (3.1) iff there exist $\nu \in \mathbb{R}$, $\lambda^m, \lambda^M \in \mathbb{R}_{\geq 0}^n$ satisfying the KKT conditions

$$P^m - P^{\text{opt}} \leq \mathbf{0}_n, \quad (\lambda^m)^\top (P^m - P^{\text{opt}}) = 0, \quad (3.11a)$$

$$P^{\text{opt}} - P^M \leq \mathbf{0}_n, \quad (\lambda^M)^\top (P^{\text{opt}} - P^M) = 0, \quad (3.11b)$$

$$\mathbf{1}_n^\top P^{\text{opt}} = P_l, \quad \nabla f(P^{\text{opt}}) - \lambda^m + \lambda^M = -\nu \mathbf{1}_n. \quad (3.11c)$$

Now, consider the partition of $[n]$ associated to P^{opt} ,

$$I_0(P^{\text{opt}}) = \{i \in [n] \mid P_i^m < P_i^{\text{opt}} < P_i^M\},$$

$$I_+(P^{\text{opt}}) = \{i \in [n] \mid P_i^{\text{opt}} = P_i^M\},$$

$$I_-(P^{\text{opt}}) = \{i \in [n] \mid P_i^{\text{opt}} = P_i^m\}.$$

If $i \in I_0(P^{\text{opt}})$, then (3.11a)-(3.11b) imply $\lambda_i^m = \lambda_i^M = 0$, and hence $\nabla f_i(P_i^{\text{opt}}) = -\nu$ by (3.11c). If $i \in I_+(P^{\text{opt}})$, then (3.11a)-(3.11b) imply $\lambda_i^m = 0$, $\lambda_i^M > 0$, and hence $\nabla f_i(P_i^{\text{opt}}) = -\nu - \lambda_i^M$ by (3.11c). Finally, if $i \in I_-(P^{\text{opt}})$, then (3.11a)-(3.11b) imply $\lambda_i^m > 0$, $\lambda_i^M = 0$, and hence $\nabla f_i(P_i^{\text{opt}}) = -\nu + \lambda_i^m$ by (3.11c). To establish the bounds on the multipliers, we distinguish between whether (a) $I_0(P^{\text{opt}})$ is non-empty or (b) $I_0(P^{\text{opt}})$ is empty. In case (a), from (3.11), $\nu = -\nabla f_i(P_i^{\text{opt}})$ for all $i \in I_0(P^{\text{opt}})$, and therefore $|\nu| \leq \|\nabla f(P^{\text{opt}})\|_\infty$. In case (b), from (3.11), we get $\nu \leq -\nabla f_j(P_j^{\text{opt}})$ for all $j \in I_+(P^{\text{opt}})$. Similarly, we obtain $\nu \geq -\nabla f_k(P_k^{\text{opt}})$ for all $k \in I_-(P^{\text{opt}})$. Therefore, $-\nabla f_k(P_k^{\text{opt}}) \leq \nu \leq -\nabla f_j(P_j^{\text{opt}})$ for all $j \in I_+(P^{\text{opt}})$ and $k \in I_-(P^{\text{opt}})$. Since $I_0(P^{\text{opt}})$ is empty and by assumption $P^m, P^M \notin \mathcal{F}_{\text{ED}}$, both $I_-(P^{\text{opt}})$ and $I_+(P^{\text{opt}})$ are non-empty. Therefore, we obtain $|\nu| \leq \|\nabla f(P^{\text{opt}})\|_\infty$. This inequality, together with (3.11c) and the fact that either λ_i^m or λ_i^M is zero for each $i \in [n]$, implies $\|\lambda^m\|_\infty, \|\lambda^M\|_\infty \leq 2\|\nabla f(P^{\text{opt}})\|_\infty \leq 2 \max_{P \in \mathcal{F}_{\text{ED}}} \|\nabla f(P)\|_\infty$. \square

Our next step is to provide an alternative formulation of the ED problem that is similar in structure to that of the rED problem. We do this by using an exact penalty function method to remove the box constraints. Specifically, let

$$f^\epsilon(P) = \sum_{i=1}^n f_i(P_i) + \frac{1}{\epsilon} \left(\sum_{i=1}^n ([P_i - P_i^M]^+ + [P_i^m - P_i]^+) \right).$$

Note that this corresponds to a scenario where generator $i \in [n]$ has local cost given by

$$f_i^\epsilon(P_i) = f_i(P_i) + \frac{1}{\epsilon} \left([P_i - P_i^M]^+ + [P_i^m - P_i]^+ \right). \quad (3.12)$$

This function is convex, locally Lipschitz, and continuously differentiable in \mathbb{R}

except at $P_i = P_i^m$ and $P_i = P_i^M$. Its generalized gradient $\partial f_i^\epsilon : \mathbb{R} \rightrightarrows \mathbb{R}$ is given by

$$\partial f_i^\epsilon(P_i) = \begin{cases} \{\nabla f_i(P_i) - \frac{1}{\epsilon}\} & \text{if } P_i < P_i^m, \\ [\nabla f_i(P_i) - \frac{1}{\epsilon}, \nabla f_i(P_i)] & \text{if } P_i = P_i^m, \\ \{\nabla f_i(P_i)\} & \text{if } P_i^m < P_i < P_i^M, \\ [\nabla f_i(P_i), \nabla f_i(P_i) + \frac{1}{\epsilon}] & \text{if } P_i = P_i^M, \\ \{\nabla f_i(P_i) + \frac{1}{\epsilon}\} & \text{if } P_i > P_i^M. \end{cases}$$

As a result, the total cost f^ϵ is convex, locally Lipschitz, and regular. Its generalized gradient at $P \in \mathbb{R}^n$ is $\partial f^\epsilon(P) = \partial f_1^\epsilon(P_1) \times \cdots \times \partial f_n^\epsilon(P_n)$. Consider the optimization

$$\text{minimize } f^\epsilon(P), \tag{3.13a}$$

$$\text{subject to } \mathbf{1}_n^\top P = P_l. \tag{3.13b}$$

We next establish the equivalence of (3.13) with the ED problem.

Proposition 3.3.2. *(Equivalence between (3.1) and (3.13)): The solutions of (3.1) and (3.13) coincide for $\epsilon \in \mathbb{R}_{>0}$ such that*

$$\epsilon < \frac{1}{2 \max_{P \in \mathcal{F}_{\text{ED}}} \|\nabla f(P)\|_\infty}. \tag{3.14}$$

Proof. Observe the parallelism between (3.1) and (2.5) on one side and (3.13) and (2.6) on the other. Recall that, for the ED problem (3.1), the set of solutions is nonempty and compact, and the refined Slater condition is satisfied. Thus, from Proposition 2.5.2, the solutions of (3.13) and (3.1) coincide if $\frac{1}{\epsilon} > \|\lambda^m\|_\infty, \|\lambda^M\|_\infty$ for some Lagrange multipliers λ^m and λ^M . From Lemma 3.3.1, there exists λ^m and λ^M satisfying $\|\lambda^m\|_\infty, \|\lambda^M\|_\infty \leq 2 \max_{P \in \mathcal{F}_{\text{ED}}} \|\nabla f(P)\|_\infty$. Thus, if $\epsilon < \frac{1}{2 \max_{P \in \mathcal{F}_{\text{ED}}} \|\nabla f(P)\|_\infty}$, then $\frac{1}{\epsilon} > 2 \max_{P \in \mathcal{F}_{\text{ED}}} \|\nabla f(P)\|_\infty \geq \|\lambda^m\|_\infty, \|\lambda^M\|_\infty$ and the claim follows. \square

3.3.2 Laplacian-nonsmooth-gradient dynamics

Here, we propose a distributed algorithm to solve the ED problem. Our design builds on the alternative formulation (3.13). Consider the Laplacian-nonsmooth-gradient dynamics

$$\dot{P} \in -\mathbf{L}\partial f^\epsilon(P). \quad (3.15)$$

The set-valued map $-\mathbf{L}\partial f^\epsilon$ is non-empty, takes compact, convex values, and is locally bounded and upper semicontinuous. Therefore, existence of solutions is guaranteed (cf. Section 2.6.3). Moreover, this dynamics is distributed in the sense that, to implement it, each generator only requires information from its out-neighbors. When convenient, we denote the dynamics (3.15) by $X_{\text{L-n-g}} : \mathbb{R}^n \rightrightarrows \mathbb{R}^n$. The next result establishes the strongly positive invariance of \mathcal{F}_{ED} .

Lemma 3.3.3. (*Invariance of the feasibility set*): *The feasibility set \mathcal{F}_{ED} is strongly positively invariant under the Laplacian-nonsmooth-gradient dynamics (3.15) provided that $\epsilon \in \mathbb{R}_{>0}$ satisfies (with $d_{\max}^{\text{out}} = \max_{i \in \mathcal{V}} d^{\text{out}}(i)$)*

$$\epsilon < \frac{\min_{(i,j) \in \mathcal{E}} a_{ij}}{2d_{\max}^{\text{out}} \max_{P \in \mathcal{F}_{\text{ED}}} \|\nabla f(P)\|_\infty}. \quad (3.16)$$

Proof. We begin by noting that, if ϵ satisfies (3.16), then there exists $\alpha > 0$ such that

$$\epsilon < \frac{\min_{(i,j) \in \mathcal{E}} a_{ij}}{2d_{\max}^{\text{out}} \max_{P \in \mathcal{F}_{\text{ED}}^\alpha} \|\nabla f(P)\|_\infty}, \quad (3.17)$$

where $\mathcal{F}_{\text{ED}}^\alpha = \{P \in \mathbb{R}^n \mid \mathbf{1}_n^\top P = P_l \text{ and } P^m - \alpha \mathbf{1}_n \leq P \leq P^M + \alpha \mathbf{1}_n\}$. Now, we reason by contradiction. Assume that \mathcal{F}_{ED} is not strongly positively invariant under the Laplacian-nonsmooth-gradient dynamics $X_{\text{L-n-g}}$. This implies that there exists a boundary point $\bar{P} \in \text{bd}(\mathcal{F}_{\text{ED}})$, a real number $\delta > 0$, and a trajectory $t \mapsto P(t)$ obeying (3.15) such that $P(0) = \bar{P}$ and $P(t) \notin \mathcal{F}_{\text{ED}}$ for all $t \in (0, \delta)$. Without loss of generality, assume that $P(t) \in \mathcal{F}_{\text{ED}}^\alpha$ for all $t \in (0, \delta)$. Now, using the same reasoning as in the proof of Theorem 3.2.1, it is not difficult to see that the load condition is preserved along $X_{\text{L-n-g}}$. Therefore, trajectories can only leave \mathcal{F}_{ED} by violating the box constraints. Thus, without loss of generality, there must

exist a unit i such that $P_i(0) = P_i^M$ and $P_i(t) > P_i^M$ for all $t \in (0, \delta)$. This means that there must exist $t \rightarrow \zeta(t) \in -\mathbf{L}\partial f^\epsilon(P(t))$ and $\delta_1 \in (0, \delta)$ such that $\zeta_i(t) \geq 0$ a.e. in $(0, \delta_1)$. Next we show that this can only happen if $P_j(t) \geq P_j^M$ for all $j \in \mathcal{N}_i^+$. Since $P_i(t) > P_i^M$ for $t \in (0, \delta_1)$, then $\partial f_i(P_i(t)) = \{\nabla f_i(P_i(t)) + \frac{1}{\epsilon}\}$. Therefore,

$$\zeta_i(t) = - \sum_{j \in \mathcal{N}_i^+} a_{ij} \left(\nabla f_i(P_i(t)) + \frac{1}{\epsilon} - \eta_j(t) \right),$$

where $\eta_j(t) \in \partial f_j(P_j(t))$. Note that if $P_j(t) \geq P_j^M$, then $\eta_j(t) \leq \nabla f_j(P_j(t)) + \frac{1}{\epsilon}$, whereas if $P_j(t) < P_j^M$, then $\eta_j(t) \leq \nabla f_j(P_j(t))$. For convenience, denote this latter set of units by $\overline{\mathcal{N}_i^+}$. Now, we can upper bound $\zeta_i(t)$ by

$$\begin{aligned} \zeta_i(t) &\leq - \sum_{j \in \mathcal{N}_i^+} a_{ij} \left(\nabla f_i(P_i(t)) - \nabla f_j(P_j(t)) \right) - \frac{1}{\epsilon} \sum_{j \in \overline{\mathcal{N}_i^+}} a_{ij} \\ &\leq 2 \max_{P \in \mathcal{F}_{\text{ED}}^\alpha} \|\nabla f(P)\|_\infty d_{\text{max}}^{\text{out}} - \frac{1}{\epsilon} \sum_{j \in \overline{\mathcal{N}_i^+}} a_{ij} < 0, \end{aligned}$$

where the last inequality follows from (3.17). Hence, $\zeta_i(t) \geq 0$ only if $P_j(t) \geq P_j^M$ for all $j \in \mathcal{N}_i^+$ and so the latter is true on $(0, \delta_1)$ by continuity of the trajectories. Extending the argument to the neighbors of each $j \in \mathcal{N}_i^+$, we obtain an interval $(0, \delta_2) \subset (0, \delta_1)$ over which all one- and two-hop neighbors of i have generation levels greater than or equal to their respective maximum limits. Recursively, and since the graph is strongly connected and the number of units finite, we get an interval $(0, \bar{\delta})$ over which $P(t) \geq P^M$, which implies $P(0) = P^M$, contradicting the fact that $P^M \notin \mathcal{F}_{\text{ED}}$. \square

We next build on this result to show that the dynamics (3.15) asymptotically converges to the set of solutions of (3.1).

Theorem 3.3.4. *(Convergence of the Laplacian-nonsmooth-gradient dynamics): For ϵ satisfying (3.16), all trajectories of the dynamics (3.15) starting from \mathcal{F}_{ED} converge to the set of solutions of the ED problem (3.1).*

Proof. Our proof strategy relies on the LaSalle Invariance principle for differential

inclusions (cf. Theorem 2.6.3). Recall that the function f^ϵ is locally Lipschitz and regular. Furthermore, the set-valued map $P \mapsto X_{L-n-g}(P) = -L\partial f^\epsilon(P)$ is locally bounded, upper semicontinuous, and takes non-empty, compact, and convex values. The set-valued Lie derivative $\mathcal{L}_{X_{L-n-g}}f^\epsilon : \mathbb{R}^n \rightrightarrows \mathbb{R}$ of f^ϵ along (3.15) is

$$\mathcal{L}_{X_{L-n-g}}f^\epsilon(P) = \{-\zeta^\top L\zeta \mid \zeta \in \partial f^\epsilon(P)\}. \quad (3.18)$$

Since \mathcal{G} is weight-balanced $-\zeta^\top L\zeta = -\zeta^\top L_s\zeta \leq 0$, which implies $\max \mathcal{L}_{X_{L-n-g}}f^\epsilon(P) \leq 0$ for all $P \in \mathbb{R}^n$. From Lemma 3.3.3, the compact set \mathcal{F}_{ED} is strongly positively invariant under X_{L-n-g} . Therefore, the application of Theorem 2.6.3 yields that all evolutions of (3.15) starting in \mathcal{F}_{ED} converge to the largest weakly invariant set M contained in $\mathcal{F}_{ED} \cap \{P \in \mathbb{R}^n \mid 0 \in \mathcal{L}_{X_{L-n-g}}f^\epsilon(P)\}$. From (3.18) and the fact that \mathcal{G} is weight-balanced, we deduce that $0 \in \mathcal{L}_{X_{L-n-g}}f^\epsilon(P)$ if and only if there exists $\mu \in \mathbb{R}$ such that $\mu \mathbf{1}_n \in \partial f^\epsilon(P)$. Using Lemma 2.5.3, this is equivalent to $P \in \mathcal{F}_{ED}$ being a solution of (3.13). This implies that M corresponds to the set of solutions of (3.13). Finally, since (3.16) implies (3.14), Proposition 3.3.2 guarantees that the solutions of (3.1) and (3.13) coincide. \square

Since, \mathcal{F}_{ED} is strongly positively invariant under X_{L-n-g} , f^ϵ is nonincreasing along X_{L-n-g} (cf. proof of Theorem 3.3.4), and f^ϵ and f coincide on \mathcal{F}_{ED} , the Laplacian-nonsmooth-gradient dynamics is an anytime algorithm for the ED problem (3.1). Because these properties do not depend on the specific graph, the convergence properties of (3.15) are the same if the communication topology is time-varying as long as it remains weight-balanced and strongly connected. Note that, following the discussion of Remark 3.1.1, the Laplacian-nonsmooth-gradient dynamics can be employed in a hierarchical way for scenarios where a set of buses form the communication network and each bus is connected to a group of generators and/or loads. At the top level, a copy of the dynamics would be implemented over the set of buses (with the cost function for each bus being the aggregated cost of the generators attached to it) and, at a lower level, a copy of the dynamics is executed in each bus among the generators connected to it. Finally, the initialization procedures of Remark 3.2.2 do not work for (3.15) because of the box

constraints. The iterative algorithms in [DGH11] provide initialization procedures that only converge asymptotically to a feasible point in \mathcal{F}_{ED} . We address this issue next.

Remark 3.3.5. (*Robustness against initialization errors*): Both the Laplacian-gradient and the Laplacian-nonsmooth-gradient dynamics preserve the total power generated by the system. Thus, if they are initialized with an error in load satisfaction, the dynamics ensures that the error stays constant while the system evolves. In this sense, these dynamics are robust. In Chapter 4, we will design a dynamics that has a more desirable property of driving the error to zero. •

3.4 Algorithm initialization and robustness against generator addition and deletion

The distributed dynamics proposed in Sections 3.2 and 3.3 rely on a proper initialization of the power levels of the units to satisfy the load condition, which remains constant throughout the execution. However, the latter is no longer the case if some generators leave the network or new generators join it. For the rED problem, this issue can easily be resolved by prescribing that the power of each unit leaving the network is compensated with a corresponding increase in the power of one of its neighbors, and that new generators join the network with zero power. However, for the ED problem, the presence of the box constraints makes the design of a distributed solution more challenging. This is the problem we address here. Interestingly, our strategy, termed DETERMINE FEASIBLE ALLOCATION, can also be used to initialize the dynamics (3.15).

We assume that the communication topology among the generators is undirected and connected at all times. A unit deletion event corresponds to removing the corresponding vertex, and all edges associated with it. A unit addition event corresponds to adding a vertex, and some additional edges associated with it. At any given time, the communication topology is represented by $\mathcal{G}_{\text{events}} = (\mathcal{V}_{\text{events}}, \mathcal{E}_{\text{events}})$.

3.4.1 Algorithm rationale and informal description

Here, we provide an informal description of the three-phase DETERMINE FEASIBLE ALLOCATION strategy that allows units to collectively adjust their powers in finite time to meet the total load while satisfying the box constraints.

(i) *Phase 1 (tree maintenance)*: This phase maintains a spanning rooted tree T_{root} whose vertices are, at any instant of time, the generators present in the network. When a unit enters the network, it sets its power to zero (all units fall into this case when this procedure is run to initialize (3.15)) and is assigned a token of the same value. A unit that leaves the network transfers a token with its power level to one of its neighbors. Every unit i , except the root, resets its current generation to $P_i + P_i^{\text{tkn}}$, where P_i^{tkn} is the summation of the tokens of i (with default value zero if no token is received). The root adds P_l to its token if the algorithm is executed for the initialization of (3.15). With these levels, the network allocation might be unfeasible and sums $P_l - P_{\text{root}}^{\text{tkn}}$.

(ii) *Phase 2 (capacity computation)*: Each unit i aggregates the difference between the current generation and the lower and upper limits, respectively, for all the units in the subtree T_i of T_{root} that has i as its root. Mathematically, $C_i^{\text{m}} = \sum_{j \in T_i} (P_j - P_j^{\text{m}})$ and $C_i^{\text{M}} = \sum_{j \in T_i} (P_j^{\text{M}} - P_j)$. These values represent the collective capacity of T_i to decrease or increase, respectively, the total power of the network while satisfying the box constraints. If $-C_{\text{root}}^{\text{m}} \leq P_{\text{root}}^{\text{tkn}} \leq C_{\text{root}}^{\text{M}}$ does not hold, then the root declares that the load cannot be met.

(iii) *Phase 3 (feasible power allocation)*: The root initiates the distribution of $P_{\text{root}}^{\text{tkn}}$, starting with itself and going down the tree until the leaves. Each unit gets a power value from its parent, which it distributes among itself (respecting its box constraints) and its children, making sure that the ulterior assignments down the tree are feasible.

We next provide a formal description and analysis of phases 2 and 3. Regarding the tree maintenance in phase 1, we do not enter into details given the ample number of solutions in literature, see e.g. [Lyn97]. We only mention that the root can be arbitrarily selected, the tree can be built via any tree construction algorithm, and addition and deletion events can be handled via tree repairing

algorithms [ACK08, SC12].

3.4.2 The GET CAPACITY strategy

Here, we describe the GET CAPACITY strategy that does capacity computation of phase 2. The method assumes that each unit i knows the identity of its parent parent_i and children children_i in the tree T_{root} , and hence is distributed. Informally,

[Informal description]: The leaves of the tree start by sending their capacities $P_i - P_i^m$ and $P_i^M - P_i$ to their parents. Each unit, i , upon receiving the capacities of all its children, adds them along with its own to get C_i^m and C_i^M , and sends the value to its parent. The routine ends upon reaching the root.

Algorithm 1: GET CAPACITY

Executed by: generators $i \in \mathcal{V}_{\text{events}}$
Data : $P_i, P_i^m, P_i^M, \text{parent}_i, \text{children}_i$
Initialize : $\vec{C}_i^m = \vec{C}_i^M := -\infty \mathbf{1}_{|\text{children}_i|}$
 if children_i *is empty* **then**
 | $C_i^m = P_i - P_i^m, C_i^M := P_i^M - P_i$
 else
 | $C_i^m = C_i^M := -\infty$
 end

1 **if** children_i *is empty* **then** send (C_i^m, C_i^M) to parent_i
2
3 **while** $(C_i^m, C_i^M) = (-\infty, -\infty)$ **do**
4 **if** message (C_j^m, C_j^M) received from child j **then**
5 update $\vec{C}_i^m(j) = C_j^m$ and $\vec{C}_i^M(j) = C_j^M$
6 **if** $(\vec{C}_i^m(k), \vec{C}_i^M(k)) \neq (-\infty, -\infty)$ for all $k \in \text{children}_i$ **then**
7 set $(C_i^m, C_i^M) = (P_i - P_i^m + \text{Sum}(\vec{C}_i^m), P_i^M - P_i + \text{Sum}(\vec{C}_i^M))$
8 **if** i *is not root* **then**
9 | send (C_i^m, C_i^M) to parent_i
10 **end**
11 **end**
12 **end**
13 **end**

Algorithm 1 formally describes GET CAPACITY. The next result summarizes its properties. The proof is straightforward.

Lemma 3.4.1. (*Correctness of GET CAPACITY*): *Starting from the spanning tree T_{root} over $\mathcal{G}_{\text{events}}$ and $P \in \mathbb{R}^{|\mathcal{V}_{\text{events}}|}$, the algorithm GET CAPACITY terminates in finite time, with each unit $i \in \mathcal{V}_{\text{events}}$ having the following information:*

(i) *the capacities $C_i^m = \sum_{k \in T_i} P_k - P_k^m$ and $C_i^M = \sum_{k \in T_i} P_k^M - P_k$ of the subtree T_i , and*

(ii) *the capacities C_j^m, C_j^M of the subtrees $\{T_j\}_{j \in \text{children}_i}$ stored in $\vec{C}_i^m, \vec{C}_i^M \in \mathbb{R}^{|\text{children}_i|}$.*

Note that the capacities C_i^m and C_i^M are non-negative if all units in the subtree T_i satisfy the box constraints. However, this might not be the case due to the resetting of generation levels in phase 1 to account for unit addition and deletion.

Lemma 3.4.2. (*Bounds on feasible power allocations to subtree*): *Given $P \in \mathbb{R}^{|\mathcal{V}_{\text{events}}|}$, the following holds*

(i) *$C^m + C^M \geq 0$ if $P^M \geq P^m$ (same holds with strict signs)*

(ii) *for each $i \in |\mathcal{V}_{\text{events}}|$, the additional power $P_i^{\text{gv}} \in \mathbb{R}$ can be further allocated to the units in T_i respecting their box constraints if and only if $-C_i^m \leq P_i^{\text{gv}} \leq C_i^M$.*

Proof. Fact (i) follows from noting that $C_i^m = \sum_{k \in T_i} (P_k - P_k^m) = \sum_{k \in T_i} (P_k^M - P_k^m) - C_i^M$. Regarding fact (ii), P_i^{gv} can be allocated among the units in T_i while satisfying the box constraints for each of them iff $\sum_{k \in T_i} P_k^m \leq \sum_{k \in T_i} P_k + P_i^{\text{gv}} \leq \sum_{k \in T_i} P_k^M$. That is, adding P_i^{gv} to the current generation of T_i gives a value that falls between the collective lower and upper limits of T_i . Rearranging the terms yields the desired result. \square

3.4.3 Algorithm: FEASIBLY ALLOCATE

Here, we describe the FEASIBLY ALLOCATE strategy that implements the feasible allocation computation of phase 3. Before this strategy is executed, the generation levels computed in phase 1 are unfeasible because their sum is $P_l - P_{\text{root}}^{\text{tkn}}$ and does not satisfy the load condition. Additionally, because of unit addition and deletion, some might not be satisfying their box constraints. The FEASIBLY ALLOCATE strategy addresses both issues. The procedure assumes that each unit i knows parent_i , children_i , and the capacities C_i^{m} , C_i^{M} , \vec{C}_i^{m} , and \vec{C}_i^{M} obtained in GET CAPACITY, and is therefore distributed. Informally,

[Informal description]: The root initiates the algorithm by setting $P_{\text{root}}^{\text{gv}} = P_{\text{root}}^{\text{tkn}}$. Each unit i , upon initializing P_i^{gv} , computes its change in power generation ($P_i^{\text{chg}} \in \mathbb{R}$) and the power to be allocated among its children ($\vec{P}_i^{\text{chg}} \in \mathbb{R}^{|\text{children}_i|}$). The unit sets its generation to $P_i + P_i^{\text{chg}}$ and sends $\vec{P}_i^{\text{chg}}(j)$ to child $j \in \text{children}_i$. The strategy ends at the leaves.

Algorithm 2 gives a formal description of FEASIBLY ALLOCATE. The next result establishes its correctness.

Proposition 3.4.3. (*Correctness of FEASIBLY ALLOCATE*): *Let $P_{\text{root}}^{\text{tkn}} \in \mathbb{R}$ with $-C_{\text{root}}^{\text{m}} \leq P_{\text{root}}^{\text{tkn}} \leq C_{\text{root}}^{\text{M}}$. Then, the FEASIBLY ALLOCATE strategy ends in finite time at an allocation $P^+ \in \mathbb{R}^{|\mathcal{V}_{\text{events}}|}$ satisfying the box constraints, $P_i^{\text{m}} \leq P_i^+ \leq P_i^{\text{M}}$, $i \in \mathcal{V}_{\text{events}}$, and the load condition, $P_l = \sum_{i \in \mathcal{V}_{\text{events}}} P_i^+$.*

Proof. By Lemma 3.4.2(ii), $-C_{\text{root}}^{\text{m}} \leq P_{\text{root}}^{\text{tkn}} \leq C_{\text{root}}^{\text{M}}$ implies that $P_{\text{root}}^{\text{tkn}}$ can be allocated to the units in T . In turn, by the same result, for a unit i , $-C_i^{\text{m}} \leq P_i^{\text{gv}} \leq C_i^{\text{M}}$ implies existence of a decomposition $P_i^{\text{chg}} \in \mathbb{R}$ and $\vec{P}_i^{\text{chg}} \in \mathbb{R}^{|\text{children}_i|}$ with

$$P_i^{\text{chg}} + \text{Sum}(\vec{P}_i^{\text{chg}}) = P_i^{\text{gv}}, \quad (3.19a)$$

$$-myP_i^{\text{dm}} \leq P_i^{\text{chg}} \leq myP_i^{\text{dM}}, \quad (3.19b)$$

$$-\vec{C}_i^{\text{m}} \leq \vec{P}_i^{\text{chg}} \leq \vec{C}_i^{\text{M}}, \quad (3.19c)$$

where we denote $myP_i^{\text{dm}} = P_i - P_i^{\text{m}}$ and $myP_i^{\text{dM}} = P_i^{\text{M}} - P_i$. Equation (3.19b) corresponds to the box constraints being satisfied for unit i if assigned the additional

Algorithm 2: FEASIBLY ALLOCATE

Executed by: generators $i \in \mathcal{V}_{\text{events}}$
Data : $P_i, P_i^m, P_i^M, \text{parent}_i, \text{children}_i, \vec{C}_i^m, \vec{C}_i^M$
Initialize : $P_i^{\text{chg}} := -\infty, \vec{P}_i^{\text{chg}} := -\infty \mathbf{1}_{|\text{children}_i|}, myP_i^{\text{dm}} := P_i - P_i^m,$
 $myP_i^{\text{dM}} := P_i^M - P_i$

- 1 **while** $P_i^{\text{chg}} = -\infty$ **do**
- 2 **if** i root or message $\vec{P}_{\text{parent}_i}^{\text{chg}}(i)$ from parent_i **then**
- 3 **if** i root **then** $P_i^{\text{gv}} = P_{\text{root}}^{\text{tkn}}$ **else** $P_i^{\text{gv}} = \vec{P}_{\text{parent}_i}^{\text{chg}}(i)$
- 4 set $P_i^{\text{chg}} = \text{argmin}_{x \in [-myP_i^{\text{dm}}, myP_i^{\text{dM}}]} |x|$
- 5 **for** $j \in \text{children}_i$ **do**
- 6 set $\vec{P}_i^{\text{chg}}(j) = \text{argmin}_{x \in [-\vec{C}_i^m(j), \vec{C}_i^M(j)]} |x|$
- 7 **end**
- 8 set $P_i^{\text{gv}} = P_i^{\text{gv}} - P_i^{\text{chg}} - \text{Sum}(\vec{P}_i^{\text{chg}})$
- 9 **if** $P_i^{\text{gv}} \geq 0$ **then**
- 10 set $X = \min\{P_i^{\text{gv}}, myP_i^{\text{dM}} - P_i^{\text{chg}}\}$
- 11 set $(P_i^{\text{chg}}, P_i^{\text{gv}}) = (P_i^{\text{chg}} + X, P_i^{\text{gv}} - X)$
- 12 **for** $j \in \text{children}_i$ **do**
- 13 set $X = \min\{P_i^{\text{gv}}, \vec{C}_i^M(j) - \vec{P}_i^{\text{chg}}(j)\}$
- 14 set $(\vec{P}_i^{\text{chg}}(j), P_i^{\text{gv}}) = (\vec{P}_i^{\text{chg}}(j) + X, P_i^{\text{gv}} - X)$
- 15 **end**
- 16 **end**
- 17 **else**
- 18 set $X = \max\{P_i^{\text{gv}}, -myP_i^{\text{dm}} - P_i^{\text{chg}}\}$
- 19 set $(P_i^{\text{chg}}, P_i^{\text{gv}}) = (P_i^{\text{chg}} + X, P_i^{\text{gv}} - X)$
- 20 **for** $j \in \text{children}_i$ **do**
- 21 set $X = \max\{P_i^{\text{gv}}, -\vec{C}_i^m(j) - \vec{P}_i^{\text{chg}}(j)\}$
- 22 set $(\vec{P}_i^{\text{chg}}(j), P_i^{\text{gv}}) = (\vec{P}_i^{\text{chg}}(j) + X, P_i^{\text{gv}} - X)$
- 23 **end**
- 24 **end**
- 25 set $P_i = P_i + P_i^{\text{chg}}$
- 26 send $\vec{P}_i^{\text{chg}}(j)$ to each $j \in \text{children}_i$
- 27 **end**
- 28 **end**
- 29 **end**

power P_i^{chg} to generate. Equation (3.19c) ensures that a feasible allocation exists for the subtree of each of its children. We compute P_i^{chg} and \vec{P}_i^{chg} in two steps. First, we find the portion of power that ensures feasibility for i and its children. This is done via

$$a_i = \operatorname{argmin}_{x \in [-myP_i^{\text{dm}}, myP_i^{\text{dM}}]} |x|,$$

$$\vec{b}_i(j) = \operatorname{argmin}_{x \in [-\vec{C}_i^{\text{m}}(j), \vec{C}_i^{\text{M}}(j)]} |x|, \text{ for } j \in \text{children}_i.$$

Observe that $P_i^{\text{chg}} = a_i$ and $\vec{P}_i^{\text{chg}} = \vec{b}_i$ satisfy (3.19b) and (3.19c) but not necessarily (3.19a). The second step takes care of this shortcoming by defining $X_i \in \mathbb{R}$ and $\vec{Y}_i \in \mathbb{R}^{|\text{children}_i|}$ as

$$P_i^{\text{chg}} = a_i + X_i, \quad \vec{P}_i^{\text{chg}} = \vec{b}_i + \vec{Y}_i.$$

In these new variables, (3.19) reads as

$$X_i + \text{Sum}(\vec{Y}_i) = P_i^{\text{gV}} - a_i - \text{Sum}(\vec{b}_i), \quad (3.20a)$$

$$-myP_i^{\text{dm}} - a_i \leq X_i \leq myP_i^{\text{dM}} - a_i, \quad (3.20b)$$

$$-\vec{C}_i^{\text{m}} - \vec{b}_i \leq \vec{Y}_i \leq \vec{C}_i^{\text{M}} - \vec{b}_i. \quad (3.20c)$$

Adding the lower limits of (3.20b) and (3.20c) yields $-C_i^{\text{m}} - a_i - \text{Sum}(\vec{b}_i)$, where we use $C_i^{\text{m}} = myP_i^{\text{dm}} + \text{Sum}(\vec{C}_i^{\text{m}})$. Similarly, the upper limits sum $C_i^{\text{M}} - a_i - \text{Sum}(\vec{b}_i)$. Therefore, with $-C_i^{\text{m}} \leq P_i^{\text{gV}} \leq C_i^{\text{M}}$, (3.20) is solvable by unit i with knowledge of P_i^{gV} , myP_i^{dm} , myP_i^{dM} , \vec{C}_i^{m} , and \vec{C}_i^{M} . Note that the lower limits of (3.20b) and (3.20c) are nonpositive and the upper ones are nonnegative. Therefore, if $P_i^{\text{gV}+} \geq 0$, FEASIBLY ALLOCATE considers first unit i and then its children sequentially and assigns the maximum power each can take (bounded by the upper limit of (3.20b) and (3.20c)) as X_i and \vec{Y}_i until there is no more to allocate. Similarly if $P_i^{\text{gV}+} < 0$ negative values are assigned (lower bounded by lower limits of (3.20b) and (3.20c)). For unit i , this corresponds to steps 11-12 (if $P_i^{\text{gV}+} \geq 0$) or 19-20 (if $P_i^{\text{gV}+} < 0$) of Algorithm 2. For the children, this corresponds to steps 13-15 (if $P_i^{\text{gV}+} \geq 0$) or steps 21-23 (if $P_i^{\text{gV}+} < 0$) of Algorithm 2. Consequently, the resulting

power allocation $P^+ = P + P^{\text{chg}}$ satisfies $P^m \leq P^+ \leq P^M$ because (3.19b) holds for each unit $i \in \mathcal{V}_{\text{events}}$. Additionally,

$$\begin{aligned} \sum_{i \in \mathcal{V}_{\text{events}}} P_i^{\text{chg}} &= P_{\text{root}}^{\text{chg}} + \sum_{i \in \mathcal{V}_{\text{events}} \setminus \text{root}} P_i^{\text{chg}} \\ &= P_{\text{root}}^{\text{chg}} + \sum_{i \in \text{children}_{\text{root}}} \vec{P}_{\text{root}}^{\text{chg}} = P_{\text{root}}^{\text{gv}}, \end{aligned}$$

where we use that (3.19a) holds for each $i \in \mathcal{V}_{\text{events}}$ in the second and third inequalities. Since $P_{\text{root}}^{\text{gv}} = P_{\text{root}}^{\text{tkn}}$ and $\sum_{i \in \mathcal{V}_{\text{events}}} P_i = P_l - P_{\text{root}}^{\text{tkn}}$, we get $\sum_{i \in \mathcal{V}_{\text{events}}} P_i^+ = P_l$. \square

Remark 3.4.4. (*Trade-offs between additional information and network-wide computation*): When dealing with the addition and deletion of generators, it is conceivable that, depending on the nature of the events, agents may use algorithmic implementations that do not involve the whole network in determining a feasible allocation. As an example, consider a scenario where network changes occur in a localized manner and do not affect substantially the network generation capacity. Then, one could envision that a feasible allocation could be found involving only a small set of generators in the computation of capacities and the allocation of the mismatch. Such localized solutions are prone to failure when faced with more extreme events (e.g., a large change to the overall network generation capacity caused by topological changes). Instead, the DETERMINE FEASIBLE ALLOCATION strategy is guaranteed to find a feasible allocation whenever it exists.

•

3.5 Simulations

Here, we illustrate the application of the Laplacian-nonsmooth-gradient dynamics to solve the ED problem (3.1) and the use of the DETERMINE FEASIBLE ALLOCATION strategy to handle unit addition and deletion. The dynamics (3.15) is simulated with a first-order Euler discretization. The optimizers are computed using an sdp solver in the YALMIP toolbox.

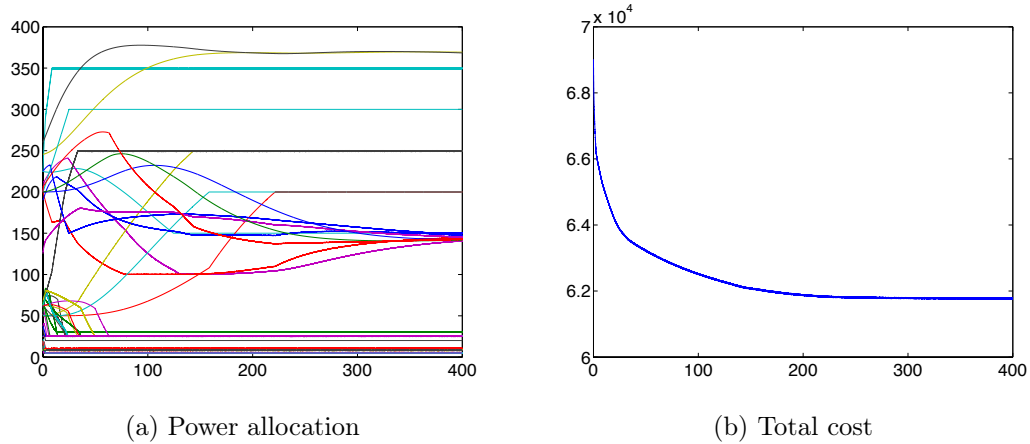


Figure 3.1: Evolution of the power allocation (a) and the network cost (b) under the Laplacian-nonsmooth-gradient dynamics in the IEEE 118 bus test case. The stepsize of the Euler time-discretization is 2.5×10^{-3} and $\epsilon = 0.006$.

IEEE 118 bus

Consider the ED problem for the IEEE 118 bus test case [IEE]. This test case has 54 generators, with quadratic cost functions for each unit i , $f_i(P_i) = a_i + b_i P_i + c_i P_i^2$, whose coefficients belong to the ranges $a_i \in [6.78, 74.33]$, $b_i \in [8.3391, 37.6968]$, and $c_i \in [0.0024, 0.0697]$. The load is $P_l = 4200$ and the capacity bounds vary as $P_i^m \in [5, 150]$ and $P_i^M \in [150, 400]$. The communication topology is a directed cycle with the additional bi-directional edges $\{1, 11\}, \{11, 21\}, \{21, 31\}, \{31, 41\}, \{41, 51\}$, with all weights equal to 1. Fig. 3.1 depicts the execution of (3.15). Note that as the network converges to the optimizer while satisfying the constraints, the total cost is monotonically decreasing.

Unit addition and deletion

Consider six power generators initially communicating over the graph in Fig. 3.2(a). The units implement (3.15) starting from the allocation $P_0 = (1.15, 2.75, 1.5, 3.35, 1.25, 2)$ that meets the load $P_l = 12$ and quickly achieve a close proximity of the optimizer $(0.94, 2, 2.4, 2.61, 1.35, 2.7)$. After 0.75 seconds, unit 7 joins the network and unit 3 leaves it, with the resulting topology shown in Fig. 3.2(b). The network then employs the DETERMINE FEASIBLE ALLOCATION

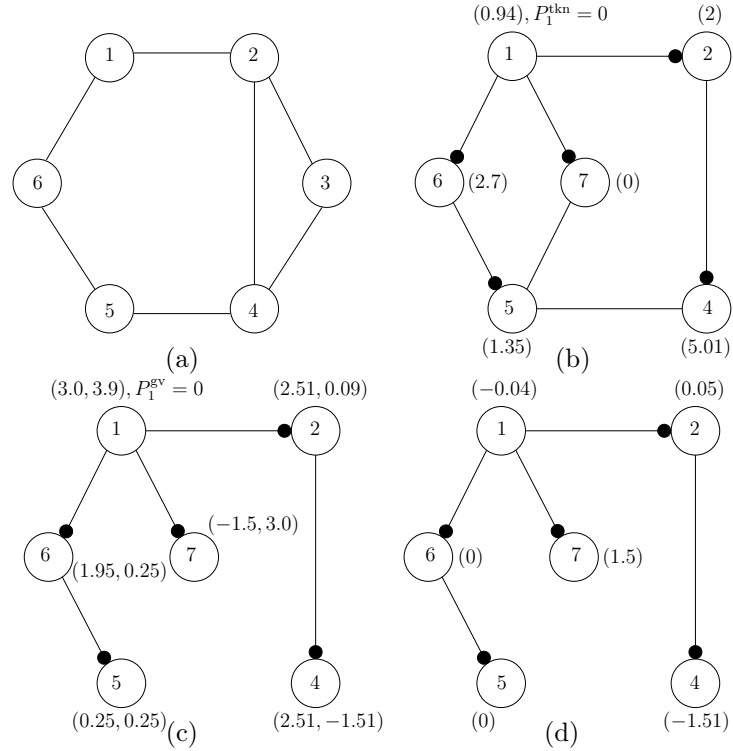


Figure 3.2: (a) Initial communication topology with all edge weights equal to 1. (b) Communication topology after the addition of unit 7 and deletion of unit 3. Generation levels at the end of Phase 1 of the DETERMINE FEASIBLE ALLOCATION strategy are in parentheses. The tree is depicted via edges with dots. When leaving, unit 3 transfers its power as a token to unit 4 and hence, after token addition, 4's generation becomes 5.01 (higher than its maximum capacity). Unit 7 enters with zero power. Thus, all units except 4 have zero token value. Unit 1, being the root of the tree, sets $P_1^{\text{tkn}} = 0$. (c) State after the execution of GET CAPACITY. For each unit i , (C_i^m, C_i^M) are indicated in parentheses. Unit 1 initiates FEASIBLY ALLOCATE to distribute $P_1^{\text{gv}} = 0$. (d) State at the end of FEASIBLY ALLOCATE, with values of the power distributed to the units in parentheses. These values sum up to 0, and when added to their respective generation levels in (b) result into the allocation $P_0^+ = (0.9, 2.05, 3.5, 1.35, 2.7, 1.5)$ that satisfies the load condition and the box constraints.

Table 3.1: Coefficients of the quadratic cost function $f_i(P_i) = a_i + b_i P_i + c_i P_i^2$ and lower P_i^m and upper P_i^M generation limits for each unit i .

Unit	a_i	b_i	c_i	P_i^m	P_i^M
1	1	4	5	0.9	1.5
2	1	2	3	2	3.6
3	4	4	1	1	2.4
4	2	3	2	2.5	3.5
5	1	0	5	1.1	1.6
6	1	1	1	1	2.7
7	2	2	1	1.5	3

strategy, whose execution is illustrated in Fig. 3.2(b)-3.2(d), and finds the new feasible allocation $(0.9, 2.05, 3.5, 1.35, 2.7, 1.5)$ from which (3.15) is re-initialized. Table 3.1 gives the cost function and the box constraints for each unit. Fig. 3.3 shows the evolution of the power allocations and the total cost. The network asymptotically converges to the optimizer $(0.9, 2, 2.5, 1.1, 2.7, 2.8)$. In Fig. 3.3(a), the discontinuity at $t = 0.75s$ corresponds to the DETERMINE FEASIBLE ALLOCATION strategy handling the addition and deletion. Note also the jump in the cost. The network eventually obtains a lower cost than the one before the events because the added unit 7 incurs a lower cost when producing the same power as the deleted unit 3.

Acknowledgments

This chapter is taken, in part, from the work [CC15c] published as “Distributed generator coordination for initialization and anytime optimization in economic dispatch” by A. Cherukuri and J. Cortés, in the IEEE Transaction on Control of Network Systems, 2015, as well as [CMC14] where it appears as “Distributed, anytime optimization in power-generator networks for economic dispatch” by A. Cherukuri, S. Martínez, and J. Cortés in the proceedings of the 2014 American Control Conference. The dissertation author was the primary investigator and author of these papers. This research was partly supported by the US National Science Foundation (NSF) Award CMMI-1300272.

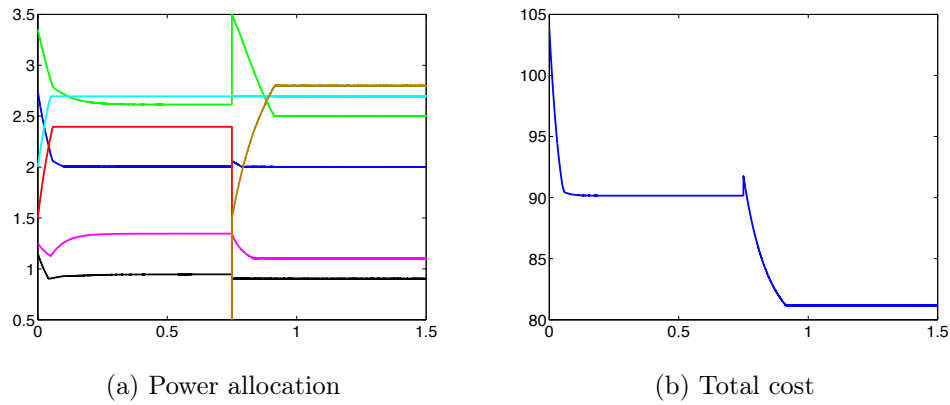


Figure 3.3: Time evolutions of the power allocation and the network cost under the Laplacian-nonsmooth-gradient dynamics. The network of 6 generators with topology depicted in Fig. 3.2(a) converges towards the optimizer $(0.94, 2, 2.4, 2.61, 1.35, 2.7)$ when, at $t = 0.75s$, unit 3 (red line) leaves and unit 7 (brown line) gets added. After executing the DETERMINE FEASIBLE ALLOCATION strategy to find a feasible power allocation, the network with topology depicted in Fig. 3.2(b) evolves along the Laplacian-nonsmooth-gradient dynamics to arrive at the optimizer $(0.9, 2, 2.5, 1.1, 2.7, 2.8)$. The stepsize of the Euler time-discretization is 2.5×10^{-5} and $\epsilon = 0.006$.

Chapter 4

Robust distributed dynamics for ED problem

In Chapter 3, we introduced a distributed anytime algorithm that finds a solution of the ED problem asymptotically. The algorithm required proper initialization, that is, a power allocation that is feasible. In Section 3.4, we addressed this problem partly by providing a finite-time convergent algorithm that finds a feasible initial condition. However, in the case that the power demand is a time-varying signal or the number of generators participating in the dispatch changes often, the finite-time convergent routine needs to be executed over and over again. To overcome this problem, this chapter presents a robust distributed algorithmic solution for the ED problem which converges from any initial power allocation.

4.1 Problem statement

This section will recall the definition of the economic dispatch problem that we defined in Section 3.1. Consider $n \in \mathbb{Z}_{\geq 1}$ power generators communicating over a strongly connected and weight-balanced digraph $\mathcal{G} = (\mathcal{V}, \mathcal{E}, \mathbf{A})$. Each generator corresponds to a vertex in the digraph and an edge (i, j) represents the ability of generator j to send information to generator i . The cost of power generation for unit i is measured by $f_i : \mathbb{R} \rightarrow \mathbb{R}_{\geq 0}$, assumed to be convex and continuously differentiable. Representing the power generated by unit i by $P_i \in \mathbb{R}$, the total

cost incurred by the network with the power allocation $P = (P_1, \dots, P_n) \in \mathbb{R}^n$ is measured by $f : \mathbb{R}^n \rightarrow \mathbb{R}_{\geq 0}$ as

$$f(P) = \sum_{i=1}^n f_i(P_i).$$

Note that f is convex and continuously differentiable. The generators aim to minimize the total cost $f(P)$ while meeting the total power load $P_l \in \mathbb{R}_{>0}$, i.e., $\sum_{i=1}^n P_i = P_l$. Each generator has an upper and a lower limit on the power it can produce, $P_i^m \leq P_i \leq P_i^M$ for $i \in [n]$. Formally, the economic dispatch (ED) problem is

$$\text{minimize } f(P), \tag{4.1a}$$

$$\text{subject to } \mathbf{1}_n^\top P = P_l, \tag{4.1b}$$

$$P^m \leq P \leq P^M. \tag{4.1c}$$

The constraint (4.1b) is the *load condition* and (4.1c) are the *box constraints*. The set of allocations satisfying the box constraints is $\mathcal{F}_B = \{P \in \mathbb{R}^n \mid P^m \leq P \leq P^M\}$. Further, we denote the feasibility set of (4.1) as $\mathcal{F}_{\text{ED}} = \mathcal{F}_B \cap \mathcal{H}_{P_l} = \{P \in \mathbb{R}^n \mid P^m \leq P \leq P^M \text{ and } \mathbf{1}_n^\top P = P_l\}$ and the set of solutions as $\mathcal{F}_{\text{ED}}^*$. Since \mathcal{F}_{ED} is compact, $\mathcal{F}_{\text{ED}}^*$ is compact. Note that $P^M \in \mathcal{F}_{\text{ED}}$ implies $\mathcal{F}_{\text{ED}} = \{P^M\}$. We assume that P^M and P^m are not feasible.

Our aim is to design a distributed algorithm that allows the team of generators to solve the ED problem (4.1) starting from any initial condition, can handle time-varying loads, and is robust to intermittent power generation.

Remark 4.1.1. (*Additional practical constraints*): We do not consider here, for simplicity, other constraints on the ED problem such as transmission losses, transmission line capacities, valve-point loading effects, ramp rate limits, and prohibited operating zones. As our forthcoming treatment will show, the design and analysis of algorithmic solutions to the ED problem without these additional constraints is already quite challenging given our performance requirements. Nevertheless, Remark 4.3.5 later comments on how to adapt our algorithm to deal with more

general scenarios. •

Our design strategy relies on the following reformulation of the ED problem without inequality constraints that was developed in Chapter 3. Consider the modified ED problem

$$\text{minimize } f^\epsilon(P), \tag{4.2a}$$

$$\text{subject to } \mathbf{1}_n^\top P = P_l, \tag{4.2b}$$

where the objective function is

$$f^\epsilon(P) = \sum_{i=1}^n f_i(P_i) + \frac{1}{\epsilon} \left(\sum_{i=1}^n ([P_i - P_i^M]^+ + [P_i^m - P_i]^+) \right).$$

This corresponds to each generator $i \in [n]$ having the modified local cost

$$f_i^\epsilon(P_i) = f_i(P_i) + \frac{1}{\epsilon} ([P_i - P_i^M]^+ + [P_i^m - P_i]^+).$$

Note that f_i^ϵ is convex, locally Lipschitz, and continuously differentiable on \mathbb{R} except at $P_i = P_i^m$ and $P_i = P_i^M$. Moreover, the total cost f^ϵ is convex, locally Lipschitz, and regular. According to Proposition 3.3.2, the solutions to the original (4.1) and the modified (4.2) ED problems coincide for $\epsilon \in \mathbb{R}_{>0}$ such that

$$\epsilon < \frac{1}{2 \max_{P \in \mathcal{F}_{\text{ED}}} \|\nabla f(P)\|_\infty}. \tag{4.3}$$

Throughout this chapter, we will assume that ϵ satisfies this condition. Recall that $P^* \in \mathbb{R}^n$ is a solution of (4.2) if and only if there exists $\mu \in \mathbb{R}$ such that

$$\mu \mathbf{1}_n \in \partial f^\epsilon(P^*) \quad \text{and} \quad \mathbf{1}_n^\top P^* = P_l. \tag{4.4}$$

4.2 Robust centralized algorithmic solution

This section presents a robust strategy to make the network power allocation converge to the solution set of the ED problem starting from any initial

condition. Even though this algorithm is centralized, its design provides enough insight to tackle later the design of a distributed algorithmic solution. Consider the “load mismatch + Laplacian-nonsmooth-gradient” (abbreviated $\mathbf{1m}+\mathbf{L}\partial$) dynamics, represented by the set-valued map $X_{\mathbf{1m}+\mathbf{L}\partial} : \mathbb{R}^n \rightrightarrows \mathbb{R}^n$,

$$\dot{P} \in -\mathbf{L}\partial f^\epsilon(P) + \frac{1}{n}(P_l - \mathbf{1}_n^\top P)\mathbf{1}_n, \quad (4.5)$$

where \mathbf{L} is the Laplacian associated to the strongly connected and weight-balanced communication digraph \mathcal{G} . For each generator, the first term seeks to minimize the total cost while leaving unchanged the total generated power. The second term is a feedback element that seeks to drive the units towards the satisfaction of the load. The first term is computable using information from its neighbors but the second term requires them to know the aggregated state of the whole network, which makes it not directly implementable in a distributed manner. The next result shows that the trajectories of (4.5) converge to the set of solutions of the ED problem.

Theorem 4.2.1. *(Convergence of the trajectories of $X_{\mathbf{1m}+\mathbf{L}\partial}$ to the solutions of the ED problem): The trajectories of (4.5) starting from any point in \mathbb{R}^n converge to the set of solutions of (4.1).*

Proof. Our proof strategy proceeds by applying the refined LaSalle Invariance Principle for differential inclusions established later in Section 4.5, cf. Proposition 4.5.1. Consider the following function $V_1 : \mathbb{R}^n \rightarrow \mathbb{R}_{\geq 0}$,

$$V_1(P) = \frac{1}{2}(P_l - \mathbf{1}_n^\top P)^2.$$

The set-valued Lie derivative of V_1 along $X_{\mathbf{1m}+\mathbf{L}\partial}$ is

$$\mathcal{L}_{X_{\mathbf{1m}+\mathbf{L}\partial}} V_1(P) = \{-(P_l - \mathbf{1}_n^\top P)^2\} = \{-2V_1(P)\}.$$

Thus, starting at any $P(0) \in \mathbb{R}^n$, the trajectory of $X_{\mathbf{1m}+\mathbf{L}\partial}$ satisfies $V_1(P(t)) = V_1(P(0))e^{-2t}$ and its omega-limit set (provided the trajectory is bounded, a fact that we assume is true for now and establish later) is contained in \mathcal{H}_{P_l} . In the

notation of Proposition 4.5.1, \mathcal{H}_{P_l} plays the role of the closed submanifold \mathcal{S} of \mathbb{R}^n . We next show that the hypotheses of this result hold. In the notation of the Lemma 4.5.3, the function f^ϵ , the map $(P, \zeta) \mapsto -\mathbf{L}\zeta$, and the set-valued map $P \rightrightarrows -\mathbf{L}\partial f^\epsilon(P)$ play the role of W , g , and F , respectively (our choice of F is because $X_{\mathbf{1}_m+\mathbf{L}\partial}$ takes the form $\dot{P} \in -\mathbf{L}\partial f^\epsilon(P)$ on $\mathcal{S} = \mathcal{H}_{P_l}$). Notice that $\zeta \mapsto -\mathbf{L}\zeta$ is a continuous map and, since \mathcal{G} is strongly connected and weight-balanced, we have $\zeta^\top(-\mathbf{L}\zeta) = -\frac{1}{2}\zeta^\top(\mathbf{L}+\mathbf{L}^\top)\zeta \leq 0$ for any $\zeta \in \partial f^\epsilon(P)$. Therefore, Lemma 4.5.3(i) is satisfied. Moreover, if $\zeta^\top(-\mathbf{L}\zeta) = 0$ for some $\zeta \in \partial f^\epsilon(P)$, then $\zeta \in \text{span}\{\mathbf{1}_n\}$. Since for $P \in \mathcal{H}_{P_l}$, we have

$$\mathcal{L}_{X_{\mathbf{1}_m+\mathbf{L}\partial}}f^\epsilon(P) = \{-\zeta^\top\mathbf{L}\zeta \mid \zeta \in \partial f^\epsilon(P)\},$$

we deduce $0 \in \mathcal{L}_{X_{\mathbf{1}_m+\mathbf{L}\partial}}f^\epsilon(P)$, i.e., Lemma 4.5.3(ii) holds. The application of Lemma 4.5.3 then yields that Proposition 4.5.1(ii) holds too. In addition, from the above analysis, note that if $0 \in \mathcal{L}_{X_{\mathbf{1}_m+\mathbf{L}\partial}}f^\epsilon(P)$ for some $P \in \mathcal{H}_{P_l}$, then there exists $\mu \in \mathbb{R}$ such that $\mu\mathbf{1}_n \in \partial f^\epsilon(P)$ and, from (4.4), P is a solution of (4.1). Therefore, $\{P \in \mathcal{H}_{P_l} \mid 0 \in \mathcal{L}_{X_{\mathbf{1}_m+\mathbf{L}\partial}}f^\epsilon(P)\}$ is the set of solutions of the ED problem and belongs to a level set of f^ϵ , which establishes that Proposition 4.5.1(i) also holds.

To be able to apply Proposition 4.5.1 and conclude the proof, it remains to show that the trajectories of $X_{\mathbf{1}_m+\mathbf{L}\partial}$ are bounded. We reason by contradiction, i.e., assume there exists a trajectory $t \mapsto P(t)$, $P(0) \in \mathbb{R}^n$ of $X_{\mathbf{1}_m+\mathbf{L}\partial}$ such that $\|P(t)\| \rightarrow \infty$. From the analysis above, we know that along this trajectory $\mathbf{1}_n^\top P(t) \rightarrow P_l$ and $f^\epsilon(P(t)) \rightarrow \infty$ (as f^ϵ is radially unbounded). Therefore, there exist a sequence of times $\{t_k\}_{k=1}^\infty$ with $t_k \rightarrow \infty$ such that for all $k \in \mathbb{Z}_{\geq 1}$,

$$|\mathbf{1}_n^\top P(t_k) - P_l| < \frac{1}{k} \text{ and } \max \mathcal{L}_{X_{\mathbf{1}_m+\mathbf{L}\partial}}f^\epsilon(P(t_k)) > 0. \quad (4.6)$$

This implies that there exists a sequence $\{\zeta_k\}_{k=1}^\infty$ with $\zeta_k \in \partial f^\epsilon(P(t_k))$ such that, for all $k \in \mathbb{Z}_{\geq 1}$,

$$-\zeta_k^\top\mathbf{L}\zeta_k + \frac{1}{n}(P_l - \mathbf{1}_n^\top P(t_k))(\mathbf{1}_n^\top\zeta_k) > 0$$

$$\begin{aligned}
&\Rightarrow -\zeta_k^\top \left(\frac{\mathbf{L} + \mathbf{L}^\top}{2} \right) \zeta_k + \frac{1}{nk} |\mathbf{1}_n^\top \zeta_k| > 0 \\
&\Rightarrow -\frac{\lambda_2(\mathbf{L} + \mathbf{L}^\top)}{2} \left\| \zeta_k - \frac{1}{n} (\mathbf{1}_n^\top \zeta_k) \mathbf{1}_n \right\|^2 + \frac{1}{nk} |\mathbf{1}_n^\top \zeta_k| > 0,
\end{aligned} \tag{4.7}$$

where we have used (4.6) in the first implication and (2.1) in the second. Next, we consider two cases depending on whether (a) $|\mathbf{1}_n^\top \zeta_k|$ is bounded or (b) $|\mathbf{1}_n^\top \zeta_k| \rightarrow \infty$. In case (a), taking the limit $k \rightarrow \infty$ in the last inequality of (4.7), we get

$$\lim_{k \rightarrow \infty} \left\| \zeta_k - \frac{1}{n} (\mathbf{1}_n^\top \zeta_k) \mathbf{1}_n \right\| = 0. \tag{4.8}$$

Since, $\|P(t)\| \rightarrow \infty$ and $\mathbf{1}_n^\top P(t) \rightarrow P_l$, there exist $i, j \in [n]$ such that $P_i(t_k) \rightarrow \infty$ and $P_j(t_k) \rightarrow -\infty$. Let $P^* \in \mathcal{F}_{\text{ED}}^*$ and $\mu \mathbf{1}_n \in \partial f^\epsilon(P^*)$ for some $\mu \in \mathbb{R}$. Then, without loss of generality, we assume that $P_i^* \leq P_i(t_k) \leq P_i(t_{k+1})$ and $P_j^* \geq P_j(t_k) \geq P_j(t_{k+1})$ for all k . This fact along with the expression of $\partial f_i^\epsilon : \mathbb{R} \rightrightarrows \mathbb{R}$,

$$\partial f_i^\epsilon(P_i) = \begin{cases} \{\nabla f_i(P_i) - \frac{1}{\epsilon}\} & \text{if } P_i < P_i^m, \\ [\nabla f_i(P_i) - \frac{1}{\epsilon}, \nabla f_i(P_i)] & \text{if } P_i = P_i^m, \\ \{\nabla f_i(P_i)\} & \text{if } P_i^m < P_i < P_i^M, \\ [\nabla f_i(P_i), \nabla f_i(P_i) + \frac{1}{\epsilon}] & \text{if } P_i = P_i^M, \\ \{\nabla f_i(P_i) + \frac{1}{\epsilon}\} & \text{if } P_i > P_i^M. \end{cases}$$

gives us the following property for all $k \in \mathbb{Z}_{\geq 1}$,

$$\min \partial f_i^\epsilon(P_i(t_k)) \geq \mu, \quad \max \partial f_j^\epsilon(P_j(t_k)) \leq \mu, \tag{4.9a}$$

$$\min \partial f_i^\epsilon(P_i(t_{k+1})) \geq \max \partial f_i^\epsilon(P_i(t_k)), \tag{4.9b}$$

$$\max \partial f_j^\epsilon(P_j(t_{k+1})) \leq \min \partial f_j^\epsilon(P_j(t_k)). \tag{4.9c}$$

Note that the limit (4.8) yields $\lim_{k \rightarrow \infty} |(\zeta_k)_i - (\zeta_k)_j| = 0$. On the other hand, from (4.9b)-(4.9c), we obtain $|(\zeta_k)_i - (\zeta_k)_j| \leq |(\zeta_{k+1})_i - (\zeta_{k+1})_j|$ for all k . Therefore, we obtain $(\zeta_k)_i = (\zeta_k)_j$ for all k and from (4.9a), we get $\mu = (\zeta_k)_i = (\zeta_k)_j$ for all k . From (4.9b)-(4.9c), this further implies that $\mu \in \partial f_i^\epsilon(x)$ for all $x \in [P_i^*, \infty)$ and that $\mu \in \partial f_j^\epsilon(x)$ for all $x \in (-\infty, P_j^*]$. Using this fact, one can construct an

unbounded set of solutions to the ED problem in the following manner. First, fix all the components of P^* except i and j . Now pick any $x \in \mathbb{R}_{\geq 0}$ and consider $P_i^* + x$ and $P_j^* - x$. From what we have reasoned so far, all such points that we obtain by varying x are solutions to the ED problem as they satisfy (4.4). This contradicts the fact that $\mathcal{F}_{\text{ED}}^*$ is bounded.

In case (b), assume without loss of generality that $\mathbf{1}_n^\top \zeta_k \rightarrow \infty$ (the argument for $\mathbf{1}_n^\top \zeta_k \rightarrow -\infty$ follows similarly). As reasoned above, there exists $j \in [n]$ such that $P_j(t_k) \rightarrow -\infty$ and there exists $\mu \in \mathbb{R}$ such that $(\zeta_k)_j \leq \mu$ for all $k \in \mathbb{Z}_{\geq 1}$. Using this fact, we upper bound the left hand side of the inequality (4.7) by

$$\begin{aligned} & -\frac{\lambda_2(\mathbf{L} + \mathbf{L}^\top)}{2} \left\| \zeta_k - \frac{1}{n}(\mathbf{1}_n^\top \zeta_k) \mathbf{1}_n \right\|^2 + \frac{1}{nk}(\mathbf{1}_n^\top \zeta_k) \\ & \leq -\frac{\lambda_2(\mathbf{L} + \mathbf{L}^\top)}{2} \left((\zeta_k)_j - \frac{1}{n}(\mathbf{1}_n^\top \zeta_k) \right)^2 + \frac{1}{nk}(\mathbf{1}_n^\top \zeta_k) \\ & \leq -\frac{\lambda_2(\mathbf{L} + \mathbf{L}^\top)}{2} \left(\mu - \frac{1}{n}(\mathbf{1}_n^\top \zeta_k) \right)^2 + \frac{1}{nk}(\mathbf{1}_n^\top \zeta_k), \end{aligned} \quad (4.10)$$

where the last inequality is valid for all but a finite number of k . Hence, as $\mathbf{1}_n^\top \zeta_k \rightarrow \infty$, there is $\bar{k} \in \mathbb{Z}_{\geq 1}$ such that the expression in (4.10) is negative for $k \geq \bar{k}$, contradicting (4.7). Thus, we conclude the trajectories are bounded. \square

From the proof above, it is interesting to note that the feedback term (4.5) drives the mismatch between generation and load to zero at an exponential rate, no matter what the initial power allocation. This is a good indication of its robustness properties: time-varying loads or scenarios with generators going down and coming back online can be handled as long as the rate of these changes is lower than the exponential rate of convergence associated to the load satisfaction. We provide a formal characterization of these properties for the distributed implementation of this strategy in the next section.

4.3 Robust distributed algorithmic solution

This section presents a distributed strategy to solve the ED problem starting from any initial power allocation. We build on the centralized design presented

in Section 4.2. We also formally characterize the robustness properties against addition and deletion of generators and time-varying loads.

Given the discussion on the centralized nature of the dynamics (4.5), the core idea of our design is to employ a dynamic average consensus algorithm that allows each unit in the network to estimate the mismatch in load satisfaction. In dynamic average consensus (cf. Section 2.7), each agent has access to a time-varying input signal and interacts with its neighbors in order to track the average of the input signals across the network. For our specific case, we assume the total load P_l is only known to one generator $r \in [n]$ (its specific identity is arbitrary). Following Section 2.7, consider

$$\begin{aligned}\dot{z} &= -\alpha z - \beta \mathbf{L}z - v + \nu_2(P_l e_r - P), \\ \dot{v} &= \alpha \beta \mathbf{L}z,\end{aligned}$$

where $e_r \in \mathbb{R}^n$ is the unit vector along the r -th direction and $\alpha, \beta, \nu_2 > 0$ are design parameters. Note that this algorithm is distributed over the communication graph \mathcal{G} . For each $i \in [n]$, z_i plays the role of an estimator associated to i which aims to track the average signal $t \mapsto \frac{1}{n}(P_l - \mathbf{1}_n^\top P(t))$. This observation justifies substituting the feedback term in (4.5) by $z \in \mathbb{R}^n$, giving rise to the “dynamic average consensus + Laplacian-nonsmooth-gradient” dynamics, abbreviated **dac+L ∂** for convenience, mathematically represented by the set-valued map $X_{\text{dac+L}\partial} : \mathbb{R}^{3n} \rightrightarrows \mathbb{R}^{3n}$,

$$\dot{P} \in -\mathbf{L}\partial f^\epsilon(P) + \nu_1 z, \tag{4.12a}$$

$$\dot{z} = -\alpha z - \beta \mathbf{L}z - v + \nu_2(P_l e_r - P), \tag{4.12b}$$

$$\dot{v} = \alpha \beta \mathbf{L}z, \tag{4.12c}$$

where $\nu_1 > 0$ is a design parameter. Unlike (4.5), this algorithm is distributed, as each agent only needs to interact with its neighbors to implement it.

Remark 4.3.1. (*Comparison with finite-time initialization approach*): Our distributed solution for the ED problem proposed in Chapter 3 involved initializing the generation levels inside the feasibility set \mathcal{F}_{ED} using a finite-time message pass-

ing algorithm. This finite-time initialization approach is best suited for scenarios with a fixed set of participating generators. In the presence of intermittent generation, every time a generator joins or leaves the network, the generators have to stop the dynamics, execute the finite-time algorithm, and then re-run the dynamics. This approach, however, cannot deliver perfect tracking of continuously time-varying loads. In contrast, the **dac+L ∂** dynamics does not suffer from these limitations, as discussed later in Section 4.3.2. \bullet

4.3.1 Convergence analysis

Here we characterize the asymptotic convergence properties of the **dac+L ∂** dynamics. We start by establishing an important fact on the omega-limit set of any trajectory of (4.12) with initial condition in $\mathbb{R}^n \times \mathbb{R}^n \times \mathcal{H}_0$.

Lemma 4.3.2. *(Characterizing the omega-limit set of the trajectories of the **dac+L ∂** dynamics): The omega-limit set of any trajectory of (4.12) with initial condition $(P_0, z_0, v_0) \in \mathbb{R}^n \times \mathbb{R}^n \times \mathcal{H}_0$ is contained in $\mathcal{H}_{P_l} \times \mathcal{H}_0 \times \mathcal{H}_0$.*

Proof. From (4.12c), note that $\mathbf{1}_n^\top \dot{v} = 0$. Since $v_0 \in \mathcal{H}_0$, this implies that $\mathbf{1}_n^\top v(t) = 0$ for all $t \geq 0$. Now, define $\zeta(t) = \mathbf{1}_n^\top P(t) - P_l$ and note that

$$\dot{\zeta}(t) = \mathbf{1}_n^\top \dot{P}(t) = \nu_1 \mathbf{1}_n^\top z(t),$$

where we have used (4.12a), and

$$\begin{aligned} \ddot{\zeta}(t) &= \nu_1 \mathbf{1}_n^\top \dot{z}(t) \\ &= \nu_1 \mathbf{1}_n^\top (-\alpha z(t) - \beta \mathbf{L}z(t) - v(t) + \nu_2(P_l e_k - P(t))) \\ &= -\nu_1 \alpha (\mathbf{1}_n^\top z(t)) - \nu_1 \nu_2 \zeta(t) = -\alpha \dot{\zeta}(t) - \nu_1 \nu_2 \zeta(t), \end{aligned}$$

where we have used (4.12b). We write this system as a first-order one by defining $x_1 = \zeta$ and $x_2 = \dot{\zeta}$ to get

$$\begin{bmatrix} \dot{x}_1 \\ \dot{x}_2 \end{bmatrix} = \begin{bmatrix} 0 & 1 \\ -\nu_1 \nu_2 & -\alpha \end{bmatrix} \begin{bmatrix} x_1 \\ x_2 \end{bmatrix}. \quad (4.13)$$

Evaluating the Lie derivative of the positive definite, radially unbounded function $V_2(x_1, x_2) = \nu_1 \nu_2 x_1^2 + x_2^2$ along the above dynamics and applying the LaSalle Invariance Principle [Kha02], we deduce that $x_1(t) \rightarrow 0$ and $x_2(t) \rightarrow 0$ as $t \rightarrow \infty$, that is, $\mathbf{1}_n^\top P(t) \rightarrow P_l$ and $\mathbf{1}_n^\top z(t) \rightarrow 0$. Since the system (4.13) is linear, the convergence is exponential. \square

The next result builds on this fact and Proposition 4.5.1 to establish that the trajectory of power allocations under (4.12) converges to the solution set of the ED problem.

Theorem 4.3.3. (*Convergence of the dac+L ∂ dynamics to the solutions of ED problem*): For $\alpha, \beta, \nu_1, \nu_2 > 0$ with

$$\frac{\nu_1}{\beta \nu_2 \lambda_2(\mathbf{L} + \mathbf{L}^\top)} + \frac{\nu_2^2 \lambda_{\max}(\mathbf{L}^\top \mathbf{L})}{2\alpha} < \lambda_2(\mathbf{L} + \mathbf{L}^\top), \quad (4.14)$$

the trajectories of (4.12) starting from any point in $\mathbb{R}^n \times \mathbb{R}^n \times \mathcal{H}_0$ converge to the set $\mathcal{F}_{\text{aug}}^* = \{(P, z, v) \in \mathcal{F}_{\text{ED}}^* \times \{0\} \times \mathbb{R}^n \mid v = \nu_2(P_l e_r - P)\}$.

Proof. Our proof strategy is based on the refined LaSalle Invariance Principle for differential inclusions established in Proposition 4.5.1. Before justifying that all its hypotheses are satisfied, we reformulate the expression for the dynamics to help simplify the analysis. Consider first the change of coordinates, $(P, z, v) \mapsto (P, z, \bar{v})$, with $\bar{v} = v - \nu_2(P_l e_r - P)$. The set-valued map $X_{\text{dac+L}\partial}$ then takes the form

$$\begin{aligned} X_{\text{dac+L}\partial}(P, z, \bar{v}) = \{ & (-\mathbf{L}\zeta + \nu_1 z, -(\alpha + \beta\mathbf{L})z - \bar{v}, \\ & (\alpha\beta\mathbf{L} + \nu_1\nu_2)z - \nu_2\mathbf{L}\zeta \in \mathbb{R}^{3n} \mid \zeta \in \partial f^c(P)\}. \end{aligned}$$

The change of coordinates shifts the equilibrium of the consensus dynamics to the origin. Under the additional change of coordinates $(P, z, \bar{v}) \mapsto (P, \xi_1, \xi_2)$, with

$$\begin{bmatrix} \xi_1 \\ \xi_2 \end{bmatrix} = \begin{bmatrix} I & 0 \\ \alpha I & I \end{bmatrix} \begin{bmatrix} z \\ \bar{v} \end{bmatrix}, \quad (4.15)$$

the set-valued map $X_{\text{dac}+\text{L}\partial}$ takes the form

$$\begin{aligned} X_{\text{dac}+\text{L}\partial}(P, \xi_1, \xi_2) = \{ & (-\text{L}\zeta + \nu_1\xi_1, -\beta\text{L}\xi_1 - \xi_2, \\ & \nu_1\nu_2\xi_1 - \alpha\xi_2 - \nu_2\text{L}\zeta) \in \mathbb{R}^{3n} \mid \zeta \in \partial f^\epsilon(P)\}. \end{aligned} \quad (4.16)$$

This extra change of coordinates makes it easier to identify the candidate Lyapunov function $V_3 : \mathbb{R}^{3n} \rightarrow \mathbb{R}_{\geq 0}$,

$$V_3(P, \xi_1, \xi_2) = f^\epsilon(P) + \frac{1}{2}(\nu_1\nu_2\|\xi_1\|^2 + \|\xi_2\|^2).$$

For convenience, denote the overall change of coordinates by $D : \mathbb{R}^{3n} \rightarrow \mathbb{R}^{3n}$,

$$(P, \xi_1, \xi_2) = D(P, z, v) = (P, z, v + \alpha z - \nu_2(P_1 e_r - P)).$$

Our analysis now focuses on proving that, in the new coordinates, the trajectories of (4.12) converge to the set

$$\overline{\mathcal{F}}_{\text{aug}} = D(\mathcal{F}_{\text{aug}}^*) = \mathcal{F}_{\text{ED}}^* \times \{0\} \times \{0\}.$$

Note that $D(\mathcal{H}_{P_1} \times \mathcal{H}_0 \times \mathcal{H}_0) = \mathcal{H}_{P_1} \times \mathcal{H}_0 \times \mathcal{H}_0$ and therefore, from Lemma 4.3.2, the omega-limit set of a trajectory $t \mapsto (P(t), \xi_1(t), \xi_2(t))$ starting in $D(\mathbb{R}^n \times \mathbb{R}^n \times \mathcal{H}_0)$ belongs to $\mathcal{H}_{P_1} \times \mathcal{H}_0 \times \mathcal{H}_0$.

Our next step is to show that the hypotheses of Proposition 4.5.1 are satisfied where $\mathcal{H}_{P_1} \times \mathcal{H}_0 \times \mathcal{H}_0$ and V_3 play the role of the closed submanifold \mathcal{S} of \mathbb{R}^{3n} and the function W , respectively. To do so, we resort to Lemma 4.5.3. Define the continuous function $g : \mathbb{R}^{3n} \times \mathbb{R}^{3n} \rightarrow \mathbb{R}^{3n}$ by

$$g(P, \xi_1, \xi_2, \hat{\zeta}) = (-\text{L}\hat{\zeta}_1 + \nu_1\xi_1, -\beta\text{L}\xi_1 - \xi_2, \nu_1\nu_2\xi_1 - \alpha\xi_2 - \nu_2\text{L}\hat{\zeta}_1),$$

and note that the dynamics (4.16) can be expressed as $X_{\text{dac}+\text{L}\partial}(P, \xi_1, \xi_2) = \{g(P, \xi_1, \xi_2, \hat{\zeta}) \mid \hat{\zeta} \in \partial V_3(P, \xi_1, \xi_2)\}$. For $(P, \xi_1, \xi_2) \in \mathcal{H}_{P_1} \times \mathcal{H}_0 \times \mathcal{H}_0$ and

$$\hat{\zeta} \in \partial V_3(P, \xi_1, \xi_2),$$

$$\hat{\zeta}^\top g(P, \xi_1, \xi_2, \hat{\zeta}) = -\zeta^\top \mathbf{L}\zeta + \nu_1 \zeta^\top \xi_1 - \beta \nu_1 \nu_2 \xi_1^\top \mathbf{L} \xi_1 - \alpha \|\xi_2\|^2 - \nu_2 \xi_2^\top \mathbf{L} \zeta, \quad (4.17)$$

where we have used that $\zeta = \hat{\zeta}_1 \in \partial f^\epsilon(P)$, $\hat{\zeta}_2 = \nu_1 \nu_2 \xi_1$, and $\hat{\zeta}_3 = \xi_2$. Since the digraph \mathcal{G} is strongly connected and weight-balanced, we apply (2.1) and the fact that $\mathbf{1}_n^\top \xi_1 = 0$ to bound the above expression as

$$\begin{aligned} -\frac{1}{2} \lambda_2 (\mathbf{L} + \mathbf{L}^\top) \|\eta\|^2 + \nu_1 \eta^\top \xi_1 - \frac{1}{2} \beta \nu_1 \nu_2 \lambda_2 (\mathbf{L} + \mathbf{L}^\top) \|\xi_1\|^2 \\ - \alpha \|\xi_2\|^2 - \nu_2 \xi_2^\top \mathbf{L} \eta = \gamma^\top M \gamma, \end{aligned}$$

where $\eta = \zeta - \frac{1}{n} (\mathbf{1}_n^\top \zeta) \mathbf{1}_n$, $\gamma^\top = [\eta^\top, \xi_1^\top, \xi_2^\top]$, and

$$M = \begin{bmatrix} -\frac{1}{2} \lambda_2 (\mathbf{L} + \mathbf{L}^\top) I & \frac{1}{2} \nu_1 I & -\frac{1}{2} \nu_2 \mathbf{L}^\top \\ \frac{1}{2} \nu_1 I & -\frac{1}{2} \beta \nu_1 \nu_2 \lambda_2 (\mathbf{L} + \mathbf{L}^\top) I & 0 \\ -\frac{1}{2} \nu_2 \mathbf{L} & 0 & -\alpha I \end{bmatrix}.$$

Reasoning with the Schur complement [BV09], $M \in \mathbb{R}^{3n \times 3n}$ is negative definite if

$$\begin{aligned} -\frac{1}{2} \lambda_2 (\mathbf{L} + \mathbf{L}^\top) I - \begin{bmatrix} \frac{1}{2} \nu_1 I & -\frac{1}{2} \nu_2 \mathbf{L}^\top \end{bmatrix} \begin{bmatrix} -\frac{1}{2} \beta \nu_1 \nu_2 \lambda_2 (\mathbf{L} + \mathbf{L}^\top) I & 0 \\ 0 & -\alpha I \end{bmatrix}^{-1} \begin{bmatrix} \frac{1}{2} \nu_1 I \\ -\frac{1}{2} \nu_2 \mathbf{L} \end{bmatrix} \\ = -\frac{1}{2} \lambda_2 (\mathbf{L} + \mathbf{L}^\top) I + \frac{\nu_1}{2\beta \nu_2 \lambda_2 (\mathbf{L} + \mathbf{L}^\top)} I + \frac{\nu_2^2}{4\alpha} \mathbf{L}^\top \mathbf{L}, \end{aligned}$$

is negative definite. This latter fact is implied by (4.14). As a consequence, $\hat{\zeta}^\top g(P, \xi_1, \xi_2, \hat{\zeta}) \leq 0$ and so, Lemma 4.5.3(i) holds. Moreover, $\hat{\zeta}^\top g(P, \xi_1, \xi_2, \hat{\zeta}) = 0$ if and only if $\eta = \xi_1 = \xi_2 = 0$, which means $\zeta \in \text{span}\{\mathbf{1}_n\}$. Using this fact along with the definition of the set-valued Lie derivative and the characterization of optimizers (4.4), we deduce that $\hat{\zeta}^\top g(P, \xi_1, \xi_2, \hat{\zeta}) = 0$ if and only if (a) $0 \in \mathcal{L}_{X_{\text{dac}+\text{L}\partial}} V_3(P, \xi_1, \xi_2)$ and (b) P is a solution of the ED problem. Fact (a) implies that Lemma 4.5.3(ii) holds and hence, Proposition 4.5.1(ii) holds too. Fact (b) implies that over the set $\mathcal{H}_{P_i} \times \mathcal{H}_0 \times \mathcal{H}_0$, we have $0 \in \mathcal{L}_{X_{\text{dac}+\text{L}\partial}} V_3(P, \xi_1, \xi_2)$ if and only if $(P, \xi_1, \xi_2) \in \overline{\mathcal{F}}_{\text{aug}}$. Since, $\overline{\mathcal{F}}_{\text{aug}}$ belongs to a level set of V_3 , we conclude that

Proposition 4.5.1(i) holds too.

To be able to apply Proposition 4.5.1 and conclude the proof, it remains to show that the trajectories starting from $D(\mathbb{R}^n \times \mathbb{R}^n \times \mathcal{H}_0)$ are bounded. We reason by contradiction, i.e., assume there exists a trajectory $t \mapsto (P(t), \xi_1(t), \xi_2(t))$, with initial condition $(P(0), \xi_1(0), \xi_2(0)) \in D(\mathbb{R}^n \times \mathbb{R}^n \times \mathcal{H}_0)$ of $X_{\text{dac}+\text{L}\partial}$ such that $\|(P(t), \xi_1(t), \xi_2(t))\| \rightarrow \infty$. Since V_3 is radially unbounded, this implies $V_3(P(t), \xi_1(t), \xi_2(t)) \rightarrow \infty$. Additionally, from Lemma 4.3.2, we know that $\mathbf{1}_n^\top P(t) \rightarrow P_l$ and $\mathbf{1}_n^\top \xi_1(t) \rightarrow 0$. Thus, there exists a sequence of times $\{t_k\}_{k=1}^\infty$ with $t_k \rightarrow \infty$ such that for all $k \in \mathbb{Z}_{\geq 1}$,

$$|\mathbf{1}_n^\top \xi_1(t_k)| < 1/k, \quad (4.18a)$$

$$\max \mathcal{L}_{X_{\text{dac}+\text{L}\partial}} V_3(P(t_k), \xi_1(t_k), \xi_2(t_k)) > 0. \quad (4.18b)$$

Note that (4.18b) implies that there exists a sequence $\{\zeta_k\}_{k=1}^\infty$ with $\zeta_k \in \partial f^\epsilon(P(t_k))$ such that

$$-\zeta_k^\top \mathbf{L} \zeta_k + \nu_1 \zeta_k^\top \xi_1(t_k) - \beta \nu_1 \nu_2 \xi_1(t_k)^\top \mathbf{L} \xi_1(t_k) - \alpha \|\xi_1(t_k)\|^2 - \nu_2 \xi_2(t_k)^\top \mathbf{L} \zeta_k > 0,$$

for all $k \in \mathbb{Z}_{\geq 1}$, where we have used the fact that an element of $\mathcal{L}_{X_{\text{dac}+\text{L}\partial}} V_3(P, \xi_1, \xi_2)$ has the form given in (4.17). Letting $\eta_k = \zeta_k - \frac{1}{n}(\mathbf{1}_n^\top \zeta_k) \mathbf{1}_n$, we use (2.1) to deduce from the above inequality that

$$\begin{aligned} & -\frac{1}{2} \lambda_2 (\mathbf{L} + \mathbf{L}^\top) \|\eta_k\|^2 + \nu_1 \eta_k^\top \xi_1(t_k) + \frac{1}{n} \nu_1 (\mathbf{1}_n^\top \zeta_k) (\mathbf{1}_n^\top \xi_1(t_k)) \\ & - \frac{1}{2} \beta \nu_1 \nu_2 \lambda_2 (\mathbf{L} + \mathbf{L}^\top) \|\xi_1(t_k) - \frac{1}{n} (\mathbf{1}_n^\top \xi_1(t_k)) \mathbf{1}_n\|^2 \\ & - \alpha \|\xi_1(t_k)\|^2 - \nu_2 \xi_2(t_k)^\top \mathbf{L} \eta_k > 0. \end{aligned}$$

Further, using the expression

$$\|\xi_1(t_k) - \frac{1}{n} (\mathbf{1}_n^\top \xi_1(t_k)) \mathbf{1}_n\|^2 = \|\xi_1(t_k)\|^2 - \frac{1}{n} (\mathbf{1}_n^\top \xi_1(t_k))^2,$$

the inequality can be rewritten as

$$\gamma_k^\top M \gamma_k + \frac{1}{n} \nu_1 (\mathbf{1}_n^\top \zeta_k) (\mathbf{1}_n^\top \xi_1(t_k)) + \frac{\beta \nu_1 \nu_2}{2n} \lambda_2(\mathbf{L} + \mathbf{L}^\top) (\mathbf{1}_n^\top \xi_1(t_k))^2 > 0,$$

where $\gamma_k^\top = [\eta_k^\top, \xi_1(t_k)^\top, \xi_2(t_k)^\top]$. Using now the bound (4.18a), we arrive at the inequality,

$$\gamma_k^\top M \gamma_k + \frac{\nu_1}{nk} |\mathbf{1}_n^\top \zeta_k| + \frac{\beta \nu_1 \nu_2}{2nk^2} \lambda_2(\mathbf{L} + \mathbf{L}^\top) > 0. \quad (4.19)$$

Next, we consider two cases, depending on whether the sequence $\{P(t_k)\}$ is (a) bounded or (b) unbounded. In case (a), the sequence $\{(\xi_1(t_k), \xi_2(t_k))\}$ must be unbounded. Since M is negative definite, we have $\gamma_k^\top M \gamma_k \leq \lambda_{\max}(M) \|(\xi_1(t_k), \xi_2(t_k))\|^2$. Thus, (4.19) implies that

$$\lambda_{\max}(M) \|(\xi_1(t_k), \xi_2(t_k))\|^2 + \frac{\nu_1}{nk} |\mathbf{1}_n^\top \zeta_k| + \frac{\beta \nu_1 \nu_2}{2nk^2} \lambda_2(\mathbf{L} + \mathbf{L}^\top) > 0.$$

Now, from the expression of ∂f^ϵ , since $\{P(t_k)\}$ is bounded, the sequence $\{\zeta_k\}$ must be bounded. Combining these facts with $\lambda_{\max}(M) < 0$, one can find $\bar{k} \in \mathbb{Z}_{\geq 1}$ such that the above inequality is violated for all $k \geq \bar{k}$, which is a contradiction. For case (b), we use the bound $\gamma_k^\top M \gamma_k \leq \lambda_{\max}(M) \|\eta_k\|^2$ to deduce from (4.19) that

$$\lambda_{\max}(M) \|\eta_k\|^2 + \frac{\nu_1}{nk} |\mathbf{1}_n^\top \zeta_k| + \frac{\beta \nu_1 \nu_2}{2nk^2} \lambda_2(\mathbf{L} + \mathbf{L}^\top) > 0.$$

One can then use a similar argument as laid out in the proof of Theorem 4.2.1, considering the two cases of $|\mathbf{1}_n^\top \zeta_k|$ being bounded or unbounded, arriving in both cases at similar contradictions. This concludes the proof. \square

Note that as a consequence of the above result, the **dac+L ∂** dynamics do not require any specific pre-processing for the initialization of the power allocations. Each generator can select any generation level, independent of the other units, and the algorithm guarantees convergence to the solutions of the ED problem.

Remark 4.3.4. (*Distributed selection of algorithm design parameters*): The convergence of the **dac+L ∂** dynamics relies on a selection of the parameters α , β , ν_1 and $\nu_2 \in \mathbb{R}_{>0}$ that satisfy (4.14). Checking this inequality requires knowledge of

the spectrum of matrices related to the Laplacian matrix, and hence the entire network structure. Here, we provide an alternative condition that implies (4.14) and can be checked by the units in a distributed way. Let n_{\max} be an upper bound on the number of units, d_{\max}^{out} be an upper bound on the out-degree of all units, and a_{\min} be a lower bound on the edge weights,

$$n \leq n_{\max}, \max_{i \in \mathcal{V}} d^{\text{out}}(i) \leq d_{\max}^{\text{out}}, \min_{(i,j) \in \mathcal{E}} a_{ij} \geq a_{\min}. \quad (4.20)$$

A straightforward generalization of [Moh91, Theorem 4.2] for weighted graphs gives rise to the following lower bound on $\lambda_2(\mathbf{L} + \mathbf{L}^\top)$,

$$\frac{4a_{\min}}{n_{\max}^2} \leq \lambda_2(\mathbf{L} + \mathbf{L}^\top). \quad (4.21)$$

On the other hand, using properties of matrix norms [Ber05, Chapter 9], one can deduce

$$\lambda_{\max}(\mathbf{L}^\top \mathbf{L}) = \|\mathbf{L}\|^2 \leq (\sqrt{n} \|\mathbf{L}\|_\infty)^2 \leq (2\sqrt{n} d_{\max}^{\text{out}})^2 \leq 4n_{\max} (d_{\max}^{\text{out}})^2. \quad (4.22)$$

Using (4.21)-(4.22), the left-hand side of (4.14) can be upper bounded by

$$\frac{\nu_1}{\beta \nu_2 \lambda_2(\mathbf{L} + \mathbf{L}^\top)} + \frac{\nu_2^2 \lambda_{\max}(\mathbf{L}^\top \mathbf{L})}{2\alpha} \leq \frac{\nu_1 n_{\max}^2}{4a_{\min} \beta \nu_2} + \frac{2\nu_2^2 n_{\max} (d_{\max}^{\text{out}})^2}{\alpha}.$$

Further, the right-hand side of (4.14) can be lower bounded using (4.21). Putting the two together, we obtain the new condition

$$\frac{\nu_1 n_{\max}^2}{4a_{\min} \beta \nu_2} + \frac{2\nu_2^2 n_{\max} (d_{\max}^{\text{out}})^2}{\alpha} < \frac{4a_{\min}}{n_{\max}^2}, \quad (4.23)$$

which implies (4.14). The network can ensure that this condition is met in various ways. For instance, if the bounds n_{\max} , d_{\max}^{out} , and a_{\min} are not available, the network can implement distributed algorithms for max- and min-consensus [RB08] to compute them in finite time. Once known, any generator can select α , β , ν_1 and ν_2 satisfying (4.23) and broadcast its choice. Alternatively, the computation of the design parameters can be implemented concurrently with the determination

of the bounds via consensus by specifying a specific formula to select them that is guaranteed to satisfy (4.23). Note that the units necessarily need to agree on the parameters, otherwise if each unit selects a different set of parameters, the dynamic average consensus would not track the average input signal. •

Remark 4.3.5. (*Distributed loads and transmission losses*): Here we expand on our observations in Remark 4.1.1 regarding the inclusion of additional constraints on the ED problem. Our algorithmic solution can be easily modified to deal with the alternative scenarios studied in [ZYC11, KH12, BDL⁺14, LV14], where each generator has the knowledge of the load at the corresponding bus that it is connected to and the total load is the aggregate of these individual loads. Mathematically, denoting the load demanded at generator bus i by $P_i^L \in \mathbb{R}$, the total load is given by $P_l = \sum_{i=1}^n P_i^L$. For this case, replacing the vector $P_l e_r$ by P^L in the **dac**+ $L\partial$ dynamics (4.12b) gives an algorithm that solves the ED problem for the load P_l . Our solution strategy can also handle transmission losses as modeled in [BDL⁺14], where it is assumed that each generator i can estimate the power loss in the transmission lines adjacent to it. With those values available, the generator could add them to the quantity P_i^L , which would make the network find a power allocation that takes care of the transmission losses. •

4.3.2 Robustness analysis

In this section, we study the robustness properties of the **dac**+ $L\partial$ dynamics in the presence of time-varying load signals and intermittent power unit generation. Our analysis relies on the exponential stability of the mismatch dynamics between total generation and load established in Lemma 4.3.2, which implies that (4.13) is input-to-state stable (ISS) [Kha02, Lemma 4.6], and consequently robust against arbitrary bounded perturbations. The following result provides an explicit, exponentially decaying, bound for the evolution of any trajectory of (4.13). While the rate of decay can also be determined by computing the eigenvalues of matrix defining the dynamics, here we employ a Lyapunov argument to obtain also the value of the gain associated to the rate.

Lemma 4.3.6. (Convergence rate of the mismatch dynamics (4.13)): Let $R \in \mathbb{R}^{2 \times 2}$ be defined by

$$R = \frac{1}{2\alpha\nu_1\nu_2} \begin{bmatrix} \alpha^2 + \nu_1\nu_2 + (\nu_1\nu_2)^2 & \alpha \\ \alpha & 1 + \nu_1\nu_2 \end{bmatrix}.$$

Then $R \succ 0$ and any trajectory $t \mapsto x(t)$ of the dynamics (4.13) satisfies $\|x(t)\| \leq c_1 e^{-c_2 t} \|x(0)\|$, where $c_1 = \sqrt{\lambda_{\max}(R)/\lambda_{\min}(R)}$ and $c_2 = 1/2\lambda_{\max}(R)$.

Proof. Let $A \in \mathbb{R}^{2 \times 2}$ be the system matrix of (4.13). Then, one can see that $A^\top R + RA = -I$, i.e., $V_4(x) = x^\top R x$ is a Lyapunov function for (4.13). Note that

$$\lambda_{\min}(R)\|x\|^2 \leq V_4(x) \leq \lambda_{\max}(R)\|x\|^2. \quad (4.24)$$

From the Lyapunov equation, we have $\mathcal{L}_{Ax} V_4(x) = -\|x\|^2 \leq -\frac{1}{\lambda_{\max}(R)} V_4(x)$, which implies $V_4(x(t)) \leq e^{-1/\lambda_{\max}(R)t} V_4(x(0))$ along any trajectory $t \mapsto x(t)$ of (4.13). Again using (4.24), we get

$$\|x(t)\|^2 \leq \frac{\lambda_{\max}(R)}{\lambda_{\min}(R)} e^{-1/\lambda_{\max}(R)t} \|x(0)\|^2,$$

which concludes the claim. \square

In the above result, it is interesting to note that the convergence rate is independent of the specific communication digraph (as long as it is weight-balanced). We use next the exponentially decaying bound obtained above to illustrate the extent to which the network can collectively track a dynamic load (which corresponds to a time-varying perturbation in the mismatch dynamics) and is robust to intermittent power generation (which corresponds to perturbations in the state of the mismatch dynamics).

Tracking dynamic loads

Here we consider a time-varying total load given by a twice continuously differentiable trajectory $\mathbb{R}_{\geq 0} \ni t \mapsto P_l(t)$ and show how the total generation of the network under the $\text{dac}+L\partial$ dynamics tracks it. We assume the signal is known to

an arbitrary unit $r \in [n]$. In this case, the dynamics (4.13) take the following form

$$\begin{bmatrix} \dot{x}_1 \\ \dot{x}_2 \end{bmatrix} = \begin{bmatrix} 0 & 1 \\ -\nu_1\nu_2 & -\alpha \end{bmatrix} \begin{bmatrix} x_1 \\ x_2 \end{bmatrix} + \begin{bmatrix} 0 \\ -\alpha\dot{P}_l - \ddot{P}_l \end{bmatrix}.$$

Using Lemma 4.3.6, one can compute the following bound on any trajectory of the above system

$$\|x(t)\| \leq c_1 e^{-c_2 t} \|x(0)\| + \frac{c_1}{c_2} \sup_{s \in [0, t]} \left| \alpha \dot{P}_l(s) + \ddot{P}_l(s) \right|.$$

In particular, for a signal with bounded \dot{P}_l and \ddot{P}_l , the mismatch between generation and load, i.e., $x_1(t)$ is bounded. Also, the mismatch has an ultimate bound as $t \rightarrow \infty$. The following result summarizes this notion formally. The proof is straightforward application of Lemma 4.3.6 following the exposition of input-to-state stability in [Kha02].

Proposition 4.3.7. (*Power mismatch is ultimately bounded for dynamic load under the $\text{dac}+\text{L}\partial$ dynamics*): Let $\mathbb{R}_{\geq 0} \ni t \mapsto P_l(t)$ be twice continuously differentiable and such that

$$\sup_{t \geq 0} \left| \dot{P}_l(t) \right| \leq d_1, \quad \sup_{t \geq 0} \left| \ddot{P}_l(t) \right| \leq d_2,$$

for some $d_1, d_2 > 0$. Then, the mismatch $\mathbf{1}_n^\top P(t) - P_l(t)$ between load and generation is bounded along the trajectories of (4.12) and has ultimate bound $\frac{c_1}{c_2}(\alpha d_1 + d_2)$, with c_1, c_2 given in Lemma 4.3.6. Moreover, if $\dot{P}_l(t) \rightarrow 0$ and $\ddot{P}_l(t) \rightarrow 0$ as $t \rightarrow \infty$, then $\mathbf{1}_n^\top P(t) \rightarrow P_l(t)$ as $t \rightarrow \infty$.

Robustness to intermittent power generation

Here, we characterize the algorithm robustness against unit addition and deletion to capture scenarios with intermittent power generation. Addition and deletion events are modeled via a time-varying communication digraph, which we assume remains strongly connected and weight-balanced at all times. When a unit stops generating power (deletion event), the corresponding vertex and its adjacent

edges are removed. When a unit starts providing power (addition event), the corresponding node is added to the digraph along with a set of edges. Given the intricacies of the convergence analysis for the $\mathbf{dac}+\mathbf{L}\partial$ dynamics, cf. Theorem 4.3.3, it is important to make sure that the state v remains in the set \mathcal{H}_0 , irrespectively of the discontinuities caused by the events. The following routine makes sure that this is the case.

TRAJECTORY INVARIANCE: When a unit i joins the network at time t , it starts with $v_i(t) = 0$. When a unit i leaves the network at time t , it passes a token with value $v_i(t)$ to one of its in-neighbors $j \in \mathcal{N}^{\text{in}}(i)$, who resets its value to $v_j(t) + v_i(t)$.

The TRAJECTORY INVARIANCE routine ensures that the dynamics (4.13) are the appropriate description for the evolution of the load satisfaction mismatch. This, together with the ISS property established in Lemma 4.3.6, implies that the mismatch effect in power generation caused by addition/deletion events vanishes exponentially fast. In particular, if the number of addition/deletion events is finite, then the set of generators converge to the solution of the ED problem. We formalize this next.

Proposition 4.3.8. *(Convergence of the $\mathbf{dac}+\mathbf{L}\partial$ dynamics under intermittent power generation): Let n_{max} be the maximum number of generators that can contribute to the power generation at any time. Let $\Sigma_{n_{max}}$ be the set of digraphs that are strongly connected and weight-balanced and whose vertex set is included in $[n_{max}]$. Let $\sigma : [0, \infty) \rightarrow \Sigma_{n_{max}}$ be a piecewise constant, right-continuous switching signal described by the set of switching times $\{t_1, t_2, \dots\} \subset \mathbb{R}_{\geq 0}$, with $t_k \leq t_{k+1}$, each corresponding to either an addition or a deletion event. Denote by $X_{\mathbf{dac}+\mathbf{L}\partial}^\sigma$ the switching $\mathbf{dac}+\mathbf{L}\partial$ dynamics corresponding to σ , defined by (4.12) with \mathbf{L} replaced by $\mathbf{L}(\sigma(t))$ for all $t \geq 0$, and assume agents execute the TRAJECTORY INVARIANCE routine when they leave or join the network. Then,*

- (i) *at any time $t \in \{0\} \cup \{t_1, t_2, \dots\}$, if the variables $(P(t), z(t))$ for the generators in $\sigma(t)$ satisfy $|\mathbf{1}_n^\top P(t) - P_l| \leq M_1$ and $|\mathbf{1}_n^\top z(t)| \leq M_2$ for some $M_1, M_2 > 0$, then the magnitude of the mismatch between generation and*

load becomes less than or equal to $\rho > 0$ in time

$$t_\rho = \frac{1}{c_2} \ln\left(\frac{c_1(M_1 + \nu_1 M_2)}{\rho}\right),$$

provided no event occurs in the interval $(t, t + t_\rho)$;

- (ii) if the number of events is finite, say N , then the trajectories of $X_{\text{dac}+\text{L}\partial}^\sigma$ converge to the set of solutions of the ED problem for the group of generators in $\sigma(t_N)$ provided (4.14) is met for $\sigma(t_N)$.

Note that the generators can ensure that the condition (4.14), required for the convergence of the **dac**+**L** ∂ dynamics, holds at all times even under addition and deletion events, if they rely on verifying that (4.23) holds and the bounds (4.20) are valid for all the topologies in $\Sigma_{n_{\max}}$.

4.4 Simulations in a IEEE 118 bus system

This section illustrates the convergence of the **dac**+**L** ∂ dynamics to the solutions of the ED problem (4.1) starting from any initial power allocation and its robustness properties. We consider the IEEE 118 bus system [IEE], that consists of 54 generators. The cost function of each generator i is quadratic, $f_i(P_i) = a_i + b_i P_i + c_i P_i^2$, with coefficients belonging to the ranges $a_i \in [6.78, 74.33]$, $b_i \in [8.3391, 37.6968]$, and $c_i \in [0.0024, 0.0697]$. The communication topology is the digraph \mathcal{G} described in Table 4.1.

We choose the design parameters as $\nu_1 = 1, \nu_2 = 1.3, \alpha = 10, \beta = 40, \epsilon = 0.0086$, which satisfy the conditions (4.3) and (4.14) for \mathcal{G} . The total load is 4600 for the first 150 seconds and 4200 for the next 150 seconds, and is known to unit 3. Figure 4.1(a)-(c) depicts the evolution of the power allocation, total cost, and the mismatch between the total generation and load under the **dac**+**L** ∂ dynamics starting at the initial condition $(P(0), z(0), v(0)) = (0.5 * (P^m + P^M), 0, 0)$. Note that the generators initially converge to a power allocation that meets the load 4600 and minimizes the total cost of generation. Later, with the decrease in desired load to 4200, the network decreases the total generation while minimizing the total

Table 4.1: Definition of the digraphs \mathcal{G} , $\hat{\mathcal{G}}$, $\hat{\mathcal{G}}_{\{4,11,25,45\}}$, and $\hat{\mathcal{G}}_{\{4,25,27\}}$.

\mathcal{G}	digraph over 54 vertices consisting of a directed cycle through vertices $1, \dots, 54$ and bi-directional edges $\{(i, \text{id}_{54}(i+5)), (i, \text{id}_{54}(i+10)), (i, \text{id}_{54}(i+15)), (i, \text{id}_{54}(i+20))\}$ for each $i \in [54]$, where $\text{id}_{54}(x) = x$ if $x \in [54]$ and $x - 54$ otherwise. All edge weights are 0.1.
$\hat{\mathcal{G}}$	obtained from \mathcal{G} by replacing the directed cycle with an undirected one keeping the edge weights same
$\hat{\mathcal{G}}_{\{4,11,25,45\}}$	obtained from $\hat{\mathcal{G}}$ by removing the vertices $\{4, 11, 25, 45\}$ and the edges adjacent to them
$\hat{\mathcal{G}}_{\{4,25,27\}}$	obtained from $\hat{\mathcal{G}}$ by removing the vertices $\{4, 25, 27\}$ and the edges adjacent to them

cost. Figure 4.1(d)-(f) shows the performance of the ratio-consensus algorithm from [DGCH12] for the same initial condition and communication topology. One can observe that the $\text{dac}+\text{L}\partial$ dynamics shows better transient behavior when the load changes.

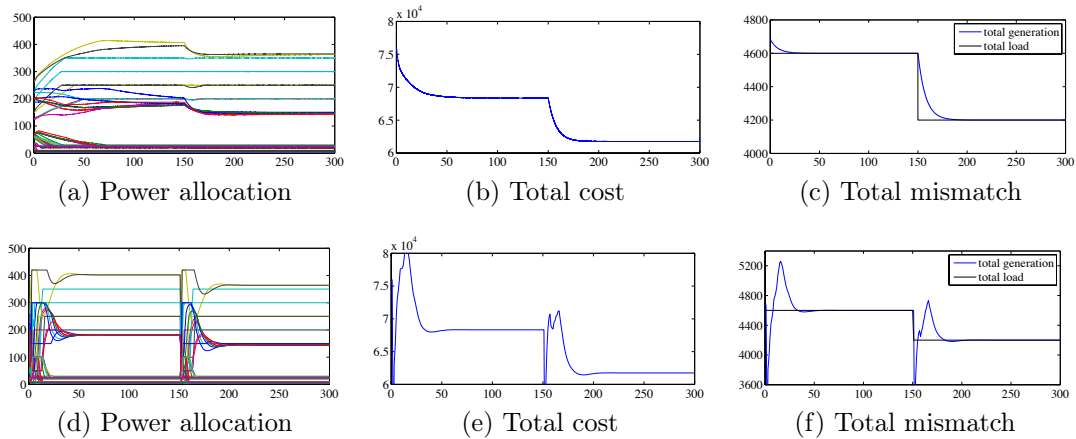


Figure 4.1: Evolution of the power allocation, the total cost, and the total mismatch between generation and load under the $\text{dac}+\text{L}\partial$ dynamics (a)-(c) and the ratio-consensus algorithm (d)-(f) from [DGCH12] for the IEEE 118 bus example. The communication topology is \mathcal{G} , the load is initially 4600 and later 4200. For $\text{dac}+\text{L}\partial$, the parameters are $\nu_1 = 1$, $\nu_2 = 1.3$, $\alpha = 10$, $\beta = 40$, and $\epsilon = 0.0086$. Both algorithms converge to the optimizer but $\text{dac}+\text{L}\partial$ shows better transient behavior when the load changes at $t = 150\text{s}$.

Next, we consider a time-varying total load given by a constant plus a sinusoid, $P_l(t) = 4300 + 100 \sin(0.05t)$. With the same communication topology, design

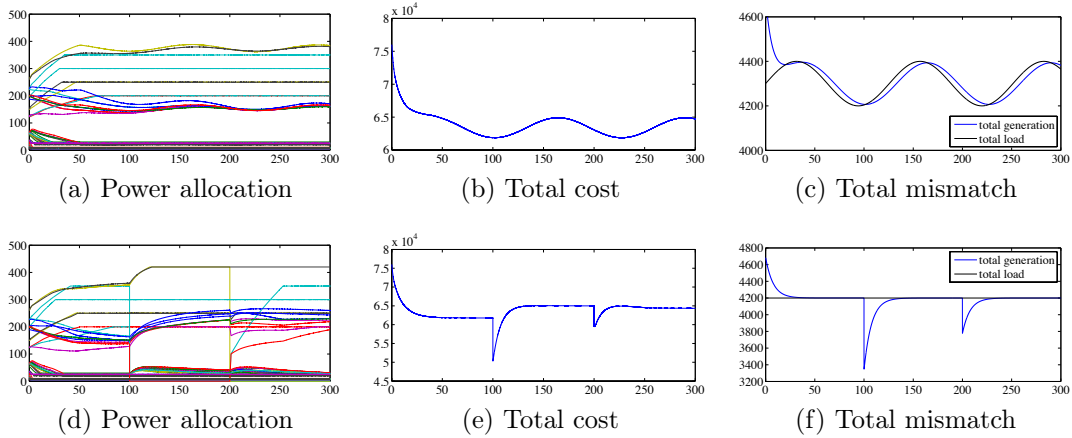


Figure 4.2: Performance of the $\text{dac}+\text{L}\partial$ dynamics for the IEEE 118 bus system under time-varying load and generator addition and deletion. Keeping the communication topology, design parameters, and the initial condition same, plots (a)-(c) show the evolution of the power allocation, total cost, and the total mismatch under the dynamics for the time-varying load given by $P_l(t) = 4300 + 100 \sin(0.05t)$. In the last case (d)-(f), the parameters remain the same, the communication graph is initially the graph $\hat{\mathcal{G}}$. At $t = 100s$, units $\{4, 11, 25, 45\}$ leave the network, resulting in the communication topology $\hat{\mathcal{G}}_{\setminus\{4,11,25,45\}}$, and the remaining agents run the TRAJECTORY INVARIANCE routine. Later, at $t = 200s$, units $\{11, 45\}$ join the network while unit 27 leaves it, resulting in the communication topology $\hat{\mathcal{G}}_{\setminus\{4,25,27\}}$. After implementing the TRAJECTORY INVARIANCE routine, the $\text{dac}+\text{L}\partial$ algorithm eventually converges to an optimizer of the ED problem for the network $\hat{\mathcal{G}}_{\setminus\{4,25,27\}}$.

parameters, and initial condition as above, Figure 4.2 (a)-(c) illustrates the behavior of the network under the $\text{dac}+\text{L}\partial$ dynamics. As established in Proposition 4.3.7, the total generation tracks the time-varying load signal and the mismatch between these values has an ultimate bound. Additionally, to illustrate how that the mismatch vanishes if the load becomes constant, we show in Figure 4.3 a load signal that consists of short bursts of sinusoidal variation that decay exponentially. The difference between generation and load becomes smaller and smaller as the load tends towards a constant signal.

Our final scenario considers addition and deletion of generators. The initial communication topology is the undirected graph $\hat{\mathcal{G}}$ described in Table 4.1. The design parameters and the initial condition are the same as above. The total load is 4200 and is same at all times. For the first 100 seconds, the power allocations converge to a neighborhood of a solution of the ED problem for the set of generators in $\hat{\mathcal{G}}$. At time $t = 100\text{s}$, the units $\{4, 11, 25, 45\}$ stop generating power and leave the network. We select these generators because of their substantial impact in the total power generation. After this event, the resulting communication graph is $\hat{\mathcal{G}}_{\setminus\{4,11,25,45\}}$, cf. Table 4.1. The generators implement the TRAJECTORY INVARIANCE routine, after which the $\text{dac}+\text{L}\partial$ algorithm drives the mismatch to zero and minimizes the total cost. At $t_2 = 200\text{s}$, another event occurs, the units $\{11, 45\}$ get added to the network while the generator 27 leaves. The resulting communication topology is $\hat{\mathcal{G}}_{\{4,25,27\}}$, cf. Table 4.1. After executing the TRAJECTORY INVARIANCE routine, the algorithm converges eventually to the optimizers of the ED problem for the set of generators in $\hat{\mathcal{G}}_{\{4,25,27\}}$, as shown in Figure 4.2(d)-(f). This example illustrates the robustness of the $\text{dac}+\text{L}\partial$ dynamics against intermittent generation by the units, as formally established in Proposition 4.3.8. In addition to the presented examples, we also successfully simulated scenarios of the kind described in Remark 4.3.5, where the total load is not known to a single generator and is instead the aggregate of the local loads connected to each of the generator buses, but we do not report them here for space reasons. We have also observed in multiple simulations that the $\text{dac}+\text{L}\partial$ dynamics respects the box constraints along its trajectories if they are satisfied at the initial condition.

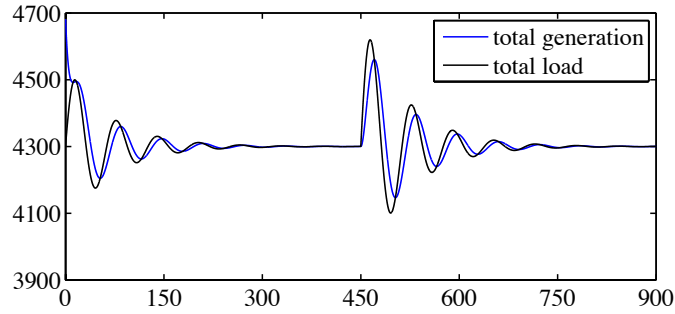


Figure 4.3: Evolution of the total power generation for the IEEE 118 bus example under the $\text{dac}+\text{L}\partial$ dynamics for the communication digraph \mathcal{G} , design parameters $\nu_1 = 1$, $\nu_2 = 1.3$, $\alpha = 10$, $\beta = 40$ and $\epsilon = 0.0086$, and time-varying total load. The example depicts the input-to-state stability of the mismatch dynamics.

4.5 Refined LaSalle Invariance Principle for differential inclusions

In this section we provide a refinement of the LaSalle Invariance Principle for differential inclusions, see e.g., [Cor08], by extending the results of [AE10] for differential equations. Our motivation for developing this refinement comes from the need to provide the necessary tools to tackle the convergence analysis of the coordination algorithms presented in Sections 4.2 and 4.3. Nevertheless, the results stated here are of independent interest.

Proposition 4.5.1. (*Refined LaSalle Invariance Principle for differential inclusions*): *Let $F : \mathbb{R}^n \rightrightarrows \mathbb{R}^n$ be upper semicontinuous, taking nonempty, convex, and compact values at every point $x \in \mathbb{R}^n$. Consider the differential inclusion $\dot{x} \in F(x)$ and let $t \mapsto \varphi(t)$ be a bounded solution whose omega-limit set $\Omega(\varphi)$ is contained in $\mathcal{S} \subset \mathbb{R}^n$, a closed embedded submanifold of \mathbb{R}^n . Let \mathcal{O} be an open neighborhood of \mathcal{S} where a locally Lipschitz, regular function $W : \mathcal{O} \rightarrow \mathbb{R}$ is defined. Assume the following holds,*

- (i) *the set $\mathcal{E} = \{x \in \mathcal{S} \mid 0 \in \mathcal{L}_F W(x)\}$ belongs to a level set of W ,*
- (ii) *for any compact set $\mathcal{M} \subset \mathcal{S}$ with $\mathcal{M} \cap \mathcal{E} = \emptyset$, there exists a compact neighborhood \mathcal{M}_c of \mathcal{M} in \mathbb{R}^n and $\delta < 0$ such that $\sup_{x \in \mathcal{M}_c} \max \mathcal{L}_F W(x) \leq \delta$.*

Then, $\Omega(\varphi) \subset \mathcal{E}$.

Before proceeding with the proof of the result, we establish an auxiliary result.

Lemma 4.5.2. *Under the hypotheses of Proposition 4.5.1, the sets $\Omega(\varphi)$ and \mathcal{E} have nonempty intersection.*

Proof. By contradiction, assume $\Omega(\varphi) \cap \mathcal{E} = \emptyset$. Then, using the hypothesis (ii) in Proposition 4.5.1, there exists $\delta < 0$ such that $\sup_{x \in \Omega(\varphi)} \max \mathcal{L}_F W(x) \leq \delta$. Let $x \in \Omega(\varphi)$. Since this set is weakly positively invariant, there exists a trajectory $t \mapsto \tilde{\varphi}(t)$ of the differential inclusion with $\tilde{\varphi}(0) = x$ such that $\tilde{\varphi}(t) \in \Omega(\varphi)$. Since $\frac{d}{dt}W(\tilde{\varphi}(t)) \in \mathcal{L}_F W(\tilde{\varphi}(t))$ for almost all $t \geq 0$, we get $W(\tilde{\varphi}(t)) - W(x) \leq \delta t$. This is in contradiction with the fact that $t \mapsto \tilde{\varphi}(t)$ belongs to the compact set $\Omega(\varphi)$, where W is lower bounded. \square

We are now ready to prove Proposition 4.5.1.

Proof of Proposition 4.5.1. We consider two cases, depending on whether the set $\Omega(\varphi)$ (a) is or (b) is not contained in a level set of W . In case (a), given any $x \in \Omega(\varphi)$, there exists a trajectory of F starting at x that remains in $\Omega(\varphi)$ (because of the weak positive invariance of the omega-limit set). If $x \notin \mathcal{E}$, then by the hypotheses (ii), there exists a compact neighborhood \mathcal{M}_x of x in \mathbb{R}^n and $\delta < 0$ such that $\sup_{y \in \mathcal{M}_x} \mathcal{L}_F W(y) \leq \delta$. Since $\Omega(\varphi) \subset \mathcal{S}$, the trajectory of F starting at x remains in the set $\mathcal{M}_x \cap \mathcal{S}$ for a finite time, say t_1 . Over the time interval $[0, t_1]$, we have $W(t) - W(0) \leq \delta t$. This, however, is in contradiction with the fact that the trajectory belongs to $\Omega(\varphi)$ which is contained in a level set of W . Therefore, $x \in \mathcal{E}$, and since this point is generic, we conclude $\Omega(\varphi) \subset \mathcal{E}$.

Next, we consider case (b) and reason by contradiction, i.e., assume that $\Omega(\varphi)$ is not contained in \mathcal{E} (see Figure 4.4). Given $\epsilon > 0$, let $\mathcal{B}_\epsilon \subset \mathcal{O}$ be a compact neighborhood of $\Omega(\varphi)$ in \mathbb{R}^n such that $d(\mathcal{B}_\epsilon, \Omega(\varphi)) \leq \epsilon$. Let \mathcal{U} be an open neighborhood of \mathcal{E} in \mathbb{R}^n and define $\mathcal{U}_\epsilon = \mathcal{U} \cap \mathcal{B}_\epsilon$. Note that \mathcal{U}_ϵ is nonempty because $\Omega(\varphi) \cap \mathcal{E}$ is nonempty by Lemma 4.5.2. Since $\Omega(\varphi)$ is not contained in a level set of W but \mathcal{E} is by hypotheses (i), we can choose $P \in \Omega(\varphi) \setminus \mathcal{E}$ such that

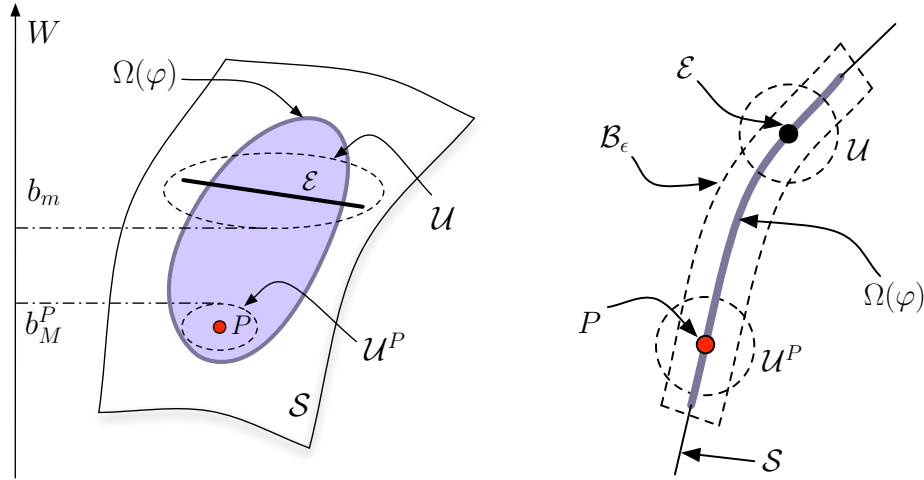


Figure 4.4: Illustration (adapted from [AE10, Figure 1]) depicting various elements involved in the case (b) of the proof of Proposition 4.5.1.

$W(P) \neq W(\mathcal{E})$. Without loss of generality, assume $W(P) < W(\mathcal{E})$ (the reasoning is analogous for the other case). Select an open neighborhood \mathcal{U}^P of P in \mathbb{R}^n and define $\mathcal{U}_\epsilon^P = \mathcal{U}^P \cap \mathcal{B}_\epsilon$. Define the following quantities

$$b_m = \inf_{x \in \mathcal{U}_\epsilon} W(x), \quad b_M^P = \sup_{x \in \mathcal{U}_\epsilon^P} W(x).$$

Note that the neighborhoods \mathcal{U} and \mathcal{U}^P can be chosen such that the set $\Omega(\varphi) \setminus (\mathcal{U} \cup \mathcal{U}^P)$ is nonempty, compact, and its intersection with \mathcal{E} is empty. Along with this, one can select ϵ in such a way that $b_m > b_M^P$ and from assumption (ii) we get

$$\sup_{x \in \mathcal{B}_\epsilon \setminus (\mathcal{U} \cup \mathcal{U}^P)} \max \mathcal{L}_F W(x) \leq \delta < 0, \quad (4.25)$$

(in the case $W(P) > W(\mathcal{E})$, we would reason with the quantities $b_M = \sup_{x \in \mathcal{U}_\epsilon} W(x)$ and $b_m^P = \inf_{x \in \mathcal{U}_\epsilon^P} W(x)$). Since $\Omega(\varphi)$ is the omega-limit set of φ and \mathcal{B}_ϵ is a compact neighborhood of $\Omega(\varphi)$, there exists $t_1 > 0$ such that $\varphi(t_1) \in \mathcal{U}_\epsilon^P$ and $\varphi(t) \in \mathcal{B}_\epsilon$ for all $t \geq t_1$. Moreover, since $\Omega(\varphi) \cap \mathcal{E}$ is nonempty, there must also exist $t_2 > t_1$ such that $\varphi(t_2) \in \mathcal{U}_\epsilon$. From continuity of the trajectory we deduce that there exist times $t_1^*, t_2^* \in (t_1, t_2)$, $t_1^* < t_2^*$ such that $\varphi(t_1^*)$ and $\varphi(t_2^*)$ lie on the boundary of the compact set $\mathcal{B}_\epsilon \setminus (\mathcal{U}_\epsilon \cup \mathcal{U}_\epsilon^P)$, with $\varphi(t_1^*)$ belonging to

the closure of \mathcal{U}_ϵ^P and $\varphi(t_2^*)$ to the closure of \mathcal{U}_ϵ . However, this is not possible as $W(\varphi(t_2^*)) \geq b_m > b_M^P \geq W(\varphi(t_1^*))$ and, in the interval $[t_1^*, t_2^*]$, the trajectory belongs to $\mathcal{B}_\epsilon \setminus (\mathcal{U}_\epsilon \cup \mathcal{U}_\epsilon^P)$, where the function W can only decrease due to (4.25), which is a contradiction. \square

Here we present an auxiliary result that aids the proof of Proposition 4.5.1.

Lemma 4.5.3. (*Continuity property of set-valued Lie derivatives*): *Let $W : \mathbb{R}^n \rightarrow \mathbb{R}$ be a locally Lipschitz and regular function. Let $g : \mathbb{R}^n \times \mathbb{R}^n \rightarrow \mathbb{R}^n$ be a continuous function and define the set-valued map $F : \mathbb{R}^n \rightrightarrows \mathbb{R}^n$ by $F(x) = \{g(x, \zeta) \mid \zeta \in \partial W(x)\}$. Assume that*

- (i) \mathcal{S} is an embedded submanifold of \mathbb{R}^n such that $\zeta^\top g(x, \zeta) \leq 0$ for all $x \in \mathcal{S}$ and all $\zeta \in \partial W(x)$,
- (ii) for any $x \in \mathcal{S}$, if $\zeta^\top g(x, \zeta) = 0$ for some $\zeta \in \partial W(x)$, then $x \in \mathcal{E} = \{z \in \mathcal{S} \mid 0 \in \mathcal{L}_F W(z)\}$.

Then, for any compact set $\mathcal{M} \subset \mathcal{S}$ with $\mathcal{M} \cap \mathcal{E} = \emptyset$, there exists a compact neighborhood \mathcal{M}_c of \mathcal{M} in \mathbb{R}^n and $\delta < 0$ such that $\sup_{x \in \mathcal{M}_c} \max \mathcal{L}_F W(x) \leq \delta$.

Proof. We reason by contradiction, i.e., assume that for all compact neighborhoods \mathcal{M}_c of \mathcal{M} in \mathbb{R}^n and all $\delta < 0$, we have

$$\sup_{x \in \mathcal{M}_c} \max \mathcal{L}_F W(x) > \delta.$$

Note that this implies that $\sup_{x \in \mathcal{M}_c} \max \mathcal{L}_F W(x) \geq 0$. Now, for each $k \in \mathbb{Z}_{\geq 1}$, consider the compact neighborhood $\mathcal{M}_k = \mathcal{M} + \overline{B_{\frac{1}{k}}(0)}$ of \mathcal{M} . From the above, we deduce the existence of a sequence $\{x_k\}_{k=1}^\infty$ with $x_k \in \mathcal{M}_k$ such that

$$\lim_{k \rightarrow \infty} \max \mathcal{L}_F W(x_k) = \ell \geq 0. \quad (4.26)$$

Since the whole sequence belongs to the compact set \mathcal{M}_1 , there exists a subsequence, which we denote with the same indices for simplicity, such that

$$\lim_{k \rightarrow \infty} x_k = \tilde{x} \in \mathcal{M}. \quad (4.27)$$

From (4.26), there exists a sequence $\zeta_k \in \partial W(x_k)$ such that

$$\lim_{k \rightarrow \infty} \zeta_k^\top g(x_k, \zeta_k) \geq 0. \quad (4.28)$$

Since ∂W is upper semicontinuous with compact values, the set $\partial W(\mathcal{M}_1)$ is compact, cf. [AC84, Proposition 3, p. 42]. This implies that the sequence $\{\zeta_k\}$ belongs to the compact set $\partial W(\mathcal{M}_1)$ and hence, there exists a subsequence, denoted again by the same indices for simplicity, such that $\zeta_k \rightarrow \tilde{\zeta}$. Now since ∂W is upper semicontinuous and takes closed values, we deduce from [AC84, Proposition 2, p. 41] that $\tilde{\zeta} \in \partial W(\tilde{x})$. From (4.27) and (4.28), since g is continuous, we obtain $\tilde{\zeta}^\top g(\tilde{x}, \tilde{\zeta}) \geq 0$. By assumption (i), this implies $\tilde{\zeta}^\top g(\tilde{x}, \tilde{\zeta}) = 0$. Assumption (ii) then implies $\tilde{x} \in \mathcal{E}$, which together with (4.27) contradicts $\mathcal{M} \cap \mathcal{E} = \emptyset$. \square

Acknowledgments

This chapter is taken, in part, from the work [CC16d] published as “Initialization-free distributed coordination for economic dispatch under varying loads and generator commitment” by A. Cherukuri and J. Cortés, in *Automatica*, 2016, as well as [CC14] where it appears as “Distributed coordination for economic dispatch with varying load and generator commitment” by A. Cherukuri and J. Cortés in the proceedings of the 2014 Annual Allerton Conference on Communication, Control, and Computing. The dissertation author was the primary investigator and author of these papers. This research was partly supported by the US National Science Foundation (NSF) Award CMMI-1300272.

Chapter 5

Robust distributed dynamics for DEDS problem

With the context of previous two chapters in mind, our objective here is to provide a distributed algorithmic solution to the dynamic economic dispatch problem with storage.

5.1 Problem statement

Consider a network of $n \in \mathbb{Z}_{\geq 1}$ distributed energy resources (DERs) whose communication topology is a strongly connected and weight-balanced digraph $\mathcal{G} = (\mathcal{V}, \mathcal{E}, \mathbf{A})$. For simplicity, assume DERs to be generator units. In our discussion, DERs can also be flexible loads (where the cost function corresponds to the negative of the load utility function). An edge (i, j) represents the capability of unit j to transmit information to unit i . Each unit i is equipped with storage capabilities with minimum $C_i^m \in \mathbb{R}_{\geq 0}$ and maximum $C_i^M \in \mathbb{R}_{>0}$ capacities. The network collectively aims to meet a power demand profile during a finite-time horizon $[\mathfrak{h}]$ specified by $L_{\mathfrak{t}} \in \mathbb{R}_{>0}^{\mathfrak{h}}$, that is, $L_{\mathfrak{t}}^{(k)}$ is the demand at time slot $k \in [\mathfrak{h}]$. This demand can either correspond to a load requested from an external entity, denoted $L_{\mathfrak{e}}^{(k)} \geq 0$ for slot k , or each DER i might have to satisfy a load at the bus it is connected to, denoted $(L_{\mathfrak{b}})_i^{(k)} \geq 0$ for slot k . Thus, for each $k \in [\mathfrak{h}]$, $L_{\mathfrak{t}}^{(k)} = L_{\mathfrak{e}}^{(k)} + \sum_{i=1}^n (L_{\mathfrak{b}})_i^{(k)}$. We assume that the external demand

$L_e = (L_e^{(1)}, \dots, L_e^{(h)})$ is known to an arbitrarily selected unit $r \in [n]$, whereas the demand at bus i , $(L_b)_i = ((L_b)_i^{(1)}, \dots, (L_b)_i^{(h)})$, is known to unit i . For convenience, $L_b = (L_b^{(1)}, \dots, L_b^{(h)})$, where $L_b^{(k)} = ((L_b)_1^{(k)}, \dots, (L_b)_n^{(k)})$ collects the load known to each unit at $k \in [h]$. Along with load satisfaction, the group aims to minimize the total cost of generation and to satisfy the constraints for each DER. These elements are explained next.

Each unit i decides at every time slot k in $[h]$ the amount of power it generates, the portion $J_i^{(k)} \in \mathbb{R}$ of it that it injects into the grid to meet the load, and the remaining part $S_i^{(k)} \in \mathbb{R}$ that it sends to the storage unit. The power generated by i at k is then $J_i^{(k)} + S_i^{(k)}$. We denote by $J^{(k)} = (J_1^{(k)}, \dots, J_n^{(k)}) \in \mathbb{R}^n$ and $S^{(k)} = (S_1^{(k)}, \dots, S_n^{(k)}) \in \mathbb{R}^n$ the collective injected and stored power at time k , respectively. The load satisfaction is then expressed as $\mathbf{1}_n^\top J^{(k)} = L_t^{(k)} = L_e^{(k)} + \mathbf{1}_n^\top L_b^{(k)}$, for all $k \in [h]$. The cost $f_i^{(k)}(J_i^{(k)} + S_i^{(k)})$ of power generation $J_i^{(k)} + S_i^{(k)}$ by i at time k is given by $f_i^{(k)} : \mathbb{R} \rightarrow \mathbb{R}_{\geq 0}$, which we assume convex and continuously differentiable. Given $(J^{(k)}, S^{(k)})$, the cost incurred by the network at slot k is

$$f^{(k)}(J^{(k)} + S^{(k)}) = \sum_{i=1}^n f_i^{(k)}(J_i^{(k)} + S_i^{(k)}).$$

The cumulative cost of generation for the network across the time horizon is $f : \mathbb{R}^{nh} \rightarrow \mathbb{R}_{\geq 0}$, $f(x) = \sum_{k=1}^h f^{(k)}(x^{(k)})$. Given injection $J = (J^{(1)}, \dots, J^{(h)}) \in \mathbb{R}^{nh}$ and storage $S = (S^{(1)}, \dots, S^{(h)}) \in \mathbb{R}^{nh}$ values, the total network cost is

$$f(J + S) = \sum_{k=1}^h f^{(k)}(J^{(k)} + S^{(k)}).$$

The functions $\{f^{(k)}\}_{k=1}^h$ and f are also convex and continuously differentiable. Next, we describe the physical constraints on the DERs. Each unit's power must belong to the range $[P_i^m, P_i^M] \subset \mathbb{R}_{>0}$, representing lower and upper bounds on the power generation at each time slot. Each unit i also respects upper and lower ramp limits: the change in the generation from any time slot k to $k + 1$ is upper and lower bounded by R_i^u and $-R_i^l$, respectively, with $R_i^u, R_i^l \in \mathbb{R}_{>0}$. At each time slot, the power injected into the grid by each unit must be nonnegative, i.e., $J_i^{(k)} \geq 0$.

Further, the power stored in any storage unit i at any time slot $k \in [\mathfrak{h}]$ must belong to the range $[C_i^m, C_i^M]$. Finally, we assume that at the beginning of the time slot $k = 1$, each storage unit i starts with some stored power $S_i^{(0)} \in [C_i^m, C_i^M]$. With the above model, the *dynamic economic dispatch with storage* (DEDS) problem is formally defined by the following convex optimization problem,

$$\underset{(J,S) \in \mathbb{R}^{2n\mathfrak{h}}}{\text{minimize}} \quad f(J + S), \quad (5.1a)$$

subject to for $k \in [\mathfrak{h}]$,

$$\mathbf{1}_n^\top J^{(k)} = L_t^{(k)}, \quad (5.1b)$$

$$P^m \leq J^{(k)} + S^{(k)} \leq P^M, \quad (5.1c)$$

$$C^m \leq S^{(0)} + \sum_{k'=1}^k S^{(k')} \leq C^M, \quad (5.1d)$$

$$\mathbf{0}_n \leq J^{(k)}, \quad (5.1e)$$

for $k \in [\mathfrak{h}] \setminus \{\mathfrak{h}\}$,

$$R^l \leq J^{(k+1)} + S^{(k+1)} - J^{(k)} - S^{(k)} \leq R^u. \quad (5.1f)$$

We refer to (5.1b)–(5.1f) as the *load conditions*, *box constraints*, *storage limits*, *injection constraints*, and *ramp constraints*, resp. We denote by $\mathcal{F}_{\text{DEDS}}$ and $\mathcal{F}_{\text{DEDS}}^*$ the feasibility and the solution set of (5.1), resp., and assume them to be nonempty. Since $\mathcal{F}_{\text{DEDS}}$ is compact, so is $\mathcal{F}_{\text{DEDS}}^*$. Moreover, the refined Slater condition is satisfied as all constraints (5.1b)–(5.1f) are affine in the decision variables. Additionally, we assume the DEDS problem satisfies the strong Slater condition with $\rho \in \mathbb{R}_{>0}$ and $(J^\rho, S^\rho) \in \mathbb{R}^{2n\mathfrak{h}}$. Our aim is to design a distributed algorithm that allows the network to solve (5.1).

Remark 5.1.1. (*Extensions to DEDS formulation*): The DEDS formulation can be modified to consider scenarios where only some DERs \mathcal{V}_{gs} are equipped with storage and others \mathcal{V}_g are not, with $[n] = \mathcal{V}_{gs} \cup \mathcal{V}_g$. The formulation can also be extended to consider the cost of storage, inefficiencies, and constraints on (dis)charging of the storage units, as in [HMMD13, ZGG13]. These factors either affect the constraint (5.1d), add additional conditions on the storage variables,

or modify the objective function. As long as the resulting cost and constraints are convex in S , all these can be treated within (5.1) without affecting the design methodology. Also, the DEDS formulation does not account for other physical constraints on the power network such as transmission losses and line capacity limits. Our ensuing discussion shows that, even with these omissions, the design of a provably correct distributed algorithm with the communication structure assumed here is challenging. •

5.2 Distributed algorithmic solution

We describe here the distributed algorithm that asymptotically solves the DEDS problem. Our design builds on an equivalent formulation of the optimization using penalty functions (cf. Section 5.2-A). This reformulation gets rid of the inequality constraints, yielding an optimization whose structure guides our algorithmic design (cf. Section 5.2-B).

A. Alternative formulation of the DEDS problem: The procedure here follows closely the theory of exact penalty functions outlined in Chapter 2. For an $\epsilon \in \mathbb{R}_{>0}$, consider the modified cost function $f^\epsilon : \mathbb{R}^{n^h} \times \mathbb{R}^{n^h} \rightarrow \mathbb{R}_{\geq 0}$,

$$f^\epsilon(J, S) = f(J + S) + \frac{1}{\epsilon} \left(\sum_{k=1}^{\mathfrak{h}} \mathbf{1}_n^\top ([T_1^{(k)}]^+ + [T_2^{(k)}]^+ + [T_3^{(k)}]^+ + [T_4^{(k)}]^+ + [T_5^{(k)}]^+) + \sum_{k=1}^{\mathfrak{h}-1} \mathbf{1}_n^\top ([T_6^{(k)}]^+ + [T_7^{(k)}]^+) \right),$$

where

$$\begin{aligned} T_1^{(k)} &= P^m - J^{(k)} - S^{(k)}, \quad T_2^{(k)} = J^{(k)} + S^{(k)} - P^M, \\ T_3^{(k)} &= C^m - S^{(0)} - \sum_{k'=1}^k S^{(k')}, \\ T_4^{(k)} &= S^{(0)} + \sum_{k'=1}^k S^{(k')} - C^M, \quad T_5^{(k)} = -J^{(k)}, \\ T_6^{(k)} &= -R^l - J^{(k+1)} - S^{(k+1)} + J^{(k)} + S^{(k)}, \end{aligned}$$

$$T_7^{(k)} = J^{(k+1)} + S^{(k+1)} - J^{(k)} - S^{(k)} - R^u. \quad (5.2)$$

This cost contains the penalty terms for all the inequality constraints of the DEDS problem. Note that f^ϵ is locally Lipschitz, jointly convex in J and S , and regular. Thus, the partial generalized gradients $\partial_J f^\epsilon$ and $\partial_S f^\epsilon$ take nonempty, convex, compact values and are locally bounded and upper semicontinuous. Consider the modified DEDS problem

$$\min\{f^\epsilon(J, S) \mid \mathbf{1}_n^\top J^{(k)} = L_t^{(k)}, \forall k \in [\mathfrak{h}]\}. \quad (5.3)$$

The difference between the optimizations (5.1) and (5.3) is that all inequality constraints of (5.1) are moved to the objective of (5.3) in the form of penalty terms. The next result provides a criteria for selecting ϵ such that the modified DEDS and the DEDS problems have the exact same solutions. This allows us to focus on solving (5.3). The proof is a direct application of Lemmas 2.5.1 and 2.5.2 using the fact that the DEDS problem satisfies the strong Slater condition with ρ and (J^ρ, S^ρ) .

Lemma 5.2.1. *(Equivalence of DEDS and modified DEDS problems): Let $(J^*, S^*) \in \mathcal{F}_{\text{DEDS}}^*$. Then, the optimizers of the problems (5.1) and (5.3) are the same for $\epsilon \in \mathbb{R}_{>0}$ satisfying*

$$\epsilon < \frac{\rho}{f(J^\rho + S^\rho) - f(J^* + S^*)}. \quad (5.4)$$

From here on, we assume that ϵ satisfies (5.4) and so problems (5.1) and (5.3) are equivalent. Writing the Lagrangian and the KKT conditions for (5.3), we obtain the following characterization of the solution set of the DEDS problem.

$$\begin{aligned} \mathcal{F}_{\text{DEDS}}^* = \{ & (J, S) \in \mathbb{R}^{2n\mathfrak{h}} \mid \mathbf{1}_n^\top J^{(k)} = L_t^{(k)} \text{ for all } k \in [\mathfrak{h}], 0 \in \partial_S f^\epsilon(J, S), \\ & \text{and } \exists \nu \in \mathbb{R}^{\mathfrak{h}} \text{ such that } (\nu^{(1)} \mathbf{1}_n; \dots; \nu^{(\mathfrak{h})} \mathbf{1}_n) \in \partial_J f^\epsilon(J, S)\}. \end{aligned} \quad (5.5)$$

Recall that $\mathcal{F}_{\text{DEDS}}^*$ is bounded. Next, we stipulate a mild regularity assumption on this set which implies that perturbing it by a small parameter does not result into

an unbounded set. This property is of use in our convergence analysis later.

Assumption 5.2.2. (Regularity of $\mathcal{F}_{\text{DEDS}}^*$): For $p \in \mathbb{R}_{\geq 0}$, define the map $p \mapsto \mathcal{F}(p) \subset \mathbb{R}^{2n\mathfrak{h}}$ as

$$\begin{aligned} \mathcal{F}(p) = \{ & (J, S) \in \mathbb{R}^{2n\mathfrak{h}} \mid \left| \mathbf{1}_n^\top J^{(k)} - L_{\mathfrak{t}}^{(k)} \right| \leq p \text{ for all } k \in [\mathfrak{h}], \\ & 0 \in \partial_S f^\epsilon(J, S) + pB_1(0), \text{ and } \exists \nu \in \mathbb{R}^{\mathfrak{h}} \text{ such that} \\ & (\nu^{(1)}\mathbf{1}_n; \dots; \nu^{(\mathfrak{h})}\mathbf{1}_n) \in \partial_J f^\epsilon(J, S) + pB_1(0) \}. \end{aligned}$$

Note that $\mathcal{F}(0) = \mathcal{F}_{\text{DEDS}}^*$. Then, there exists a $\bar{p} > 0$ such that $\mathcal{F}(p)$ is bounded for all $p \in [0, \bar{p})$. •

The equivalent reformulation (5.3), has a desirable structure: it does not have inequality constraints and the equalities have the special property that their coefficient vector lies in the null space of the Laplacian matrix. In the following section, we see how these facts help in the algorithm design and analysis.

B. The $\text{dac}+(\mathbf{L}\partial, \partial)$ coordination algorithm: Here, we present our distributed algorithm and establish its asymptotic convergence to the set of solutions of the DEDS problem starting from any initial condition. Our design combines ideas of Laplacian-gradient dynamics [CC15c] and dynamic average consensus [KCM15b]. Consider the set-valued dynamics,

$$\dot{J} \in -(\mathbf{I}_{\mathfrak{h}} \otimes \mathbf{L})\partial_J f^\epsilon(J, S) + \nu_1 z, \quad (5.6a)$$

$$\dot{S} \in -\partial_S f^\epsilon(J, S), \quad (5.6b)$$

$$\dot{z} = -\alpha z - \beta(\mathbf{I}_{\mathfrak{h}} \otimes \mathbf{L})z - v + \nu_2(L_{\mathbf{e}} \otimes e_r + L_{\mathbf{b}} - J), \quad (5.6c)$$

$$\dot{v} = \alpha\beta(\mathbf{I}_{\mathfrak{h}} \otimes \mathbf{L})z, \quad (5.6d)$$

where $\alpha, \beta, \nu_2, \nu_2 \in \mathbb{R}_{>0}$ are design parameters and $e_r \in \mathbb{R}^n$ is the unit vector along the r -th coordinate. We refer to (5.6) as $\text{dac}+(\mathbf{L}\partial, \partial)$ dynamics and below we explain its components.

[Description of $\text{dac}+(\mathbf{L}\partial, \partial)$ dynamics]: The dynamics (5.6) consists of “dynamic average consensus in (z, v) + Laplacian gradient in J + gradient in S ”, and so we use

the terminology $\text{dac}+(\mathbf{L}\partial, \partial)$. The (z, v) -component corresponds to the dynamic average consensus part. Here, $z_i^{(k)}$ is aiming to track, for unit i , the quantity $\mathbf{1}_n^\top (L_e^{(k)} e_r + L_b^{(k)} - J^{(k)})$, that is, the difference between the total load $L_t^{(k)} = L_e^{(k)} + \mathbf{1}_n^\top L_b^{(k)}$ and the current injection level $\mathbf{1}_n^\top J^{(k)}$ (recall that the external demand $L_e = (L_e^{(1)}, \dots, L_e^{(h)})$ is known to unit $r \in [n]$). The J -dynamics has two terms. The first term seeks to minimize f^ϵ keeping constant the total power generation. The second term gets the feedback of the mismatch between the total generation and the total load from the z -dynamics and drives the network towards load satisfaction. Finally, the S -component is gradient descent and seeks to minimize f^ϵ with respect to the variable S . From this description, one can see that getting rid of the inequalities of (5.1) using penalty functions simplifies the design.

For convenience, we denote the right-hand side of (5.6) by $X_{\text{dac}+(\mathbf{L}\partial, \partial)} : \mathbb{R}^{4nh} \rightrightarrows \mathbb{R}^{4nh}$. Note that $\text{Eq}(X_{\text{dac}+(\mathbf{L}\partial, \partial)}) = \mathcal{F}_{\text{DEDS}}^*$ and since $\partial_J f^\epsilon$ and $\partial_S f^\epsilon$ are locally bounded, upper semicontinuous and take nonempty convex compact values, the solutions of $X_{\text{dac}+(\mathbf{L}\partial, \partial)}$ exist (cf. Chapter 2).

Remark 5.2.3. (*Distributed implementation of $\text{dac}+(\mathbf{L}\partial, \partial)$ dynamics*): For (5.6), each $i \in [n]$ implements the dynamics of its decision variables, which are $\{J_i^{(k)}, S_i^{(k)}, z_i^{(k)}, v_i^{(k)}\}_{k=1}^h$. That is, for each $k \in [h]$, unit i implements

$$\dot{J}_i^{(k)} \in - \sum_{j \in \mathcal{N}_\zeta^{+i}} a_{ij} (\zeta_i^{(k)} - \zeta_j^{(k)}) + \nu_1 z_i^{(k)}, \quad (5.7a)$$

$$\dot{S}_i^{(k)} \in -\xi_i^{(k)}, \quad (5.7b)$$

$$\begin{aligned} \dot{z}_i^{(k)} = & -\alpha z_i^{(k)} - \beta \sum_{j \in \mathcal{N}_\zeta^{+i}} a_{ij} (z_i^{(k)} - z_j^{(k)}) - v_i^{(k)} \\ & + \nu_2 (L_e^{(k)}(e_r)_i + (L_b)_i^{(k)} - J_i^{(k)}), \end{aligned} \quad (5.7c)$$

$$\dot{v}_i^{(k)} = \alpha \beta \sum_{j \in \mathcal{N}_\zeta^{+i}} a_{ij} (z_i^{(k)} - z_j^{(k)}), \quad (5.7d)$$

where $\zeta \in \partial_J f^\epsilon(J, S) \subset \mathbb{R}^{nh}$, and $\xi \in \partial_S f^\epsilon(J, S) \subset \mathbb{R}^{nh}$. Hence, (5.7c) and (5.7d) can be implemented by i using information from its out-neighbors. Subsequently,

f^ϵ can be written in the separable form

$$f^\epsilon(J, S) = \sum_{i=1}^n f_i^\epsilon(J_i^{(1)}, \dots, J_i^{(\mathfrak{h})}, S_i^{(1)}, \dots, S_i^{(\mathfrak{h})}).$$

Thus, the entities $\zeta_i^{(k)} \in \partial_{J_i^{(k)}} f^\epsilon(J, S)$ and $\xi_i^{(k)} \in \partial_{S_i^{(k)}} f^\epsilon(J, S)$, for all $k \in [\mathfrak{h}]$, only depend on the decision variables of unit i and so are computable by it. This further implies that (5.7b) can be implemented by i using its own state and, to execute (5.7a), i needs information from its out-neighbors. Hence, the dynamics can be executed in a distributed manner. For real-time implementation, we discretize (5.6): selecting a small enough stepsize results in trajectories that follow closely the continuous-time trajectories leading to the optimizers. \bullet

Next, we state our main convergence result.

Theorem 5.2.4. (Convergence of the $\text{dac}+(\mathbf{L}\partial, \partial)$ dynamics to the solutions of the DEDS problem): *Let $\mathcal{F}_{\text{DEDS}}^*$ satisfy Assumption 5.2.2, ϵ satisfy (5.4), and $\alpha, \beta, \nu_1, \nu_2 > 0$ satisfy*

$$\frac{\nu_1}{\beta\nu_2\lambda_2(\mathbf{L} + \mathbf{L}^\top)} + \frac{\nu_2^2\lambda_{\max}(\mathbf{L}^\top\mathbf{L})}{2\alpha} < \lambda_2(\mathbf{L} + \mathbf{L}^\top). \quad (5.8)$$

Then, any trajectory of (5.6) starting in $\mathbb{R}^{n\mathfrak{h}} \times \mathbb{R}^{n\mathfrak{h}} \times \mathbb{R}^{n\mathfrak{h}} \times (\mathcal{H}_0)^\mathfrak{h}$ converges to $\mathcal{F}_{\text{aug}}^ = \{(J, S, z, v) \in \mathcal{F}_{\text{DEDS}}^* \times \{0\} \times \mathbb{R}^{n\mathfrak{h}} \mid v = \nu_2(L_e \otimes e_r + L_b - J)\}$.*

Proof of Theorem 5.2.4. For convenience, let $\mathfrak{M}_g = \mathbb{R}^{n\mathfrak{h}} \times \mathbb{R}^{n\mathfrak{h}} \times \mathbb{R}^{n\mathfrak{h}} \times (\mathcal{H}_0)^\mathfrak{h}$ and $\mathfrak{M}_o = \prod_{k=1}^\mathfrak{h} \mathcal{H}_{L_t^{(k)}} \times \mathbb{R}^{n\mathfrak{h}} \times (\mathcal{H}_0)^\mathfrak{h} \times (\mathcal{H}_0)^\mathfrak{h}$. We divide the proof into three broad steps.

Step 1: Characterizing the ω -limit set: We show that the ω -limit set of any trajectory of (5.6) with initial condition $(J_0, S_0, z_0, v_0) \in \mathfrak{M}_g$ belongs to \mathfrak{M}_o . For this, write (5.6d) as

$$\dot{v}^{(k)} = \alpha\beta\mathbf{L}z^{(k)} \quad \text{for all } k \in [\mathfrak{h}].$$

Note that $\mathbf{1}_n^\top \dot{v}^{(k)} = \alpha\beta\mathbf{1}_n^\top \mathbf{L}z^{(k)} = 0$ for all $k \in [\mathfrak{h}]$ because \mathcal{G} is weight-balanced. Therefore, the initial condition $v_0 \in (\mathcal{H}_0)^\mathfrak{h}$ implies that $v(t) \in (\mathcal{H}_0)^\mathfrak{h}$ for all $t \geq 0$

along any trajectory of (5.6) starting at (J_0, S_0, z_0, v_0) . Now, if $\zeta \in \partial_J f^\epsilon(J, S)$ then, from (5.6a) and (5.6c), we get for any $k \in [\mathfrak{h}]$

$$\begin{aligned} \dot{j}^{(k)} &= -\mathbf{L}\zeta^{(k)} + \nu_1 z^{(k)}, \\ \dot{z}^{(k)} &= -\alpha z^{(k)} - \beta \mathbf{L}z^{(k)} - v^{(k)} + \nu_2(L_e^{(k)} e_r + L_b^{(k)} - J^{(k)}). \end{aligned}$$

Let $\xi_k = \mathbf{1}_n^\top J^{(k)} - L_t^{(k)}$. Then, from the above equations we get $\dot{\xi}_k = \mathbf{1}_n^\top \dot{j}^{(k)} = \nu_1 \mathbf{1}_n^\top \dot{z}^{(k)}$. Further, we have

$$\begin{aligned} \ddot{\xi}_k &= \nu_1 \mathbf{1}_n^\top \dot{z}^{(k)} = -\alpha \nu_1 \mathbf{1}_n^\top z^{(k)} + \nu_1 \nu_2 (L_t^{(k)} - \mathbf{1}_n^\top J^{(k)}) \\ &= -\alpha \dot{\xi}_k - \nu_1 \nu_2 \xi_k, \end{aligned}$$

forming a second-order linear system for ξ_k . The LaSalle Invariance Principle [Kha02] with the function $\nu_1 \nu_2 \|\xi_k\|^2 + \|\dot{\xi}_k\|^2$ implies that as $t \rightarrow \infty$ we have $(\xi_k(t); \dot{\xi}_k(t)) \rightarrow 0$ and so $\mathbf{1}_n^\top J^{(k)}(t) \rightarrow L_t^{(k)}$ and $\mathbf{1}_n^\top z^{(k)}(t) \rightarrow 0$ as $t \rightarrow \infty$.

Step 2: Applying the refined LaSalle Invariance Principle: Consider the change of coordinates $D : \mathbb{R}^{4n\mathfrak{h}} \rightarrow \mathbb{R}^{4n\mathfrak{h}}$,

$$(J, S, \omega_1, \omega_2) = D(J, S, z, v) = (J, S, z, v + \alpha z - \nu_2(L_e \otimes e_r + L_b - J)).$$

In these coordinates, the set-valued map (5.6) takes the form

$$\begin{aligned} X_{\text{dac}+(\mathbf{L}\partial, \partial)}(J, S, \omega_1, \omega_2) &= \{(-(\mathbf{I}_\mathfrak{h} \otimes \mathbf{L})\zeta_1 + \nu_1 \omega_1, -\zeta_2, -\beta(\mathbf{I}_\mathfrak{h} \otimes \mathbf{L})\omega_1 - \omega_2, \\ &\quad \nu_1 \nu_2 \omega_1 - \alpha \omega_2 - \nu_2(\mathbf{I}_\mathfrak{h} \otimes \mathbf{L})\zeta_1) \in \mathbb{R}^{4n\mathfrak{h}} \mid \\ &\quad \zeta_1 \in \partial_J f^\epsilon(J, S), \zeta_2 \in \partial_S f^\epsilon(J, S)\}. \end{aligned} \quad (5.9)$$

This transformation helps in identifying the LaSalle-type function for the dynamics. We now focus on proving that, in the new coordinates, the trajectories of (5.6) converge to the set

$$\overline{\mathcal{F}}_{\text{aug}} = D(\mathcal{F}_{\text{aug}}^*) = \mathcal{F}_{\text{DEDS}}^* \times \{0\} \times \{0\}.$$

Note that $D(\mathfrak{M}_o) = \mathfrak{M}_o$ and so, from the property of the ω -limit set of trajectories above, we get that $t \mapsto (J(t), S(t), \omega_1(t), \omega_2(t))$ starting in $D(\mathfrak{M}_g)$ belongs to \mathfrak{M}_o . Next, we show the hypotheses of Proposition 4.5.1 are satisfied, where \mathfrak{M}_o plays the role of $\mathcal{S} \subset \mathbb{R}^{4n\mathfrak{h}}$ and $V : \mathbb{R}^{4n\mathfrak{h}} \rightarrow \mathbb{R}_{\geq 0}$,

$$V(J, S, \omega_1, \omega_2) = f^\epsilon(J, S) + \frac{1}{2}(\nu_1\nu_2\|\omega_1\|^2 + \|\omega_2\|^2).$$

plays the role of W , respectively. Let $(J, S, \omega_1, \omega_2) \in \mathfrak{M}_o$ then any element of $\mathcal{L}_{X_{\text{dac}}+(L\partial, \partial)} V(J, S, \omega_1, \omega_2)$ can be written as

$$\begin{aligned} & -\zeta_1^\top (\mathbf{I}_{\mathfrak{h}} \otimes \mathbf{L}) \zeta_1 + \nu_1 \zeta_1^\top \omega_1 - \|\zeta_2\|^2 - \beta \nu_1 \nu_2 \omega_1^\top (\mathbf{I}_{\mathfrak{h}} \otimes \mathbf{L}) \omega_1 \\ & - \alpha \|\omega_2\|^2 - \nu_2 \omega_2^\top (\mathbf{I}_{\mathfrak{h}} \otimes \mathbf{L}) \zeta_1, \end{aligned} \quad (5.10)$$

where $\zeta_1 \in \partial_J f^\epsilon(J, S)$ and $\zeta_2 \in \partial_S f^\epsilon(J, S)$. Since the digraph \mathcal{G} is strongly connected and weight-balanced, we use (2.1) and $\mathbf{1}_{n\mathfrak{h}}^\top \omega_1 = 0$ to bound the above expression as

$$\begin{aligned} & -\frac{1}{2}\lambda_2(\mathbf{L} + \mathbf{L}^\top)\|\eta\|^2 + \nu_1\eta^\top \omega_1 - \|\zeta_2\|^2 \\ & -\frac{1}{2}\beta\nu_1\nu_2\lambda_2(\mathbf{L} + \mathbf{L}^\top)\|\omega_1\|^2 - \alpha\|\omega_2\|^2 - \nu_2\omega_2^\top (\mathbf{I}_{\mathfrak{h}} \otimes \mathbf{L})\eta \\ & = \gamma^\top M\gamma - \|\zeta_2\|^2, \end{aligned}$$

where $\eta = (\eta^{(1)}; \dots; \eta^{(\mathfrak{h})})$ with $\eta^{(k)} = \zeta^{(k)} - \frac{1}{n}(\mathbf{1}_n^\top \zeta^{(k)})\mathbf{1}_n$, the vector $\gamma = (\eta; \omega_1; \omega_2)$, and the matrix

$$M = \begin{bmatrix} -\frac{1}{2}\lambda_2(\mathbf{L} + \mathbf{L}^\top)\mathbf{I}_{n\mathfrak{h}} & B^\top \\ B & C \end{bmatrix},$$

with $B^\top = \left[\frac{1}{2}\nu_1\mathbf{I}_{n\mathfrak{h}} \quad -\frac{1}{2}\nu_2(\mathbf{I}_{\mathfrak{h}} \otimes \mathbf{L})^\top \right]$, and

$$C = \begin{bmatrix} -\frac{1}{2}\beta\nu_1\nu_2\lambda_2(\mathbf{L} + \mathbf{L}^\top)\mathbf{I}_{n\mathfrak{h}} & 0 \\ 0 & -\alpha\mathbf{I}_{n\mathfrak{h}} \end{bmatrix}.$$

Resorting to the Schur complement [BV09], $M \in \mathbb{R}^{3n\mathfrak{h} \times 3n\mathfrak{h}}$ is neg. definite if $-\frac{1}{2}\lambda_2(\mathbf{L} + \mathbf{L}^\top)\mathbf{I}_{n\mathfrak{h}} - B^\top C^{-1}B$, that equals

$$-\frac{1}{2}\lambda_2(\mathbf{L} + \mathbf{L}^\top)\mathbf{I}_{n\mathfrak{h}} + \frac{\nu_1}{2\beta\nu_2\lambda_2(\mathbf{L} + \mathbf{L}^\top)}\mathbf{I}_{n\mathfrak{h}} + \frac{\nu_2^2}{4\alpha}(\mathbf{I}_{\mathfrak{h}} \otimes \mathbf{L})^\top(\mathbf{I}_{\mathfrak{h}} \otimes \mathbf{L}),$$

is negative definite, which follows from (5.8). Hence, for any $(J, S, \omega_1, \omega_2) \in \mathfrak{M}_o$, we have $\max \mathcal{L}_{X_{\text{dac}^+(\mathbf{L}\partial, \partial)}} V(J, S, \omega_1, \omega_2) \leq 0$ and also $0 \in \mathcal{L}_{X_{\text{dac}^+(\mathbf{L}\partial, \partial)}} V(J, S, \omega_1, \omega_2)$ iff $\eta = \zeta_2 = \omega_1 = \omega_2 = 0$, which means $\zeta^{(k)} \in \text{span}\{\mathbf{1}_n\}$ for each $k \in [\mathfrak{h}]$. Consequently, using (5.5), we deduce that (J, S) is a solution of (5.3) and so, $(J, S, \omega_1, \omega_2) \in \overline{\mathcal{F}}_{\text{aug}}$. Since, $\overline{\mathcal{F}}_{\text{aug}}$ belongs to a level set of V , we conclude that Proposition 4.5.1(i) holds. Further, using Lemma 4.5.3 one can show that Proposition 4.5.1(ii) holds too.

Step 3: Showing boundedness of trajectories: To apply Proposition 4.5.1, it remains to show that the trajectories starting from $D(\mathfrak{M}_g)$ are bounded. We reason by contradiction. Assume there exists $t \mapsto (J(t), S(t), \omega_1(t), \omega_2(t))$, with $(J(0), S(0), \omega_1(0), \omega_2(0)) \in D(\mathfrak{M}_g)$, of $X_{\text{dac}^+(\mathbf{L}\partial, \partial)}$ such that $\|(J(t), S(t), \omega_1(t), \omega_2(t))\| \rightarrow \infty$. Since V is radially unbounded, this implies $V(J(t), S(t), \omega_1(t), \omega_2(t)) \rightarrow \infty$. Also, as established above, we know $\mathbf{1}_n^\top J^{(k)}(t) \rightarrow L_t^{(k)}$ and $\mathbf{1}_n^\top \omega_1^{(k)}(t) \rightarrow 0$ for each $k \in [\mathfrak{h}]$. Thus, there exist times $\{t_m\}_{m=1}^\infty$ with $t_m \rightarrow \infty$ such that for all $m \in \mathbb{Z}_{\geq 1}$,

$$\begin{aligned} \left| \mathbf{1}_n^\top \omega_1^{(k)}(t_m) \right| &< 1/m \text{ for all } k \in [\mathfrak{h}], \\ \max \mathcal{L}_{X_{\text{dac}^+(\mathbf{L}\partial, \partial)}} V(J(t_m), S(t_m), \omega_1(t_m), \omega_2(t_m)) &> 0. \end{aligned} \tag{5.11}$$

The second inequality implies the existence of $\{\zeta_{1,m}\}_{m=1}^\infty$ and $\{\zeta_{2,m}\}_{m=1}^\infty$ with $(\zeta_{1,m}, \zeta_{2,m}) \in (\partial_J f^\epsilon(J(t_m), S(t_m)), \partial_S f^\epsilon(J(t_m), S(t_m)))$, such that

$$\begin{aligned} &-\zeta_{1,m}^\top(\mathbf{I}_{\mathfrak{h}} \otimes \mathbf{L})\zeta_{1,m} + \nu_1 \zeta_{1,m}^\top \omega_1(t_m) - \|\zeta_{2,m}\|^2 \\ &\quad - \beta\nu_1\nu_2\omega_1(t_m)^\top(\mathbf{I}_{\mathfrak{h}} \otimes \mathbf{L})\omega_1(t_m) - \alpha\|\omega_2(t_m)\|^2 \\ &\quad - \nu_2\omega_2(t_m)^\top(\mathbf{I}_{\mathfrak{h}} \otimes \mathbf{L})\zeta_{1,m} > 0, \end{aligned}$$

for all $m \in \mathbb{Z}_{\geq 1}$, where we have used (5.10) to write an element of

$\mathcal{L}_{X_{\text{dac}}+(\mathbf{L}\partial, \partial)} V(J, S, \omega_1, \omega_2)$. Letting $\eta_m^{(k)} = \zeta_{1,m}^{(k)} - \frac{1}{n}(\mathbf{1}_n^\top \zeta_{1,m}^{(k)})\mathbf{1}_n$, using (2.1), and using the relation $\|\omega_1^{(k)}(t_m) - \frac{1}{n}(\mathbf{1}_n^\top \omega_1^{(k)}(t_m))\mathbf{1}_n\|^2 = \|\omega_1^{(k)}(t_m)\|^2 - \frac{1}{n}(\mathbf{1}_n^\top \omega_1^{(k)}(t_m))^2$, the above inequality can be rewritten as

$$\begin{aligned} \gamma_m^\top M \gamma_m + \frac{1}{n} \nu_1 \sum_{k \in [\mathfrak{h}]} (\mathbf{1}_n^\top \zeta_{1,m}^{(k)}) (\mathbf{1}_n^\top \omega_1^{(k)}(t_m)) - \|\zeta_{2,m}\|^2 \\ + \frac{\beta \nu_1 \nu_2}{2n} \lambda_2(\mathbf{L} + \mathbf{L}^\top) \sum_{k \in [\mathfrak{h}]} (\mathbf{1}_n^\top \omega_1^{(k)}(t_m))^2 > 0, \end{aligned} \quad (5.12)$$

with $\gamma_m = (\eta_m; \omega_1(t_m); \omega_2(t_m))$. Using (5.11) on (5.12),

$$\gamma_m^\top M \gamma_m - \|\zeta_{2,m}\|^2 + \frac{\nu_1}{nm} \sum_{k \in [\mathfrak{h}]} \left| \mathbf{1}_n^\top \zeta_{1,m}^{(k)} \right| + \frac{\beta \nu_1 \nu_2 \mathfrak{h}}{2nm^2} \lambda_2(\mathbf{L} + \mathbf{L}^\top) > 0 \quad (5.13)$$

for all $m \in \mathbb{Z}_{\geq 1}$. Next, we consider two cases, depending on whether the sequence $\{(J(t_m), S(t_m))\}_{m=1}^\infty$ is (a) bounded or (b) unbounded. In case (a), $\{(\omega_1(t_m), \omega_2(t_m))\}_{m=1}^\infty$ must be unbounded. Since M is negative definite, we have $\gamma_m^\top M \gamma_m \leq \lambda_{\max}(M) \|(\omega_1(t_m), \omega_2(t_m))\|^2$. Thus, by (5.13)

$$\lambda_{\max}(M) \|(\omega_1(t_m), \omega_2(t_m))\|^2 + \frac{\nu_1}{nm} \sum_{k \in [\mathfrak{h}]} \left| \mathbf{1}_n^\top \zeta_{1,m}^{(k)} \right| + \frac{\beta \nu_1 \nu_2 \mathfrak{h}}{2nm^2} \lambda_2(\mathbf{L} + \mathbf{L}^\top) > 0. \quad (5.14)$$

Since $\partial_J f^\epsilon$ is locally bounded and $\{(J(t_m), S(t_m))\}_{m=1}^\infty$ is bounded, we deduce $\{\zeta_{1,m}\}$ is bounded [HUL93, Proposition 6.2.2]. Combining these facts with $\lambda_{\max}(M) < 0$ and $\|(\omega_1(t_m), \omega_2(t_m))\| \rightarrow \infty$, one can find $\bar{m} \in \mathbb{Z}_{\geq 1}$ such that (5.14) is violated for all $m \geq \bar{m}$, a contradiction. Now consider case (b) where $\{(J(t_m), S(t_m))\}_{m=1}^\infty$ is unbounded. We divide this case further into two, based on the sequence $\{\sum_{k=1}^{\mathfrak{h}} \left| \mathbf{1}_n^\top \zeta_{1,m}^{(k)} \right|\}_{m=1}^\infty$ being bounded or not. Using $\gamma_m^\top M \gamma_m \leq \lambda_{\max}(M) \|\eta_m\|^2$, the inequality (5.13) implies

$$\lambda_{\max}(M) \|\eta_m\|^2 - \|\zeta_{2,m}\|^2 + \frac{\nu_1}{nm} \sum_{k=1}^{\mathfrak{h}} \left| \mathbf{1}_n^\top \zeta_{1,m}^{(k)} \right| + \frac{\beta \nu_1 \nu_2 \mathfrak{h}}{2nm^2} \lambda_2(\mathbf{L} + \mathbf{L}^\top) > 0. \quad (5.15)$$

Consider the case when $\{\sum_{k=1}^{\mathfrak{h}} \left| \mathbf{1}_n^\top \zeta_{1,m}^{(k)} \right|\}_{m=1}^\infty$ is unbounded. Partition $[\mathfrak{h}]$ into

disjoint sets \mathcal{K}_u and \mathcal{K}_b such that $\left| \mathbf{1}_n^\top \zeta_{1,m}^{(k)} \right| \rightarrow \infty$ for all $k \in \mathcal{K}_u$ and $\left\{ \left| \mathbf{1}_n^\top \zeta_{1,m}^{(k)} \right| \right\}_{m=1}^\infty$ is uniformly bounded for all $k \in \mathcal{K}_b$. For convenience, rewrite (5.15) as $\sum_{k=1}^{\mathfrak{h}} U_{k,m} + \frac{Z_1}{m} > 0$, where $Z_1 = \frac{\beta \nu_1 \nu_2 \mathfrak{h}}{2nm} \lambda_2(\mathbf{L} + \mathbf{L}^\top)$ and, for each $k \in [\mathfrak{h}]$,

$$U_{k,m} = \lambda_{\max}(M) \|\eta_m^{(k)}\|^2 - \|\zeta_{2,m}^{(k)}\|^2 + \frac{\nu_1}{nm} \left| \mathbf{1}_n^\top \zeta_{1,m}^{(k)} \right|.$$

By definition of \mathcal{K}_b , there exists $Z_2 > 0$ with $\sum_{k \in \mathcal{K}_b} U_{k,m} \leq \frac{Z_2}{m}$. Hence, if (5.15) holds for all $m \in \mathbb{Z}_{\geq 1}$, then so is

$$\sum_{k \in \mathcal{K}_u} U_{k,m} + \frac{Z_1 + Z_2}{m} > 0.$$

Next we show that for each $k \in \mathcal{K}_u$ there exists $m_k \in \mathbb{Z}_{\geq 1}$ such that $U_{k,m} + \frac{Z_1 + Z_2}{m} < 0$ for all $m \geq m_k$. This will lead to the desired contradiction. Assume without loss of generality that $\mathbf{1}_n^\top \zeta_{1,m}^{(k)} \rightarrow \infty$ (reasoning for the case when the sequence approaches negative infinity follows analogously). Then, for

$$\lambda_{\max}(M) \|\eta_m^{(k)}\|^2 - \|\zeta_{2,m}^{(k)}\|^2 + \frac{\nu_1}{nm} \left| \mathbf{1}_n^\top \zeta_{1,m}^{(k)} \right| + \frac{Z_1 + Z_2}{m} > 0,$$

for all $m \in \mathbb{Z}_{\geq 1}$, we require $(\zeta_{1,m}^{(k)})_i \rightarrow \infty$ for all $i \in [n]$. Indeed, otherwise, recalling that $\eta_m^{(k)} = \zeta_{1,m}^{(k)} - \frac{1}{n}(\mathbf{1}_n^\top \zeta_{1,m}^{(k)})\mathbf{1}_n$, it can be shown that there exist an \bar{m} such that

$$\lambda_{\max} \|\eta_m^{(k)}\|^2 < \frac{\nu_1}{nm} \left| \mathbf{1}_n^\top \zeta_{1,m}^{(k)} \right| + \frac{Z_1 + Z_2}{m} \quad \text{for all } m \geq \bar{m}.$$

Note that from Lemma 5.2.5 we have $\|\zeta_{1,m}^{(k)} - \zeta_{2,m}^{(k)}\|_\infty \leq \frac{\mathfrak{h}+4}{\epsilon}$ which further implies that $(\zeta_{2,m}^{(k)})_i \rightarrow \infty$ for all $i \in [n]$. With these facts in place, we write

$$U_{k,m} + \frac{Z_1 + Z_2}{m} < - \sum_{i=1}^n (\zeta_{2,m}^{(k)})_i^2 + \frac{\nu_1}{m} \left| \sum_{i=1}^n (\zeta_{1,m}^{(k)})_i \right| + \frac{Z_1 + Z_2}{m}$$

and deduce that there exists an $m_k \in \mathbb{Z}_{\geq 1}$ such that the right-hand side of the above expression is negative for all $m \geq m_k$, which is what we wanted to show.

Finally, consider the case when $\left\{ \sum_{k=1}^{\mathfrak{h}} \left| \mathbf{1}_n^\top \zeta_{1,m}^{(k)} \right| \right\}_{m=1}^{\infty}$ is bounded. For (5.15) to be true for all m , we need $\|\gamma_m\| \rightarrow 0$ and $\|\zeta_{2,m}\| \rightarrow 0$ as $m \rightarrow \infty$. This further implies that $\eta_m \rightarrow 0$ and, from Assumption 5.2.2, this is only possible if $\{(J(t_m), S(t_m))\}_{m=1}^{\infty}$ is bounded, a contradiction. \square

The next result aids the above outlined proof.

Lemma 5.2.5. *(Bound on the difference between $\partial_J f^\epsilon$ and $\partial_S f^\epsilon$): For $(J, S) \in \mathbb{R}^{2n\mathfrak{h}}$, any two elements $\zeta_1 \in \partial_J f^\epsilon(J, S)$ and $\zeta_2 \in \partial_S f^\epsilon(J, S)$ satisfy $\|\zeta_1 - \zeta_2\|_\infty \leq (\mathfrak{h} + 4)/\epsilon$.*

Proof. Write $f^\epsilon(J, S) = f_a(J + S) + f_b(J) + f_c(S)$ where the functions $f_a, f_b, f_c : \mathbb{R}^{n\mathfrak{h}} \rightarrow \mathbb{R}_{\geq 0}$ are

$$\begin{aligned} f_a(J + S) &= f(J + S) + \frac{1}{\epsilon} \left(\sum_{k=1}^{\mathfrak{h}} \mathbf{1}_n^\top ([T_1^{(k)}]^+ + [T_2^{(k)}]^+) + \sum_{k=1}^{\mathfrak{h}-1} \mathbf{1}_n^\top ([T_6^{(k)}]^+ + [T_7^{(k)}]^+) \right), \\ f_b(J) &= \frac{1}{\epsilon} \sum_{k=1}^{\mathfrak{h}} \mathbf{1}_n^\top [T_5^{(k)}]^+, \\ f_c(S) &= \frac{1}{\epsilon} \sum_{k=1}^{\mathfrak{h}} \mathbf{1}_n^\top ([T_3^{(k)}]^+ + [T_4^{(k)}]^+). \end{aligned}$$

See (5.2) for the definition of the right-hand side terms. From the sum rule of generalized gradients [Cor08], any element $\zeta_1 \in \partial_J f^\epsilon(J, S)$ can be expressed as a sum of the vectors $\zeta_{1,a}$ and $\zeta_{1,b} \in \mathbb{R}^{n\mathfrak{h}}$ such that $\zeta_{1,a} \in \partial f_a(J + S)$ and $\zeta_{1,b} \in \partial f_b(J)$. Similarly, $\zeta_2 = \zeta_{2,a} + \zeta_{2,c}$ where $\zeta_{2,a} \in \partial f_a(J + S)$ and $\zeta_{2,c} \in \partial f_c(S)$. By the definition of f_b , we get $\|\zeta_{1,b}\|_\infty \leq \frac{1}{\epsilon}$. For the function f_c , note that for any $i \in [n]$ and any $k \in [\mathfrak{h}]$, either $([T_3^{(k)}]^+)_i$ is zero or $([T_4^{(k)}]^+)_i$ is zero. Considering extreme case, if for a particular i , either $([T_3^{(k)}]^+)_i > 0$ or $([T_4^{(k)}]^+)_i > 0$ for all $k \in [\mathfrak{h}]$ then, we obtain $\left| (\zeta_{2,c})_i^{(1)} \right| = \frac{\mathfrak{h}}{\epsilon}$. This implies that $\|\zeta_{2,c}\|_\infty \leq \frac{\mathfrak{h}}{\epsilon}$. Now consider any two elements $\zeta_{1,a}, \zeta_{2,a} \in \partial f_a(J + S)$. Note that for any $i \in [n]$, either $([T_1^{(k)}]^+)_i$ is zero or $([T_2^{(k)}]^+)_i$ is zero. Similarly, either $([T_6^{(k)}]^+)_i$ or $([T_7^{(k)}]^+)_i$ is zero. Further, note that $J_i^{(k)} + S_i^{(k)}$ appears in $([T_6^{(k)}]^+)_i$ and $([T_7^{(k)}]^+)_i$ as well as in $([T_6^{(k-1)}]^+)_i$ and $([T_7^{(k-1)}]^+)_i$. At the same time, only two of these four terms are nonzero for any $k \in [\mathfrak{h}] \setminus \mathfrak{h}$ and any $i \in [n]$. Using these facts we get $\|\zeta_{1,a} - \zeta_{2,a}\|_\infty \leq \frac{3}{\epsilon}$.

Finally, the proof concludes noting $\|\zeta_1 - \zeta_2\|_\infty = \|\zeta_{1,a} + \zeta_{1,b} - \zeta_{2,a} - \zeta_{2,c}\|_\infty \leq \|\zeta_{1,a} - \zeta_{2,a}\|_\infty + \|\zeta_{1,b}\|_\infty + \|\zeta_{2,c}\|_\infty \leq (\mathfrak{h} + 4)/\epsilon$. \square

From the first step in the proof of Theorem 5.2.4, one sees that the mismatch between the network power injection and the load profile converges exponentially fast to zero. This guarantees robustness of the algorithm, in the sense that during its execution, the load can vary or agents can join or leave the network (provided that there is always a participating node that knows the external demand), and the dynamics adjusts for these perturbations.

Remark 5.2.6. (*General setup for storage: revisited*): The $\text{dac}+(\text{L}\partial, \partial)$ dynamics (5.6) can be modified to scenarios that include more general descriptions of storage capabilities, as in Remark 5.1.1. For instance, if only a subset of units have storage capabilities, the only modification is to set the variables $\{S_i^{(k)}\}_{i \in \mathcal{V}_g, k \in [h]}$ to zero and execute (5.6b) only for the variables $\{S_i^{(k)}\}_{i \in \mathcal{V}_{gs}, k \in [h]}$. The resulting strategy converges to the solution set of the corresponding DEDS problem. \bullet

Remark 5.2.7. (*Distributed selection of design parameters*): The implementation of (5.6) requires the selection of parameters $\alpha, \beta, \nu_1, \nu_2, \epsilon$ satisfying (5.4) and (5.8). Instead of condition (5.8), one can check a different, stronger inequality that requires knowledge of the maximum and minimum of various network-wide quantities. In turn, these can be computed in finite time by the units resorting to distributed consensus-based procedures [RB08] in order to collectively select appropriate values, see e.g., Remark 4.3.4. Regarding (5.4), an upper bound on the denominator of the right-hand side can be computed by aggregating, using consensus, the difference between the max and the min values that each DER's aggregate cost function takes in its respective feasibility set (neglecting load conditions). The challenge for the units, however, is to estimate ρ . This can be accomplished by considering the optimization “find the largest ρ for which the DEDS problem satisfies the strong Slater condition” and having the units employ a distributed algorithm to solve it, see e.g., [CC16b]. \bullet

5.3 Simulations

We illustrate the application of the $\text{dac}+(\mathbf{L}\partial, \partial)$ dynamics to solve the DEDS problem for a group of $n = 10$ generators with communication defined by a directed ring with bi-directional edges $\{(1, 5), (2, 6), (3, 7), (4, 8)\}$ (all edge weights are 1). The planning horizon is $\mathfrak{h} = 6$ and the load profile consists of the external load $L_e = (1950, 1980, 2700, 2370, 1900, 1850)$ and the load at each generator i for each slot k given by $(L_b)_i^{(k)} = 10i$. Thus, for each slot k , $(L_b)^{(k)} = \sum_{i=1}^{10} (L_b)_i^{(k)} = 550$ and so, $L_t = (2500, 2530, 3250, 2920, 2450, 2400)$. Generators have storage capacities determined by $C^M = 100\mathbf{1}_n$ and $C^m = S^{(0)} = 5\mathbf{1}_n$. The cost function of each unit is quadratic and constant across time. Table 5.1 details the cost function coefficients, generation limits, and ramp constraints, which are modified from the data for 39-bus New England system [ZMST11].

Table 5.1: Cost coefficients (a_i, b_i, c_i) and bounds $P_i^M, P_i^m, R_i^l, R_i^u$. The cost function of i is $f_i(P_i) = a_i + b_i P_i + c_i P_i^2$.

Unit	a_i	b_i	c_i	P_i^m	P_i^M	R_i^l	R_i^u
1	240	7.0	0.0070	0	1040	120	80
2	200	10.0	0.0095	0	646	90	50
3	220	8.5	0.0090	0	725	100	65
4	200	11.0	0.0090	0	652	90	50
5	220	10.5	0.0080	0	508	90	50
6	190	12.0	0.0075	0	687	90	50
7	200	10.0	0.0100	0	580	120	80
8	170	9.0	0.0090	0	564	90	50
9	190	11.0	0.0072	0	865	100	65
10	220	8.8	0.0080	0	1100	90	50

Figure 5.1 illustrates the evolution of the total power injected at each time slot and the total cost incurred by the network, respectively. As established in Theorem 5.2.4 and shown in Figure 5.2, the total injection asymptotically converges to the load profile l , the total aggregate cost converges to the minimum 201092 and the converged solution satisfies (5.1c)-(5.1f). The number of variables maintained and updated by each generator is linear in the length of the time horizon \mathfrak{h} , and therefore, at each iteration, the computation time and the communication volume increase linearly with \mathfrak{h} .

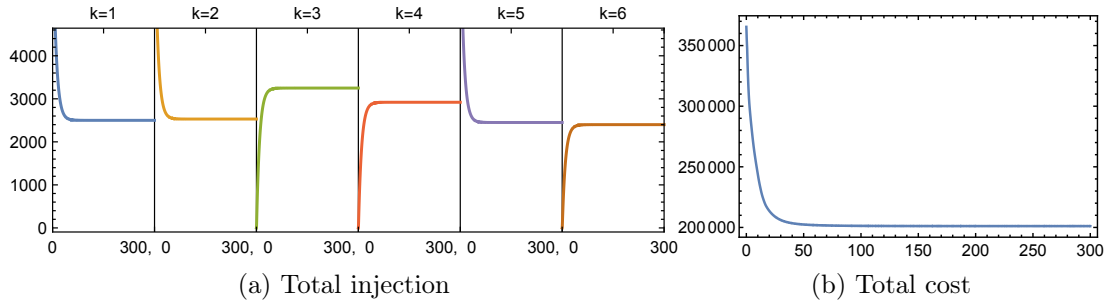


Figure 5.1: Illustration of the execution of $\text{dac}+(\mathbf{L}\partial, \partial)$ dynamics for a network of 10 generators with communication topology given by a directed ring among the generators with bi-directional edges $\{(1, 5), (2, 6), (3, 7), (4, 8)\}$ where all edge weights are 1. Table 5.1 gives the box constraints, the ramp constraints, and the cost functions. The load profile is $L_t = (2500, 2530, 3250, 2920, 2450, 2400)$ and $C^M = 100\mathbf{1}_n$, $C^m = S^{(0)} = 5\mathbf{1}_n$. Plots (a) and (b) show the time evolution of the total injection at each time slot and the aggregate cost along a trajectory of the $\text{dac}+(\mathbf{L}\partial, \partial)$ dynamics starting at $J(0) = (P^M, P^M, P^m, P^m, P^M, P^m)$, $S(0) = z(0) = v(0) = \mathbf{0}_{nb}$. The parameters are $\epsilon = 0.007$, $\alpha = 4$, $\beta = 10$, and $\nu_1 = \nu_2 = 0.65$ (which satisfy conditions (5.4) and (5.8)). The dynamics is simulated using a first-order Euler discretization with stepsize 5×10^{-4} . Without accounting for communication, the computation time (i.e., the time spent by any unit updating its variables) is 16.3642 seconds. In contrast, the (centralized) Quadprog solver from the YALMIP toolbox takes 2.2361 seconds to find an optimizer. With stepsize 5×10^{-3} , the computation time of the distributed algorithm reduces to 2.6915 seconds while the total incurred cost at the converged point is 0.1% higher.

Acknowledgments

This chapter is taken, in part, from the work [CC18] submitted as “Distributed coordination of DERs with storage for dynamic economic dispatch” by A. Cherukuri and J. Cortés, to the IEEE Transactions on Automatic Control, as well as [CC15b] where it appears as “Distributed dynamic economic dispatch of power generators with storage” by A. Cherukuri and J. Cortés in the proceedings of the 2015 IEEE Conference on Decision and Control. The dissertation author was the primary investigator and author of these papers. This research was partly supported by the US National Science Foundation (NSF) Award ECCS-1307176.

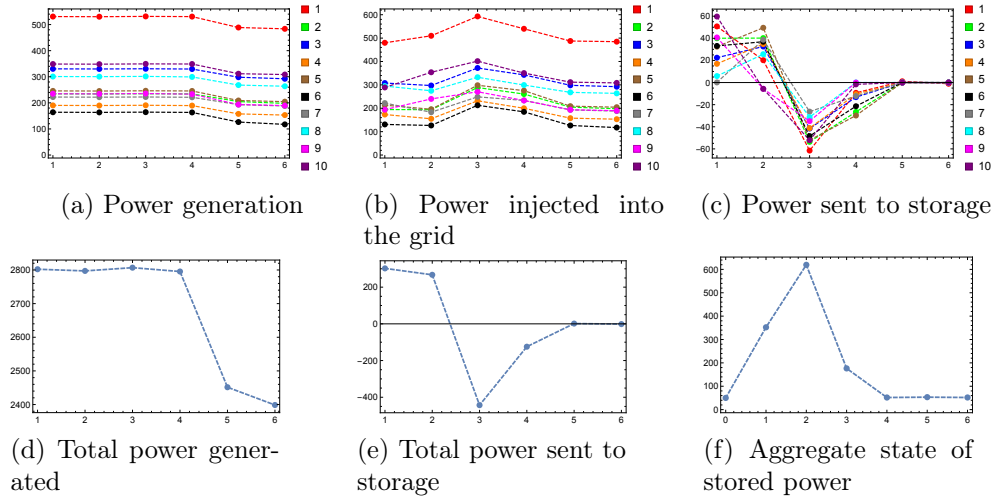


Figure 5.2: Plots (a) to (f) illustrate the solution obtained in Figure 5.1. Plots (b) and (c) show the power injected and power sent to storage across the time horizon, with unique colors for each generator. These values add up to the total generation in (a). The collective behavior is represented in (d)-(f), where we plot the total power generated, the total power sent to storage, and the aggregate of the power stored in the storage units, respectively. The profile of total injection is the same as that of load profile. Since the time-independent cost is quadratic with positive coefficients and the storage capacity is large enough, one can show that the optimal strategy is to produce the same power unless ramp constraints become active. This can be seen in (a) and (d). The initial excess generation (due to the lower required load) at slots $k = 1, 2$ is stored and used in slots $k = 3, 4, 5, 6$, as indicated in (e) and (f).

Chapter 6

Asymptotic convergence of saddle-point dynamics

It is well known that the trajectories of the gradient dynamics of a continuously differentiable function with bounded sublevel sets converge asymptotically to its set of critical points, see e.g. [HS74]. This fact, however, is not true in general for the saddle-point dynamics (gradient descent in one variable and gradient ascent in the other) of a continuously differentiable function of two variables, see e.g. [AHU58, DSS58]. This chapter investigates conditions under which the above statement is true for the case where the critical points are min-max saddle points and they possibly form a continuum.

6.1 Problem statement

Given a continuously differentiable function $F : \mathbb{R}^n \times \mathbb{R}^m \rightarrow \mathbb{R}$, which we refer to as a *saddle function*, we consider its saddle-point dynamics, i.e., gradient-descent in one argument and gradient-ascent in the other,

$$\dot{x} = -\nabla_x F(x, z), \tag{6.1a}$$

$$\dot{z} = \nabla_z F(x, z). \tag{6.1b}$$

When convenient, we use the shorthand notation $X_{\text{sp}} : \mathbb{R}^n \times \mathbb{R}^m \rightarrow \mathbb{R}^n \times \mathbb{R}^m$ to refer to this dynamics. Our aim is to provide conditions on F under which the trajectories of its saddle-point dynamics (6.1) locally asymptotically converge to its set of saddle points, and possibly to a point in the set. We are also interested in identifying conditions to establish global asymptotic convergence. Throughout this chapter, we assume that the set $\text{Saddle}(F)$ is nonempty. This assumption is valid under mild conditions in the application areas that motivate our study: for the Lagrangian of the constrained optimization problem [BV04] and the value function for zero-sum games [BO82]. Our forthcoming discussion is divided in two threads, one for the case of convex-concave functions, cf. Section 6.2, and one for the case of general functions, cf. Section 6.3. In each case, we provide illustrative examples to show the applicability of the results. For preliminary concepts on saddle-points and convex-concave functions, we refer to Section 2.4.

6.2 Convergence analysis for convex-concave saddle functions

This section presents conditions for the asymptotic stability of saddle points under the saddle-point dynamics (6.1) that rely on the convexity-concavity properties of the saddle function.

6.2.1 Stability under strict convexity-concavity

Our first result provides conditions that guarantee the local asymptotic stability of the set of saddle points.

Proposition 6.2.1. *(Local asymptotic stability of the set of saddle points via convexity-concavity): For $F : \mathbb{R}^n \times \mathbb{R}^m \rightarrow \mathbb{R}$ continuously differentiable and locally strictly convex-concave on $\text{Saddle}(F)$, each isolated path connected component of $\text{Saddle}(F)$ is locally asymptotically stable under the saddle-point dynamics X_{sp} and, moreover, the convergence of each trajectory is to a point.*

Proof. Let \mathcal{S} be an isolated path connected component of $\text{Saddle}(F)$ and take $(x_*, z_*) \in \mathcal{S}$. Without loss of generality, we consider the case when $x \mapsto F(x, z_*)$ is locally strictly convex (the proof for the case when $z \mapsto F(x_*, z)$ is locally strictly concave is analogous). Consider the function $V : \mathbb{R}^n \times \mathbb{R}^m \rightarrow \mathbb{R}_{\geq 0}$,

$$V(x, z) = \frac{1}{2} \left(\|x - x_*\|^2 + \|z - z_*\|^2 \right), \quad (6.2)$$

which we note is radially unbounded (and hence has bounded sublevel sets). We refer to V as a LaSalle function because locally, as we show next, its Lie derivative is negative, but not strictly negative. Let \mathcal{U} be the neighborhood of (x_*, z_*) where local convexity-concavity holds. The Lie derivative of V along the dynamics (6.1) at $(x, z) \in \mathcal{U}$ can be written as,

$$\begin{aligned} \mathcal{L}_{X_{\text{sp}}} V(x, z) &= -(x - x_*)^\top \nabla_x F(x, z) + (z - z_*)^\top \nabla_z F(x, z) \quad (6.3) \\ &\leq F(x_*, z) - F(x, z) + F(x, z) - F(x, z_*) \\ &= F(x_*, z) - F(x_*, z_*) + F(x_*, z_*) - F(x, z_*) \leq 0, \end{aligned}$$

where the first inequality follows from the first-order condition for convexity and concavity, and the last inequality follows from the definition of saddle point. As a consequence, for $\alpha > 0$ small enough such that $V^{-1}(\leq V(\alpha)) \subset \mathcal{U}$, we conclude that $V^{-1}(\leq V(\alpha))$ is positively invariant under X_{sp} . The application of the LaSalle Invariance Principle [Kha02, Theorem 4.4] yields that any trajectory starting from a point in $V^{-1}(\leq V(\alpha))$ converges to the largest invariant set M contained in $\{(x, z) \in V^{-1}(\leq V(\alpha)) \mid \mathcal{L}_{X_{\text{sp}}} V(x, z) = 0\}$. Let $(x, z) \in M$. From (6.3), $\mathcal{L}_{X_{\text{sp}}} V(x, z) = 0$ implies that $F(x_*, z) = F(x_*, z_*) = F(x, z_*)$. In turn, the local strict convexity of $x \mapsto F(x, z_*)$ implies that $x = x_*$. Since M is positively invariant, the trajectory $t \mapsto (x(t), z(t))$ of X_{sp} starting at (x, z) is contained in M . This implies that along the trajectory, for all $t \geq 0$, (a) $x(t) = x_*$ i.e., $\dot{x}(t) = \nabla_x F(x(t), z(t)) = 0$, and (b) $F(x_*, z(t)) = F(x_*, z_*)$. The later implies

$$0 = \mathcal{L}_{X_{\text{sp}}} F(x_*, z(t)) = X_{\text{sp}}(x_*, z(t)) \cdot (0, \nabla_z F(x_*, z(t))) = \|\nabla_z F(x(t), z(t))\|^2,$$

for all $t \geq 0$. Thus, we get $\nabla_x F(x, z) = 0$ and $\nabla_z F(x, z) = 0$. Further, since $(x, z) \in \mathcal{U}$, local convexity-concavity holds over \mathcal{U} , and \mathcal{S} is an isolated component, we obtain $(x, z) \in \mathcal{S}$, which shows $M \subset \mathcal{S}$. Since (x_*, z_*) is arbitrary, the asymptotic convergence property holds in a neighborhood of \mathcal{S} . The pointwise convergence follows from the application of Lemma 6.4.3. \square

The result above shows that each saddle point is stable and that each path connected component of $\text{Saddle}(F)$ is asymptotically stable. Note that each saddle point might not be asymptotically stable. However, if a component consists of a single point, then that point is asymptotically stable. Interestingly, a close look at the proof of Proposition 6.2.1 reveals that, if the assumptions hold globally, then the asymptotic stability of the set of saddle points is also global, as stated next.

Corollary 6.2.2. (*Global asymptotic stability of the set of saddle points via convexity-concavity*): For $F : \mathbb{R}^n \times \mathbb{R}^m \rightarrow \mathbb{R}$ continuously differentiable and globally strictly convex-concave, $\text{Saddle}(F)$ is globally asymptotically stable under the saddle-point dynamics X_{sp} and the convergence of trajectories is to a point.

Remark 6.2.3. (*Relationship with results on primal-dual dynamics: I*): Corollary 6.2.2 is an extension to more general functions and less stringent assumptions of the results stated for Lagrangian functions of constrained convex (or concave) optimization problems in [WE11, AHU58, FP10] and cost functions of differential games in [RBS13]. In [AHU58, FP10], for a concave optimization, the matrix $\nabla_{xx}F$ is assumed to be negative definite at every saddle point and in [WE11] the set $\text{Saddle}(F)$ is assumed to be a singleton. The work [RBS13] assumes a sufficient condition on the cost functions to guarantee convergence that in the current setup is equivalent to having $\nabla_{xx}F$ and $\nabla_{zz}F$ positive and negative definite, respectively.

•

6.2.2 Stability under convexity-linearity or linearity-concavity

Here we study the asymptotic convergence properties of the saddle-point dynamics when the convexity-concavity of the saddle function is not strict but,

instead, the function depends linearly on its second argument. The analysis follows analogously for saddle functions that are linear in the first argument and concave in the other. The consideration of this class of functions is motivated by equality constrained optimization problems.

Proposition 6.2.4. *(Local asymptotic stability of the set of saddle points via convexity-linearity): For a continuously differentiable function $F : \mathbb{R}^n \times \mathbb{R}^m \rightarrow \mathbb{R}$, if*

(i) *F is locally convex-concave on $\text{Saddle}(F)$ and linear in z ,*

(ii) *for each $(x_*, z_*) \in \text{Saddle}(F)$, there exists a neighborhood $\mathcal{U}_{x_*} \subset \mathbb{R}^n$ of x_* where, if $F(x, z_*) = F(x_*, z_*)$ with $x \in \mathcal{U}_{x_*}$, then $(x, z_*) \in \text{Saddle}(F)$,*

then each isolated path connected component of $\text{Saddle}(F)$ is locally asymptotically stable under the saddle-point dynamics X_{sp} and, moreover, the convergence of trajectories is to a point.

Proof. Given an isolated path connected component \mathcal{S} of $\text{Saddle}(F)$, Lemma 6.4.1 implies that $F|_{\mathcal{S}}$ is constant. Our proof proceeds along similar lines as those of Proposition 6.2.1. With the same notation, given $(x_*, z_*) \in \mathcal{S}$, the arguments follow verbatim until the identification of the largest invariant set M contained in $\{(x, z) \in V^{-1}(\leq V(\alpha)) \mid \mathcal{L}_{X_{sp}}V(x, z) = 0\}$. Let $(x, z) \in M$. From (6.3), $\mathcal{L}_{X_{sp}}V(x, z) = 0$ implies $F(x_*, z) = F(x_*, z_*) = F(x, z_*)$. By assumption (ii), this means $(x, z_*) \in \mathcal{S}$, and by assumption (i), the linearity property gives $\nabla_z F(x, z) = \nabla_z F(x, z_*) = 0$. Therefore $\nabla_z F|_M = 0$. For $(x, z) \in M$, the trajectory $t \mapsto (x(t), z(t))$ of X_{sp} starting at (x, z) is contained in M . Consequently, $z(t) = z$ for all $t \in [0, \infty)$ and $\dot{x}(t) = -\nabla_x F(x(t), z)$ corresponds to the gradient dynamics of the (locally) convex function $y \mapsto F(y, z)$. Therefore, $x(t)$ converges to a minimizer x' of this function, i.e., $\nabla_x F(x', z) = 0$. Since $\nabla_z F|_M = 0$, the continuity of $\nabla_z F$ implies that $\nabla_z F(x', z) = 0$, and hence $(x', z) \in \mathcal{S}$. By continuity of F , it follows that $F(x(t), z) \rightarrow F(x', z) = F(x_*, z_*)$, where for the equality we use the fact that $F|_{\mathcal{S}}$ is constant. On the other hand, note that $0 = \mathcal{L}_{X_{sp}}V(x(t), z) =$

$-(x(t) - x_*)^\top \nabla_x F(x(t), z) \leq F(x_*, z) - F(x(t), z)$ implies

$$F(x(t), z) \leq F(x_*, z) = F(x_*, z_*),$$

for all $t \in [0, \infty)$. Therefore, the monotonically nonincreasing sequence $\{F(x(t), z)\}$ converges to $F(x_*, z_*)$, which is also an upper bound on the whole sequence. This can only be possible if $F(x(t), z) = F(x_*, z_*)$ for all $t \in [0, \infty)$. This further implies $\nabla_x F(x(t), z) = 0$ for all $t \in [0, \infty)$, and hence, $(x, z) \in \mathcal{S}$. Consequently, $M \subset \mathcal{S}$. Since (x_*, z_*) has been chosen arbitrarily, the convergence property holds in a neighborhood of \mathcal{S} . The pointwise convergence follows now from the application of Lemma 6.4.3. \square

The assumption (ii) in the above result is a generalization of the local strict convexity condition for the function $F(\cdot, z_*)$. That is, (ii) allows other points in the neighborhood of x_* to have the same value of the function $F(\cdot, z_*)$ as that at x_* , as long as they are saddle points (whereas, under local strict convexity, x_* is the local unique minimizer of $F(\cdot, z_*)$). The next result extends the conclusions of Proposition 6.2.4 globally when the assumptions hold globally.

Corollary 6.2.5. (*Global asymptotic stability of the set of saddle points via convexity-linearity*): For a \mathcal{C}^1 function $F : \mathbb{R}^n \times \mathbb{R}^m \rightarrow \mathbb{R}$, if

(i) F is globally convex-concave and linear in z ,

(ii) for each $(x_*, z_*) \in \text{Saddle}(F)$, if $F(x, z_*) = F(x_*, z_*)$, then $(x, z_*) \in \text{Saddle}(F)$,

then $\text{Saddle}(F)$ is globally asymptotically stable under the saddle-point dynamics X_{sp} and, moreover, convergence of trajectories is to a point.

Example 6.2.6. (*Saddle-point dynamics for convex optimization*): Consider the following convex optimization problem on \mathbb{R}^3 ,

$$\text{minimize } (x_1 + x_2 + x_3)^2, \tag{6.4a}$$

$$\text{subject to } x_1 = x_2. \tag{6.4b}$$

The set of solutions of this optimization is $\{x \in \mathbb{R}^3 \mid 2x_1 + x_3 = 0, x_2 = x_1\}$, with Lagrangian

$$L(x, z) = (x_1 + x_2 + x_3)^2 + z(x_1 - x_2), \quad (6.5)$$

where $z \in \mathbb{R}$ is the Lagrange multiplier. The set of saddle points of L (which correspond to the set of primal-dual solutions to (6.4)) are $\text{Saddle}(L) = \{(x, z) \in \mathbb{R}^3 \times \mathbb{R} \mid 2x_1 + x_3 = 0, x_1 = x_2, \text{ and } z = 0\}$. However, L is not strictly convex-concave and hence, it does not satisfy the hypotheses of Corollary 6.2.2. While L is globally convex-concave and linear in z , it does not satisfy assumption (ii) of Corollary 6.2.5. Therefore, to identify a dynamics that renders $\text{Saddle}(L)$ asymptotically stable, we form the augmented Lagrangian

$$\tilde{L}(x, z) = L(x, z) + (x_1 - x_2)^2, \quad (6.6)$$

that has the same set of saddle points as L . Note that \tilde{L} is not strictly convex-concave but it is globally convex-concave (this can be seen by computing its Hessian) and is linear in z . Moreover, given any $(x_*, z_*) \in \text{Saddle}(L)$, we have $\tilde{L}(x_*, z_*) = 0$, and if $\tilde{L}(x, z_*) = \tilde{L}(x_*, z_*) = 0$, then $(x, z_*) \in \text{Saddle}(L)$. By Corollary 6.2.5, the trajectories of the saddle-point dynamics of \tilde{L} converge to a point in \mathcal{S} and hence, solve the optimization problem (6.4). Figure 6.1 illustrates this fact. Note that the point of convergence depends on the initial condition. •

Remark 6.2.7. (*Relationship with results on primal-dual dynamics: II*): The work [FP10, Section 4] considers concave optimization problems under inequality constraints where the objective function is not strictly concave but analyzes the convergence properties of a different dynamics. Specifically, the paper studies a discontinuous dynamics based on the saddle-point information of an augmented Lagrangian combined with a projection operator that restricts the dual variables to the nonnegative orthant. We have verified that, for the formulation of the concave optimization problem in [FP10] but with equality constraints, the augmented Lagrangian satisfies the hypotheses of Corollary 6.2.5, implying that the dynamics X_{sp} renders the primal-dual optima of the problem asymptotically stable. •

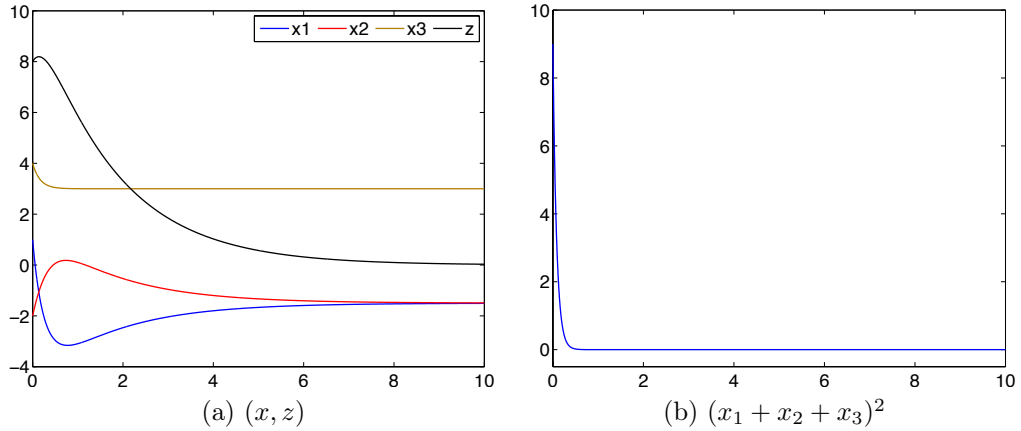


Figure 6.1: (a) Trajectory of the saddle-point dynamics of the augmented Lagrangian \tilde{L} in (6.6) for the optimization problem (6.4). The initial condition is $(x, z) = (1, -2, 4, 8)$. The trajectory converges to $(-1.5, -1.5, 3, 0) \in \text{Saddle}(L)$. (b) Evolution of the objective function of the optimization (6.4) along the trajectory. The value converges to the minimum, 0.

6.2.3 Stability under strong quasiconvexity-quasiconcavity

Motivated by the aim of further relaxing the conditions for asymptotic convergence, we conclude this section by weakening the convexity-concavity requirement on the saddle function. The next result shows that strong quasiconvexity-quasiconcavity is sufficient to ensure convergence of the saddle-point dynamics.

Proposition 6.2.8. *(Local asymptotic stability of the set of saddle points via strong quasiconvexity-quasiconcavity): Let $F : \mathbb{R}^n \times \mathbb{R}^m \rightarrow \mathbb{R}$ be \mathcal{C}^2 and the map $(x, z) \mapsto \nabla_{xz}F(x, z)$ be locally Lipschitz. Assume that F is locally jointly strongly quasiconvex-quasiconcave on $\text{Saddle}(F)$. Then, each isolated path connected component of $\text{Saddle}(F)$ is locally asymptotically stable under the saddle-point dynamics X_{sp} and, moreover, the convergence of trajectories is to a point. Further, if F is globally jointly strongly quasiconvex-quasiconcave and $\nabla_{xz}F$ is constant over $\mathbb{R}^n \times \mathbb{R}^m$, then $\text{Saddle}(F)$ is globally asymptotically stable under X_{sp} and the convergence of trajectories is to a point.*

Proof. Let $(x_*, z_*) \in \mathcal{S}$, where \mathcal{S} is an isolated path connected component of $\text{Saddle}(F)$, and consider the function $V : \mathbb{R}^n \times \mathbb{R}^m \rightarrow \mathbb{R}_{\geq 0}$ defined in (6.2). Let \mathcal{U} be the neighborhood of (x_*, z_*) where the local joint strong quasiconvexity-

quasiconcavity holds. The Lie derivative of V along the saddle-point dynamics at $(x, z) \in \mathcal{U}$ can be written as,

$$\begin{aligned}\mathcal{L}_{X_{\text{sp}}}V(x, z) &= -(x - x_*)^\top \nabla_x F(x, z) + (z - z_*)^\top \nabla_z F(x, z), \\ &= -(x - x_*)^\top \nabla_x F(x, z_*) + (z - z_*)^\top \nabla_z F(x_*, z) + M_1 + M_2,\end{aligned}\quad (6.7)$$

where

$$\begin{aligned}M_1 &= -(x - x_*)^\top (\nabla_x F(x, z) - \nabla_x F(x, z_*)), \\ M_2 &= (z - z_*)^\top (\nabla_z F(x, z) - \nabla_z F(x_*, z)).\end{aligned}$$

Writing

$$\begin{aligned}\nabla_x F(x, z) - \nabla_x F(x, z_*) &= \int_0^1 \nabla_{zx} F(x, z_* + t(z - z_*))(z - z_*) dt, \\ \nabla_z F(x, z) - \nabla_z F(x_*, z) &= \int_0^1 \nabla_{xz} F(x_* + t(x - x_*), z)(x - x_*) dt,\end{aligned}$$

we get

$$\begin{aligned}M_1 + M_2 &= (z - z_*)^\top \left(\int_0^1 (\nabla_{xz} F(x_* + t(x - x_*), z) \right. \\ &\quad \left. - \nabla_{xz} F(x, z_* + t(z - z_*))) dt \right) (x - x_*) \\ &\leq \|z - z_*\| (L\|x - x_*\| + L\|z - z_*\|) \|x - x_*\|,\end{aligned}\quad (6.8)$$

where in the inequality, we have used the fact that $\nabla_{xz} F$ is locally Lipschitz with some constant $L > 0$. From the first-order property of a strong quasiconvex function, cf. Lemma 6.4.2, there exist constants $s_1, s_2 > 0$ such that

$$-(x - x_*)^\top \nabla_x F(x, z_*) \leq -s_1 \|x - x_*\|^2, \quad (6.9a)$$

$$(z - z_*)^\top \nabla_z F(x_*, z) \leq -s_2 \|z - z_*\|^2, \quad (6.9b)$$

for all $(x, z) \in \mathcal{U}$. Substituting (6.8) and (6.9) into the expression for the Lie

derivative (6.7), we obtain

$$\begin{aligned} \mathcal{L}_{X_{\text{sp}}}V(x, z) &\leq -s_1\|x - x_*\|^2 - s_2\|z - z_*\|^2 + L\|x - x_*\|^2\|z - z_*\| \\ &\quad + L\|x - x_*\|\|z - z_*\|^2. \end{aligned}$$

To conclude the proof, note that if $\|z - z_*\| < \frac{s_1}{L}$ and $\|x - x_*\| < \frac{s_2}{L}$, then $\mathcal{L}_{X_{\text{sp}}}V(x, z) < 0$, which implies local asymptotic stability. The pointwise convergence follows from Lemma 6.4.3. The global asymptotic stability can be reasoned using similar arguments as above using the fact that here $M_1 + M_2 = 0$ because $\nabla_{xz}F$ is constant. \square

In the following, we present an example where the above result is employed to explain local asymptotic convergence. In this case, none of the results from Section 6.2.1 and 6.2.2 apply, thereby justifying the importance of the above result.

Example 6.2.9. (*Convergence for locally jointly strongly quasiconvex-quasiconcave function*): Consider $F : \mathbb{R} \times \mathbb{R} \rightarrow \mathbb{R}$ given by,

$$F(x, z) = (2 - e^{-x^2})(1 + e^{-z^2}). \quad (6.10)$$

Note that F is \mathcal{C}^2 and $\nabla_{xz}F(x, z) = -4xze^{-x^2}e^{-z^2}$ is locally Lipschitz. To see this, note that the function $x \mapsto xe^{-x^2}$ is bounded and is locally Lipschitz (as its derivative is bounded). Further, the product of two bounded and locally Lipschitz functions is locally Lipschitz [Soh03, Theorem 4.6.3] and so, $(x, z) \mapsto \nabla_{xz}F(x, z)$ is locally Lipschitz. The set of saddle points of F is $\text{Saddle}(F) = \{0\}$. Next, we show that $x \mapsto f(x) = c_1 - c_2e^{-x^2}$, $c_2 > 0$, is locally strongly quasiconvex at 0. Fix $\delta > 0$ and let $x, y \in B_\delta(0)$ such that $f(y) \leq f(x)$. Then, $|y| \leq |x|$ and

$$\begin{aligned} &\max\{f(x), f(y)\} - f(\lambda x + (1 - \lambda)y) - s\lambda(1 - \lambda)(x - y)^2 \\ &\quad = c_2(-e^{-x^2} + e^{-(\lambda x + (1 - \lambda)y)^2}) - s\lambda(1 - \lambda)(x - y)^2 \\ &\quad \geq c_2e^{-x^2}(x^2 - (\lambda x + (1 - \lambda)y)^2) - s\lambda(1 - \lambda)(x - y)^2 \\ &\quad = (1 - \lambda)(x - y)\left(c_2e^{-x^2}(x + y) + \lambda(x - y)(c_2e^{-x^2} - s)\right) \geq 0, \end{aligned}$$

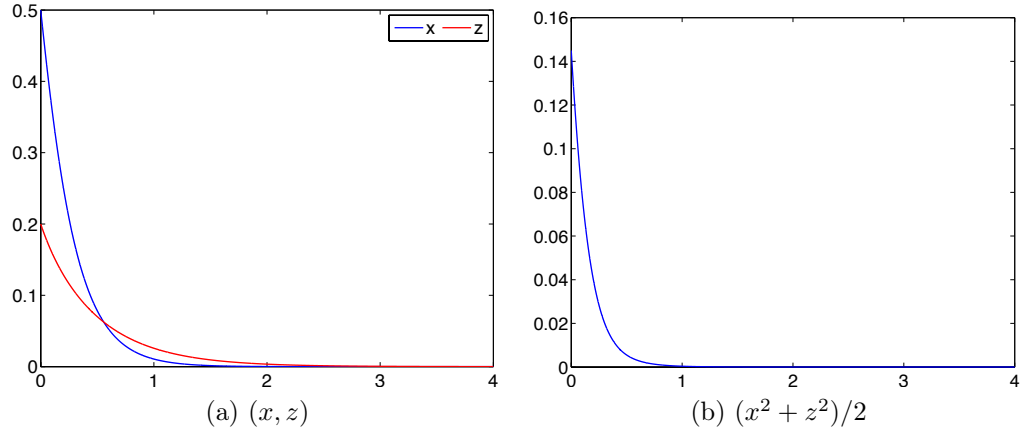


Figure 6.2: (a) Trajectory of the saddle-point dynamics for F given in (6.10). The initial condition is $(x, z) = (0.5, 0.2)$. The trajectory converges to the saddle point $(0, 0)$. (b) Evolution of the function V along the trajectory.

for $s \leq c_2 e^{-\delta^2}$, given the fact that $|y| \leq |x|$. Therefore, f is locally strongly quasiconvex and so $-f$ is locally strongly quasiconcave. Using these facts, we deduce that F is locally jointly strongly quasiconvex-quasiconcave. Thus, the hypotheses of Proposition 6.2.8 are met, implying local asymptotic stability of $\text{Saddle}(F)$ under the saddle-point dynamics. Figure 6.2 illustrates this fact in simulation. Note that F does not satisfy the conditions outlined in results of Section 6.2.1 and 6.2.2. •

6.3 Convergence analysis for general saddle functions

We study here the convergence properties of the saddle-point dynamics associated to functions that are not convex-concave. Our first result explores conditions for local asymptotic stability based on the linearization of the dynamics and properties of the eigenstructure of the Jacobian matrices. In particular, we assume that X_{sp} is piecewise \mathcal{C}^2 and that the set of limit points of the Jacobian of X_{sp} at any saddle point have a common kernel and negative real parts for the nonzero eigenvalues. The proof is a direct consequence of Proposition 6.4.5.

Proposition 6.3.1. *(Local asymptotic stability of manifold of saddle points via*

linearization – piecewise \mathcal{C}^3 saddle function): Given $F : \mathbb{R}^n \times \mathbb{R}^m \rightarrow \mathbb{R}$, let $\mathcal{S} \subset \text{Saddle}(F)$ be a p -dimensional submanifold of saddle points. Assume that F is \mathcal{C}^1 with locally Lipschitz gradient on a neighborhood of \mathcal{S} and that the vector field X_{sp} is piecewise \mathcal{C}^2 . Assume that at each $(x_*, z_*) \in \mathcal{S}$, the set of matrices $\mathcal{A}_* \subset \mathbb{R}^{n+m \times n+m}$ defined as

$$\mathcal{A}_* = \left\{ \lim_{k \rightarrow \infty} DX_{sp}(x_k, z_k) \mid (x_k, z_k) \rightarrow (x, z), (x_k, z_k) \in \mathbb{R}^{n+m} \setminus \Omega_{X_{sp}} \right\},$$

where $\Omega_{X_{sp}}$ is the set of points where X_{sp} is not differentiable, satisfies the following:

(i) there exists an orthogonal matrix $Q \in \mathbb{R}^{n+m \times n+m}$ such that

$$Q^\top A Q = \begin{bmatrix} 0 & 0 \\ 0 & \tilde{A} \end{bmatrix}, \quad (6.11)$$

for all $A \in \mathcal{A}_*$, where $\tilde{A} \in \mathbb{R}^{n+m-p \times n+m-p}$,

(ii) the nonzero eigenvalues of the matrices in \mathcal{A}_* have negative real parts,

(iii) there exists a positive definite matrix $P \in \mathbb{R}^{n+m-p \times n+m-p}$ such that

$$\tilde{A}^\top P + P \tilde{A} \prec 0,$$

for all \tilde{A} obtained by applying transformation (6.11) on each $A \in \mathcal{A}_*$.

Then, \mathcal{S} is locally asymptotically stable under (6.30) and the trajectories converge to a point in \mathcal{S} .

When F is sufficiently smooth, we can refine the above result as follows.

Corollary 6.3.2. (Local asymptotic stability of manifold of saddle points via linearization – \mathcal{C}^3 saddle function): Given $F : \mathbb{R}^n \times \mathbb{R}^m \rightarrow \mathbb{R}$, let $\mathcal{S} \subset \text{Saddle}(F)$ be a p -dimensional manifold of saddle points. Assume F is \mathcal{C}^3 on a neighborhood of \mathcal{S} and that the Jacobian of X_{sp} at each point in \mathcal{S} has no eigenvalues in the imaginary axis other than 0, which is semisimple with multiplicity p . Then, \mathcal{S} is locally asymptotically stable under the saddle-point dynamics X_{sp} and the trajectories converge to a point.

Proof. Since F is \mathcal{C}^3 , the map X_{sp} is \mathcal{C}^2 and so, the limit point of Jacobian matrices at a saddle point $(x_*, z_*) \in \mathcal{S}$ is the Jacobian at that point itself, that is,

$$DX_{\text{sp}} = \begin{bmatrix} -\nabla_{xx}F & -\nabla_{xz}F \\ \nabla_{zx}F & \nabla_{zz}F \end{bmatrix}_{(x_*, z_*)}.$$

From the definition of saddle point, we have $\nabla_{xx}F(x_*, z_*) \succeq 0$ and $\nabla_{zz}F(x_*, z_*) \preceq 0$. In turn, we obtain $DX_{\text{sp}} + DX_{\text{sp}}^\top \preceq 0$, and since $\text{Re}(\lambda_i(DX_{\text{sp}})) \leq \lambda_{\max}(\frac{1}{2}(DX_{\text{sp}} + DX_{\text{sp}}^\top))$ [Ber05, Fact 5.10.28], we deduce that $\text{Re}(\lambda_i(DX_{\text{sp}})) \leq 0$. The statement now follows from Proposition 6.3.1 using the fact that the properties of the eigenvalues of DX_{sp} shown here imply existence of an orthonormal transformation leading to a form of DX_{sp} that satisfies assumptions (i)-(iii) of Proposition 6.3.1. \square

Next, we provide a sufficient condition under which the Jacobian of X_{sp} for a saddle function F that is linear in its second argument satisfies the hypothesis of Corollary 6.3.2 regarding the lack of eigenvalues on the imaginary axis other than 0.

Lemma 6.3.3. *(Sufficient condition for absence of imaginary eigenvalues of the Jacobian of X_{sp}): Let $F : \mathbb{R}^n \times \mathbb{R}^m \rightarrow \mathbb{R}$ be \mathcal{C}^2 and linear in the second argument. Then, the Jacobian of X_{sp} at any saddle point (x_*, z_*) of F has no eigenvalues on the imaginary axis except for 0 if $\text{range}(\nabla_{zx}F(x_*, z_*)) \cap \text{null}(\nabla_{xx}F(x_*, z_*)) = \{0\}$.*

Proof. The Jacobian of X_{sp} at a saddle point (x_*, z_*) for a saddle function F that is linear in z is given as

$$DX_{\text{sp}} = \begin{bmatrix} A & B \\ -B^\top & 0 \end{bmatrix},$$

where $A = -\nabla_{xx}F(x_*, z_*)$ and $B = -\nabla_{zx}F(x_*, z_*)$. We reason by contradiction. Let $i\lambda$, $\lambda \neq 0$ be an imaginary eigenvalue of DX_{sp} with the corresponding eigenvector $a + ib$. Let $a = (a_1; a_2)$ and $b = (b_1; b_2)$ where $a_1, b_1 \in \mathbb{R}^n$ and $a_2, b_2 \in \mathbb{R}^m$. Then the real and imaginary parts of the condition $DX_{\text{sp}}(a + ib) = (i\lambda)(a + ib)$

yield

$$Aa_1 + Ba_2 = -\lambda b_1, \quad -B^\top a_1 = -\lambda b_2, \quad (6.12)$$

$$Ab_1 + Bb_2 = \lambda a_1, \quad -B^\top b_1 = \lambda a_2. \quad (6.13)$$

Pre-multiplying the first equation of (6.12) with a_1^\top gives $a_1^\top Aa_1 + a_1^\top Ba_2 = -\lambda a_1^\top b_1$. Using the second equation of (6.12), we get $a_1^\top Aa_1 = -\lambda(a_1^\top b_1 + a_2^\top b_2)$. A similar procedure for the set of equations in (6.13) gives $b_1^\top Ab_1 = \lambda(a_1^\top b_1 + a_2^\top b_2)$. These conditions imply that $a_1^\top Aa_1 = -b_1^\top Ab_1$. Since A is negative semi-definite, we obtain $a_1, b_1 \in \text{null}(A)$. Note that $a_1, b_1 \neq 0$, because otherwise it would mean that $a = b = 0$. Further, using this fact in the first equations of (6.12) and (6.13), respectively, we get

$$Ba_2 = -\lambda b_1, \quad Bb_2 = \lambda a_1.$$

That is, $a_1, b_1 \in \text{range}(B)$, a contradiction. \square

The following example illustrates an application of the above results to a nonconvex constrained optimization problem.

Example 6.3.4. (*Saddle-point dynamics for nonconvex optimization*): Consider the following constrained optimization on \mathbb{R}^3 ,

$$\text{minimize} \quad (\|x\| - 1)^2, \quad (6.14a)$$

$$\text{subject to} \quad x_3 = 0.5, \quad (6.14b)$$

where $x = (x_1, x_2, x_3) \in \mathbb{R}^3$. The optimizers are $\{x \in \mathbb{R}^3 \mid x_3 = 0.5, x_1^2 + x_2^2 = 0.75\}$. The Lagrangian $L : \mathbb{R}^3 \times \mathbb{R} \rightarrow \mathbb{R}$ is given by

$$L(x, z) = (\|x\| - 1)^2 + z(x_3 - 0.5),$$

and its set of saddle points is the one-dimensional manifold $\text{Saddle}(L) = \{(x, z) \in \mathbb{R}^3 \times \mathbb{R} \mid x_3 = 0.5, x_1^2 + x_2^2 = 0.75, z = 0\}$. The saddle-point dynamics of L takes

the form

$$\dot{x} = -2\left(1 - \frac{1}{\|x\|}\right)x - [0, 0, z]^\top, \quad (6.15a)$$

$$\dot{z} = x_3 - 0.5. \quad (6.15b)$$

Note that $\text{Saddle}(L)$ is nonconvex and that L is nonconvex in its first argument on any neighborhood of any saddle point. Therefore, results that rely on the convexity-concavity properties of L are not applicable to establish the asymptotic convergence of (6.15) to the set of saddle points. This can, however, be established through Corollary 6.3.2 by observing that the Jacobian of X_{sp} at any point of $\text{Saddle}(L)$ has 0 as an eigenvalue with multiplicity one and the rest of the eigenvalues are not on the imaginary axis. To show this, consider $(x_*, z_*) \in \text{Saddle}(L)$. Note that $DX_{\text{sp}}(x_*, z_*) = \begin{bmatrix} -2x_*^\top x_* & -e_3 \\ e_3^\top & 0 \end{bmatrix}$, where $e_3 = [0, 0, 1]^\top$. One can deduce from this that $v \in \text{null}(DX_{\text{sp}}(x_*, z_*))$ if and only if $x_*^\top [v_1, v_2, v_3]^\top = 0$, $v_3 = 0$, and $v_4 = 0$. These three conditions define a one-dimensional space and so 0 is an eigenvalue of $DX_{\text{sp}}(x_*, z_*)$ with multiplicity 1. To show that the rest of eigenvalues do not lie on the imaginary axis, we show that the hypotheses of Lemma 6.3.3 are met. At any saddle point (x_*, z_*) , we have $\nabla_{zx}L(x_*, z_*) = e_3$ and $\nabla_{xx}L(x_*, z_*) = 2x_*^\top x_*$. If $v \in \text{range}(\nabla_{zx}L(x_*, z_*)) \cap \text{null}(\nabla_{xx}L(x_*, z_*))$ then $v = [0, 0, \lambda]^\top$, $\lambda \in \mathbb{R}$, and $x_*^\top v = 0$. Since $(x_*)_3 = 0.5$, we get $\lambda = 0$ and hence, the hypotheses of Lemma 6.3.3 are satisfied. Figure 6.3 illustrates in simulation the convergence of the trajectories to a saddle point. The point of convergence depends on the initial condition. •

There are functions that do not satisfy the hypotheses of Proposition 6.3.1 whose saddle-point dynamics still seems to enjoy local asymptotic convergence properties. As an example, consider the function $F : \mathbb{R}^2 \times \mathbb{R} \rightarrow \mathbb{R}$,

$$F(x, z) = (\|x\| - 1)^4 - z^2\|x\|^2, \quad (6.16)$$

whose set of saddle points is the one-dimensional manifold $\text{Saddle}(F) = \{(x, z) \in \mathbb{R}^2 \times \mathbb{R} \mid \|x\| = 1, z = 0\}$. The Jacobian of the saddle-point dynamics at any $(x, z) \in \text{Saddle}(F)$ has -2 as an eigenvalue and 0 as the other eigenvalue, with

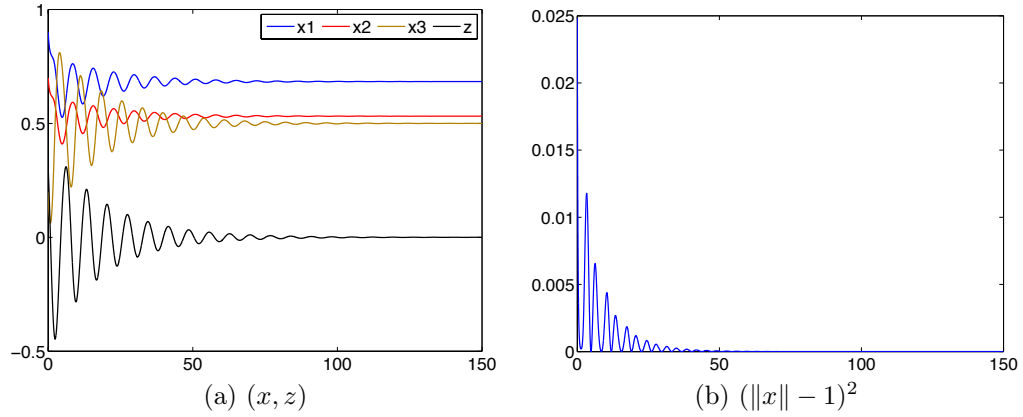


Figure 6.3: (a) Trajectory of the saddle-point dynamics (6.15) for the Lagrangian of the constrained optimization problem (6.14). The initial condition is $(x, z) = (0.9, 0.7, 0.2, 0.3)$. The trajectory converges to $(0.68, 0.53, 0.50, 0) \in \text{Saddle}(L)$. (b) Evolution of the objective function of the optimization (6.14) along the trajectory. The value converges to the minimum, 0.

multiplicity 2, which is greater than the dimension of $\text{Saddle}(F)$ (and therefore Proposition 6.3.1 cannot be applied). Simulations show that the trajectories of the saddle-point dynamics asymptotically approach $\text{Saddle}(S)$ if the initial condition is close enough to this set. Our next result allows us to formally establish this fact by studying the behavior of the distance function along the proximal normals to $\text{Saddle}(F)$.

Proposition 6.3.5. (*Asymptotic stability of manifold of saddle points via proximal normals*): Let $F : \mathbb{R}^n \times \mathbb{R}^m \rightarrow \mathbb{R}$ be \mathcal{C}^2 and $\mathcal{S} \subset \text{Saddle}(F)$ be a closed set. Assume there exist constants $\lambda_M, k_1, k_2, \alpha_1, \beta_1 > 0$ and $L_x, L_z, \alpha_2, \beta_2 \geq 0$ such that the following hold

- (i) either $L_x = 0$ or $\alpha_1 \leq \alpha_2 + 1$,
- (ii) either $L_z = 0$ or $\beta_1 \leq \beta_2 + 1$,
- (iii) for every $(x_*, z_*) \in \mathcal{S}$ and every proximal normal $\eta = (\eta_x, \eta_z) \in \mathbb{R}^n \times \mathbb{R}^m$ to \mathcal{S} at (x_*, z_*) with $\|\eta\| = 1$, the functions

$$[0, \lambda_M) \ni \lambda \mapsto F(x_* + \lambda\eta_x, z_*),$$

$$[0, \lambda_M) \ni \lambda \mapsto F(x_*, z_* + \lambda\eta_z),$$

are convex and concave, respectively, with

$$F(x_* + \lambda\eta_x, z_*) - F(x_*, z_*) \geq k_1 \|\lambda\eta_x\|^{\alpha_1}, \quad (6.17a)$$

$$F(x_*, z_* + \lambda\eta_z) - F(x_*, z_*) \leq -k_2 \|\lambda\eta_z\|^{\beta_1}, \quad (6.17b)$$

and, for all $\lambda \in [0, \lambda_M)$ and all $t \in [0, 1]$,

$$\begin{aligned} \|\nabla_{xz}F(x_* + t\lambda\eta_x, z_* + \lambda\eta_z) - \nabla_{xz}F(x_* + \lambda\eta_x, z_* + t\lambda\eta_z)\| \\ \leq L_x \|\lambda\eta_x\|^{\alpha_2} + L_z \|\lambda\eta_z\|^{\beta_2}. \end{aligned} \quad (6.18)$$

Then, \mathcal{S} is locally asymptotically stable under the saddle-point dynamics X_{sp} . Moreover, the convergence of the trajectories is to a point if every point of \mathcal{S} is stable. The convergence is global if, for every $\lambda_M \in \mathbb{R}_{\geq 0}$, there exist $k_1, k_2, \alpha_1, \beta_1 > 0$ such that the above hypotheses (i)-(iii) are satisfied by these constants along with $L_x = L_z = 0$.

Proof. Our proof is based on showing that there exists $\bar{\lambda} \in (0, \lambda_M]$ such that the distance function $d_{\mathcal{S}}$ decreases monotonically and converges to zero along the trajectories of X_{sp} that start in $\mathcal{S} + B_{\bar{\lambda}}(0)$. From (2.3),

$$\partial d_{\mathcal{S}}^2(x, z) = \text{co}\{2(x - x_*; z - z_*) \mid (x_*, z_*) \in \text{proj}_{\mathcal{S}}(x, z)\}.$$

Following [Cor08], we compute the set-valued Lie derivative of $d_{\mathcal{S}}^2$ along X_{sp} , denoted $\mathcal{L}_{X_{sp}} d_{\mathcal{S}}^2 : \mathbb{R}^n \times \mathbb{R}^m \rightrightarrows \mathbb{R}$, as

$$\begin{aligned} \mathcal{L}_{X_{sp}} d_{\mathcal{S}}^2(x, z) = \text{co}\{-2(x - x_*)^\top \nabla_x F(x, z) + \\ 2(z - z_*)^\top \nabla_z F(x, z) \mid (x_*, z_*) \in \text{proj}_{\mathcal{S}}(x, z)\}. \end{aligned}$$

Since $d_{\mathcal{S}}^2$ is globally Lipschitz and regular, cf. Section 2.3, the evolution of the function $d_{\mathcal{S}}^2$ along any trajectory $t \mapsto (x(t), z(t))$ of (6.1) is differentiable at almost all $t \in \mathbb{R}_{\geq 0}$, and furthermore, cf. [Cor08, Proposition 10],

$$\frac{d}{dt}(d_{\mathcal{S}}^2(x(t), z(t)) \in \mathcal{L}_{X_{sp}} d_{\mathcal{S}}^2(x(t), z(t))$$

for almost all $t \in \mathbb{R}_{\geq 0}$. Therefore, our goal is to show that $\max \mathcal{L}_{X_{\text{sp}}} d_{\mathcal{S}}^2(x, z) < 0$ for all $(x, z) \in (\mathcal{S} + B_{\bar{\lambda}}(0)) \setminus \mathcal{S}$ for some $\bar{\lambda} \in (0, \lambda_M]$. Let $(x, z) \in \mathcal{S} + B_{\lambda_M}(0)$ and take $(x_*, z_*) \in \text{proj}_{\mathcal{S}}(x, z)$. By definition, there exists a proximal normal $\eta = (\eta_x, \eta_z)$ to \mathcal{S} at (x_*, z_*) with $\|\eta\| = 1$ and $x = x_* + \lambda\eta_x$, $z = z_* + \lambda\eta_z$, and $\lambda \in [0, \lambda_M]$. Let $2\xi \in \mathcal{L}_{X_{\text{sp}}} d_{\mathcal{S}}^2(x, z)$ denote

$$\xi = -(x - x_*)^\top \nabla_x F(x, z) + (z - z_*)^\top \nabla_z F(x, z). \quad (6.19)$$

Writing

$$\begin{aligned} \nabla_x F(x, z) &= \nabla_x F(x, z_*) + \int_0^1 \nabla_{zx} F(x, z_* + t(z - z_*))(z - z_*) dt, \\ \nabla_z F(x, z) &= \nabla_z F(x_*, z) + \int_0^1 \nabla_{xz} F(x_* + t(x - x_*), z)(x - x_*) dt, \end{aligned}$$

and substituting in (6.19) we get

$$\xi = -(x - x_*)^\top \nabla_x F(x, z_*) + (z - z_*)^\top \nabla_z F(x_*, z) + (z - z_*)^\top M(x - x_*), \quad (6.20)$$

where $M = \int_0^1 (\nabla_{xz} F(x_* + t(x - x_*), z) - \nabla_{xz} F(x, z_* + t(z - z_*))) dt$. Using the convexity and concavity along the proximal normal and applying the bounds (6.17), we obtain

$$-(x - x_*)^\top \nabla_x F(x, z_*) \leq F(x_*, z_*) - F(x, z_*) \leq -k_1 \|\lambda\eta_x\|^{\alpha_1}, \quad (6.21a)$$

$$(z - z_*)^\top \nabla_z F(x_*, z) \leq F(x_*, z) - F(x_*, z_*) \leq -k_2 \|\lambda\eta_z\|^{\beta_1}. \quad (6.21b)$$

On the other hand, using (6.18), we bound M by

$$\|M\| \leq L_x \|\lambda\eta_x\|^{\alpha_2} + L_z \|\lambda\eta_z\|^{\beta_2}. \quad (6.22)$$

Using (6.21) and (6.22) in (6.20), and rearranging the terms yields

$$\xi \leq (-k_1 \|\lambda\eta_x\|^{\alpha_1} + L_x \|\lambda\eta_x\|^{\alpha_2+1} \|\lambda\eta_z\|) + (-k_2 \|\lambda\eta_z\|^{\beta_1} + L_z \|\lambda\eta_z\|^{\beta_2+1} \|\lambda\eta_x\|).$$

If $L_x = 0$, then the first parenthesis is negative whenever $\lambda\eta_x \neq 0$ (i.e., $x \neq x_*$). If $L_x \neq 0$ and $\alpha_1 \leq \alpha_2 + 1$, then for $\|\lambda\eta_x\| < 1$ and $\|\lambda\eta_z\| < \min(1, k_1/L_x)$, the first parenthesis is negative whenever $\lambda\eta_x \neq 0$. Analogously, the second parenthesis is negative for $z \neq z_*$ if either $L_z = 0$ or $\beta_1 \leq \beta_2 + 1$ with $\|\lambda\eta_z\| < 1$ and $\|\lambda\eta_x\| < \min(1, k_2/L_z)$. Thus, if $\lambda < \min\{1, k_1/L_x, k_2/L_z\}$ (excluding from the min operation the elements that are not well defined due to the denominator being zero), then hypotheses (i)-(ii) imply that $\xi < 0$ whenever $(x, z) \neq (x_*, z_*)$. Moreover, since $(x_*, z_*) \in \text{proj}_{\mathcal{S}}(x, z)$ was chosen arbitrarily, we conclude that $\max \mathcal{L}_{X_{\text{sp}}} d_{\mathcal{S}}^2(x, z) < 0$ for all $(x, z) \in \mathcal{S} + B_{\bar{\lambda}}(0)$ where $\bar{\lambda} \in (0, \lambda_M]$ satisfies $\bar{\lambda} < \min\{1, k_1/L_x, k_2/L_z\}$. This proves the local asymptotic stability. Finally, convergence to a point follows from Lemma 6.4.3 and global convergence follows from the analysis done above. \square

Intuitively, the hypotheses of Proposition 6.3.5 imply that along the proximal normal to the saddle set, the convexity (resp. concavity) in the x -coordinate (resp. z -coordinate) is ‘stronger’ than the influence of the x - and z -dynamics on each other, represented by the off-diagonal Hessian terms. When this coupling is absent (i.e., $\nabla_{xz}F \equiv 0$), the x - and z -dynamics are independent of each other and they function as individually aiming to minimize (resp. maximize) a function of one variable, thereby, reaching a saddle point. Note that the assumptions of Proposition 6.3.5 do not imply that F is locally convex-concave. As an example, the function in (6.16) is not convex-concave in any neighborhood of any saddle point but we show next that it satisfies the assumptions of Proposition 6.3.5, establishing local asymptotic convergence of the respective saddle-point dynamics.

Example 6.3.6. (*Convergence analysis via proximal normals*): Consider the function F defined in (6.16). Consider a saddle point $(x_*, z_*) = (\cos \theta, \sin \theta, 0) \in \text{Saddle}(F)$, where $\theta \in [0, 2\pi)$. Let

$$\eta = (\eta_x, \eta_z) = ((a_1 \cos \theta, a_1 \sin \theta), a_2),$$

with $a_1, a_2 \in \mathbb{R}$ and $a_1^2 + a_2^2 = 1$, be a proximal normal to $\text{Saddle}(F)$ at (x_*, z_*) . Note that the function $\lambda \mapsto F(x_* + \lambda\eta_x, z_*) = (\lambda a_1)^4$ is convex, satisfying (6.17a)

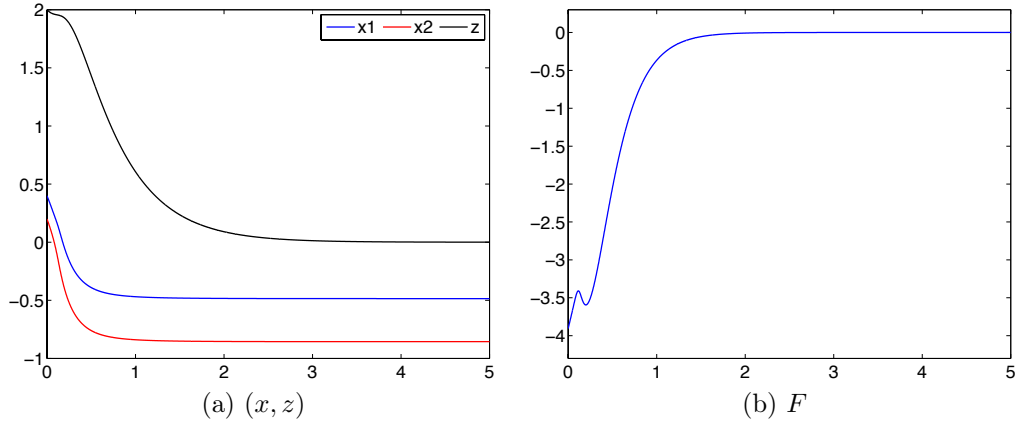


Figure 6.4: (a) Trajectory of the saddle-point dynamics for the function defined by (6.16). The initial condition is $(x, z) = (0.1, 0.2, 4)$. The trajectory converges to $(0.49, 0.86, 0) \in \text{Saddle}(F)$. (b) Evolution of the function F along the trajectory. The value converges to 0, the value that the function takes on its saddle set.

with $k_1 = 1$ and $\alpha_1 = 4$. The function $\lambda \mapsto F(x_*, z_* + \lambda\eta_z) = -(\lambda a_2)^2$ is concave, satisfying (6.17b) with $k_2 = 1$, $\beta_1 = 2$. Also, given any $\lambda_M > 0$ and for all $t \in [0, 1]$, we can write

$$\begin{aligned}
 & \|\nabla_{xz}F(x_* + t\lambda\eta_x, z_* + \lambda\eta_z) - \nabla_{xz}F(x_* + \lambda\eta_x, z_* + t\lambda\eta_z)\| \\
 &= \left\| -4(\lambda a_2)(1 + t\lambda a_1) \begin{pmatrix} \cos\theta \\ \sin\theta \end{pmatrix} + 4(t\lambda a_2)(1 + \lambda a_1) \begin{pmatrix} \cos\theta \\ \sin\theta \end{pmatrix} \right\|, \\
 &\leq \|4(\lambda a_2)(1 + t\lambda a_1) - 4(t\lambda a_2)(1 + \lambda a_1)\|, \\
 &\leq 8(1 + \lambda a_1)(\lambda a_2) \leq L_z(\lambda a_2),
 \end{aligned}$$

for $\lambda \leq \lambda_M$, where $L_z = 8(1 + \lambda_M a_1)$. This implies that $L_x = 0$, $L_z \neq 0$ and $\beta_2 = 1$. Therefore, hypotheses (i)-(iii) of Proposition 6.3.5 are satisfied and this establishes asymptotic convergence of the saddle-point dynamics. Figure 6.4 illustrates this fact. Note that since $L_z \neq 0$, we cannot guarantee global convergence. \bullet

Interestingly, Propositions 6.3.1 and 6.3.5 complement each other. The function (6.16) satisfies the hypotheses of Proposition 6.3.5 but not those of Proposition 6.3.1. Conversely, the Lagrangian of the constrained optimization (6.14) satisfies the hypotheses of Proposition 6.3.1 but not those of Proposition 6.3.5.

In the next result, we consider yet another scenario where the saddle function might not be convex-concave in its arguments but the saddle-point dynam-

ics converges to the set of equilibrium points. As a motivation, consider the function $F : \mathbb{R} \times \mathbb{R} \rightarrow \mathbb{R}$, $F(x, z) = xz^2$. The set of saddle points of F are $\text{Saddle}(F) = \mathbb{R}_{\leq 0} \times \{0\}$. One can show that, at the saddle point $(0, 0)$, neither the hypotheses of Proposition 6.3.1 nor those of Proposition 6.3.5 are satisfied. Yet, simulations show that the trajectories of the dynamics converge to the saddle points from almost all initial conditions in \mathbb{R}^2 , see Figure 6.5 below. This asymptotic behavior can be characterized through the following result which generalizes [KP87, Theorem 3].

Proposition 6.3.7. (*Global asymptotic stability of equilibria of saddle-point dynamics for saddle functions linear in one argument*): For $F : \mathbb{R}^n \times \mathbb{R}^m \rightarrow \mathbb{R}$, assume the following form $F(x, z) = g(z)^\top x$, where $g : \mathbb{R}^m \rightarrow \mathbb{R}^n$ is \mathcal{C}^1 . Assume that there exists $(x_*, z_*) \in \text{Saddle}(F)$ such that

- (i) $F(x_*, z_*) \geq F(x_*, z)$ for all $z \in \mathbb{R}^m$,
- (ii) for any $z \in \mathbb{R}^m$, the condition $g(z)^\top x_* = 0$ implies $g(z) = 0$,
- (iii) any trajectory of X_{sp} is bounded.

Then, all trajectories of the saddle-point dynamics X_{sp} converge asymptotically to the set of equilibrium points of X_{sp} .

Proof. Consider the function $V : \mathbb{R}^n \times \mathbb{R}^m \rightarrow \mathbb{R}$,

$$V(x, z) = -x_*^\top x.$$

The Lie derivative of V along the saddle-point dynamics X_{sp} is

$$\mathcal{L}_{X_{sp}} V(x, z) = x_*^\top \nabla_x F(x, z) = x_*^\top g(z) = F(x_*, z) \leq F(x_*, z_*) = 0, \quad (6.23)$$

where in the inequality we have used assumption (i), and $F(x_*, z_*) = 0$ is implied by the definition of the saddle point, that is, $\nabla_x F(x_*, z_*) = g(z_*) = 0$. Now consider any trajectory $t \mapsto (x(t), z(t))$, $(x(0), z(0)) \in \mathbb{R}^n \times \mathbb{R}^m$ of X_{sp} . Since the trajectory is bounded by assumption (iii), the application of the LaSalle Invariance Principle [Kha02, Theorem 4.4] yields that the trajectory converges to the

largest invariant set \mathcal{M} contained in $\{(x, z) \in \mathbb{R}^n \times \mathbb{R}^m \mid \mathcal{L}_{X_{\text{sp}}} V(x, z) = 0\}$, which from (6.23) is equal to the set $\{(x, z) \in \mathbb{R}^n \times \mathbb{R}^m \mid F(x_*, z) = 0\}$. Let $(x, z) \in \mathcal{M}$. Then, we have $F(x_*, z) = g(z)^\top x_* = 0$ and by hypotheses (ii) we get $g(z) = 0$. Therefore, if $(x, z) \in \mathcal{M}$ then $g(z) = 0$. Consider the trajectory $t \mapsto (x(t), z(t))$ of X_{sp} with $(x(0), z(0)) = (x, z)$ which is contained in \mathcal{M} . Then, along the trajectory we have

$$\dot{x}(t) = -\nabla_x F(x(t), z(t)) = -g(z(t)) = 0.$$

Further, note that along this trajectory we have $g(z(t)) = 0$ for all $t \geq 0$. Thus, $\frac{d}{dt}g(z(t)) = 0$ for all $t \geq 0$, which implies that

$$\frac{d}{dt}g(z(t)) = Dg(z(t))\dot{z}(t) = Dg(z(t))Dg(z(t))^\top x = 0.$$

From the above expression we deduce that $\dot{z}(t) = Dg(z(t))^\top x = 0$. This can be seen from the fact that $Dg(z(t))Dg(z(t))^\top x = 0$ implies $x^\top Dg(z(t))Dg(z(t))^\top x = (Dg(z(t))^\top x)^2 = 0$. From the above reasoning, we conclude that (x, z) is an equilibrium point of X_{sp} . \square

The proof of Proposition 6.3.7 hints at the fact that hypothesis (ii) can be omitted if information about other saddle points of F is known. Specifically, consider the case where n saddle points $(x_*^{(1)}, z_*^{(1)}), \dots, (x_*^{(n)}, z_*^{(n)})$ of F exist, each satisfying hypothesis (i) of Proposition 6.3.7 and such that the vectors $x_*^{(1)}, \dots, x_*^{(n)}$ are linearly independent. In this scenario, for those points $z \in \mathbb{R}^m$ such that $g(z)^\top x_*^{(i)} = 0$ for all $i \in [n]$ (as would be obtained in the proof), the linear independence of $x_*^{(i)}$'s already implies that $g(z) = 0$, making hypothesis (ii) unnecessary.

Corollary 6.3.8. *(Almost global asymptotic stability of saddle points for saddle functions linear in one argument): If, in addition to the hypotheses of Proposition 6.3.7, the set of equilibria of X_{sp} other than those belonging to $\text{Saddle}(F)$ are unstable, then the trajectories of X_{sp} converge asymptotically to $\text{Saddle}(F)$ from almost all initial conditions (all but the unstable equilibria). Moreover, if each point in $\text{Saddle}(F)$ is stable under X_{sp} , then $\text{Saddle}(F)$ is almost globally asymptotically*

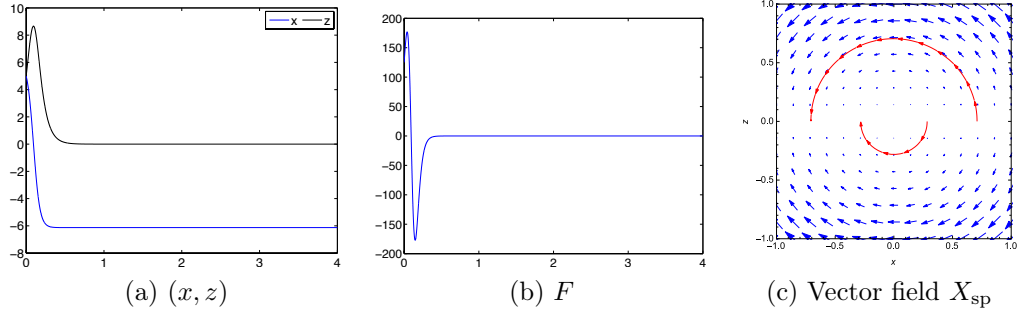


Figure 6.5: (a) Trajectory of the saddle-point dynamics for the function $F(x, z) = xz^2$. The initial condition is $(x, z) = (5, 5)$. The trajectory converges to $(-6.13, 0) \in \text{Saddle}(F)$. (b) Evolution of the function F along the trajectory. The value converges to 0, the value that the function takes on its saddle set. (c) The vector field X_{sp} , depicting that the set of saddle points are attractive while the other equilibrium points $\mathbb{R}_{>0} \times \{0\}$ are unstable.

stable under the saddle-point dynamics X_{sp} and the trajectories converge to a point in $\text{Saddle}(F)$.

Next, we illustrate how the above result can be applied to the motivating example given before Proposition 6.3.7 to infer almost global convergence of the trajectories.

Example 6.3.9. (*Convergence for saddle functions linear in one argument*): Consider again $F(x, z) = xz^2$ with $\text{Saddle}(F) = \{(x, z) \in \mathbb{R} \times \mathbb{R} \mid x \leq 0 \text{ and } z = 0\}$. Pick $(x_*, z_*) = (-1, 0)$. One can verify that this saddle point satisfies the hypotheses (i) and (ii) of Proposition 6.3.7. Moreover, along any trajectory of the saddle-point dynamics for F , the function $x^2 + \frac{z^2}{2}$ is preserved, which implies that all trajectories are bounded. One can also see that the equilibria of the saddle-point dynamics that are not saddle points, that is the set $\mathbb{R}_{>0} \times \{0\}$, are unstable. Therefore, from Corollary 6.3.8, we conclude that the trajectories of the saddle-point dynamics asymptotically converge to the set of saddle points from almost all initial conditions. Figure 6.5 illustrates these observations. •

6.4 Auxiliary results

This section contains some auxiliary results for our convergence analysis in Sections 6.2 and 6.3. Our first result establishes the constant value of the saddle function over its set of (local) saddle points.

Lemma 6.4.1. (*Constant function value over saddle points*): For $F : \mathbb{R}^n \times \mathbb{R}^m \rightarrow \mathbb{R}$ continuously differentiable, let $\mathcal{S} \subset \text{Saddle}(F)$ be a path connected set. If F is locally convex-concave on \mathcal{S} , then $F|_{\mathcal{S}}$ is constant.

Proof. We start by considering the case when \mathcal{S} is compact. Given $(x, z) \in \mathcal{S}$, let $\delta(x, z) > 0$ be such that $B_{\delta(x, z)}(x, z) \subset (\mathcal{U}_x \times \mathcal{U}_z) \cap \mathcal{U}$, where \mathcal{U}_x and \mathcal{U}_z are neighborhoods where the saddle property (2.4) holds and \mathcal{U} is the neighborhood of (x, z) where local convexity-concavity holds (cf. Section 2.4). This defines a covering of \mathcal{S} by open sets as

$$\mathcal{S} \subset \cup_{(x, z) \in \mathcal{S}} B_{\delta(x, z)}(x, z).$$

Since \mathcal{S} is compact, there exist a finite number of points $(x_1, z_1), (x_2, z_2), \dots, (x_n, z_n)$ in \mathcal{S} such that $\cup_{i=1}^n B_{\delta(x_i, z_i)}(x_i, z_i)$ covers \mathcal{S} . For convenience, denote $B_{\delta(x_i, z_i)}(x_i, z_i)$ by B_i . Next, we show that $F|_{\mathcal{S} \cap B_i}$ is constant for all $i \in [n]$. To see this, let $(\bar{x}, \bar{z}) \in \mathcal{S} \cap B_i$. From (2.4), we have

$$F(x_i, \bar{z}) \leq F(x_i, z_i) \leq F(\bar{x}, z_i). \quad (6.24)$$

From the convexity of $x \mapsto F(x, \bar{z})$ over $\mathcal{U} \cap (\mathbb{R}^n \times \{\bar{z}\})$, (cf. definition of local convexity-concavity in Section 2.4), and the fact that $\nabla_x F(\bar{x}, \bar{z}) = 0$, we obtain $F(x_i, \bar{z}) \geq F(\bar{x}, \bar{z}) + (x_i - \bar{x})^\top \nabla_x F(\bar{x}, \bar{z}) = F(\bar{x}, \bar{z})$. Similarly, using the concavity of $z \mapsto F(\bar{x}, z)$, we get $F(\bar{x}, z_i) \leq F(\bar{x}, \bar{z})$. These inequalities together with (6.24) yield

$$F(x_i, z_i) \leq F(\bar{x}, z_i) \leq F(\bar{x}, \bar{z}) \leq F(x_i, \bar{z}) \leq F(x_i, z_i).$$

That is, $F(\bar{x}, \bar{z}) = F(x_i, z_i)$ and hence $F|_{\mathcal{S} \cap B_i}$ is constant. Using this reasoning,

if $\mathcal{S} \cap B_i \cap B_j \neq \emptyset$ for any $i, j \in [n]$, then $F_{|\mathcal{S} \cap (B_i \cup B_j)}$ is constant. Using that \mathcal{S} is path connected, the fact [Dug66, p. 117] states that, for any two points $(x_l, z_l), (x_m, z_m) \in \mathcal{S}$, there exist distinct members i_1, i_2, \dots, i_k of the set $[n]$ such that $(x_l, z_l) \in \mathcal{S} \cap B_{i_1}$, $(x_m, z_m) \in \mathcal{S} \cap B_{i_k}$ and $\mathcal{S} \cap B_{i_t} \cap B_{i_{t+1}} \neq \emptyset$ for all $t \in [k-1]$. Hence, we conclude that $F_{|\mathcal{S}}$ is constant. Finally, in the case when \mathcal{S} is not compact, pick any two points $(x_l, z_l), (x_m, z_m) \in \mathcal{S}$ and let $\gamma : [0, 1] \rightarrow \mathcal{S}$ be a continuous map with $\gamma(0) = (x_l, z_l)$ and $\gamma(1) = (x_m, z_m)$ denoting the path between these points. The image $\gamma([0, 1]) \subset \mathcal{S}$ is closed and bounded, hence compact, and therefore, $F_{|\gamma([0, 1])}$ is constant. Since the two points are arbitrary, we conclude that $F_{|\mathcal{S}}$ is constant. \square

The difficulty in Lemma 6.4.1 arises due to the local nature of the saddle points (the result is instead straightforward for global saddle points). The next result provides a first-order condition for strongly quasiconvex functions.

Lemma 6.4.2. (*First-order property of a strongly quasiconvex function*): *Let $f : \mathbb{R}^n \rightarrow \mathbb{R}$ be a C^1 function that is strongly quasiconvex on a convex set $\mathcal{D} \subset \mathbb{R}^n$. Then, there exists a constant $s > 0$ such that*

$$f(x) \leq f(y) \Rightarrow \nabla f(y)^\top (x - y) \leq -s \|x - y\|^2, \quad (6.25)$$

for any $x, y \in \mathcal{D}$.

Proof. Consider $x, y \in \mathcal{D}$ such that $f(x) \leq f(y)$. From strong quasiconvexity we have $f(y) \geq f(\lambda x + (1 - \lambda)y) + s\lambda(1 - \lambda)\|x - y\|^2$, for any $\lambda \in [0, 1]$. Rearranging,

$$f(\lambda x + (1 - \lambda)y) - f(y) \leq -s\lambda(1 - \lambda)\|x - y\|^2. \quad (6.26)$$

On the other hand, the Taylor's approximation of f at y yields the following equality at point $y + \lambda(x - y)$, which is equal to $\lambda x + (1 - \lambda)y$, as

$$\begin{aligned} f(\lambda x + (1 - \lambda)y) - f(y) &= \nabla f(y)^\top (\lambda x + (1 - \lambda)y - y) + g(\lambda x + (1 - \lambda)y - y) \\ &= \lambda \nabla f(y)^\top (x - y) + g(\lambda(x - y)), \end{aligned} \quad (6.27)$$

for some function g with the property $\lim_{\lambda \rightarrow 0} \frac{g(\lambda(x-y))}{\lambda} = 0$. Using (6.27) in (6.26), dividing by λ , and taking the limit $\lambda \rightarrow 0$ yields the result. \square

The next result is helpful when dealing with dynamical systems that have non-isolated equilibria to establish the asymptotic convergence of the trajectories to a point, rather than to a set.

Lemma 6.4.3. (*Asymptotic convergence to a point [BB03, Corollary 5.2]*): *Consider the nonlinear system*

$$\dot{x}(t) = f(x(t)), \quad x(0) = x_0, \quad (6.28)$$

where $f : \mathbb{R}^n \rightarrow \mathbb{R}^n$ is locally Lipschitz. Let $\mathcal{W} \subset \mathbb{R}^n$ be a compact set that is positively invariant under (6.28) and let $\mathcal{E} \subset \mathcal{W}$ be a set of stable equilibria. If a trajectory $t \mapsto x(t)$ of (6.28) with $x_0 \in \mathcal{W}$ satisfies $\lim_{t \rightarrow \infty} d_{\mathcal{E}}(x(t)) = 0$, then the trajectory converges to a point in \mathcal{E} .

Finally, we establish the asymptotic stability of a manifold of equilibria through linearization techniques. We start with a useful intermediary result.

Lemma 6.4.4. (*Limit points of Jacobian of a piecewise \mathcal{C}^2 function*): *Let $f : \mathbb{R}^n \rightarrow \mathbb{R}^n$ be piecewise \mathcal{C}^2 . Then, for every $x \in \mathbb{R}^n$, there exists a finite index set $\mathcal{I}_x \subset \mathbb{Z}_{\geq 1}$ and a set of matrices $\{A_{x,i} \in \mathbb{R}^{n \times n}\}_{i \in \mathcal{I}_x}$ such that*

$$\{A_{x,i} \mid i \in \mathcal{I}_x\} = \left\{ \lim_{k \rightarrow \infty} Df(x_k) \mid x_k \rightarrow x, x_k \in \mathbb{R}^n \setminus \Omega_f \right\}, \quad (6.29)$$

where Ω_f is the set of points where f is not differentiable.

Proof. Since f is piecewise \mathcal{C}^2 , cf. Section 2.1, let $\mathcal{D}_1, \dots, \mathcal{D}_m \subset \mathbb{R}^n$ be the finite collection of disjoint open sets such that f is \mathcal{C}^2 on \mathcal{D}_i for each $i \in [m]$ and $\mathbb{R}^n = \cup_{i=1}^m \text{cl}(\mathcal{D}_i)$. Let $x \in \mathbb{R}^n$ and define $\mathcal{I}_x = \{i \in [m] \mid x \in \text{cl}(\mathcal{D}_i)\}$ and $A_{x,i} = \{\lim_{k \rightarrow \infty} Df(x_k) \mid x_k \rightarrow x, x_k \in \mathcal{D}_i\}$. Note that $A_{x,i}$ is uniquely defined for each i as, by definition, $f|_{\text{cl}(\mathcal{D}_i)}$ is \mathcal{C}^2 . To show that (6.29) holds for the above defined matrices, first note that the set $\{A_{x,i} \mid i \in \mathcal{I}_x\}$ is included in the right

hand side of (6.29) by definition. To show the other inclusion, consider any sequence $\{x_k\}_{k=1}^\infty \subset \mathbb{R}^n \setminus \Omega_f$ with $x_k \rightarrow x$. One can partition this sequence into subsequences, each contained in one of the sets \mathcal{D}_i , $i \in \mathcal{I}_x$ and each converging to x . Thus, the limit $\lim_{k \rightarrow \infty} Df(x_k)$ is contained in the set $\{A_{x,i}\}_{i \in \mathcal{I}_x}$, proving the other inclusion and yielding (6.29). Note that, in the nonsmooth analysis literature [Cla83, Chapter 2], the convex hull of matrices $\{A_{x,i}\}_{i \in \mathcal{I}_x}$ is known as the generalized Jacobian of f at x . \square

The following statement is an extension of [Hen81, Exercise 6] to vector fields that are only piecewise twice continuously differentiable. Its proof is inspired, but cannot be directly implied from, center manifold theory [Car82].

Proposition 6.4.5. (*Asymptotic stability of a manifold of equilibrium points for piecewise C^2 vector fields*): *Consider the system*

$$\dot{x} = f(x), \tag{6.30}$$

where $f : \mathbb{R}^n \rightarrow \mathbb{R}^n$ is piecewise C^2 and locally Lipschitz in a neighborhood of a p -dimensional submanifold of equilibrium points $\mathcal{E} \subset \mathbb{R}^n$ of (6.30). Assume that at each $x_* \in \mathcal{E}$, the set of matrices $\{A_{x_*,i}\}_{i \in \mathcal{I}_{x_*}}$ from Lemma 6.4.4 satisfy:

(i) *there exists an orthogonal matrix $Q \in \mathbb{R}^{n \times n}$ such that, for all $i \in \mathcal{I}_{x_*}$,*

$$Q^\top A_{x_*,i} Q = \begin{bmatrix} 0 & 0 \\ 0 & \tilde{A}_{x_*,i} \end{bmatrix},$$

where $\tilde{A}_{x_*,i} \in \mathbb{R}^{n-p \times n-p}$,

(ii) *the eigenvalues of the matrices $\{\tilde{A}_{x_*,i}\}_{i \in \mathcal{I}_{x_*}}$ have negative real parts,*

(iii) *there exists a positive definite matrix $P \in \mathbb{R}^{n-p \times n-p}$ such that*

$$\tilde{A}_{x_*,i}^\top P + P \tilde{A}_{x_*,i} \prec 0, \quad \text{for all } i \in \mathcal{I}_{(x_*, z_*)}.$$

Then, \mathcal{E} is locally asymptotically stable under (6.30) and the trajectories converge to a point in \mathcal{E} .

Proof. Our strategy to prove the result is to linearize the vector field f on each of the patches around any equilibrium point and employ a common Lyapunov function and a common upper bound on the growth of the second-order term to establish the convergence of the trajectories. This approach is an extension of the proof of [Kha02, Theorem 8.2], where the vector field f is assumed to be \mathcal{C}^2 everywhere. Let $x_* \in \mathcal{E}$. For convenience, translate x_* to the origin of (6.30). We divide the proof in its various parts to make it easier to follow the technical arguments.

Step I: linearization of the vector field on patches around the equilibrium point. From Lemma 6.4.4, define $\mathcal{I}_0 = \{i \in [m] \mid 0 \in \text{cl}(\mathcal{D}_i)\}$ and matrices $\{A_{0,i}\}_{i \in \mathcal{I}_0}$ as the limit points of the Jacobian matrices. From the definition of piecewise \mathcal{C}^2 function, there exist \mathcal{C}^2 functions $\{f_i : \mathcal{D}_i^e \rightarrow \mathbb{R}^n\}_{i \in \mathcal{I}_0}$ with \mathcal{D}_i^e open such that with $\text{cl}(\mathcal{D}_i) \subset \mathcal{D}_i^e$ and the maps $f|_{\text{cl}(\mathcal{D}_i)}$ and f_i take the same value over the set $\text{cl}(\mathcal{D}_i)$. Note that $0 \in \mathcal{D}_i^e$ for every $i \in \mathcal{I}_0$. By definition of the matrices $\{A_{0,i}\}_{i \in \mathcal{I}_0}$, we deduce that $Df_i(0) = A_{0,i}$ for each $i \in \mathcal{I}_0$. Therefore, there exists a neighborhood $\mathcal{N}_0 \subset \mathbb{R}^n$ of the origin and a set of \mathcal{C}^2 functions $\{g_i : \mathbb{R}^n \rightarrow \mathbb{R}^n\}_{i \in \mathcal{I}_0}$ such that, for all $i \in \mathcal{I}_0$, $f_i(x) = A_{0,i}x + g_i(x)$, for all $x \in \mathcal{N}_0 \cap \mathcal{D}_i^e$, where

$$g_i(0) = 0 \quad \text{and} \quad \frac{\partial g_i}{\partial x}(0) = 0. \quad (6.31)$$

Without loss of generality, select \mathcal{N}_0 such that $\mathcal{N}_0 \cap \mathcal{D}_i$ is empty for every $i \notin \mathcal{I}_0$. That is, $\cup_{i \in \mathcal{I}_0} (\mathcal{N}_0 \cap \text{cl}(\mathcal{D}_i))$ contains a neighborhood of the origin. With the above construction, the vector field f in a neighborhood around the origin is written as

$$f(x) = f_i(x) = A_{0,i}x + g_i(x), \text{ for all } x \in \mathcal{N}_0 \cap \text{cl}(\mathcal{D}_i), i \in \mathcal{I}_0, \quad (6.32)$$

where for each $i \in \mathcal{I}_0$, g_i satisfies (6.31).

Step II: change of coordinates. Subsequently, from hypothesis (i), there exists an orthogonal matrix $Q \in \mathbb{R}^{n \times n}$, defining an orthonormal transformation

denoted by $\mathcal{T}_Q : \mathbb{R}^n \rightarrow \mathbb{R}^n$, $x \mapsto (u, v)$, that yields the new form of (6.32) as

$$\begin{bmatrix} \dot{u} \\ \dot{v} \end{bmatrix} = \begin{bmatrix} 0 & 0 \\ 0 & \tilde{A}_{0,i} \end{bmatrix} \begin{bmatrix} u \\ v \end{bmatrix} + \begin{bmatrix} \tilde{g}_{i,1}(u, v) \\ \tilde{g}_{i,2}(u, v) \end{bmatrix}, \text{ for all } (u, v) \in \mathcal{T}_Q(\mathcal{N}_0 \cap \text{cl}(\mathcal{D}_i)), i \in \mathcal{I}_0, \quad (6.33)$$

where for each $i \in \mathcal{I}_0$, the matrix $\tilde{A}_{0,i}$ has eigenvalues with negative real parts (cf. hypothesis (ii)) and for each $i \in \mathcal{I}_0$ and $k \in \{1, 2\}$ we have

$$\tilde{g}_{i,k}(0, 0) = 0, \quad \frac{\partial \tilde{g}_{i,k}}{\partial u}(0, 0) = 0, \quad \text{and} \quad \frac{\partial \tilde{g}_{i,k}}{\partial v}(0, 0) = 0. \quad (6.34)$$

With a slight abuse of notation, denote the manifold of equilibrium points in the transformed coordinates by \mathcal{E} itself, i.e., $\mathcal{E} = \mathcal{T}_Q(\mathcal{E})$. From (6.33), we deduce that the tangent and the normal spaces to the equilibrium manifold \mathcal{E} at the origin are $\{(u, v) \in \mathbb{R}^p \times \mathbb{R}^{n-p} \mid v = 0\}$ and $\{(u, v) \in \mathbb{R}^p \times \mathbb{R}^{n-p} \mid u = 0\}$, respectively. Due to this fact and since \mathcal{E} is a submanifold of \mathbb{R}^n , there exists a smooth function $h : \mathbb{R}^p \rightarrow \mathbb{R}^{n-p}$ and a neighborhood $\mathcal{U} \subset \mathcal{T}_Q(\mathcal{N}_0) \subset \mathbb{R}^n$ of the origin such that for any $(u, v) \in \mathcal{U}$, $v = h(u)$ if and only if $(u, v) \in \mathcal{E} \cap \mathcal{U}$. Moreover,

$$h(0) = 0 \text{ and } \frac{\partial h}{\partial u}(0) = 0. \quad (6.35)$$

Now, consider the coordinate $w = v - h(u)$ to quantify the distance of a point (u, v) from the set \mathcal{E} in the neighborhood \mathcal{U} . To conclude the proof, we focus on showing that there exists a neighborhood of the origin such that along a trajectory of (6.33) initialized in this neighborhood, we have $w(t) \rightarrow 0$ and $(u(t), h(u(t))) \in \mathcal{U}$ at all $t \geq 0$. In (u, w) -coordinates, over the set \mathcal{U} , the system (6.33) reads as

$$\begin{bmatrix} \dot{u} \\ \dot{w} \end{bmatrix} = \begin{bmatrix} 0 & 0 \\ 0 & \tilde{A}_{0,i} \end{bmatrix} \begin{bmatrix} u \\ w \end{bmatrix} + \begin{bmatrix} \bar{g}_{i,1}(u, w) \\ \bar{g}_{i,2}(u, w) \end{bmatrix}, \text{ for } (u, w + h(u)) \in \mathcal{U} \cap \mathcal{T}_Q(\text{cl}(\mathcal{D}_i)), i \in \mathcal{I}_0, \quad (6.36)$$

where $\bar{g}_{i,1}(u, w) = \tilde{g}_{i,1}(u, w + h(u))$ and $\bar{g}_{i,2}(u, w) = \tilde{A}_{0,i}h(u) + \tilde{g}_{i,2}(u, w + h(u)) - \frac{\partial h}{\partial u}(u)(\tilde{g}_{i,1}(u, w + h(u)))$. Further, the equilibrium points $\mathcal{E} \cap \mathcal{U}$ in these coordinates

are represented by the set of points $(u, 0)$, where u satisfies $(u, h(u)) \in \mathcal{E} \cap \mathcal{U}$. These facts, along with the conditions on the first-order derivatives of $\tilde{g}_{i,1}$, $\tilde{g}_{i,2}$ in (6.34) and that of h in (6.35) yield

$$\bar{g}_{i,k}(u, 0) = 0 \text{ and } \frac{\partial \bar{g}_{i,k}}{\partial w}(0, 0) = 0, \quad (6.37)$$

for all $i \in \mathcal{I}_0$ and $k \in \{1, 2\}$. Note that the functions $\bar{g}_{i,1}$ and $\bar{g}_{i,2}$ are \mathcal{C}^2 . This implies that, for small enough $\epsilon > 0$, we have $\|\bar{g}_{i,k}(u, w)\| \leq M_{i,k}\|w\|$, for $k \in \{1, 2\}$, $i \in \mathcal{I}_0$, and $(u, w) \in B_\epsilon(0)$, where the constants $\{M_{i,k}\}_{i \in \mathcal{I}_0, k \in \{1, 2\}} \subset \mathbb{R}_{>0}$ can be made arbitrarily small by selecting smaller ϵ . Defining $M_\epsilon = \max\{M_{i,k} \mid i \in \mathcal{I}_0, k \in \{1, 2\}\}$,

$$\|\bar{g}_{i,k}(u, w)\| \leq M_\epsilon \|w\|, \text{ for } k \in \{1, 2\} \text{ and } i \in \mathcal{I}_0. \quad (6.38)$$

Step III: Lyapunov analysis. With the bounds above, we proceed to carry out the Lyapunov analysis for (6.36). Using the matrix P from assumption (iii), define the candidate Lyapunov function $V : \mathbb{R}^{n-p} \rightarrow \mathbb{R}_{\geq 0}$ for (6.36) as $V(w) = w^\top P w$ whose Lie derivative along (6.36) is

$$\begin{aligned} \mathcal{L}_{(6.36)} V(w) &= w^\top (\tilde{A}_{0,i}^\top P + P \tilde{A}_{0,i}) w + 2w^\top P \bar{g}_{i,2}(u, w), \\ &\text{for } (u, w + h(u)) \in \mathcal{U} \cap \mathcal{T}_Q(\text{cl}(\mathcal{D}_i)), i \in \mathcal{I}_0. \end{aligned}$$

By assumption (iii), there exists $\lambda > 0$ such that $w^\top (\tilde{A}_{0,i}^\top P + P \tilde{A}_{0,i}) w \leq -\lambda \|w\|^2$. Pick ϵ such that $(u, w) \in B_\epsilon(0)$ implies $(u, h(u) + w) \in \mathcal{U}$. Then, the above Lie derivative can be upper bounded as

$$\mathcal{L}_{(6.36)} V(w) \leq -\lambda \|w\|^2 + 2M_\epsilon \|P\| \|w\|^2 = -\beta_1 \|w\|^2, \text{ for } (u, w) \in B_\epsilon(0),$$

where $\beta_1 = \lambda - 2M_\epsilon$. Let ϵ small enough so that $\beta_1 > 0$ and therefore $\mathcal{L}_{(6.36)} V(w) \leq -\beta_1 \|w\|^2 < 0$ for $w \neq 0$. Now assume that there exists a trajectory $t \mapsto (u(t), w(t))$ of (6.36) that satisfies $(u(t), w(t)) \in B_\epsilon(0)$ for all $t \geq 0$. Then, using the following

$$\lambda_{\min}(P) \|w\|^2 \leq w^\top P w \leq \lambda_{\max}(P) \|w\|^2,$$

we get $V(w(t)) \leq e^{-\beta_1 t / \lambda_{\max}(P)} V(w(0))$ along this trajectory. Employing the same inequalities again, we get

$$\|w(t)\| \leq K \|w(0)\| e^{-\beta_2 t}, \quad (6.39)$$

where $K = \sqrt{\frac{\lambda_{\max}(P)}{\lambda_{\min}(P)}}$ and $\beta_2 = \frac{\beta_1}{2\lambda_{\max}(P)} > 0$. This proves that $w(t) \rightarrow 0$ exponentially for the considered trajectory. Finally, we show that there exists $\delta > 0$ such that all trajectories of (6.36) with initial condition $(u(0), w(0)) \in B_\delta(0)$ satisfy $(u(t), w(t)) \in B_\epsilon(0)$ for all $t \geq 0$ and hence, converge to \mathcal{E} . From (6.36), (6.38) and (6.39), we have

$$\|u(t)\| \leq \|u(0)\| + \int_0^t M_\epsilon K e^{-\beta_2 s} \|w(0)\| ds, \leq \|u(0)\| + \frac{M_\epsilon K}{\beta_2} \|w(0)\|. \quad (6.40)$$

By choosing ϵ small enough, M_ϵ can be made arbitrarily small and β_2 can be bounded away from the origin. With this, from (6.39) and (6.40), one can select a small enough $\delta > 0$ such that $(u(0), w(0)) \in B_\delta(0)$ imply $(u(t), w(t)) \in B_\epsilon(0)$ for all $t \geq 0$ and $w(t) \rightarrow 0$. From this, we deduce that the trajectories starting in $B_\delta(0)$ converge to the set \mathcal{E} and the origin is stable. Since x_* was arbitrary, we conclude local asymptotic stability of \mathcal{E} . Convergence to a point follows from the application of Lemma 6.4.3. \square

The next example illustrates the application of the above result to conclude local convergence of trajectories to a point in the manifold of equilibria.

Example 6.4.6. (*Asymptotic stability of a manifold of equilibria for piecewise \mathcal{C}^2*)

vector fields): Consider the system $\dot{x} = f(x)$, where $f : \mathbb{R}^3 \rightarrow \mathbb{R}^3$ is given by

$$f(x) = \begin{cases} \begin{bmatrix} -1 & 1 & 0 \\ 1 & -2 & 1 \\ 0 & 1 & -1 \end{bmatrix} \begin{bmatrix} x_1 \\ x_2 \\ x_3 \end{bmatrix} + (x_1 - x_3)^2 \begin{bmatrix} 1 \\ 1 \\ 1 \end{bmatrix}, & \text{if } x_1 - x_3 \geq 0, \\ \begin{bmatrix} -2 & 1 & 1 \\ 1 & -2 & 1 \\ 1 & 1 & -2 \end{bmatrix} \begin{bmatrix} x_1 \\ x_2 \\ x_3 \end{bmatrix} + (x_1 - x_3)^2(1 - x_1 + x_3) \begin{bmatrix} 1 \\ 1 \\ 1 \end{bmatrix}, & \text{if } x_1 - x_3 < 0. \end{cases} \quad (6.41)$$

The set of equilibria of f is the one-dimensional manifold $\mathcal{E} = \{x \in \mathbb{R}^3 \mid x_1 = x_2 = x_3\}$. Consider the regions $\mathcal{D}_1 = \{x \in \mathbb{R}^2 \mid x_1 - x_3 > 0\}$ and $\mathcal{D}_2 = \{x \in \mathbb{R}^2 \mid x_1 - x_3 < 0\}$. Note that f is locally Lipschitz on \mathbb{R}^3 and \mathcal{C}^2 on \mathcal{D}_1 and \mathcal{D}_2 . At any equilibrium point $x_* \in \mathcal{E}$, the limit point of the generalized Jacobian belongs to $\{A_1, A_2\}$, where

$$A_1 = \begin{bmatrix} -1 & 1 & 0 \\ 1 & -2 & 1 \\ 0 & 1 & -1 \end{bmatrix} \quad \text{and} \quad A_2 = \begin{bmatrix} -2 & 1 & 1 \\ 1 & -2 & 1 \\ 1 & 1 & -2 \end{bmatrix}.$$

With the orthogonal matrix $Q = \begin{bmatrix} 1 & 1 & 1 \\ 1 & -1 & 1 \\ 1 & 0 & -2 \end{bmatrix}$ we get,

$$Q^\top A_1 Q = \begin{bmatrix} 0 & 0 & 0 \\ 0 & -5 & 3 \\ 0 & 3 & -9 \end{bmatrix}, \quad Q^\top A_2 Q = \begin{bmatrix} 0 & 0 & 0 \\ 0 & -6 & 0 \\ 0 & 0 & -18 \end{bmatrix}.$$

The nonzero 2×2 -submatrices obtained in the above equation have eigenvalues with negative real parts and have the identity matrix as a common Lyapunov function. Therefore, from Proposition 6.4.5, we conclude that \mathcal{E} is locally asymptotically stable under $\dot{x} = f(x)$, as illustrated in Figure 6.6. •

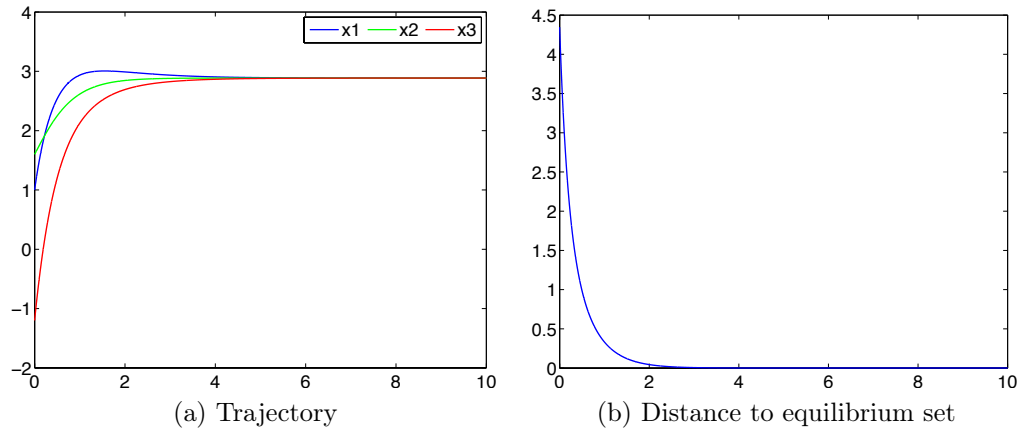


Figure 6.6: (a) Trajectory of the vector field f defined in (6.41). The initial condition is $x = (1, 1.6, -1.2)$. The trajectory converges to the equilibrium point $(2.88, 2.88, 2.88)$. (b) Evolution of the distance to the equilibrium set \mathcal{E} of the trajectory.

Acknowledgments

This chapter is taken, in part, from the work [CGC17] published as “Saddle-point dynamics: conditions for asymptotic stability of saddle points” by A. Cherukuri, B. Gharesifard, and J. Cortés, in *SIAM Journal on Control and Optimization*, as well as [CC15a] where it appears as “Asymptotic stability of saddle points under the saddle-point dynamics” by A. Cherukuri and J. Cortés in the proceedings of the 2015 American Control Conference. The dissertation author was the primary investigator and author of these papers. This research was partly supported by the US National Science Foundation (NSF) Award ECCS-1307176.

Chapter 7

Asymptotic convergence of primal-dual dynamics

Our objective in chapter is to provide a rigorous treatment of the convergence analysis of the primal-dual dynamics using classical notions from stability analysis.

7.1 Problem statement

This section reviews the primal-dual dynamics for solving constrained optimization problems and justifies the need to rigorously characterize its convergence properties. Consider the concave optimization problem on \mathbb{R}^n ,

$$\text{maximize } f(x), \tag{7.1a}$$

$$\text{subject to } g(x) \leq \mathbf{0}_m, \tag{7.1b}$$

where the continuously differentiable functions $f : \mathbb{R}^n \rightarrow \mathbb{R}$ and $g : \mathbb{R}^n \rightarrow \mathbb{R}^m$ are strictly concave and convex, respectively, and have locally Lipschitz gradients. The Lagrangian of the problem (7.1) is given as

$$L(x, \lambda) = f(x) - \lambda^\top g(x), \tag{7.2}$$

where $\lambda \in \mathbb{R}^m$ is the Lagrange multiplier corresponding to the inequality constraint (7.1b). Note that the Lagrangian is concave in x and convex (in fact linear) in λ . Assume that the Slater's conditions is satisfied for the problem (7.1), that is, there exists $x \in \mathbb{R}^n$ such that $g(x) < \mathbf{0}_m$. Under this assumption, the duality gap between the primal and dual optimizers is zero and a point $(x_*, \lambda_*) \in \mathcal{D}$ is a primal-dual optimizer of (7.1) if and only if it is a saddle point of L over the domain \mathcal{D} , i.e.,

$$L(x, \lambda) \leq L(x_*, \lambda_*) \quad \text{and} \quad L(x_*, \lambda) \geq L(x_*, \lambda_*),$$

for all $x \in \mathbb{R}^n$ and $\lambda \in \mathbb{R}_{\geq 0}^m$. For convenience, we denote the set of saddle points of L (equivalently the primal-dual optimizers) by $\mathbf{X} \times \Lambda \subset \mathbb{R}^n \times \mathbb{R}^m$. Note that since f is strictly concave, the set \mathbf{X} is a singleton. Furthermore, (x_*, λ_*) is a primal-dual optimizer if and only if it satisfies the following Karush-Kuhn-Tucker (KKT) conditions (cf. [BV09, Chapter 5]),

$$\nabla f(x_*) - \sum_{i=1}^m (\lambda_*)_i \nabla g_i(x_*) = 0, \quad (7.3a)$$

$$g(x_*) \leq \mathbf{0}_m, \quad \lambda_* \geq \mathbf{0}_m, \quad \lambda_*^\top g(x_*) = 0. \quad (7.3b)$$

Given this characterization of the solutions of the optimization problem, it is natural to consider the *primal-dual dynamics* on $\mathbb{R}^n \times \mathbb{R}_{\geq 0}^m$ to find them

$$\dot{x} = \nabla_x L(x, \lambda) = \nabla f(x) - \sum_{i=1}^m \lambda_i \nabla g_i(x), \quad (7.4a)$$

$$\dot{\lambda} = [-\nabla_\lambda L(x, \lambda)]_\lambda^+ = [g(x)]_\lambda^+. \quad (7.4b)$$

When convenient, we use the notation $X_{\text{p-d}} : \mathbb{R}^n \times \mathbb{R}_{\geq 0}^m \rightarrow \mathbb{R}^n \times \mathbb{R}^m$ to refer to the dynamics (7.4). Given that the primal-dual dynamics is discontinuous, we consider solutions in the Caratheodory sense. The reason for this is that, with this notion of solution, a point is an equilibrium of (7.4) if and only if it satisfies the KKT conditions (7.3).

Our objective is to establish that the solutions of (7.4) exist and asymptot-

ically converge to a solution of the concave optimization problem (7.1) using classical notions and tools from stability analysis. Our motivation for this aim comes from the conceptual simplicity and versatility of Lyapunov-like methods and their amenability for performing robustness analysis and studying generalizations of the dynamics. One way of tackling this problem, see e.g., [FP10], is to interpret the dynamics as a state-dependent switched system, formulate the latter as a hybrid automaton as defined in [LJS⁺03], and then employ the invariance principle for hybrid automata to characterize its asymptotic convergence properties. However, this route is not valid in general because one of the key assumptions required by the invariance principle for hybrid automata is not satisfied by the primal-dual dynamics. The next example justifies this claim.

Example 7.1.1. (*The hybrid automaton corresponding to the primal-dual dynamics is not continuous*): Consider the concave optimization problem (7.1) on \mathbb{R} with $f(x) = -(x - 5)^2$ and $g(x) = x^2 - 1$, whose set of primal-dual optimizers is $\mathbf{X} \times \Lambda = \{(1, 4)\}$. The associated primal-dual dynamics takes the form

$$\dot{x} = -2(x - 5) - 2x\lambda, \quad (7.5a)$$

$$\dot{\lambda} = [x^2 - 1]_{\lambda}^+. \quad (7.5b)$$

We next formulate this dynamics as a hybrid automaton as defined in [LJS⁺03, Definition II.1]. The idea to build the hybrid automaton is to divide the state space $\mathbb{R} \times \mathbb{R}_{\geq 0}$ into two domains over which the vector field (7.5) is continuous. To this end, we define two modes represented by the discrete variable q , taking values in $\mathbf{Q} = \{1, 2\}$. The value $q = 1$ represents the mode where the projection in (7.5b) is active and $q = 2$ represents the mode where it is not. Formally, the projection is *active* at (x, λ) if $[g(x)]_{\lambda}^+ \neq g(x)$, i.e. $\lambda = 0$ and $g(x) < 0$. The hybrid automaton is then given by the collection $H = (Q, X, f, \text{Init}, D, E, G, R)$, where $Q = \{q\}$ is the set of discrete variables, taking values in \mathbf{Q} ; $X = \{x, \lambda\}$ is the set of continuous variables, taking values in $\mathbf{X} = \mathbb{R} \times \mathbb{R}_{\geq 0}$; the vector field $f : \mathbf{Q} \times \mathbf{X} \rightarrow T\mathbf{X}$ is

defined by

$$f(1, (x, \lambda)) = \begin{bmatrix} -2(x-5) - 2x\lambda \\ 0 \end{bmatrix},$$

$$f(2, (x, \lambda)) = \begin{bmatrix} -2(x-5) - 2x\lambda \\ x^2 - 1 \end{bmatrix};$$

$\text{Init} = \mathbf{X}$ is the set of initial conditions; $D : \mathbf{Q} \rightrightarrows \mathbf{X}$ specifies the domain of each discrete mode,

$$D(1) = (-1, 1) \times \{0\}, \quad D(2) = \mathbf{X} \setminus D(1),$$

i.e., the dynamics is defined by the vector field $(x, \lambda) \rightarrow f(1, (x, \lambda))$ over $D(1)$ and by $(x, \lambda) \rightarrow f(2, (x, \lambda))$ over $D(2)$; $E = \{(1, 2), (2, 1)\}$ is the set of edges specifying the transitions between modes; the guard map $G : \mathbf{Q} \rightrightarrows \mathbf{X}$ specifies when a solution can jump from one mode to the other,

$$G(1, 2) = \{(1, 0), (-1, 0)\}, \quad G(2, 1) = (-1, 1) \times \{0\},$$

i.e., $G(q, q')$ is the set of points where a solution jumps from mode q to mode q' ; and, finally, the reset map $R : \mathbf{Q} \times \mathbf{X} \rightrightarrows \mathbf{X}$ specifies that the state is preserved after a jump from one mode to another,

$$R((1, 2), (x, \lambda)) = R((2, 1), (x, \lambda)) = \{(x, \lambda)\}.$$

We are now ready to show that the hybrid automaton is not continuous in the sense defined by [LJS⁺03, Definition III.3]. This notion plays a key role in the study of omega-limit sets and their stability, and is in fact a basic assumption of the invariance principle developed in [LJS⁺03, Theorem IV.1]. Roughly speaking, H is continuous if two executions of H starting close to one another remain close to one another. An execution of H consists of a tuple (τ, q, x) , where τ is a hybrid time trajectory (a sequence of intervals specifying where mode transitions and continuous evolution take place), q is a map that gives the discrete mode

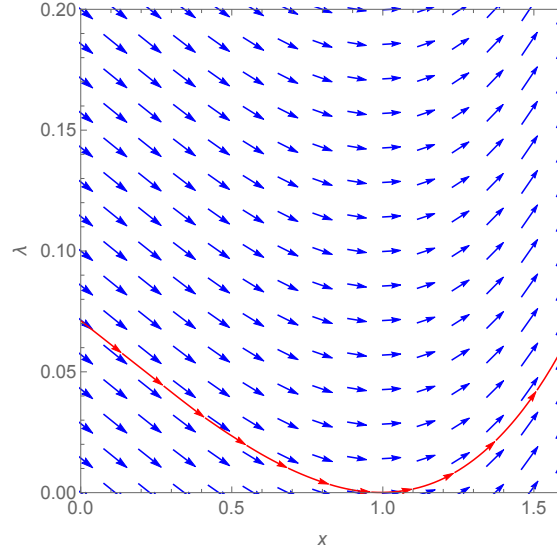


Figure 7.1: An illustration depicting the vector field (7.5) in the range $(x, \lambda) \in [0, 1.6] \times [0, 0.2]$. As shown (with a red streamline), there exists a solution of (7.5) that starts at a point $(x(0), \lambda(0))$ with $x(0) < 1$ and $\lambda(0) > 0$ such that it remains in the domain $\lambda > 0$ at all times except at one time instant t' when $(x(t'), \lambda(t')) = (1, 0)$.

of the execution at each interval of τ , and x is a set of differentiable maps that represent the evolution of the continuous state of the execution along intervals of τ . A necessary condition for two executions to “remain close” is to have the time instants of transitions in their mode for the executions (if there are any) close to one another. To disprove the continuity of H , it is enough then to show that there exist two executions that start arbitrarily close and yet experience their first mode transitions at time instants that are not arbitrarily close. Select an initial condition $(x(0), \lambda(0)) \in (0, 1) \times (0, \infty)$ that gives rise to a solution of (7.5) that remains in the set $(0, 1) \times (0, \infty)$ for a finite time interval $(0, t')$, $t' > 0$, satisfies $(x(t'), \lambda(t')) = (1, 0)$, and stays in the set $(1, \infty) \times (0, \infty)$ for some finite time interval (t', T) , $T > t'$. The existence of such a solution becomes clear by plotting the vector field (7.5), see Figure 7.1. Note that by construction, this also corresponds to an execution of the hybrid automaton H that starts and remains in domain $D(2)$ for the time interval $[0, T]$ and so it does not encounter any jumps in its discrete mode. Specifically, for this execution, the hybrid time trajectory is

the interval $[0, T]$, the discrete mode q is always 2 and the continuous state evolves as $t \mapsto (x(t), \lambda(t))$. Further, by observing the vector field, we deduce that in every neighborhood of $(x(0), \lambda(0))$, there exists a point $(\tilde{x}(0), \tilde{\lambda}(0))$ such that a solution of (7.5) $t \mapsto (\tilde{x}(t), \tilde{\lambda}(t))$ starting at $(\tilde{x}(0), \tilde{\lambda}(0))$ reaches the set $(0, 1) \times \{0\}$ in finite time $t_1 > 0$, remains in $(0, 1) \times \{0\}$ for a finite time interval $[t_1, t_2]$, and then enters the set $(1, \infty) \times (0, \infty)$ upon reaching the point $(1, 0)$. Indeed, this is true whenever $\tilde{x} < x(0)$ and $\tilde{\lambda} < \lambda(0)$. The execution of H corresponding to this solution starts in $D(2)$, enters $D(1)$ in finite time t_1 , and returns to $D(2)$ at time t_2 . Specifically, the hybrid time trajectory consists of three intervals $\{[0, t_1], [t_1, t_2], [t_2, T']\}$, where we assume $T' > t_2$. The discrete mode q takes value 2 for the interval $[0, t_1]$, 1 for the interval $[t_1, t_2]$, and 2 for the interval $[t_2, T']$. The continuous state $t \mapsto (\tilde{x}(t), \tilde{\lambda}(t))$ takes the same values as the solution of (7.5) explained above. Thus, the value of the discrete variable representing the mode of the execution switches from 2 to 1 and back to 2, whereas the execution corresponding to the solution of (7.5) starting at $(x(0), \lambda(0))$ never switches mode. This shows that the hybrid automaton is not continuous. •

Interestingly, even though the hybrid automaton H described in Example 7.1.1 is not continuous, one can infer from Figure 7.1 that two solutions of (7.5) remain close to each other if they start close enough. This suggests that continuity with respect to the initial condition might hold provided this notion is formalized the way it is done for traditional nonlinear systems (and not as done for hybrid automata where both discrete and continuous states have to be aligned). The next section shows that this in fact is the case. This, along with the existence and uniqueness of solutions, allows us to characterize the asymptotic convergence properties of the primal-dual dynamics.

7.2 Convergence analysis of primal-dual dynamics

In this section we show that the solutions of the primal-dual dynamics (7.4) asymptotically converge to a solution of the constrained optimization problem (7.1). Our proof strategy is to employ the invariance principle for

Caratheodory solutions of discontinuous dynamical systems stated in Proposition 2.6.1. Our first step is then to verify that all its hypotheses hold.

We start by stating a useful monotonicity property of the primal-dual dynamics with respect to the set of primal-dual optimizers $\mathbf{X} \times \Lambda$. This property can be found in [AHU58, FP10] and we include here its proof for completeness.

Lemma 7.2.1. (*Monotonicity of the primal-dual dynamics with respect to primal-dual optimizers*): *Let $(x_*, \lambda_*) \in \mathbf{X} \times \Lambda$ and define $V : \mathbb{R}^n \times \mathbb{R}^m \rightarrow \mathbb{R}_{\geq 0}$,*

$$V(x, \lambda) = \frac{1}{2}(\|x - x_*\|^2 + \|\lambda - \lambda_*\|^2). \quad (7.6)$$

Then $\mathcal{L}_{X_{p-d}}V(x, \lambda) \leq 0$ for all $(x, \lambda) \in \mathcal{D}$.

Proof. By definition of $\mathcal{L}_{X_{p-d}}V$ (cf. Section 2.6.1), we have

$$\begin{aligned} \mathcal{L}_{X_{p-d}}V(x, \lambda) &= (x - x_*)^\top \nabla_x L(x, \lambda) + (\lambda - \lambda_*)^\top [-\nabla_\lambda L(x, \lambda)]_\lambda^+ \\ &= (x - x_*)^\top \nabla_x L(x, \lambda) - (\lambda - \lambda_*)^\top \nabla_\lambda L(x, \lambda) \\ &\quad + (\lambda - \lambda_*)^\top ([-\nabla_\lambda L(x, \lambda)]_\lambda^+ + \nabla_\lambda L(x, \lambda)). \end{aligned}$$

Since L is concave in x and convex in λ , applying the first order condition of concavity and convexity for the first two terms of the above expression yields the following bound

$$\begin{aligned} \mathcal{L}_{X_{p-d}}V(x, \lambda) &\leq L(x, \lambda) - L(x_*, \lambda) + L(x, \lambda_*) - L(x, \lambda) \\ &\quad + (\lambda - \lambda_*)^\top ([-\nabla_\lambda L(x, \lambda)]_\lambda^+ + \nabla_\lambda L(x, \lambda)) \\ &= L(x_*, \lambda_*) - L(x_*, \lambda) + L(x, \lambda_*) - L(x_*, \lambda_*) \\ &\quad + (\lambda - \lambda_*)^\top ([-\nabla_\lambda L(x, \lambda)]_\lambda^+ + \nabla_\lambda L(x, \lambda)). \end{aligned}$$

Define the shorthand notation $M_1 = L(x_*, \lambda_*) - L(x_*, \lambda)$, $M_2 = L(x, \lambda_*) - L(x_*, \lambda_*)$, and $M_3 = (\lambda - \lambda_*)^\top ([-\nabla_\lambda L(x, \lambda)]_\lambda^+ + \nabla_\lambda L(x, \lambda))$, so that the above inequality reads

$$\mathcal{L}_{X_{p-d}}V(x, \lambda) \leq M_1 + M_2 + M_3.$$

Since λ_* is a minimizer of the map $\lambda \rightarrow L(x_*, \lambda)$ over the domain $\mathbb{R}_{\geq 0}^m$ and x_*

is a maximizer of the map $x \rightarrow L(x, \lambda_*)$, we obtain $M_1, M_2 \leq 0$. Replacing $-\nabla_\lambda L(x, \lambda) = g(x)$, one can write $M_3 = \sum_{i=1}^m T_i$, where for each i ,

$$T_i = (\lambda_i - (\lambda_*)_i)([g_i(x)]_{\lambda_i}^+ - g_i(x)).$$

If $\lambda_i > 0$, then $[g_i(x)]_{\lambda_i}^+ = g_i(x)$ and so $T_i = 0$. If $\lambda_i = 0$, then $\lambda_i - (\lambda_*)_i \leq 0$ and $[g_i(x)]_{\lambda_i}^+ - g_i(x) \geq 0$, which implies that $T_i \leq 0$. Therefore, we get $M_3 \leq 0$, and the result follows. \square

Next, we show that the primal-dual dynamics can be written as a projected dynamical system.

Lemma 7.2.2. (*Primal-dual dynamics as a projected dynamical system*): *The primal-dual dynamics can be written as a projected dynamical system.*

Proof. Consider the vector field $X : \mathbb{R}^n \times \mathbb{R}^m \rightarrow \mathbb{R}^n \times \mathbb{R}^m$ defined by

$$X(x, \lambda) = \begin{bmatrix} \nabla_x L(x, \lambda) \\ -\nabla_\lambda L(x, \lambda) \end{bmatrix}. \quad (7.7)$$

We wish to show that $X_{\text{p-d}}(x, \lambda) = \Pi_{\mathcal{D}}((x, \lambda), X(x, \lambda))$ for all $(x, \lambda) \in \mathcal{D}$. To see this, note that the maps $X_{\text{p-d}}$ and X take the same values over $\text{int}(\mathcal{D}) = \mathbb{R}^n \times \mathbb{R}_{>0}^m$. Now consider any point $(x, \lambda) \in \text{bd}(\mathcal{D})$. Let $I \subset [m]$ be the set of indices for which $\lambda_i = 0$ and $(-\nabla_\lambda L(x, \lambda))_i < 0$. Then, there exist $\tilde{\delta} > 0$ such that, for all $\delta \in [0, \tilde{\delta})$ and for any $j \in [n + m]$, we have

$$(\text{proj}_{\mathcal{D}}((x, \lambda) + \delta X(x, \lambda)))_j = \begin{cases} 0, & \text{if } j - n \in I, \\ (x, \lambda)_j + \delta(X(x, \lambda))_j, & \text{otherwise.} \end{cases}$$

Consequently, using the definition of the projection operator, cf. Section 2.6.2, we get

$$(\Pi_{\mathcal{D}}((x, \lambda), X(x, \lambda)))_j = \begin{cases} 0, & \text{if } j - n \in I, \\ (X(x, \lambda))_j, & \text{otherwise,} \end{cases}$$

which implies $X_{p-d}(x, \lambda) = \Pi_{\mathcal{D}}((x, \lambda), X(x, \lambda))$ for all $(x, \lambda) \in \text{bd}(\mathcal{D})$. This concludes the proof. \square

Next, we use Lemmas 7.2.1 and 7.2.2 to show the existence, uniqueness, and continuity of the solutions of X_{p-d} starting from \mathcal{D} . Our proof strategy consists of using Lemma 7.2.2 and Proposition 2.6.2 to conclude the result. A minor technical hurdle in this process is ensuring the Lipschitz property of the vector field (7.7), the projection of which on \mathcal{D} is X_{p-d} . We tackle this by using the monotonicity property of the primal-dual dynamics stated in Lemma 7.2.1 implying that a solution of X_{p-d} (if it exists) remains in a bounded set, which we know explicitly. This further implies that, given a starting point, there exists a bounded set such that the values of the vector field outside this set do not affect the solution starting at that point and hence, the vector field can be modified at the outside points without loss of generality to obtain the Lipschitz property. We make this construction explicit in the proof.

Lemma 7.2.3. (*Existence, uniqueness, and continuity of solutions of the primal-dual dynamics*): *Starting from any point $(x, \lambda) \in \mathcal{D}$, a unique solution $t \mapsto \gamma(t)$ of the primal-dual dynamics X_{p-d} exists and remains in $(\mathcal{D}) \cap V^{-1}(\leq V(x, \lambda))$. Moreover, if a sequence of points $\{(x_k, \lambda_k)\}_{k=1}^{\infty} \subset \mathcal{D}$ converge to (x, λ) as $k \rightarrow \infty$, then the sequence of solutions $\{t \mapsto \gamma_k(t)\}_{k=1}^{\infty}$ of X_{p-d} starting at these points converge uniformly to the solution $t \mapsto \gamma(t)$ on every compact set of $[0, \infty)$.*

Proof. Consider $(x(0), \lambda(0)) \in \mathcal{D}$ and let $\epsilon > 0$. Define $V_0 = V(x(0), \lambda(0))$, where V is given in (7.6), and let $\mathcal{W}_\epsilon = V^{-1}(\leq V_0 + \epsilon)$. Note that \mathcal{W}_ϵ is convex, compact, and $V^{-1}(\leq V_0) \subset \text{int}(\mathcal{W}_\epsilon)$. Let $X^{\mathcal{W}_\epsilon} : \mathbb{R}^n \times \mathbb{R}^m \rightarrow \mathbb{R}^n \times \mathbb{R}^m$ be a vector field defined as follows: equal to X on \mathcal{W}_ϵ and, for any $(x, \lambda) \in (\mathbb{R}^n \times \mathbb{R}^m) \setminus \mathcal{W}_\epsilon$,

$$X^{\mathcal{W}_\epsilon}(x, \lambda) = X(\text{proj}_{\mathcal{W}_\epsilon}(x, \lambda)).$$

The vector field $X^{\mathcal{W}_\epsilon}$ is Lipschitz on the domain $\mathbb{R}^n \times \mathbb{R}^m$. To see this, note that X is Lipschitz on the compact set \mathcal{W}_ϵ with some Lipschitz constant $K > 0$ because

f and g have locally Lipschitz gradients. Let $(x_1, \lambda_1), (x_2, \lambda_2) \in \mathbb{R}^n \times \mathbb{R}^m$. Then,

$$\begin{aligned} \|X^{\mathcal{W}_\epsilon}(x_1, \lambda_1) - X^{\mathcal{W}_\epsilon}(x_2, \lambda_2)\| &= \|X(\text{proj}_{\mathcal{W}_\epsilon}(x_1, \lambda_1)) - X(\text{proj}_{\mathcal{W}_\epsilon}(x_2, \lambda_2))\| \\ &\leq K\|\text{proj}_{\mathcal{W}_\epsilon}(x_1, \lambda_1) - \text{proj}_{\mathcal{W}_\epsilon}(x_2, \lambda_2)\| \\ &\leq K\|(x_1, \lambda_1) - (x_2, \lambda_2)\|. \end{aligned}$$

The last inequality follows from the Lipschitz property of the map $\text{proj}_{\mathcal{W}_\epsilon}$ (cf. Section 2.6.2).

Next, we employ Proposition 2.6.2 to establish the existence, uniqueness, and continuity with respect to the initial condition of the solutions of the projected dynamical system, $X_{\text{p-d}}^{\mathcal{W}_\epsilon}$, associated with $X^{\mathcal{W}_\epsilon}$ and \mathcal{D} . Our proof then concludes by showing that in fact all solutions of the projected system $X_{\text{p-d}}^{\mathcal{W}_\epsilon}$ starting in $\mathcal{W}_\epsilon \cap \mathcal{D}$ are in one-to-one correspondence with the solutions of $X_{\text{p-d}}$ starting in $\mathcal{W}_\epsilon \cap \mathcal{D}$. Let $X_{\text{p-d}}^{\mathcal{W}_\epsilon} : \mathcal{D} \rightarrow \mathbb{R}^n \times \mathbb{R}^m$ be the map obtained by projecting $X^{\mathcal{W}_\epsilon}$ with respect to \mathcal{D} ,

$$X_{\text{p-d}}^{\mathcal{W}_\epsilon}(x, \lambda) = \Pi_{\mathcal{D}}((x, \lambda), X^{\mathcal{W}_\epsilon}(x, \lambda)),$$

for all $(x, \lambda) \in \mathcal{D}$. Since $X_{\text{p-d}}$ is the projection of X with respect to \mathcal{D} , we deduce that $X_{\text{p-d}}^{\mathcal{W}_\epsilon} = X_{\text{p-d}}$ over the set $\mathcal{W}_\epsilon \cap \mathcal{D}$. Since $X^{\mathcal{W}_\epsilon}$ is Lipschitz, following Proposition 2.6.2, we obtain that starting from any point in \mathcal{D} , a unique solution of $X_{\text{p-d}}^{\mathcal{W}_\epsilon}$ exists over $[0, \infty)$ and is continuous with respect to the initial condition. Consider any solution $t \mapsto (\tilde{x}(t), \tilde{\lambda}(t))$ of $X_{\text{p-d}}^{\mathcal{W}_\epsilon}$ that starts in $\mathcal{W}_\epsilon \cap \mathcal{D}$. Note that since the solution is absolutely continuous and V is continuously differentiable, the map $t \mapsto V(\tilde{x}(t), \tilde{\lambda}(t))$ is differentiable almost everywhere on $[0, \infty)$, and hence

$$\frac{d}{dt}V(\tilde{x}(t), \tilde{\lambda}(t)) = \mathcal{L}_{X_{\text{p-d}}^{\mathcal{W}_\epsilon}}V(\tilde{x}(t), \tilde{\lambda}(t)),$$

almost everywhere on $[0, \infty)$. From Lemma 7.2.1 and the fact that $\mathcal{L}_{X_{\text{p-d}}^{\mathcal{W}_\epsilon}}V$ and $\mathcal{L}_{X_{\text{p-d}}}V$ are the same over $\mathcal{W}_\epsilon \cap \mathcal{D}$, we conclude that V is non-increasing along the solution. This means the solution remains in the set $\mathcal{W}_\epsilon \cap \mathcal{D}$. Finally, since $X_{\text{p-d}}^{\mathcal{W}_\epsilon}$ and $X_{\text{p-d}}$ are same on $\mathcal{W}_\epsilon \cap \mathcal{D}$, we conclude that $t \mapsto (\tilde{x}(t), \tilde{\lambda}(t))$ is also a solution

of $X_{\text{p-d}}$. Therefore, starting at any point in $\mathcal{W}_\epsilon \cap \mathcal{D}$, a solution of $X_{\text{p-d}}$ exists. Using Lemma 7.2.1, one can show that, if a solution of $X_{\text{p-d}}$ that starts from a point in $\mathcal{W}_\epsilon \cap \mathcal{D}$ exists, then it remains in $\mathcal{W}_\epsilon \cap \mathcal{D}$ and so is a solution of $X_{\text{p-d}}^{\mathcal{W}_\epsilon}$. This, combined with the uniqueness of solutions of $X_{\text{p-d}}^{\mathcal{W}_\epsilon}$, implies that a unique solution of $X_{\text{p-d}}$ exists starting from any point in $\mathcal{W}_\epsilon \cap \mathcal{D}$. In particular, this is true for the point $(x(0), \lambda(0))$. Finally, from the continuity of solutions of $X_{\text{p-d}}^{\mathcal{W}_\epsilon}$ and the one-to-one correspondence of solutions of $X_{\text{p-d}}$ and $X_{\text{p-d}}^{\mathcal{W}_\epsilon}$ starting $\mathcal{W}_\epsilon \cap \mathcal{D}$, we conclude the continuity with respect to initial condition for solutions of $X_{\text{p-d}}$ starting in $V^{-1}(x(0), \lambda(0))$. Since $(x(0), \lambda(0))$ is arbitrary, the result follows. \square

The next result states the invariance of the omega-limit set of any solution of the primal-dual dynamics. This ensures that all hypotheses of the invariance principle for Caratheodory solutions of discontinuous dynamical systems, cf. Proposition 2.6.1, are satisfied.

Lemma 7.2.4. (*Omega-limit set of solution of primal-dual dynamics is invariant*):
The omega-limit set of any solution of the primal-dual dynamics starting from any point in $\mathbb{R}^n \times \mathbb{R}_{\geq 0}^m$ is invariant under (7.4).

Proof. For $(x(0), \lambda(0)) \in \mathcal{D}$, let $t \mapsto (x(t), \lambda(t))$ be the solution of $X_{\text{p-d}}$ starting at $(x(0), \lambda(0))$ and let $\Omega(x, \lambda)$ be its omega-limit set. Since every solution of $X_{\text{p-d}}$ is bounded (cf. Lemma 7.2.3), the set $\Omega(x, \lambda)$ is nonempty. Let $(\bar{x}, \bar{\lambda}) \in \Omega(x, \lambda)$. From the definition of omega-limit set (cf. Section 2.6.1), there exists a sequence $\{t_k\}_{k=1}^\infty$ with $\lim_{k \rightarrow \infty} t_k = \infty$ such that $\lim_{k \rightarrow \infty} (x(t_k), \lambda(t_k)) = (\bar{x}, \bar{\lambda})$. From Lemma 7.2.3, we know that $(\bar{x}, \bar{\lambda}) \in (\mathcal{D}) \cap V^{-1}(\leq V(x(0), \lambda(0)))$ and thus a unique solution of $X_{\text{p-d}}$ exists starting at $(\bar{x}, \bar{\lambda})$. We denote it by $t \mapsto \phi(t)$, $\phi(0) = (\bar{x}, \bar{\lambda})$. We need to show that $\phi(t) \in \Omega(x, \lambda)$ for all $t \geq 0$. Pick any $\tilde{t} \in [0, \infty)$. Consider the sequence of solutions $\{t \mapsto (x_k(t), \lambda_k(t))\}_{k=1}^\infty$ where $(x_k(0), \lambda_k(0)) = (x(t_k), \lambda(t_k))$ for all $k \in \mathbb{Z}_{\geq 1}$. Since $(x_k(0), \lambda_k(0)) \rightarrow (\bar{x}, \bar{\lambda})$, by the continuity property of solutions (cf. Lemma 7.2.3), the sequence of solutions $\{t \mapsto (x_k(t), \lambda_k(t))\}_{k=1}^\infty$ converges uniformly to $t \mapsto \phi(t)$ over the interval $[0, \tilde{t}]$. In

particular, from uniqueness of solutions, we have

$$\phi(\tilde{t}) = \lim_{k \rightarrow \infty} (x_k(\tilde{t}), \lambda_k(\tilde{t})) = \lim_{k \rightarrow \infty} (x(t_k + \tilde{t}), \lambda(t_k + \tilde{t})),$$

or equivalently, $\phi(\tilde{t}) \in \Omega(x, \lambda)$. Since \tilde{t} is arbitrary, we deduce that $\phi(t) \in \Omega(x, \lambda)$ for all $t \geq 0$, concluding the proof. \square

We are now ready to establish our main result, the asymptotic convergence of the solutions of the primal-dual dynamics to a solution of the constrained optimization problem.

Theorem 7.2.5. *(Convergence of the primal-dual dynamics to a primal-dual optimizer): The set of primal-dual solutions of (7.1) is globally asymptotically stable on $\mathbb{R}^n \times \mathbb{R}_{\geq 0}^m$ under the primal-dual dynamics (7.4), and the convergence of each solution is to a point.*

Proof. Let $(x_*, \lambda_*) \in \mathbf{X} \times \Lambda$ and consider the function V defined in (7.6). For $\delta > 0$, consider the compact set $\mathcal{S} = V^{-1}(\leq \delta) \cap (\mathbb{R}^n \times \mathbb{R}_{\geq 0}^m)$. From Lemma 7.2.3, we deduce that a unique solution of $X_{\text{p-d}}$ exists starting from any point in \mathcal{S} , which remains in \mathcal{S} . Moreover, from Lemma 7.2.4, the omega-limit set of each solution starting from any point in \mathcal{S} is invariant. Finally, from Lemma 7.2.1, $\mathcal{L}_{X_{\text{p-d}}} V(x, \lambda) \leq 0$ for all $(x, \lambda) \in \mathcal{S}$. Therefore, Proposition 2.6.1 implies that any solution of $X_{\text{p-d}}$ starting in \mathcal{S} converges to the largest invariant set M contained in $\text{cl}(Z)$, where $Z = \{(x, \lambda) \in \mathcal{S} \mid \mathcal{L}_{X_{\text{p-d}}} V(x, \lambda) = 0\}$. From the proof of Lemma 7.2.1, $\mathcal{L}_{X_{\text{p-d}}} V(x, \lambda) = 0$ implies

$$\begin{aligned} L(x_*, \lambda_*) - L(x_*, \lambda) &= 0, \\ L(x, \lambda_*) - L(x_*, \lambda_*) &= 0, \\ (\lambda_i - (\lambda_*)_i)([g_i(x)]_{\lambda_i}^+ - g_i(x)) &= 0, \quad \text{for all } i \in [m]. \end{aligned}$$

Since f is strictly concave, so is the function $x \mapsto L(x, \lambda_*)$ and thus $L(x, \lambda_*) = L(x_*, \lambda_*)$ implies $x = x_*$. The equality $L(x_*, \lambda_*) - L(x_*, \lambda) = 0$ implies $\lambda^\top g(x_*) = 0$. Therefore $Z = \{(x, \lambda) \in \mathcal{S} \mid x = x_*, \lambda^\top g(x_*) = 0\}$ is closed. Let $(x_*, \lambda) \in M \subset Z$. The solution of $X_{\text{p-d}}$ starting at (x_*, λ) remains in M (and hence in Z) only

if $\nabla f(x_*) - \sum_{i=1}^m \lambda_i \nabla g_i(x_*) = 0$. This implies that (x_*, λ) satisfies the KKT conditions (7.3) and hence, $M \subset \mathbf{X} \times \Lambda$. Since the initial choice $\delta > 0$ is arbitrary, we conclude that the set $\mathbf{X} \times \Lambda$ is globally asymptotically stable on $\mathbb{R}^n \times \mathbb{R}_{\geq 0}^m$. Finally, we note that convergence is to a point in $\mathbf{X} \times \Lambda$. This is equivalent to saying that the omega-limit set $\Omega(x, \lambda) \subset \mathbf{X} \times \Lambda$ of any solution $t \mapsto (x(t), \lambda(t))$ of $X_{\text{p-d}}$ is a singleton. This fact follows from the definition of omega-limit set and the fact that, by Lemma 7.2.1, primal-dual optimizers are Lyapunov stable. This concludes the proof. \square

Remark 7.2.6. (*Alternative proof strategy via evolution variational inequalities*):

We briefly describe here an alternative proof strategy to the one we have used here to establish the asymptotic convergence of the primal-dual dynamics. The Caratheodory solutions of the primal-dual dynamics can also be seen as solutions of an evolution variational inequality (EVI) problem [BG05]. Then, one can show that the resulting EVI problem has a unique solution starting from each point in \mathcal{D} , which moreover remains in \mathcal{D} . With this in place, the LaSalle Invariance Principle [BG05, Theorem 4] for the solutions of the EVI problem can be applied to conclude the convergence to the set of primal-dual optimizers. \bullet

Remark 7.2.7. (*Primal-dual dynamics with gains*): In power network optimization problems [ZTLL14, MZL14a, ZP14] and network congestion control problems [WA04, LPD02], it is common to see generalizations of the primal-dual dynamics involving gain matrices. Formally, these dynamics take the form

$$\dot{x} = K_1 \nabla_x L(x, \lambda), \quad (7.8a)$$

$$\dot{\lambda} = K_2 [-\nabla_\lambda L(x, \lambda)]_\lambda^+, \quad (7.8b)$$

where $K_1 \in \mathbb{R}^{n \times n}$ and $K_2 \in \mathbb{R}^{m \times m}$ are diagonal, positive definite matrices. In such cases, the analysis performed here can be replicated following the same steps but using instead the Lyapunov function

$$V'(x, \lambda) = \frac{1}{2}((x - x_*)^\top K_1^{-1}(x - x_*) + (\lambda - \lambda_*)^\top K_2^{-1}(\lambda - \lambda_*)),$$

to establish the required monotonicity and convergence properties of (7.8). •

Acknowledgments

This chapter is taken, in part, from the work [CMC16] published as “Asymptotic convergence of primal-dual dynamics” by A. Cherukuri, E. Mallada, and J. Cortés, in *Systems and Control Letters*, as well as [CMC15] where it appears as “Convergence of Caratheodory solutions for primal-dual dynamics in constrained concave optimization” by A. Cherukuri, E. Mallada, and J. Cortés in the proceedings of the 2015 SIAM Conference on Control and its Applications. The dissertation author was the primary investigator and author of these papers. This research was partly supported by the US National Science Foundation (NSF) Award ECCS-1307176.

Chapter 8

Role of convexity in saddle-point dynamics

The main aim of this chapter is to refine the analysis of the saddle-point dynamics by unveiling two ways in which convexity-concavity of the saddle function plays a role. First, we show that local strong convexity-concavity is enough to conclude global asymptotic convergence, thus generalizing previous results that rely on global strong/strict convexity-concavity instead. Second, we show that, if global strong convexity-concavity holds, then one can identify a novel Lyapunov function for the projected saddle-point dynamics for the case when the saddle function is the Lagrangian of a constrained optimization problem. This, in turn, implies a stronger form of convergence, that is, input-to-state stability (ISS) and has important implications in the practical implementation of the saddle-point dynamics.

8.1 Problem statement

In this section, we provide a formal statement of the problem of interest. Consider a twice continuously differentiable function $F : \mathbb{R}^n \times \mathbb{R}_{\geq 0}^p \times \mathbb{R}^m \rightarrow \mathbb{R}$, $(x, y, z) \mapsto F(x, y, z)$, which we refer to as *saddle function*. With the notation of Section 2.4, we set $\mathcal{X} = \mathbb{R}^n$ and $\mathcal{Y} = \mathbb{R}_{\geq 0}^p \times \mathbb{R}^m$, and assume that F is convex-concave on $(\mathbb{R}^n) \times (\mathbb{R}_{\geq 0}^p \times \mathbb{R}^m)$. Let $\text{Saddle}(F)$ denote its (non-empty) set of saddle

points. We define the *projected saddle-point dynamics* for F as

$$\dot{x} = -\nabla_x F(x, y, z), \quad (8.1a)$$

$$\dot{y} = [\nabla_y F(x, y, z)]_y^+, \quad (8.1b)$$

$$\dot{z} = \nabla_z F(x, y, z). \quad (8.1c)$$

When convenient, we use the map $X_{\text{p-sp}} : \mathbb{R}^n \times \mathbb{R}_{\geq 0}^p \times \mathbb{R}^m \rightarrow \mathbb{R}^n \times \mathbb{R}^p \times \mathbb{R}^m$ to refer to the dynamics (8.1). Note that the domain $\mathbb{R}^n \times \mathbb{R}_{\geq 0}^p \times \mathbb{R}^m$ is invariant under $X_{\text{p-sp}}$ (this follows from the definition of the projection operator) and its set of equilibrium points precisely corresponds to $\text{Saddle}(F)$ (this follows from the defining property of saddle points and the first-order condition for convexity-concavity of F). Thus, a saddle point (x_*, y_*, z_*) satisfies

$$\nabla_x F(x_*, y_*, z_*) = 0, \quad \nabla_z F(x_*, y_*, z_*) = 0, \quad (8.2a)$$

$$\nabla_y F(x_*, y_*, z_*) \leq 0, \quad y_*^\top \nabla_y F(x_*, y_*, z_*) = 0. \quad (8.2b)$$

Our interest in the dynamics (8.1) is motivated by two bodies of work in the literature: one that analyzes primal-dual dynamics, corresponding to (8.1a) together with (8.1b), for solving inequality constrained network optimization problems, see e.g., [AHU58, FP10, MZL14b, ZTLL14]; and the other one analyzing saddle-point dynamics, corresponding to (8.1a) together with (8.1c), for solving equality constrained problems and finding Nash equilibrium of zero-sum games, see e.g., [CGC17] and references therein. By considering (8.1a)-(8.1c) together, we aim to unify these lines of work. Below we explain further the significance of the dynamics in solving specific network optimization problems.

Remark 8.1.1. (*Motivating examples*): Consider the following constrained convex optimization problem

$$\min\{f(x) \mid g(x) \leq 0, Ax = b\},$$

where $f : \mathbb{R}^n \rightarrow \mathbb{R}$ and $g : \mathbb{R}^n \rightarrow \mathbb{R}^p$ are convex continuously differentiable functions, $A \in \mathbb{R}^{m \times n}$, and $b \in \mathbb{R}^m$. Under zero duality gap, saddle points of the

associated Lagrangian $L(x, y, z) = f(x) + y^\top g(x) + z^\top (Ax - b)$ correspond to the primal-dual optimizers of the problem. This observation motivates the search for the saddle points of the Lagrangian, which can be done via the projected saddle-point dynamics (8.1). In many network optimization problems, f is the summation of individual costs of agents and the constraints, defined by g and A , are such that each of its components is computable by one agent interacting with its neighbors. This structure renders the projected saddle-point dynamics of the Lagrangian implementable in a distributed manner. Motivated by this, the dynamics is widespread in network optimization scenarios. For example, in optimal dispatch of power generators [ZTLL14, LZC16, SPvdS17, MZL14b], the objective function is the sum of the individual cost function of each generator, the inequalities consist of generator capacity constraints and line limits, and the equality encodes the power balance at each bus. In congestion control of communication networks [CLCD07, PM09, FP10], the cost function is the summation of the negative of the utility of the communicated data, the inequalities define constraints on channel capacities, and equalities encode the data balance at each node. •

Our main objectives are to identify conditions that guarantee that the set of saddle points is globally asymptotically stable under the dynamics (8.1) and formally characterize the robustness properties using the concept of input-to-state stability. The rest of the chapter is structured as follows. Section 8.2 investigates novel conditions that guarantee global asymptotic convergence relying on LaSalle-type arguments. Section 8.3 instead identifies a strict Lyapunov function for constrained convex optimization problems. This finding allows us in Section 8.4 to go beyond convergence guarantees and explore the robustness properties of the saddle-point dynamics.

8.2 Local properties of the saddle function imply global convergence

Our first result of this section provides a novel characterization of the omega-limit set of the trajectories of the projected saddle-point dynamics (8.1).

Proposition 8.2.1. (*Characterization of the omega-limit set of solutions of X_{p-sp}*): Given a twice continuously differentiable, convex-concave function F , each point in the set $\text{Saddle}(F)$ is stable under the projected saddle-point dynamics X_{p-sp} and the omega-limit set of every solution is contained in the largest invariant set \mathcal{M} in $\mathcal{E}(F)$, where

$$\begin{aligned} \mathcal{E}(F) = \{ & (x, y, z) \in \mathbb{R}^n \times \mathbb{R}_{\geq 0}^p \times \mathbb{R}^m \mid \\ & (x - x_*; y - y_*; z - z_*) \in \ker(\overline{H}(x, y, z, x_*, y_*, z_*)), \\ & \text{for all } (x_*, y_*, z_*) \in \text{Saddle}(F)\}, \end{aligned} \quad (8.3)$$

and

$$\begin{aligned} \overline{H}(x, y, z, x_*, y_*, z_*) &= \int_0^1 H(x(s), y(s), z(s)) ds, \\ (x(s), y(s), z(s)) &= (x_*, y_*, z_*) + s(x - x_*, y - y_*, z - z_*), \\ H(x, y, z) &= \begin{bmatrix} -\nabla_{xx}F & 0 & 0 \\ 0 & \nabla_{yy}F & \nabla_{yz}F \\ 0 & \nabla_{zy}F & \nabla_{zz}F \end{bmatrix}_{(x,y,z)}. \end{aligned} \quad (8.4)$$

Proof. The proof follows from the application of the LaSalle Invariance Principle for discontinuous Caratheodory systems (cf. Proposition 2.6.1). Let $(x_*, y_*, z_*) \in \text{Saddle}(F)$ and $V_1 : \mathbb{R}^n \times \mathbb{R}_{\geq 0}^p \times \mathbb{R}^m \rightarrow \mathbb{R}_{\geq 0}$ be defined as

$$V_1(x, y, z) = \frac{1}{2} (\|x - x_*\|^2 + \|y - y_*\|^2 + \|z - z_*\|^2). \quad (8.5)$$

The Lie derivative of V_1 along (8.1) is

$$\begin{aligned} \mathcal{L}_{X_{p-sp}} V_1(x, y, z) &= -(x - x_*)^\top \nabla_x F(x, y, z) + (y - y_*)^\top [\nabla_y F(x, y, z)]_y^+ \\ &\quad + (z - z_*)^\top \nabla_z F(x, y, z) \\ &= -(x - x_*)^\top \nabla_x F(x, y, z) + (y - y_*)^\top \nabla_y F(x, y, z) \\ &\quad + (z - z_*)^\top \nabla_z F(x, y, z) \\ &\quad + (y - y_*)^\top ([\nabla_y F(x, y, z)]_y^+ - \nabla_y F(x, y, z)) \end{aligned}$$

$$\begin{aligned} &\leq -(x - x_*)^\top \nabla_x F(x, y, z) + (y - y_*)^\top \nabla_y F(x, y, z) \\ &\quad + (z - z_*)^\top \nabla_z F(x, y, z), \end{aligned} \tag{8.6}$$

where the last inequality follows from the fact that $T_i = (y - y_*)_i([\nabla_y F(x, y, z)]_y^+ - \nabla_y F(x, y, z))_i \leq 0$ for each $i \in [p]$. Indeed if $y_i > 0$, then $T_i = 0$ and if $y_i = 0$, then $(y - y_*)_i \leq 0$ and $([\nabla_y F(x, y, z)]_y^+ - \nabla_y F(x, y, z))_i \geq 0$ which implies that $T_i \leq 0$. Next, denoting $\lambda = (y; z)$ and $\lambda^* = (y_*, z_*)$, we simplify the above inequality as

$$\begin{aligned} \mathcal{L}_{X_{p\text{-sp}}} V_1(x, y, z) &\leq -(x - x_*)^\top \nabla_x F(x, \lambda) + (\lambda - \lambda^*)^\top \nabla_\lambda F(x, \lambda) \\ &\stackrel{(a)}{=} -(x - x_*)^\top \int_0^1 \left(\nabla_{xx} F(x(s), \lambda(s))(x - x_*) \right. \\ &\quad \left. + \nabla_{\lambda x} F(x(s), \lambda(s))(\lambda - \lambda^*) \right) ds \\ &\quad + (\lambda - \lambda^*)^\top \int_0^1 \left(\nabla_{x\lambda} F(x(s), \lambda(s))(x - x_*) \right. \\ &\quad \left. + \nabla_{\lambda\lambda} F(x(s), \lambda(s))(\lambda - \lambda^*) \right) ds \\ &\stackrel{(b)}{=} [x - x_*; \lambda - \lambda^*]^\top \overline{H}(x, \lambda, x_*, \lambda^*) \stackrel{(c)}{\leq} 0, \end{aligned}$$

where (a) follows from the fundamental theorem of calculus using the notation $x(s) = x_* + s(x - x_*)$ and $\lambda(s) = \lambda^* + s(\lambda - \lambda^*)$ and recalling from (8.2) that $\nabla_x F(x_*, \lambda^*) = 0$ and $(\lambda - \lambda^*)^\top \nabla_\lambda F(x_*, \lambda^*) \leq 0$; (b) follows from the definition of \overline{H} using $(\nabla_{\lambda x} F(x, \lambda))^\top = \nabla_{x\lambda} F(x, \lambda)$; and (c) follows from the fact that \overline{H} is negative semi-definite. Now using this fact that $\mathcal{L}_{X_{p\text{-sp}}} V_1$ is nonpositive at any point, one can deduce, see e.g. [CMC16, Lemma 4.2-4.4], that starting from any point $(x(0), y(0), z(0))$ a unique trajectory of $X_{p\text{-sp}}$ exists, is contained in the compact set $V_1^{-1}(V_1(x(0), y(0), z(0))) \cap (\mathbb{R}^n \times \mathbb{R}_{\geq 0}^p \times \mathbb{R}^m)$ at all times, and its omega-limit set is invariant. These facts imply that the hypotheses of Proposition 2.6.1 hold and so, we deduce that the solutions of the dynamics $X_{p\text{-sp}}$ converge to the largest invariant set where the Lie derivative is zero, that is, the set

$$\begin{aligned} \mathcal{E}(F, x_*, y_*, z_*) &= \{(x, y, z) \in \mathbb{R}^n \times \mathbb{R}_{\geq 0}^p \times \mathbb{R}^m \mid \\ &\quad (x; y; z) - (x_*; y_*; z_*) \in \ker(\overline{H}(x, y, z, x_*, y_*, z_*))\}. \end{aligned} \tag{8.7}$$

Finally, since (x_*, y_*, z_*) was chosen arbitrary, we get that the solutions converge to the largest invariant set \mathcal{M} contained in $\mathcal{E}(F) = \bigcap_{(x_*, y_*, z_*) \in \text{Saddle}(F)} \mathcal{E}(F, x_*, y_*, z_*)$, concluding the proof. \square

Note that the proof of Proposition 8.2.1 shows that the Lie derivative of the function V_1 is negative, but not strictly negative, outside the set $\text{Saddle}(F)$. From Proposition 8.2.1 and the definition (8.3), we deduce that if a point (x, y, z) belongs to the omega-limit set (and is not a saddle point), then the line integral of the Hessian block matrix (8.4) from the any saddle point to (x, y, z) cannot be full rank. Elaborating further,

- (i) if $\nabla_{xx}F$ is full rank at a saddle point (x_*, y_*, z_*) and if the point $(x, y, z) \notin \text{Saddle}(F)$ belongs to the omega-limit set, then $x = x_*$, and
- (ii) if $\begin{bmatrix} \nabla_{yy}F & \nabla_{yz}F \\ \nabla_{zy}F & \nabla_{zz}F \end{bmatrix}$ is full rank at a saddle point (x_*, y_*, z_*) , then $(y, z) = (y_*, z_*)$.

These properties are used in the next result which shows that local strong convexity-concavity at a saddle point together with global convexity-concavity of the saddle function are enough to guarantee global convergence.

Theorem 8.2.2. *(Global asymptotic stability of the set of saddle points under X_{p-sp}): Given a twice continuously differentiable, convex-concave function F which is locally strongly convex-concave at a saddle point, the set $\text{Saddle}(F)$ is globally asymptotically stable under the projected saddle-point dynamics X_{p-sp} and the convergence of trajectories is to a point.*

Proof. Our proof proceeds by characterizing the set $\mathcal{E}(F)$ defined in (8.3). Let (x_*, y_*, z_*) be a saddle point at which F is locally strongly convex-concave. Without loss of generality, assume that $\nabla_{xx}F(x_*, y_*, z_*) \succ 0$ (the case of negative definiteness of the other Hessian block can be reasoned analogously). Let $(x, y, z) \in \mathcal{E}(F, x_*, y_*, z_*)$ (recall the definition of this set in (8.7)). Since $\nabla_{xx}F(x_*, y_*, z_*) \succ 0$ and F is twice continuously differentiable, we have that $\nabla_{xx}F$ is positive definite

in a neighborhood of (x_*, y_*, z_*) and so

$$\int_0^1 \nabla_{xx} F(x(s), y(s), z(s)) ds \succ 0,$$

where $x(s) = x_* + s(x - x_*)$, $y(s) = y_* + s(y - y_*)$, and $z(s) = z_* + s(z - z_*)$. Therefore, by definition of $\mathcal{E}(F, x_*, y_*, z_*)$, it follows that $x = x_*$ and so, $\mathcal{E}(F, x_*, y_*, z_*) \subseteq \{x_*\} \times (\mathbb{R}_{\geq 0}^p \times \mathbb{R}^m)$. From Proposition 8.2.1 the trajectories of $X_{\text{p-sp}}$ converge to the largest invariant set \mathcal{M} contained in $\mathcal{E}(F, x_*, y_*, z_*)$. To characterize this set, let $(x_*, y, z) \in \mathcal{M}$ and $t \mapsto (x_*, y(t), z(t))$ be a trajectory of $X_{\text{p-sp}}$ that is contained in \mathcal{M} and hence in $\mathcal{E}(F, x_*, y_*, z_*)$. From (8.6), we get

$$\begin{aligned} \mathcal{L}_{X_{\text{p-sp}}} V_1(x, y, z) &\leq -(x - x_*)^\top \nabla_x F(x, y, z) + (y - y_*)^\top \nabla_y F(x, y, z) \\ &\quad + (z - z_*)^\top \nabla_z F(x, y, z) \\ &\leq F(x, y, z) - F(x, y_*, z_*) + F(x_*, y, z) - F(x, y, z) \\ &\leq F(x_*, y_*, z_*) - F(x, y_*, z_*) + F(x_*, y, z) \\ &\quad - F(x_*, y_*, z_*) \leq 0, \end{aligned} \tag{8.8}$$

where in the second inequality we have used the first-order convexity and concavity property of the maps $x \mapsto F(x, y, z)$ and $(y, z) \mapsto F(x, y, z)$. Now since $\mathcal{E}(F, x_*, y_*, z_*) = \{(x_*, y, z) \mid \mathcal{L}_{X_{\text{p-sp}}} V_1(x_*, y, z) = 0\}$, using the above inequality, we get $F(x_*, y(t), z(t)) = F(x_*, y_*, z_*)$ for all $t \geq 0$. Thus, for all $t \geq 0$, $\mathcal{L}_{X_{\text{p-sp}}} F(x_*, y(t), z(t)) = 0$ which yields

$$\nabla_y F(x_*, y(t), z(t))^\top [\nabla_y F(x_*, y(t), z(t))]_{y(t)}^+ + \|\nabla_z F(x_*, y(t), z(t))\|^2 = 0$$

Note that both terms in the above expression are nonnegative and so, we get $[\nabla_y F(x_*, y(t), z(t))]_{y(t)}^+ = 0$ and $\nabla_z F(x_*, y(t), z(t)) = 0$ for all $t \geq 0$. In particular, this holds at $t = 0$ and so, $(x, y, z) \in \text{Saddle}(F)$, and we conclude $\mathcal{M} \subset \text{Saddle}(F)$. Hence $\text{Saddle}(F)$ is globally asymptotically stable. Combining this with the fact that individual saddle points are stable, one deduces the pointwise convergence of trajectories along the same lines as in [BB03, Corollary 5.2]. \square

A closer look at the proof of the above result reveals that the same conclusion also holds under milder conditions on the saddle function. In particular, F need only be twice continuously differentiable in a neighborhood of the saddle point and the local strong convexity-concavity can be relaxed to a condition on the line integral of Hessian blocks of F . We state next this stronger result.

Theorem 8.2.3. (*Global asymptotic stability of the set of saddle points under $X_{p\text{-sp}}$*): Let F be convex-concave and continuously differentiable with locally Lipschitz gradient. Suppose there is a saddle point (x_*, y_*, z_*) and a neighborhood of this point $\mathcal{U}_* \subset \mathbb{R}^n \times \mathbb{R}_{\geq 0}^p \times \mathbb{R}^m$ such that F is twice continuously differentiable on \mathcal{U}_* and either of the following holds

(i) for all $(x, y, z) \in \mathcal{U}_*$,

$$\int_0^1 \nabla_{xx} F(x(s), y(s), z(s)) ds \succ 0,$$

(ii) for all $(x, y, z) \in \mathcal{U}_*$,

$$\int_0^1 \begin{bmatrix} \nabla_{yy} F & \nabla_{yz} F \\ \nabla_{zy} F & \nabla_{zz} F \end{bmatrix}_{(x(s), y(s), z(s))} ds \prec 0,$$

where $(x(s), y(s), z(s))$ are given in (8.4). Then, $\text{Saddle}(F)$ is globally asymptotically stable under the projected saddle-point dynamics $X_{p\text{-sp}}$ and the convergence of trajectories is to a point.

We omit the proof of this result as the argument is analogous to the proof of Theorem 8.2.2, where one replaces the integral of Hessian blocks by the integral of generalized Hessian blocks (see [Cla83, Chapter 2] for the definition of the latter), as the function is not twice continuously differentiable everywhere.

Example 8.2.4. (*Illustration of global asymptotic convergence*): Consider $F : \mathbb{R}^2 \times \mathbb{R}_{\geq 0} \times \mathbb{R} \rightarrow \mathbb{R}$ given as

$$F(x, y, z) = f(x) + y(-x_1 - 1) + z(x_1 - x_2), \quad (8.9)$$

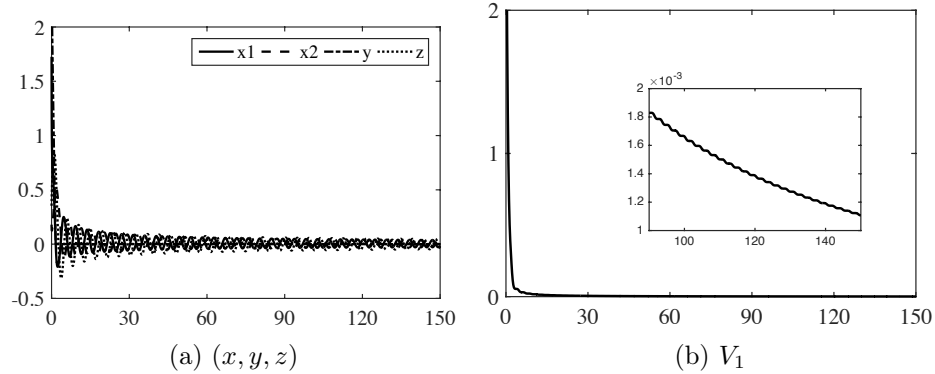


Figure 8.1: Execution of the projected saddle-point dynamics (8.1) starting from $(1.7256, 0.1793, 2.4696, 0.3532)$ for Example 8.2.4. As guaranteed by Theorem 8.2.3, the trajectory converges to the unique saddle point 0 and the function V_1 defined in (8.5) decreases monotonically.

where

$$f(x) = \begin{cases} \|x\|^4, & \text{if } \|x\| \leq \frac{1}{2}, \\ \frac{1}{16} + \frac{1}{2}(\|x\| - \frac{1}{2}), & \text{if } \|x\| \geq \frac{1}{2}. \end{cases}$$

Note that F is convex-concave on $(\mathbb{R}^2) \times (\mathbb{R}_{\geq 0} \times \mathbb{R})$ and $\text{Saddle}(F) = \{0\}$. Also, F is continuously differentiable on the entire domain and its gradient is locally Lipschitz. Finally, F is twice continuously differentiable on the neighborhood $\mathcal{U}_* = B_{1/2}(0) \cap (\mathbb{R}^2 \times \mathbb{R}_{\geq 0} \times \mathbb{R})$ of the saddle point 0 and hypothesis (i) of Theorem 8.2.3 holds on \mathcal{U}_* . Therefore, we conclude from Theorem 8.2.3 that the trajectories of the projected saddle-point dynamics of F converge globally asymptotically to the saddle point 0. Figure 8.1 shows an execution. •

Remark 8.2.5. (*Comparison with the literature*): Theorems 8.2.2 and 8.2.3 complement the available results in the literature concerning the asymptotic convergence properties of saddle-point [AHU58, CGC17, NC16] and primal-dual dynamics [FP10, CMC16]. The former dynamics corresponds to (8.1) when the variable y is absent and the later to (8.1) when the variable z is absent. For both saddle-point and primal-dual dynamics, existing global asymptotic stability results require assumptions on the global properties of F , in addition to the global convexity-concavity of F , such as global strong convexity-concavity [AHU58], global strict

convexity-concavity, and its generalizations [CGC17]. In contrast, the novelty of our results lies in establishing that certain local properties of the saddle function are enough to guarantee global asymptotic convergence. •

8.3 Lyapunov function for constrained convex optimization problems

Our discussion above has established the global asymptotic stability of the set of saddle points resorting to LaSalle-type arguments (because the function V_1 defined in (8.5) is not a strict Lyapunov function). In this section, we identify instead a strict Lyapunov function for the projected saddle-point dynamics when the saddle function F corresponds to the Lagrangian of a constrained optimization problem, cf. Remark 8.1.1. The relevance of this result stems from two facts. On the one hand, the projected saddle-point dynamics has been employed profusely to solve network optimization problems. On the other hand, although the conclusions on the asymptotic convergence of this dynamics that can be obtained with the identified Lyapunov function are the same as in the previous section, having a Lyapunov function available is advantageous for a number of reasons, including the study of robustness against disturbances, the characterization of the algorithm convergence rate, or as a design tool for developing opportunistic state-triggered implementations. We come back to this point in Section 8.4 below.

Theorem 8.3.1. (*Lyapunov function for $X_{p\text{-sp}}$*): *Let $F : \mathbb{R}^n \times \mathbb{R}_{\geq 0}^p \times \mathbb{R}^m \rightarrow \mathbb{R}$ be defined as*

$$F(x, y, z) = f(x) + y^\top g(x) + z^\top (Ax - b), \quad (8.10)$$

where $f : \mathbb{R}^n \rightarrow \mathbb{R}$ is strongly convex, twice continuously differentiable, $g : \mathbb{R}^n \rightarrow \mathbb{R}^p$ is convex, twice continuously differentiable, $A \in \mathbb{R}^{m \times n}$, and $b \in \mathbb{R}^m$. For each $(x, y, z) \in \mathbb{R}^n \times \mathbb{R}_{\geq 0}^p \times \mathbb{R}^m$, define the index set of active constraints

$$\mathcal{J}(x, y, z) = \{j \in [p] \mid y_j = 0 \text{ and } (\nabla_y F(x, y, z))_j < 0\}.$$

Then, the function $V_2 : \mathbb{R}^n \times \mathbb{R}_{\geq 0}^p \times \mathbb{R}^m \rightarrow \mathbb{R}$,

$$V_2(x, y, z) = \frac{1}{2} \left(\|\nabla_x F(x, y, z)\|^2 + \|\nabla_z F(x, y, z)\|^2 \right. \\ \left. + \sum_{j \in [p] \setminus \mathcal{J}(x, y, z)} ((\nabla_y F(x, y, z))_j)^2 \right) + \frac{1}{2} \|(x, y, z)\|_{\text{Saddle}(F)}^2$$

is nonnegative everywhere in its domain and $V_2(x, y, z) = 0$ if and only if $(x, y, z) \in \text{Saddle}(F)$. Moreover, for any trajectory $t \mapsto (x(t), y(t), z(t))$ of $X_{p\text{-sp}}$, the map $t \mapsto V_2(x(t), y(t), z(t))$

(i) is differentiable almost everywhere and if $(x(t), y(t), z(t)) \notin \text{Saddle}(F)$ for some $t \geq 0$, then $\frac{d}{dt} V_2(x(t), y(t), z(t)) < 0$ provided the derivative exists. Furthermore, for any sequence of times $\{t_k\}_{k=1}^{\infty}$ such that $t_k \rightarrow t$ and $\frac{d}{dt} V_2(x(t_k), y(t_k), z(t_k))$ exists for every t_k , we have $\limsup_{k \rightarrow \infty} \frac{d}{dt} V_2(x(t_k), y(t_k), z(t_k)) < 0$,

(ii) is right-continuous and at any point of discontinuity $t' \geq 0$, we have $V_2(x(t'), y(t'), z(t')) \leq \lim_{t \uparrow t'} V_2(x(t), y(t), z(t))$.

As a consequence, $\text{Saddle}(F)$ is globally asymptotically stable under $X_{p\text{-sp}}$ and convergence of trajectories is to a point.

Proof. We start by partitioning the domain based on the active constraints. Let $\mathcal{I} \subset [p]$ and

$$\mathcal{D}(\mathcal{I}) = \{(x, y, z) \in \mathbb{R}^n \times \mathbb{R}_{\geq 0}^p \times \mathbb{R}^m \mid \mathcal{J}(x, y, z) = \mathcal{I}\}.$$

Note that for $\mathcal{I}_1, \mathcal{I}_2 \subset [p]$, $\mathcal{I}_1 \neq \mathcal{I}_2$, we have $\mathcal{D}(\mathcal{I}_1) \cap \mathcal{D}(\mathcal{I}_2) = \emptyset$. Moreover,

$$\mathbb{R}^n \times \mathbb{R}_{\geq 0}^p \times \mathbb{R}^m = \bigcup_{\mathcal{I} \subset [p]} \mathcal{D}(\mathcal{I}).$$

For each $\mathcal{I} \subset [p]$, define the function

$$V_2^{\mathcal{I}}(x, y, z) = \frac{1}{2} \left(\|\nabla_x F(x, y, z)\|^2 + \|\nabla_z F(x, y, z)\|^2 \right)$$

$$+ \sum_{j \notin \mathcal{I}} ((\nabla_y F(x, y, z))_j)^2 + \frac{1}{2} \|(x, y, z)\|_{\text{Saddle}(F)}^2. \quad (8.11)$$

These functions will be used later for analyzing the evolution of V_2 . Consider a trajectory $t \mapsto (x(t), y(t), z(t))$ of $X_{\text{p-sp}}$ starting at some point $(x(0), y(0), z(0)) \in \mathbb{R}^n \times \mathbb{R}_{\geq 0}^p \times \mathbb{R}^m$. Our proof strategy consists of proving assertions (i) and (ii) for two scenarios, depending on whether or not there exists $\delta > 0$ such that the difference between two consecutive time instants when the trajectory switches from one partition set to another is lower bounded by δ .

Scenario 1: time elapsed between consecutive switches is lower bounded: Let $(a, b) \subset \mathbb{R}_{\geq 0}$, $b - a \geq \delta$, be a time interval for which the trajectory belongs to a partition $\mathcal{D}(\mathcal{I}')$, $\mathcal{I}' \subset [p]$, for all $t \in (a, b)$. In the following, we show that $\frac{d}{dt} V_2(x(t), y(t), z(t))$ exists for almost all $t \in (a, b)$ and its value is negative whenever $(x(t), y(t), z(t)) \notin \text{Saddle}(F)$. Consider the function $V_2^{\mathcal{I}'}$ defined in (8.11) and note that $t \mapsto V_2^{\mathcal{I}'}(x(t), y(t), z(t))$ is absolutely continuous as $V_2^{\mathcal{I}'}$ is continuously differentiable on $\mathbb{R}^n \times \mathbb{R}_{\geq 0}^p \times \mathbb{R}^m$ and the trajectory is absolutely continuous. Employing Rademacher's Theorem [Cla83], we deduce that the map $t \mapsto V_2^{\mathcal{I}'}(x(t), y(t), z(t))$ is differentiable almost everywhere. By definition, $V_2(x(t), y(t), z(t)) = V_2^{\mathcal{I}'}(x(t), y(t), z(t))$ for all $t \in (a, b)$. Therefore

$$\frac{d}{dt} V_2(x(t), y(t), z(t)) = \frac{d}{dt} V_2^{\mathcal{I}'}(x(t), y(t), z(t)) \quad (8.12)$$

for almost all $t \in (a, b)$. Further, since $V_2^{\mathcal{I}'}$ is continuously differentiable, we have

$$\frac{d}{dt} V_2^{\mathcal{I}'}(x(t), y(t), z(t)) = \mathcal{L}_{X_{\text{p-sp}}} V_2^{\mathcal{I}'}(x(t), y(t), z(t)). \quad (8.13)$$

Now consider any $(x, y, z) \in \mathcal{D}(\mathcal{I}') \setminus \text{Saddle}(F)$. Our next computation shows that $\mathcal{L}_{X_{\text{p-sp}}} V_2^{\mathcal{I}'}(x, y, z) < 0$. We have

$$\begin{aligned} \mathcal{L}_{X_{\text{p-sp}}} V_2^{\mathcal{I}'}(x, y, z) &= -\nabla_x F(x, y, z)^\top \nabla_{xx} F(x, y, z) \nabla_x F(x, y, z) \\ &\quad + \begin{bmatrix} [\nabla_y F(x, y, z)]_y^+ \\ \nabla_z F(x, y, z) \end{bmatrix}^\top \begin{bmatrix} \nabla_{yy} F & \nabla_{yz} F \\ \nabla_{zy} F & \nabla_{zz} F \end{bmatrix}_{(x,y,z)} \begin{bmatrix} [\nabla_y F(x, y, z)]_y^+ \\ \nabla_z F(x, y, z) \end{bmatrix} \end{aligned}$$

$$+ \mathcal{L}_{X_{p\text{-sp}}} \left(\frac{1}{2} \|(x, y, z)\|_{\text{Saddle}(F)}^2 \right). \quad (8.14)$$

The first two terms in the above expression are the Lie derivative of $(x, y, z) \mapsto V_2^{\mathcal{I}'}(x, y, z) - \frac{1}{2} \|(x, y, z)\|_{\text{Saddle}(F)}^2$. This computation can be shown using the properties of the operator $[\cdot]_y^+$. Now let $(x_*, y_*, z_*) = \text{proj}_{\text{Saddle}(F)}(x, y, z)$. Then, by Danskin's Theorem [CLSW98, p. 99], we have

$$\nabla \|(x, y, z)\|_{\text{Saddle}(F)}^2 = 2(x - x_*; y - y_*; z - z_*) \quad (8.15)$$

Using this expression, we get

$$\begin{aligned} \mathcal{L}_{X_{p\text{-sp}}} \left(\frac{1}{2} \|(x, y, z)\|_{\text{Saddle}(F)}^2 \right) &= -(x - x_*)^\top \nabla_x F(x, y, z) + (y - y_*)^\top [\nabla_y F(x, y, z)]_y^+ \\ &\quad + (z - z_*)^\top \nabla_z F(x, y, z) \\ &\leq F(x_*, y, z) - F(x_*, y_*, z_*) + F(x_*, y_*, z_*) \\ &\quad - F(x, y_*, z_*), \end{aligned}$$

where the last inequality follows from (8.8). Now using the above expression in (8.14) we get

$$\begin{aligned} \mathcal{L}_{X_{p\text{-sp}}} V_2^{\mathcal{I}'}(x, y, z) &\leq -\nabla_x F(x, y, z) \nabla_{xx} F(x, y, z) \nabla_x F(x, y, z) \\ &\quad + \begin{bmatrix} [\nabla_y F(x, y, z)]_y^+ \\ \nabla_z F(x, y, z) \end{bmatrix}^\top \begin{bmatrix} \nabla_{yy} F & \nabla_{yz} F \\ \nabla_{zy} F & \nabla_{zz} F \end{bmatrix}_{(x, y, z)} \begin{bmatrix} [\nabla_y F(x, y, z)]_y^+ \\ \nabla_z F(x, y, z) \end{bmatrix} \\ &\quad + F(x_*, y, z) - F(x_*, y_*, z_*) + F(x_*, y_*, z_*) \\ &\quad - F(x, y_*, z_*) \leq 0. \end{aligned}$$

If $\mathcal{L}_{X_{p\text{-sp}}} V_2^{\mathcal{I}'}(x, y, z) = 0$, then (a) $\nabla_x F(x, y, z) = 0$; (b) $x = x_*$; and (c) $F(x_*, y, z) = F(x_*, y_*, z_*)$. From (b) and (8.2), we conclude that $\nabla_z F(x, y, z) = 0$. From (c) and (8.10), we deduce that $(y - y_*)^\top g(x_*) = 0$. Note that for each $i \in [p]$, we have $(y_i - (y_*)_i)(g(x_*)_i) \leq 0$. This is because either $(g(x_*)_i) = 0$ in which case it is trivial or $(g(x_*)_i) < 0$ in which case $(y_*)_i = 0$ (as y_* maximizes the map $y \mapsto y^\top g(x_*)$) thereby making $y_i - (y_*)_i \geq 0$. Since, $(y_i - (y_*)_i)(g(x_*)_i) \leq 0$ for

each i and $(y - y_*)^\top g(x_*) = 0$, we get that for each $i \in [p]$, either $(g(x_*))_i = 0$ or $y_i = (y_*)_i$. Thus, $[\nabla_y F(x, y, z)]_y^+ = 0$. These facts imply that $(x, y, z) \in \text{Saddle}(F)$. Therefore, if $(x, y, z) \in \mathcal{D}(\mathcal{I}') \setminus \text{Saddle}(F)$ then $\mathcal{L}_{X_{p\text{-sp}}} V_2^{\mathcal{I}'}(x, y, z) < 0$. Combining this with (8.12) and (8.13), we deduce

$$\frac{d}{dt} V_2(x(t), y(t), z(t)) < 0$$

for almost all $t \in (a, b)$. Therefore, between any two switches in the partition, the evolution of V_2 is differentiable and the value of the derivative is negative. Since the number of time instances when a switch occurs is countable, the first part of assertion (i) holds. To show the limit condition, consider $t \geq 0$ such that $(x(t), y(t), z(t)) \notin \text{Saddle}(F)$. Let $\{t_k\}_{k=1}^\infty$ be such that $t_k \rightarrow t$ and $\frac{d}{dt} V_2(x(t_k), y(t_k), z(t_k))$ exists for every t_k . By continuity, $\lim_{k \rightarrow \infty} (x(t_k), y(t_k), z(t_k)) = (x(t), y(t), z(t))$. Let $\mathcal{B} \subset \mathbb{R}^n \times \mathbb{R}_{\geq 0}^p \times \mathbb{R}^m$ be a compact neighborhood of $(x(t), y(t), z(t))$ such that $\mathcal{B} \cap \text{Saddle}(F) = \emptyset$. Without loss of generality, assume that $\{(x(t_k), y(t_k), z(t_k))\}_{k=1}^\infty \subset \mathcal{B}$. Define

$$S = \max\{\mathcal{L}_{X_{p\text{-sp}}} V_2^{\mathcal{J}(x, y, z)}(x, y, z) \mid (x, y, z) \in \mathcal{B}\}.$$

The Lie derivatives in the above expression are well-defined and continuous as each $V_2^{\mathcal{J}(x, y, z)}$ is continuously differentiable. Note that $S < 0$ as $\mathcal{B} \cap \text{Saddle}(F) = \emptyset$. Moreover, as established above, for each k , $\frac{d}{dt} V_2(x(t_k), y(t_k), z(t_k)) = \mathcal{L}_{X_{p\text{-sp}}} V_2^{\mathcal{J}(x(t_k), y(t_k), z(t_k))}(x(t_k), y(t_k), z(t_k)) \leq S$. Thus, we get $\limsup_{k \rightarrow \infty} \frac{d}{dt} V_2(x(t_k), y(t_k), z(t_k)) \leq S < 0$, establishing (i) for Scenario 1.

To prove assertion (ii), note that discontinuity in V_2 can only happen when the trajectory switches the partition. In order to analyze this, consider any time instant $t' \geq 0$ and let $(x(t'), y(t'), z(t')) \in \mathcal{D}(\mathcal{I}')$ for some $\mathcal{I}' \subset [p]$. Looking at times $t \geq t'$, two cases arise:

- (a) There exists $\tilde{\delta} > 0$ such that $(x(t), y(t), z(t)) \in \mathcal{D}(\mathcal{I}')$ for all $t \in [t', t' + \tilde{\delta})$.
- (b) There exists $\tilde{\delta} > 0$ and $\mathcal{I} \neq \mathcal{I}'$ such that $(x(t), y(t), z(t)) \in \mathcal{D}(\mathcal{I})$ for all $t \in (t', t' + \tilde{\delta})$.

One can show that for Scenario 1, the trajectory cannot show any behavior other than the above mentioned two cases. We proceed to show that in both the above outlined cases, $t \mapsto V_2(x(t), y(t), z(t))$ is right-continuous at t' . Case (a) is straightforward as V_2 is continuous in the domain $\mathcal{D}(\mathcal{I}')$ and the trajectory is absolutely continuous. In case (b), $\mathcal{I} \neq \mathcal{I}'$ implies that there exists $j \in [p]$ such that either $j \in \mathcal{I} \setminus \mathcal{I}'$ or $j \in \mathcal{I}' \setminus \mathcal{I}$. Note that the later scenario, i.e., $j \in \mathcal{I}'$ and $j \notin \mathcal{I}$ cannot happen. Indeed by definition $(y(t'))_j = 0$ and $(\nabla_y F(x(t'), y(t'), z(t')))_j < 0$ and by continuity of the trajectory and the map $\nabla_y F$, these conditions also hold for some finite time interval starting at t' . Therefore, we focus on the case that $j \in \mathcal{I} \setminus \mathcal{I}'$. Then, either $(y(t'))_j > 0$ or $(\nabla_y F(x(t'), y(t'), z(t')))_j \geq 0$. The former implies, due to continuity of trajectories, that it is not possible to have $j \in \mathcal{I}$. Similarly, by continuity if $(\nabla_y F(x(t'), y(t'), z(t')))_j > 0$, then one cannot have $j \in \mathcal{I}$. Therefore, the only possibility is $(y(t'))_j = 0$ and $(\nabla_y F(x(t'), y(t'), z(t')))_j = 0$. This implies that the term $t \mapsto (\nabla_y F(x(t), y(t), z(t)))_j^2$ is right-continuous at t' . Since this holds for any $j \in \mathcal{I} \setminus \mathcal{I}'$, we conclude right-continuity of V_2 at t' . Therefore, for both cases (a) and (b), we conclude right-continuity of V_2 .

Next we show the limit condition of assertion (ii). Let $t' \geq 0$ be a point of discontinuity. Then, from the preceding discussion, there must exist $\mathcal{I}, \mathcal{I}' \subset [p]$, $\mathcal{I} \neq \mathcal{I}'$, such that $(x(t'), y(t'), z(t')) \in \mathcal{D}(\mathcal{I}')$ and $(x(t), y(t), z(t)) \in \mathcal{D}(\mathcal{I})$ for all $t \in (t' - \delta, t')$. By continuity, $\lim_{t \uparrow t'} V_2(x(t), y(t), z(t))$ exists. Note that if $j \in \mathcal{I}$ and $j \notin \mathcal{I}'$, then the term getting added to V_2 at time t' which was absent at times $t \in (t' - \delta, t')$, i.e., $(\nabla_y F(x(t), y(t), z(t)))_j^2$, is zero at t' . Therefore, the discontinuity at t' can only happen due to the existence of $j \in \mathcal{I}' \setminus \mathcal{I}$. That is, a constraint becomes active at time t' which was inactive in the time interval $(t' - \delta, t')$. Thus, the function V_2 loses a nonnegative term at time t' . This can only mean at t' the value of V_2 decreases. Hence, the limit condition of assertion (ii) holds.

Scenario 2: time elapsed between consecutive switches is not lower bounded: Observe that three cases arise. First is when there are only a finite number of switches in partition in any compact time interval. In this case, the analysis of Scenario 1 applies to every compact time interval and so assertions (i) and (ii) hold. The second case is when there exist time instants $t' > 0$ where

there is absence of “finite dwell time”, that is, there exist index sets $\mathcal{I}_1 \neq \mathcal{I}_2$ and $\mathcal{I}_2 \neq \mathcal{I}_3$ such that $(x(t), y(t), z(t)) \in \mathcal{D}(\mathcal{I}_1)$ for all $t \in (t' - \epsilon_1, t')$ and some $\epsilon_1 > 0$; $(x(t'), y(t'), z(t')) \in \mathcal{D}(\mathcal{I}_2)$; and $(x(t), y(t), z(t)) \in \mathcal{D}(\mathcal{I}_3)$ for all $t \in (t', t' + \epsilon_2)$ and some $\epsilon_2 > 0$. Again using the arguments of Scenario 1, one can show that both assertions (i) and (ii) hold for this case if there is no accumulation point of such time instants t' .

The third case instead is when there are infinite switches in a finite time interval. We analyze this case in parts. Assume that there exists a sequence of times $\{t_k\}_{k=1}^{\infty}$, $t_k \uparrow t'$, such that trajectory switches partition at each t_k . The aim is to show left-continuity of $t \mapsto V(x(t), y(t), z(t))$ at t' . Let $\mathcal{I}^s \subset [p]$ be the set of indices that switch between being active and inactive an infinite number of times along the sequence $\{t_k\}$ (note that the set is nonempty as there are an infinite number of switches and a finite number of indices). To analyze the left-continuity at t' , we only need to study the possible occurrence of discontinuity due to terms in V_2 corresponding to the indices in \mathcal{I}^s , since all other terms do not affect the continuity. Pick any $j \in \mathcal{I}^s$. Then, the term in V_2 corresponding to the index j satisfies

$$\lim_{k \rightarrow \infty} (\nabla_y F(x(t_k), y(t_k), z(t_k)))_j^2 = 0. \quad (8.16)$$

In order to show this, assume the contrary. This implies the existence of $\epsilon > 0$ such that

$$\liminf_{k \rightarrow \infty} (\nabla_y F(x(t_k), y(t_k), z(t_k)))_j^2 \geq \epsilon.$$

As a consequence, the set of k for which $(\nabla_y F(x(t_k), y(t_k), z(t_k)))_j^2 \geq \epsilon/2$ is infinite. Recall that if the constraint j becomes active at t_k , then V_2 decreases by at least $(\nabla_y F(x(t_k), y(t_k), z(t_k)))_j^2$ at t_k . Further, V_2 decreases monotonically between any consecutive t_k 's. These facts lead to the conclusion that V_2 tends to $-\infty$ as $t_k \rightarrow t'$. However, V_2 takes nonnegative values, yielding a contradiction. Hence, (8.16) is

true for all $j \in \mathcal{I}^s$ and so,

$$\lim_{k \rightarrow \infty} V_2(x(t_k), y(t_k), z(t_k)) = V_2(x(t'), y(t'), z(t')),$$

proving left-continuity of V_2 at t' . Using this reasoning, one can also conclude that if the infinite number of switches happen on a sequence $\{t_k\}_{k=1}^{\infty}$ with $t_k \downarrow t'$, then one has right-continuity at t' . Therefore, at each time instant when a switch happens, we have right-continuity of $t \mapsto V_2(x(t), y(t), z(t))$ and at points where there is accumulation of switches we have continuity (depending on which side of the time instance the accumulation takes place). This proves assertion (ii). Note that in this case too we have a countable number of time instants where the partition set switches and so the map $t \mapsto V_2(x(t), y(t), z(t))$ is differentiable almost everywhere. Moreover, one can also analyze, as done in Scenario 1, that the limit condition of assertion (i) holds in this case. These facts together establish the condition of assertion (ii), completing the proof. \square

Remark 8.3.2. (*Multiple Lyapunov functions*): The Lyapunov function V_2 is discontinuous on the domain $\mathbb{R}^n \times \mathbb{R}_{\geq 0}^p \times \mathbb{R}^m$. However, it can be seen as multiple (continuously differentiable) Lyapunov functions [Bra98], each valid on a domain, patched together in an appropriate way such that along the trajectories of $X_{\text{p-sp}}$, the evolution of V_2 is continuously differentiable with negative derivative at intervals where it is continuous and at times of discontinuity the value of V_2 only decreases. Note that in the absence of the projection in $X_{\text{p-sp}}$ (that is, no y -component of the dynamics), the function V_2 takes a much simpler form with no discontinuities and is continuously differentiable on the entire domain. \bullet

Remark 8.3.3. (*Connection with the literature: II*): The two functions whose sum defines V_2 are, individually by themselves, sufficient to establish asymptotic convergence of $X_{\text{p-sp}}$ using LaSalle Invariance arguments, see e.g., [FP10, CMC16]. However, the fact that their combination results in a strict Lyapunov function for the projected saddle-point dynamics is a novelty of our analysis here. In [NC16], a different Lyapunov function is proposed and an exponential rate of convergence is established for a saddle-point-like dynamics which is similar to $X_{\text{p-sp}}$ but without

projection components. •

8.4 ISS and self-triggered implementation of the saddle-point dynamics

Here, we build on the novel Lyapunov function identified in Section 8.3 to explore other properties of the projected saddle-point dynamics beyond global asymptotic convergence. Throughout this section, we consider saddle functions F that corresponds to the Lagrangian of an equality-constrained optimization problem, i.e.,

$$F(x, z) = f(x) + z^\top(Ax - b), \quad (8.17)$$

where $A \in \mathbb{R}^{m \times n}$, $b \in \mathbb{R}^m$, and $f : \mathbb{R}^n \rightarrow \mathbb{R}$. The reason behind this focus is that, in this case, the dynamics (8.1) is smooth and the Lyapunov function identified in Theorem 8.3.1 is continuously differentiable. These simplifications allow us to analyze input-to-state stability of the dynamics using the theory of ISS-Lyapunov functions (cf. Section 2.8). On the other hand, we do not know of such a theory for projected systems, which precludes us from carrying out ISS analysis for dynamics (8.1) for a general saddle function. The projected saddle-point dynamics (8.1) for the class of saddle functions given in (8.17) takes the form

$$\dot{x} = -\nabla_x F(x, z) = -\nabla f(x) - A^\top z, \quad (8.18a)$$

$$\dot{z} = \nabla_z F(x, z) = Ax - b, \quad (8.18b)$$

corresponding to equations (8.1a) and (8.1c). We term these dynamics simply *saddle-point dynamics* and denote it as $X_{\text{sp}} : \mathbb{R}^n \times \mathbb{R}^m \rightarrow \mathbb{R}^n \times \mathbb{R}^m$.

8.4.1 Input-to-state stability

Here, we establish that the saddle-point dynamics (8.18) is ISS with respect to the set $\text{Saddle}(F)$ when disturbance inputs affect it additively. Disturbance inputs can arise when implementing the saddle-point dynamics as a controller of a physical system because of a variety of malfunctions, including errors in the gradient computation, noise in state measurements, and errors in the controller implementation. In such scenarios, the following result shows that the dynamics (8.18) exhibits a graceful degradation of its convergence properties, one that scales with the size of the disturbance.

Theorem 8.4.1. (*ISS of saddle-point dynamics*): *Let the saddle function F be of the form (8.17), with f strongly convex, twice continuously differentiable, and satisfying $mI \preceq \nabla^2 f(x) \preceq MI$ for all $x \in \mathbb{R}^n$ and some constants $0 < m \leq M < \infty$. Then, the dynamics*

$$\begin{bmatrix} \dot{x} \\ \dot{z} \end{bmatrix} = \begin{bmatrix} -\nabla_x F(x, z) \\ \nabla_z F(x, z) \end{bmatrix} + \begin{bmatrix} u_x \\ u_z \end{bmatrix}, \quad (8.19)$$

where $(u_x, u_z) : \mathbb{R}_{\geq 0} \rightarrow \mathbb{R}^n \times \mathbb{R}^m$ is a measurable and locally essentially bounded map, is ISS with respect to $\text{Saddle}(F)$.

Proof. For notational convenience, we refer to (8.19) by $X_{\text{sp}}^{\text{p}} : \mathbb{R}^n \times \mathbb{R}^m \times \mathbb{R}^n \times \mathbb{R}^m \rightarrow \mathbb{R}^n \times \mathbb{R}^m$. Our proof consists of establishing that the function $V_3 : \mathbb{R}^n \times \mathbb{R}^m \rightarrow \mathbb{R}_{\geq 0}$,

$$V_3(x, z) = \frac{\beta_1}{2} \|X_{\text{sp}}(x, z)\|^2 + \frac{\beta_2}{2} \|(x, z)\|_{\text{Saddle}(F)}^2 \quad (8.20)$$

with $\beta_1 > 0$, $\beta_2 = \frac{4\beta_1 M^4}{m^2}$, is an ISS-Lyapunov function with respect to $\text{Saddle}(F)$ for X_{sp}^{p} . The statement then directly follows from Proposition 2.8.1.

We first show (2.14) for V_3 , that is, there exist $\alpha_1, \alpha_2 > 0$ such that $\alpha_1 \|(x, z)\|_{\text{Saddle}(F)}^2 \leq V_3(x, z) \leq \alpha_2 \|(x, z)\|_{\text{Saddle}(F)}^2$ for all $(x, z) \in \mathbb{R}^n \times \mathbb{R}^m$. The lower bound follows by choosing $\alpha_1 = \beta_2/2$. For the upper bound, define the

function $U : \mathbb{R}^n \times \mathbb{R}^n \rightarrow \mathbb{R}^{n \times n}$ by

$$U(x_1, x_2) = \int_0^1 \nabla^2 f(x_1 + s(x_2 - x_1)) ds. \quad (8.21)$$

By assumption, it holds that $mI \preceq U(x_1, x_2) \preceq MI$ for all $x_1, x_2 \in \mathbb{R}^n$. Also, from the fundamental theorem of calculus, we have $\nabla f(x_2) - \nabla f(x_1) = U(x_1, x_2)(x_2 - x_1)$ for all $x_1, x_2 \in \mathbb{R}^n$. Now pick any $(x, z) \in \mathbb{R}^n \times \mathbb{R}^m$. Let $(x_*, z_*) = \text{proj}_{\text{Saddle}(F)}(x, z)$, that is, the projection of (x, z) on the set $\text{Saddle}(F)$. This projection is unique as $\text{Saddle}(F)$ is convex. Then, one can write

$$\begin{aligned} \nabla_x F(x, z) &= \nabla_x F(x_*, z_*) + \int_0^1 \nabla_{xx} F(x(s), z(s))(x - x_*) ds \\ &\quad + \int_0^1 \nabla_{zx} F(x(s), z(s))(z - z_*) ds, \\ &= U(x_*, x)(x - x_*) + A^\top(z - z_*), \end{aligned} \quad (8.22)$$

where $x(s) = x_* + s(x - x_*)$ and $z(s) = z_* + s(z - z_*)$. Also, note that

$$\begin{aligned} \nabla_z F(x, z) &= \nabla_z F(x_*, z_*) + \int_0^1 \nabla_{xz} F(x(s), z(s))(x - x_*) ds \\ &= A(x - x_*). \end{aligned} \quad (8.23)$$

The expressions (8.22) and (8.23) use $\nabla_x F(x_*, z_*) = 0$, $\nabla_z F(x_*, z_*) = 0$, and $\nabla_{zx} F(x, z) = \nabla_{xz} F(x, z)^\top = A^\top$ for all (x, z) . From (8.22) and (8.23), we get

$$\|X_{\text{sp}}(x, z)\|^2 \leq \tilde{\alpha}_2(\|x - x_*\|^2 + \|z - z_*\|^2) = \tilde{\alpha}_2 \|(x, z)\|_{\text{Saddle}(F)}^2,$$

where $\tilde{\alpha}_2 = \frac{3}{2}(M^2 + \|A\|^2)$. In the above computation, we have used the inequality $(a + b)^2 \leq 3(a^2 + b^2)$ for any $a, b \in \mathbb{R}$. The above inequality gives the upper bound $V_3(x, z) \leq \alpha_2 \|(x, z)\|_{\text{Saddle}(F)}^2$, where $\alpha_2 = \frac{3\beta_1}{2}(M^2 + \|A\|^2) + \frac{\beta_2}{2}$.

The next step is to show that the Lie derivative of V_3 along the dynamics X_{sp}^p satisfies the ISS property (2.15). Again, pick any $(x, z) \in \mathbb{R}^n \times \mathbb{R}^m$ and let $(x_*, z_*) = \text{proj}_{\text{Saddle}(F)}(x, z)$. Then, by Danskin's Theorem [CLSW98, p. 99], we

get

$$\nabla \|(x, z)\|_{\text{Saddle}(F)}^2 = 2(x - x_*; z - z_*).$$

Using the above expression, one can compute the Lie derivative of V_3 along the dynamics X_{sp}^{P} as

$$\begin{aligned} \mathcal{L}_{X_{\text{sp}}^{\text{P}}} V_3(x, z) &= -\beta_1 \nabla_x F(x, z) \nabla_{xx} F(x, z) \nabla_x F(x, z) \\ &\quad - \beta_2 (x - x_*)^\top \nabla_x F(x, z) + \beta_2 (z - z_*)^\top \nabla_z F(x, z) \\ &\quad + \beta_1 \nabla_x F(x, z)^\top \nabla_{xx} F(x, z) u_x + \beta_1 \nabla_x F(x, z)^\top \nabla_{xz} F(x, z) u_z \\ &\quad + \beta_1 \nabla_z F(x, z)^\top \nabla_{zx} F(x, z) u_x + \beta_2 (x - x_*)^\top u_x + \beta_2 (z - z_*)^\top u_z. \end{aligned}$$

Due to the particular form of F , we have

$$\begin{aligned} \nabla_x F(x, z) &= \nabla f(x) + A^\top z, & \nabla_z F(x, z) &= Ax - b, \\ \nabla_{xx} F(x, z) &= \nabla^2 f(x), & \nabla_{xz} F(x, z) &= A^\top, \\ \nabla_{zx} F(x, z) &= A, & \nabla_{zz} F(x, z) &= 0. \end{aligned}$$

Also, $\nabla_x F(x_*, z_*) = \nabla_x f(x_*) + A^\top z_* = 0$ and $\nabla_z F(x_*, z_*) = Ax_* - b = 0$. Substituting these values in the expression of $\mathcal{L}_{X_{\text{sp}}^{\text{P}}} V_3$, replacing $\nabla_x F(x, z) = \nabla_x F(x, z) - \nabla_x F(x_*, z_*) = \nabla f(x) - \nabla f(x_*) + A^\top (z - z_*) = U(x_*, x)(x - x_*) + A^\top (z - z_*)$, and simplifying,

$$\begin{aligned} \mathcal{L}_{X_{\text{sp}}^{\text{P}}} V_3(x, z) &= -\beta_1 (U(x_*, x)(x - x_*) + A^\top (z - z_*))^\top \nabla^2 f(x) (U(x_*, x)(x - x_*)) \\ &\quad - \beta_1 (z - z_*)^\top A \nabla^2 f(x) A^\top (z - z_*) \\ &\quad - \beta_1 (U(x_*, x)(x - x_*) + A^\top (z - z_*))^\top \nabla^2 f(x) A^\top (z - z_*) \\ &\quad - \beta_1 (z - z_*)^\top A \nabla^2 f(x) (U(x_*, x)(x - x_*)) \\ &\quad - (x - x_*)^\top U(x_*, x)(x - x_*) \\ &\quad + \beta_1 (U(x_*, x)(x - x_*) + A^\top (z - z_*))^\top \nabla^2 f(x) u_x \\ &\quad + \beta_1 (U(x_*, x)(x - x_*) + A^\top (z - z_*))^\top A^\top u_z \\ &\quad + \beta_2 (x - x_*)^\top u_x + \beta_1 (A(x - x_*))^\top A u_x + \beta_2 (z - z_*)^\top u_z. \end{aligned}$$

Upper bounding now the terms using $\|\nabla^2 f(x)\|, \|U(x_*, x)\| \leq M$ for all $x \in \mathbb{R}^n$ yields

$$\begin{aligned} \mathcal{L}_{X_{\text{sp}}^{\text{p}}} V_3(x, z) &\leq -[x - x_*; A^\top(z - z_*)]^\top \bar{U}(x_*, x) [x - x_*; A^\top(z - z_*)] \\ &\quad + C_x(x, z) \|u_x\| + C_z(x, z) \|u_z\|, \end{aligned} \quad (8.24)$$

where

$$\begin{aligned} C_x(x, z) &= \left(\beta_1 M^2 \|x - x_*\| + \beta_1 M \|A\| \|z - z_*\| \right. \\ &\quad \left. + \beta_2 \|x - x_*\| + \beta_1 \|A\|^2 \|x - x_*\| \right), \\ C_z(x, z) &= \left(\beta_1 M \|A\| \|x - x_*\| + \beta_1 \|A\|^2 \|z - z_*\| \right. \\ &\quad \left. + \beta_2 \|z - z_*\| \right), \end{aligned}$$

and $\bar{U}(x_*, x)$ is

$$\begin{bmatrix} \beta_1 U \nabla^2 f(x) U + \beta_2 U & \beta_1 U \nabla^2 f(x) \\ \beta_1 \nabla^2 f(x) U & \beta_1 \nabla^2 f(x) \end{bmatrix}.$$

where $U = U(x_*, x)$. Note that $C_x(x, z) \leq \tilde{C}_x \|x - x_*; z - z_*\| = \tilde{C}_x \|(x, z)\|_{\text{Saddle}(F)}$ and $C_z(x, z) \leq \tilde{C}_z \|x - x_*; z - z_*\| = \tilde{C}_z \|(x, z)\|_{\text{Saddle}(F)}$, where

$$\begin{aligned} \tilde{C}_x &= \beta_1 M^2 + \beta_1 M \|A\| + \beta_2 + \beta_1 \|A\|^2, \\ \tilde{C}_z &= \beta_1 M \|A\| + \beta_1 \|A\|^2 + \beta_2. \end{aligned}$$

From Lemma 8.5.1, we have $\bar{U}(x_*, x) \succeq \lambda_m I$, where $\lambda_m > 0$. Employing these facts in (8.24), we obtain

$$\begin{aligned} \mathcal{L}_{X_{\text{sp}}^{\text{p}}} V_3(x, z) &\leq -\lambda_m (\|x - x_*\|^2 + \|A^\top(z - z_*)\|^2) \\ &\quad + (\tilde{C}_x + \tilde{C}_z) \|(x, z)\|_{\text{Saddle}(F)} \|u\| \end{aligned}$$

From Lemma 8.5.2, we get

$$\begin{aligned} \mathcal{L}_{X_{\text{sp}}^{\text{p}}} V_3(x, z) &\leq -\lambda_m(\|x - x_*\|^2 + \lambda_s(AA^\top)\|z - z_*\|^2) \\ &\quad + (\tilde{C}_x + \tilde{C}_z)\|(x, z)\|_{\text{Saddle}(F)}\|u\| \\ &\leq -\tilde{\lambda}_m\|(x, z)\|_{\text{Saddle}(F)}^2 \\ &\quad + (\tilde{C}_x + \tilde{C}_z)\|(x, z)\|_{\text{Saddle}(F)}\|u\|, \end{aligned}$$

where $\tilde{\lambda}_m = \lambda_m \min\{1, \lambda_s(AA^\top)\}$. Now pick any $\theta \in (0, 1)$. Then,

$$\begin{aligned} \mathcal{L}_{X_{\text{sp}}^{\text{p}}} V_3(x, z) &\leq -(1 - \theta)\tilde{\lambda}_m\|(x, z)\|_{\text{Saddle}(F)}^2 \\ &\quad - \theta\tilde{\lambda}_m\|(x, z)\|_{\text{Saddle}(F)}^2 \\ &\quad + (\tilde{C}_x + \tilde{C}_z)\|(x, z)\|_{\text{Saddle}(F)}\|u\| \\ &\leq -(1 - \theta)\tilde{\lambda}_m\|(x, z)\|_{\text{Saddle}(F)}^2, \end{aligned}$$

whenever $\|(x, z)\|_{\text{Saddle}(F)} \geq \frac{\tilde{C}_x + \tilde{C}_z}{\theta\tilde{\lambda}_m}\|u\|$, which proves the ISS property. \square

Remark 8.4.2. (*Relaxing global bounds on Hessian of f*): The assumption on the Hessian of f in Theorem 8.4.1 is restrictive, but there are functions other than quadratic that satisfy it, see e.g. [KCM15a, Section 6]. We conjecture that the global upper bound on the Hessian can be relaxed by resorting to the notion of semiglobal ISS, and we will explore this in the future. \bullet

The above result has the following consequence.

Corollary 8.4.3. (*Lyapunov function for saddle-point dynamics*): *Let the saddle function F be of the form (8.17), with f strongly convex, twice continuously differentiable, and satisfying $mI \preceq \nabla^2 f(x) \preceq MI$ for all $x \in \mathbb{R}^n$ and some constants $0 < m \leq M < \infty$. Then, the function V_3 (8.20) is a Lyapunov function with respect to the set $\text{Saddle}(F)$ for the saddle-point dynamics (8.18).*

Remark 8.4.4. (*ISS with respect to $\text{Saddle}(F)$ does not imply bounded trajectories*): Note that Theorem 8.4.1 bounds only the distance of the trajectories of (8.19) to $\text{Saddle}(F)$. Thus, if $\text{Saddle}(F)$ is unbounded, the trajectories of (8.19) can be

unbounded under arbitrarily small constant disturbances. However, if matrix A has full row-rank, then $\text{Saddle}(F)$ is a singleton and the ISS property implies that the trajectory of (8.19) remains bounded under bounded disturbances. •

As pointed out in the above remark, if $\text{Saddle}(F)$ is not unique, then the trajectories of the dynamics might not be bounded. We next look at a particular type of disturbance input which guarantees bounded trajectories even when $\text{Saddle}(F)$ is unbounded. Pick any $(x_*, z_*) \in \text{Saddle}(F)$ and define the function $\tilde{V}_3 : \mathbb{R}^n \times \mathbb{R}^m \rightarrow \mathbb{R}_{\geq 0}$ as

$$\tilde{V}_3(x, z) = \frac{\beta_1}{2} \|X_{\text{sp}}(x, z)\|^2 + \frac{\beta_2}{2} (\|x - x_*\|^2 + \|z - z_*\|^2)$$

with $\beta_1 > 0$, $\beta_2 = \frac{4\beta_1 M^4}{m^2}$. One can show, following similar steps as those of proof of Theorem 8.4.1, that the function \tilde{V}_3 is an ISS Lyapunov function with respect to the point (x_*, z_*) for the dynamics X_{sp}^{p} when the disturbance input to z -dynamics has the special structure $u_z = A\tilde{u}_z$, $\tilde{u}_z \in \mathbb{R}^n$. This type of disturbance is motivated by scenarios with measurement errors in the values of x and z used in (8.18) and without any computation error of the gradient term in the z -dynamics. The following statement makes precise the ISS property for this particular disturbance.

Corollary 8.4.5. (*ISS of saddle-point dynamics*): *Let the saddle function F be of the form (8.17), with f strongly convex, twice continuously differentiable, and satisfying $mI \preceq \nabla^2 f(x) \preceq MI$ for all $x \in \mathbb{R}^n$ and some constants $0 < m \leq M < \infty$. Then, the dynamics*

$$\begin{bmatrix} \dot{x} \\ \dot{z} \end{bmatrix} = \begin{bmatrix} -\nabla_x F(x, z) \\ \nabla_z F(x, z) \end{bmatrix} + \begin{bmatrix} u_x \\ A\tilde{u}_z \end{bmatrix}, \quad (8.25)$$

where $(u_x, \tilde{u}_z) : \mathbb{R}_{\geq 0} \rightarrow \mathbb{R}^{2n}$ is measurable and locally essentially bounded input, is ISS with respect to every point of $\text{Saddle}(F)$.

The proof is analogous to that of Theorem 8.4.1 with the key difference that the terms $C_x(x, z)$ and $C_z(x, z)$ appearing in (8.24) need to be upper bounded in terms of $\|x - x_*\|$ and $\|A^\top(z - z_*)\|$. This can be done due to the special structure

of u_z . With these bounds, one arrives at the condition (2.15) for Lyapunov \tilde{V}_3 and dynamics (8.25). One can deduce from Corollary 8.4.5 that the trajectory of (8.25) remains bounded for bounded input even when $\text{Saddle}(F)$ is unbounded.

Example 8.4.6. (*ISS property of saddle-point dynamics*): Consider $F : \mathbb{R}^2 \times \mathbb{R}^2 \rightarrow \mathbb{R}$ of the form (8.17) with

$$f(x) = x_1^2 + (x_2 - 2)^2, \quad (8.26)$$

$$A = \begin{bmatrix} 1 & -1 \\ -1 & 1 \end{bmatrix}, \text{ and } b = \begin{bmatrix} 0 \\ 0 \end{bmatrix}.$$

Then, $\text{Saddle}(F) = \{(x, z) \in \mathbb{R}^2 \times \mathbb{R}^2 \mid x = (1, 1), z = (0, 2) + \lambda(1, 1), \lambda \in \mathbb{R}\}$ is a continuum of points. Note that $\nabla^2 f(x) = 2I$, thus, satisfying the assumption of bounds on the Hessian of f . By Theorem 8.4.1, the saddle-point dynamics for this saddle function F is input-to-state stable with respect to the set $\text{Saddle}(F)$. This fact is illustrated in Figure 8.2, which also depicts how the specific structure of the disturbance input in (8.25) affects the boundedness of the trajectories. •

Remark 8.4.7. (*Quadratic ISS-Lyapunov function*): For the saddle-point dynamics (8.18), the ISS property stated in Theorem 8.4.1 and Corollary 8.4.5 can also be shown using a quadratic Lyapunov function. Let $V_4 : \mathbb{R}^n \times \mathbb{R}^m \rightarrow \mathbb{R}_{\geq 0}$ be

$$V_4(x, z) = \frac{1}{2} \|(x, z)\|_{\text{Saddle}(F)}^2 + \epsilon(x - x_p)^\top A^\top (z - z_p),$$

where $(x_p, z_p) = \text{proj}_{\text{Saddle}(F)}(x, z)$ and $\epsilon > 0$. Then, one can show that there exists $\epsilon_{\max} > 0$ such that V_4 for any $\epsilon \in (0, \epsilon_{\max})$ is an ISS-Lyapunov function for the dynamics (8.18). •

8.4.2 Self-triggered implementation

In this section we develop an opportunistic state-triggered implementation of the (continuous-time) saddle-point dynamics. Our aim is to provide a discrete-time execution of the algorithm, either on a physical system or as an optimization strategy, that do not require the continuous evaluation of the vector field and

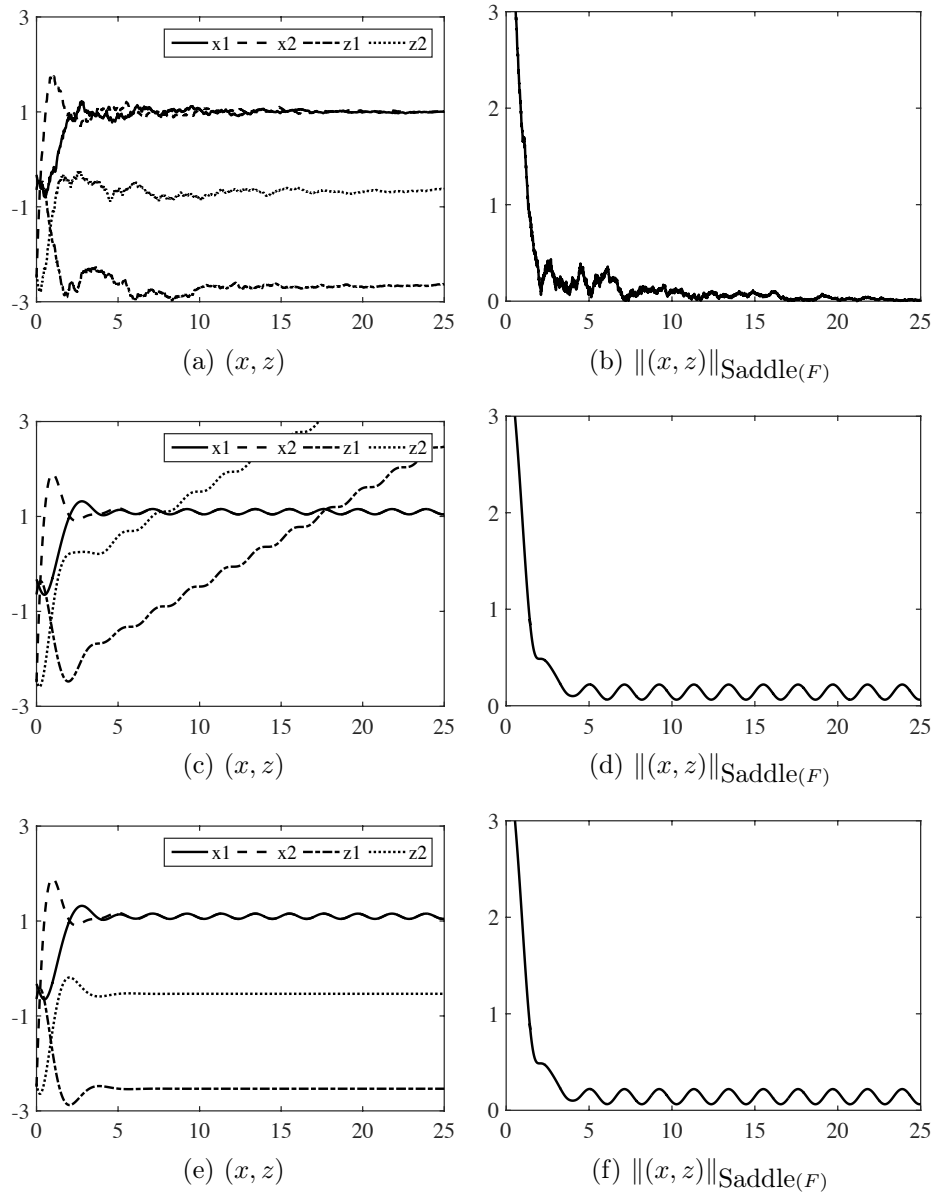


Figure 8.2: Plots (a)-(b) show the ISS property, cf. Theorem 8.4.1, of the dynamics (8.19) for the saddle function F defined by (8.26). The initial condition is $x(0) = (-0.3254, -2.4925)$ and $z(0) = (-0.6435, -2.4234)$ and the input u is exponentially decaying in magnitude. As shown in (a)-(b), the trajectory converges asymptotically to a saddle point as the input is vanishing. Plots (c)-(d) have the same initial condition but the disturbance input consists of a constant plus a sinusoid. The trajectory is unbounded under bounded input while the distance to the set of saddle points remains bounded, cf. Remark 8.4.4. Plots (e)-(f) have the same initial condition but the disturbance input to the z -dynamics is of the form (8.25). In this case, the trajectory remains bounded as the dynamics is ISS with respect to each saddle point, cf. Corollary 8.4.5.

instead adjust the stepsize based on the current state of the system. Formally, given a sequence of triggering time instants $\{t_k\}_{k=0}^\infty$, with $t_0 = 0$, we consider the following implementation of the saddle-point dynamics

$$\dot{x}(t) = -\nabla_x F(x(t_k), z(t_k)), \quad (8.27a)$$

$$\dot{z}(t) = \nabla_z F(x(t_k), z(t_k)). \quad (8.27b)$$

for $t \in [t_k, t_{k+1})$ and $k \in \mathbb{Z}_{\geq 0}$. The objective is then to design a criterium to opportunistically select the sequence of triggering instants, guaranteeing at the same time the feasibility of the execution and global asymptotic convergence, see e.g., [HJT12]. Towards this goal, we look at the evolution of the Lyapunov function V_3 in (8.20) along (8.27),

$$\begin{aligned} & \nabla V_3(x(t), z(t))^\top X_{\text{sp}}(x(t_k), z(t_k)) \\ &= \mathcal{L}_{X_{\text{sp}}} V_3(x(t_k), z(t_k)) \\ &+ \left(\nabla V_3(x(t), z(t)) - \nabla V_3(x(t_k), z(t_k)) \right)^\top X_{\text{sp}}(x(t_k), z(t_k)). \end{aligned} \quad (8.28)$$

We know from Corollary 8.4.3 that the first summand is negative outside $\text{Saddle}(F)$. Clearly, for $t = t_k$, the second summand vanishes, and by continuity, for t sufficiently close to t_k , this summand remains smaller in magnitude than the first, ensuring the decrease of V_3 . To make this argument precise, we employ Proposition 8.5.3 in (8.28) and obtain

$$\begin{aligned} \nabla V_3(x(t), z(t))^\top X_{\text{sp}}(x(t_k), z(t_k)) &\leq \mathcal{L}_{X_{\text{sp}}} V_3(x(t_k), z(t_k)) + \xi(x(t_k), z(t_k)) \\ &\quad \| (x(t) - x(t_k)); (z(t) - z(t_k)) \| \| X_{\text{sp}}(x(t_k), z(t_k)) \| \\ &= \mathcal{L}_{X_{\text{sp}}} V_3(x(t_k), z(t_k)) \\ &\quad + (t - t_k) \xi(x(t_k), z(t_k)) \| X_{\text{sp}}(x(t_k), z(t_k)) \|^2, \end{aligned}$$

where the equality follows from writing $(x(t), z(t))$ in terms of $(x(t_k), z(t_k))$ by integrating (8.27). Therefore, in order to ensure the monotonic decrease of V_3 , we

require the above expression to be nonpositive. That is,

$$t_{k+1} \leq t_k - \frac{\mathcal{L}_{X_{\text{sp}}} V_3(x(t_k), z(t_k))}{\xi(x(t_k), z(t_k)) \|X_{\text{sp}}(x(t_k), z(t_k))\|^2}. \quad (8.29)$$

Note that to set t_{k+1} equal to the right-hand side of the above expression, one needs to compute the Lie derivative at $(x(t_k), z(t_k))$. We then distinguish between two possibilities. If the self-triggered saddle-point dynamics acts as a closed-loop physical system and its equilibrium points are known, then computing the Lie derivative is feasible and one can use (8.29) to determine the triggering times. If, however, the dynamics is employed to seek the primal-dual optimizers of an optimization problem, then computing the Lie derivative is infeasible as it requires knowledge of the optimizer. To overcome this limitation, we propose the following alternative triggering criterium which satisfies (8.29) as shown later in our convergence analysis,

$$t_{k+1} = t_k + \frac{\tilde{\lambda}_m}{3(M^2 + \|A\|^2)\xi(x(t_k), z(t_k))}, \quad (8.30)$$

where $\tilde{\lambda}_m = \lambda_m \min\{1, \lambda_s(AA^\top)\}$, λ_m is given in Lemma 8.5.1, and $\lambda_s(AA^\top)$ is the smallest nonzero eigenvalue of AA^\top . In either (8.29) or (8.30), the right-hand side depends only on the state $(x(t_k), z(t_k))$. These triggering times for the dynamics (8.27) define a first-order Euler discretization of the saddle-point dynamics with step-size selection based on the current state of the system. It is for this reason that we refer to (8.27) together with either the triggering criterium (8.29) or (8.30) as the *self-triggered saddle-point dynamics*. In integral form, this dynamics results in a discrete-time implementation of (8.18) given as

$$\begin{bmatrix} x(t_{k+1}) \\ z(t_{k+1}) \end{bmatrix} = \begin{bmatrix} x(t_k) \\ z(t_k) \end{bmatrix} + (t_{k+1} - t_k) X_{\text{sp}}(x(t_k), z(t_k)).$$

Note that this dynamics can also be regarded as a state-dependent switched system with a single continuous mode and a reset map that updates the sampled state at the switching times, cf. [Lib03]. We understand the solution of (8.27) in the

Caratheodory sense (note that this dynamics has a discontinuous right-hand side). The existence of such solutions, possibly defined only on a finite time interval, is guaranteed from the fact that along any trajectory of the dynamics there are only countable number of discontinuities encountered in the vector field. The next result however shows that solutions of (8.27) exist over the entire domain $[0, \infty)$ as the difference between consecutive triggering times of the solution is lower bounded by a positive constant. Also, it establishes the asymptotic convergence of solutions to the set of saddle points.

Theorem 8.4.8. *(Convergence of the self-triggered saddle-point dynamics): Let the saddle function F be of the form (8.17), with A having full row rank, f strongly convex, twice differentiable, and satisfying $mI \preceq \nabla^2 f(x) \preceq MI$ for all $x \in \mathbb{R}^n$ and some constants $0 < m \leq M < \infty$. Let the map $x \mapsto \nabla^2 f(x)$ be Lipschitz with some constant $L > 0$. Then, $\text{Saddle}(F)$ is singleton. Let $\text{Saddle}(F) = \{(x_*, z_*)\}$. Then, for any initial condition $(x(0), z(0)) \in \mathbb{R}^n \times \mathbb{R}^m$, we have*

$$\lim_{k \rightarrow \infty} (x(t_k), z(t_k)) = (x_*, z_*)$$

for the solution of the self-triggered saddle-point dynamics, defined by (8.27) and (8.30), starting at $(x(0), z(0))$. Further, there exists $\mu_{(x(0), z(0))} > 0$ such that the triggering times of this solution satisfy

$$t_{k+1} - t_k \geq \mu_{(x(0), z(0))}, \quad \text{for all } k \in \mathbb{Z}_{\geq 1}.$$

Proof. Note that there is a unique equilibrium point to the saddle-point dynamics (8.18) for F satisfying the stated hypotheses. Therefore, the set of saddle point is singleton for this F . Now, given $(x(0), z(0)) \in \mathbb{R}^n \times \mathbb{R}^m$, let $V_3^0 = V_3(x(0), z(0))$ and define

$$G = \max\{\|\nabla_x F(x, z)\| \mid (x, z) \in V_3^{-1}(\leq V_3(V_3^0))\},$$

where, we use the notation for the sublevel set of V_3 as

$$V_3^{-1}(\leq V_3(\alpha)) = \{(x, z) \in \mathbb{R}^n \times \mathbb{R}^m \mid V_3(x, z) \leq \alpha\}$$

for any $\alpha \geq 0$. Since V_3 is radially unbounded, the set $V_3^{-1}(\leq V_3(V_3^0))$ is compact and so, G is well-defined and finite. If the trajectory of the self-triggered saddle-point dynamics is contained in $V_3^{-1}(\leq V_3(V_3^0))$, then we can bound the difference between triggering times in the following way. From Proposition 8.5.3 for all $(x, z) \in V_3^{-1}(\leq V_3(V_3^0))$, we have $\xi_1(x, z) = M\xi_2 + L\|\nabla_x F(x, z)\| \leq M\xi_2 + LG =: T_1$. Hence, for all $(x, z) \in V_3^{-1}(\leq V_3(V_3^0))$, we get

$$\begin{aligned} \xi(x, z) &= \left(\beta_1^2(\xi_1(x, z))^2 + \|A\|^4 + \|A\|^2\xi_2^2 + \beta_2^2 \right)^{\frac{1}{2}} \\ &\leq \left(\beta_1^2(T_1^2 + \|A\|^4 + \|A\|^2 + \xi_2^2) + \beta_2^2 \right)^{\frac{1}{2}} \\ &=: T_2. \end{aligned}$$

Using the above bound in (8.30), we get for all $k \in \mathbb{Z}_{\geq 1}$

$$\begin{aligned} t_{k+1} - t_k &= \frac{\tilde{\lambda}_m}{3(M^2 + \|A\|^2)\xi(x(t_k), z(t_k))} \\ &\geq \frac{\tilde{\lambda}_m}{3(M^2 + \|A\|^2)T_2} > 0. \end{aligned}$$

This implies that as long as the trajectory is contained in $V_3^{-1}(\leq V_3(V_3^0))$, the inter-trigger times are lower bounded by a positive quantity. Our next step is to show that the trajectory is contained in $V_3^{-1}(\leq V_3(V_3^0))$. Note that if (8.29) is satisfied for the triggering condition (8.30), then the sequence $\{V_3(x(t_k), z(t_k))\}_{k \in \mathbb{Z}_{\geq 1}}$ is strictly decreasing. Since V_3 is nonnegative, this implies that $\lim_{k \rightarrow \infty} V_3(x(t_k), z(t_k)) = 0$ and so, by continuity, $\lim_{k \rightarrow \infty} (x(t_k), z(t_k)) = (x_*, z_*)$. Thus, it remains to show that (8.30) implies (8.29). To this end, first note the following inequalities shown in the proof of Theorem 8.4.1

$$\frac{\|X_{\text{sp}}(x, z)\|^2}{3(M^2 + \|A\|^2)} \leq \|(x - x_*); (z - z_*)\|^2, \quad (8.31a)$$

$$|\mathcal{L}_{X_{\text{sp}}} V_3(x, z)| \geq \tilde{\lambda}_m \|(x - x_*); (z - z_*)\|^2. \quad (8.31b)$$

Using these bounds, we get from (8.30)

$$\begin{aligned} t_{k+1} - t_k &= \frac{\tilde{\lambda}_m}{3(M^2 + \|A\|^2)\xi(x(t_k), z(t_k))} \\ &\stackrel{(a)}{=} \frac{\tilde{\lambda}_m \|X_{\text{sp}}(x(t_k), z(t_k))\|^2}{3(M^2 + \|A\|^2)\xi(x(t_k), z(t_k))\|X_{\text{sp}}(x(t_k), z(t_k))\|^2} \\ &\stackrel{(b)}{\leq} \frac{\tilde{\lambda}_m \|(x(t_k) - x_*); (z(t_k) - z_*)\|^2}{\xi(x(t_k), z(t_k))\|X_{\text{sp}}(x(t_k), z(t_k))\|^2} \\ &\stackrel{(c)}{\leq} \frac{|\mathcal{L}_{X_{\text{sp}}} V_3(x(t_k), z(t_k))|}{\xi(x(t_k), z(t_k))\|X_{\text{sp}}(x(t_k), z(t_k))\|^2} \\ &= -\frac{\mathcal{L}_{X_{\text{sp}}} V_3(x(t_k), z(t_k))}{\xi(x(t_k), z(t_k))\|X_{\text{sp}}(x(t_k), z(t_k))\|^2}, \end{aligned}$$

where (a) is valid as $\|X_{\text{sp}}(x(t_k), z(t_k))\| \neq 0$, (b) follows from (8.31a), and (c) follows from (8.31b). Thus, (8.30) implies (8.29) which completes the proof. \square

Note from the above proof that the convergence implication of Theorem 8.4.8 is also valid when the triggering criterium is given by (8.29) with the inequality replaced by the equality.

Example 8.4.9. (*Self-triggered saddle-point dynamics*): Consider the function $F : \mathbb{R}^3 \times \mathbb{R} \rightarrow \mathbb{R}$,

$$F(x, z) = \|x\|^2 + z(x_1 + x_2 + x_3 - 1). \quad (8.32)$$

Then, with the notation of (8.17), we have $f(x) = \|x\|^2$, $A = [1, 1, 1]$, and $b = 1$. The set of saddle points is a singleton, $\text{Saddle}(F) = \{((\frac{1}{3}, \frac{1}{3}, \frac{1}{3}), -\frac{2}{3})\}$. Note that $\nabla^2 f(x) = 2I$ and A has full row-rank, thus, the hypotheses of Theorem 8.4.8 are met. Hence, for this F , the self-triggered saddle-point dynamics (8.27) with triggering times (8.30) converges asymptotically to the saddle point of F . Moreover, the difference between two consecutive triggering times is lower bounded by a finite quantity. Figure 8.3 illustrates a simulation of dynamics (8.27) with triggering criteria (8.29) (replacing inequality with equality), showing that this triggering criteria also ensures convergence as commented above. Finally, Figure 8.4 compares

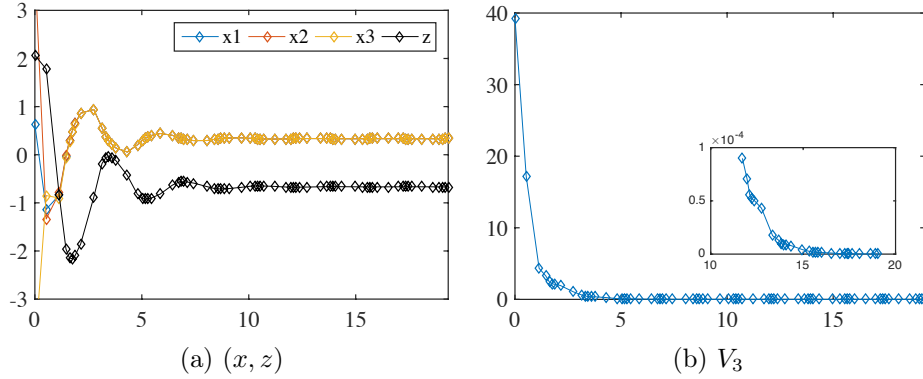


Figure 8.3: Illustration of the self-triggered saddle-point dynamics defined by (8.27) with the triggering criterium (8.29). The saddle function F is defined in (8.32). With respect to the notation of Theorem 8.4.8, we have $m = M = 2$ and $\|A\| = \sqrt{3}$. We select $\beta_1 = 0.1$, then $\beta_2 = 1.6$, and from (8.35), $\xi_1 = 2$. These constants define functions V_3 (cf. (8.20)), ξ , and ξ_2 (cf. (8.35)) and also, the triggering times (8.30). In plot (a), the initial condition is $x(0) = (0.6210, 3.9201, -4.0817)$, $z(0) = 2.0675$. The trajectory converges to the unique saddle-point and the inter-trigger times are lower bounded by a positive quantity.

the self-triggered implementation of the saddle-point dynamics with a constant-stepsize and a decaying-stepsize first-order Euler discretization. In both cases, the the self-triggered dynamics achieves convergence faster, and this may be attributed to the fact that it tunes the stepsize in a state-dependent way. •

8.5 Auxiliary results

Here we collect a couple of supporting results used in the proof of Theorem 8.4.1.

Lemma 8.5.1. (Auxiliary result for Theorem 8.4.1: I): Let $B_1, B_2 \in \mathbb{R}^{n \times n}$ be symmetric matrices satisfying $mI \preceq B_1, B_2 \preceq MI$ for some $0 < m \leq M < \infty$. Let $\beta_1 > 0$, $\beta_2 = \frac{4\beta_1 M^4}{m^2}$, and $\lambda_m = \min\{\frac{1}{2}\beta_1 m, \beta_1 m^3\}$. Then,

$$W := \begin{bmatrix} \beta_1 B_1 B_2 B_1 + \beta_2 B_1 & \beta_1 B_1 B_2 \\ \beta_1 B_2 B_1 & \beta_1 B_2 \end{bmatrix} \succ \lambda_m I.$$

Proof. Reasoning with Schur complement [BV09, Section A.5.5], the expression

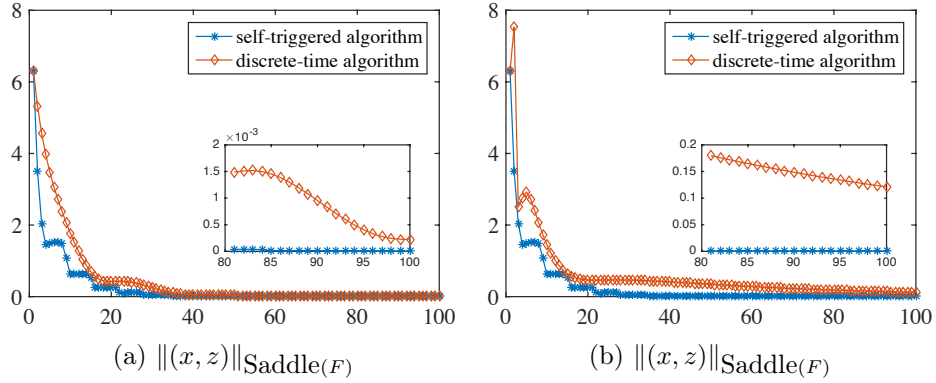


Figure 8.4: Comparison between the self-triggered saddle-point dynamics and a first-order Euler discretization of the saddle-point dynamics with two different stepsize rules. The initial condition and implementation details are the same as in Figure 8.3. Both plots show the evolution of the distance to the saddle point, compared in (a) against a constant-stepsize implementation with value 0.1 and in (b) against a decaying-stepsize implementation with value $1/k$ at the k -th iteration. The self-triggered dynamics converges faster in both cases.

$W - \lambda_m I \succ 0$ holds if and only if the following hold

$$\begin{aligned}
 & \beta_1 B_1 B_2 B_1 + \beta_2 B_1 - \lambda_m I \succ 0, \\
 & \beta_1 B_2 - \lambda_m I - \\
 & \beta_1 B_2 B_1 (\beta_1 B_1 B_2 B_1 + \beta_2 B_1 - \lambda_m I)^{-1} \beta_1 B_1 B_2 \succ 0.
 \end{aligned} \tag{8.33}$$

The first of the above inequalities is true since $\beta_1 B_1 B_2 B_1 + \beta_2 B_1 - \lambda_m I \succeq \beta_1 m^3 I + \beta_2 m I - \lambda_m I \succ 0$ as $\lambda_m \leq \beta_1 m^3$. For the second inequality note that

$$\begin{aligned}
 & \beta_1 B_2 - \lambda_m I \\
 & - \beta_1 B_2 B_1 (\beta_1 B_1 B_2 B_1 + \beta_2 B_1 - \lambda_m I)^{-1} \beta_1 B_1 B_2 \\
 & \succeq (\beta_1 m - \lambda_m) I \\
 & - \beta_1^2 M^4 \lambda_{\max} \left((\beta_1 B_1 B_2 B_1 + \beta_2 B_1 - \lambda_m I)^{-1} \right) I \\
 & \succeq \left(\frac{1}{2} \beta_1 m - \frac{\beta_1^2 M^4}{\lambda_{\min}(\beta_1 B_1 B_2 B_1 + \beta_2 B_1 - \lambda_m I)} \right) I,
 \end{aligned}$$

where in the last inequality we have used the fact that $\lambda_m \leq \beta_1 m/2$. Note that $\lambda_{\min}(\beta_1 B_1 B_2 B_1 + \beta_2 B_1 - \lambda_m I) \geq \beta_1 m^3 + \beta_2 m - \lambda_m \geq \beta_2 m$. Using this lower

bound, the following holds

$$\frac{1}{2}\beta_1 m - \frac{\beta_1^2 M^4}{\lambda_{\min}(\beta_1 B_1 B_2 B_1 + \beta_2 B_1 - \lambda_m I)} \geq \frac{1}{2}\beta_1 m - \frac{\beta_1^2 M^4}{\beta_2 m} = \frac{1}{4}\beta_1 m.$$

The above set of inequalities show that the second inequality in (8.33) holds, which concludes the proof. \square

Lemma 8.5.2. (Auxiliary result for Theorem 8.4.1: II): *Let F be of the form (8.17) with f strongly convex. Let $(x, z) \in \mathbb{R}^n \times \mathbb{R}^m$ and $(x_*, z_*) = \text{proj}_{\text{Saddle}(F)}(x, z)$. Then, $z - z_*$ is orthogonal to the kernel of A^\top , and*

$$\|A^\top(z - z_*)\|^2 \geq \lambda_s(AA^\top)\|z - z_*\|^2,$$

where $\lambda_s(AA^\top)$ is the smallest nonzero eigenvalue of AA^\top .

Proof. Our first step is to show that there exists $x_* \in \mathbb{R}^n$ such that if $(x, z) \in \text{Saddle}(F)$, then $x = x_*$. By contradiction, assume that $(x_1, z_1), (x_2, z_2) \in \text{Saddle}(F)$ and $x_1 \neq x_2$. The saddle point property at (x_1, z_1) and (x_2, z_2) yields

$$F(x_1, z_1) \leq F(x_2, z_1) \leq F(x_2, z_2) \leq F(x_1, z_2) \leq F(x_1, z_1).$$

This implies that $F(x_1, z_1) = F(x_2, z_1)$, which is a contradiction as $x \mapsto F(x, z_1)$ is strongly convex and x_1 is a minimizer of this map. Therefore, $\text{Saddle}(F) = \{x_*\} \times \mathcal{Z}$, $\mathcal{Z} \subset \mathbb{R}^m$. Further, recall that the set of saddle points of F are the set of equilibrium points of the saddle point dynamics (8.18). Hence, $(x_*, z) \in \text{Saddle}(F)$ if and only if

$$\nabla f(x_*) + A^\top z = 0.$$

We conclude from this that

$$\mathcal{Z} = -(A^\top)^\dagger \nabla f(x_*) + \ker(A^\top), \quad (8.34)$$

where $(A^\top)^\dagger$ and $\ker(A^\top)$ are the Moore-Penrose pseudoinverse [BV09, Section A.5.4] and the kernel of A^\top , respectively. By definition of the projection operator,

if $(x_*, z_*) = \text{proj}_{\text{Saddle}(F)}(x, z)$, then $z_* = \text{proj}_{\mathcal{Z}}(z)$ and so, from (8.34), we deduce that $(z - z_*)^\top v = 0$ for all $v \in \ker(A^\top)$. Using this fact, we conclude the proof by writing

$$\|A^\top(z - z_*)\|^2 = (z - z_*)^\top AA^\top(z - z_*) \geq \lambda_s(AA^\top)\|z - z_*\|^2,$$

where the inequality follows by writing the eigenvalue decomposition of AA^\top , expanding the quadratic expression in $(z - z_*)$, and lower-bounding the terms. \square

Proposition 8.5.3. (*Gradient of V_3 is locally Lipschitz*): *Let the saddle function F be of the form (8.17), with f twice differentiable, map $x \mapsto \nabla^2 f(x)$ Lipschitz with some constant $L > 0$, and $mI \preceq \nabla^2 f(x) \preceq MI$ for all $x \in \mathbb{R}^n$ and some constants $0 < m \leq M < \infty$. Then, for V_3 given in (8.20), the following holds*

$$\|\nabla V_3(x_2, z_2) - \nabla V_3(x_1, z_1)\| \leq \xi(x_1, z_1)\|x_2 - x_1; z_2 - z_1\|,$$

for all $(x_1, z_1), (x_2, z_2) \in \mathbb{R}^n \times \mathbb{R}^m$, where

$$\begin{aligned} \xi(x_1, z_1) &= \sqrt{3} \left(\beta_1^2 (\xi_1(x_1, z_1))^2 + \|A\|^4 + \|A\|^2 \xi_2^2 + \beta_2^2 \right)^{\frac{1}{2}}, \\ \xi_1(x_1, z_1) &= M\xi_2 + L\|\nabla_x F(x_1, z_1)\|, \\ \xi_2 &= \max\{M, \|A\|\}. \end{aligned} \tag{8.35}$$

Proof. For the map $(x, z) \mapsto \nabla_x F(x, z)$, note that

$$\begin{aligned} &\|\nabla_x F(x_2, z_2) - \nabla_x F(x_1, z_1)\| \\ &= \left\| \int_0^1 \nabla_{xx} F(x(s), z(s))(x_2 - x_1) ds \right. \\ &\quad \left. + \int_0^1 \nabla_{zx} F(x(s), z(s))(z_2 - z_1) ds \right\| \\ &\leq M\|x_2 - x_1\| + \|A\|\|z_2 - z_1\| \\ &\leq \xi_2\|x_2 - x_1; z_2 - z_1\|, \end{aligned} \tag{8.36}$$

where $x(s) = x_1 + s(x_2 - x_1)$, $z(s) = z_1 + s(z_2 - z_1)$ and $\xi_2 = \max\{M, \|A\|\}$. In

the above inequalities we have used the fact that $\|\nabla_{xx}F(x, z)\| = \|\nabla^2 f(x)\| \leq M$ for any (x, z) . Further, the following Lipschitz condition holds by assumption

$$\|\nabla_{xx}F(x_2, z_2) - \nabla_{xx}F(x_1, z_1)\| \leq L\|x_2 - x_1\| \quad (8.37)$$

Using (8.36) and (8.37), we get

$$\begin{aligned} & \|\nabla_{xx}F(x_2, z_2)\nabla_xF(x_2, z_2) - \nabla_{xx}F(x_1, z_1)\nabla_xF(x_1, z_1)\| \\ & \leq \|\nabla_{xx}F(x_2, z_2)(\nabla_xF(x_2, z_2) - \nabla_xF(x_1, z_1))\| \\ & \quad + \|(\nabla_{xx}F(x_2, z_2) - \nabla_{xx}F(x_1, z_1))\nabla_xF(x_1, z_1)\| \\ & \leq \xi_1(x_1, z_1)\|x_2 - x_1; z_2 - z_1\|, \end{aligned} \quad (8.38)$$

where $\xi_1(x_1, z_1) = M\xi_2 + L\|\nabla_xF(x_1, z_1)\|$. Also,

$$\begin{aligned} \|\nabla_zF(x_2, z_2) - \nabla_zF(x_1, z_1)\| &= \|A(x_2 - x_1)\| \\ &\leq \|A\|\|x_2 - x_1; z_2 - z_1\| \end{aligned} \quad (8.39)$$

Now note that

$$\begin{aligned} \nabla_xV_3(x, z) &= \beta_1\left(\nabla_{xx}F(x, z)\nabla_xF(x, z) + A^\top\nabla_zF(x, z)\right) \\ &\quad + \beta_2(x - x_*), \\ \nabla_zV_3(x, z) &= \beta_1A\nabla_xF(x, z) + \beta_2(z - z_*). \end{aligned}$$

Finally, using (8.36), (8.38), and (8.39), we get

$$\begin{aligned} & \|\nabla V_3(x_2, z_2) - \nabla V_3(x_1, z_1)\|^2 = \|\nabla_xV_3(x_2, z_2) \\ & \quad - \nabla_xV_3(x_1, z_1)\|^2 + \|\nabla_zV_3(x_2, z_2) - \nabla_zV_3(x_1, z_1)\|^2 \\ & \stackrel{(a)}{\leq} 3\beta_1^2\|\nabla_{xx}F(x_2, z_2)\nabla_xF(x_2, z_2) \\ & \quad - \nabla_{xx}F(x_1, z_1)\nabla_xF(x_1, z_1)\|^2 \\ & \quad + 3\beta_1^2\|A^\top(\nabla_zF(x_2, z_2) - \nabla_zF(x_1, z_1))\|^2 + 3\beta_2^2\|x_2 - x_1\|^2 \\ & \quad + 3\beta_1^2\|A(\nabla_xF(x_2, z_2) - \nabla_xF(x_1, z_1))\|^2 + 3\beta_2^2\|z_2 - z_1\|^2 \end{aligned}$$

$$\leq \xi(x_1, z_1)^2 \|x_2 - x_1; z_2 - z_1\|^2,$$

where in (a), we have used the inequality $(a + b)^2 \leq 3(a^2 + b^2)$ for any $a, b \in \mathbb{R}$. This concludes the proof. \square

Acknowledgments

This chapter is taken, in part, from the work [CMLC16a] submitted as “The role of convexity in saddle-point dynamics: Lyapunov function and robustness” by A. Cherukuri, E. Mallada, S. Low, and J. Cortés, to the IEEE Transactions on Automatic Control, as well as [CMLC16b] where it appears as “The role of strong convexity- concavity in the convergence and robustness of the saddle-point dynamics” by A. Cherukuri, E. Mallada, S. Low, and J. Cortés in the proceedings of the 2016 Annual Allerton Conference on Communication, Control, and Computing. The dissertation author was the primary investigator and author of these papers. This research was partly supported by the US National Science Foundation (NSF) Award ECCS-1307176 and the ARPA-e Cooperative Agreement DE-AR0000695.

Chapter 9

Iterative bidding in markets

In this chapter, we focus on the competition aspect among the aggregators. We use the term generators and aggregators alternatively. We study policies that individual generators, in conjunction with the ISO, can implement to solve the OPF problem while acting in a selfish and rational fashion.

9.1 Problem statement

Consider an electrical power network with $N_b \in \mathbb{Z}_{\geq 1}$ buses. The physical interconnection between the buses is given by a digraph $\mathcal{G} = (\mathcal{V}, \mathcal{E})$, where nodes correspond to buses and edges to physical power lines. The direction for each edge represents the convention of positive power flow. The power flow on the line $(i, j) \in \mathcal{E}$ is $z_{ij} \in \mathbb{R}$. Each line $(i, j) \in \mathcal{E}$ has a limit on the power flowing through it (in either direction), represented by $\bar{z}_{ij} > 0$. Assume that each bus $i \in [N_b]$ is connected to $n_i \in \mathbb{Z}_{\geq 0}$ strategic generators. We let $N = \sum_{i=1}^{N_b} n_i$ be the total number of generators and assign them a unique identity in $[N]$. Let the set of generators at node i be $G_i \subset [N]$ (this set is empty if there are no generators connected to bus i). The power demand at bus i is denoted by $y_i \geq 0$ and is assumed to be fixed and known to the Independent System Operator (ISO) that acts as the central regulating authority. The total demand is $\bar{y} = \sum_{i=1}^{N_b} y_i$. The cost $f_n(x_n)$ of generating $x_n \in \mathbb{R}_{\geq 0}$ amount of power by the n -th generator is given

by a quadratic function

$$f_n(x) = a_n x^2 + c_n x, \quad (9.1)$$

where $a_n > 0$ and $c_n \geq 0$. Given a power allocation $x = (x_1, \dots, x_N) \in \mathbb{R}_{\geq 0}^N$, the aggregate cost is $\sum_{n=1}^N f_n(x_n)$. The *dc optimal power flow problem* (DC-OPF) consists of

$$\underset{(x,z)}{\text{minimize}} \quad \sum_{n=1}^N f_n(x_n), \quad (9.2a)$$

$$\text{subject to} \quad \sum_{j \in \mathcal{N}_i^+} z_{ij} - \sum_{j \in \mathcal{N}_i^-} z_{ij} = \sum_{n \in G_i} x_n - y_i, \forall i, \quad (9.2b)$$

$$- \bar{z}_{ij} \leq z_{ij} \leq \bar{z}_{ij}, \quad \forall (i, j), \quad (9.2c)$$

$$x \geq \mathbf{0}_N. \quad (9.2d)$$

This problem finds the generation profile that meets the load at each bus (ensured by (9.2b)), respects the line constraints (due to (9.2c)), and minimizes the total cost (given by the objective function (9.2a)). In (9.2b) we make the convention that if $G_i = \emptyset$, then the first term on the right-hand side is zero. We assume that (9.2) is feasible. Since the individual costs are quadratic, the optimizer of the problem, denoted (x^*, z^*) , is unique [BV04].

The goal for the ISO is to solve (9.2). The ISO can interact with the generators, whereas each generator can only communicate with the ISO and is not aware of the number of other generators participating in the market and their respective cost functions, or the load at its own bus. While the ISO knows the loads and the limits on the power lines, it does not have any information about the cost functions of the generators. Therefore, power allocation is decided following a bidding process, resulting into a game-theoretic formulation. Instead of sharing their cost with the ISO, the generators bid the price per unit of power that they are willing to provide the power at. This price-based bidding is well known in the economics literature as Bertrand competition [MCWG95, Chapter 12]. Specifically, generator n bids the cost per unit power $b_n \in \mathbb{R}_{\geq 0}$ and, when convenient, we denote

the bids of all other generators except n by $b_{-n} = (b_1, \dots, b_{n-1}, b_{n+1}, \dots, b_N)$. Given the bids $b = (b_1, \dots, b_N) \in \mathbb{R}_{\geq 0}^N$, the ISO solves the following *strategic dc optimal power flow problem* (S-DC-OPF)

$$\underset{(x,z)}{\text{minimize}} \quad \sum_{n=1}^N b_n x_n, \quad (9.3a)$$

$$\text{subject to} \quad \sum_{j \in \mathcal{N}_i^+} z_{ij} - \sum_{j \in \mathcal{N}_i^-} z_{ij} = \sum_{n \in G_i} x_n - y_i, \quad \forall i, \quad (9.3b)$$

$$-\bar{z}_{ij} \leq z_{ij} \leq \bar{z}_{ij}, \quad \forall (i, j), \quad (9.3c)$$

$$x \geq \mathbf{0}_N. \quad (9.3d)$$

The difference between (9.3) and (9.2) is the objective function which is linear in the former and nonlinear, convex in the latter. The ISO solves (9.3) once all the bids are gathered. Let $(x^{\text{opt}}(b), z^{\text{opt}}(b))$ be the optimizer of (9.3) that the ISO selects (note that there might not be a unique optimizer) given bids b . This determines the power requested from each generator, given by the vector $x^{\text{opt}}(b)$. Knowing this process, the objective of each generator n is to bid a quantity $b_n \geq 0$ that maximizes its payoff $u_n : \mathbb{R}_{\geq 0}^2 \rightarrow \mathbb{R}$,

$$u_n(b_n, x_n^{\text{opt}}(b)) = b_n x_n^{\text{opt}}(b) - f_n(x_n^{\text{opt}}(b)), \quad (9.4)$$

where $x_n^{\text{opt}}(b)$ is the n -th component of the optimizer $x^{\text{opt}}(b)$.

Definition 9.1.1. (*Inelastic electricity market game*): The *inelastic electricity market game* is defined by the following

- (i) Players: the set of generators $[N]$,
- (ii) Action: for each player n , the bid $b_n \in \mathbb{R}_{\geq 0}$,
- (iii) Payoff: for each player n , the payoff u_n in (9.4).

Wherever convenient, for any $n \in [N]$, we use interchangeably the notation b and (b_n, b_{-n}) , as well as, $x^{\text{opt}}(b)$ and $x^{\text{opt}}(b_n, b_{-n})$. Note that the payoff of the players is not only defined by the bids of other players but also by the optimizer

of (9.3) that the ISO selects. For this reason, the definition of the pure Nash equilibrium for the game described below is slightly different from the standard one, see e.g. [FT91].

Definition 9.1.2. (*Nash equilibrium*): The (*pure*) *Nash equilibrium* of the inelastic electricity market game is the bid profile of the group $b^* \in \mathbb{R}_{\geq 0}^N$ for which there exists an optimizer $(x^{\text{opt}}(b^*), z^{\text{opt}}(b^*))$ of the optimization (9.3) that satisfies

$$u_n(b_n, x_n^{\text{opt}}(b_n, b_{-n}^*)) \leq u_n(b_n^*, x_n^{\text{opt}}(b^*)), \quad (9.5)$$

for all $n \in [N]$, all bids $b_n \in \mathbb{R}_{\geq 0}$, and all optimizers $(x^{\text{opt}}(b_n, b_{-n}^*), z^{\text{opt}}(b_n, b_{-n}^*))$ of (9.3) given bids (b_n, b_{-n}^*) .

We are specifically interested in bid profiles for which the optimizer of the DC-OPF problem is also a solution to the S-DC-OPF problem. This is captured in the following definition.

Definition 9.1.3. (*Efficient bid*): An *efficient bid* of the inelastic electricity market is a bid $b^* \in \mathbb{R}_{\geq 0}^N$ for which the optimizer (x^*, z^*) of (9.2) is also an optimizer of (9.3) given bids b^* and

$$x_n^* = \operatorname{argmax}_{x \geq 0} b_n^* x - f_n(x), \quad \text{for all } n \in [N]. \quad (9.6)$$

The right-hand side of (9.6) is unique as costs are quadratic.

Definition 9.1.4. (*Efficient Nash equilibrium*): A bid b^* is an *efficient Nash equilibrium* of the inelastic electricity market game if it is an efficient bid and is a Nash equilibrium.

At the efficient Nash equilibrium, the production that the generators are willing to provide, maximizing their profit, coincides with the optimal generation for the DC-OPF problem (9.2). This property justifies the study of efficient Nash equilibria. Note that given the efficient bid profile, there might be many solutions to (9.3) because the problem is linear. Thus, the ISO might not be able to find x^* given the efficient bid. However, once the ISO knows that an efficient Nash

equilibrium bid is submitted, it can ask the generators to also submit the desirable generation levels at that bid, which would exactly correspond to the solution of the DC-OPF problem.

9.2 Existence and uniqueness of efficient Nash equilibrium

Here, we establish the existence of an efficient Nash equilibrium of the inelastic electricity market game described in Section 9.1 and provide a condition for its uniqueness.

Proposition 9.2.1. (*Existence of efficient Nash equilibrium*): *Assume that at each bus of the network either there is more than one generator or there is none, i.e., either $n_i = 0$ or $n_i \geq 2$ for each $i \in [N_b]$. Then, there exists an efficient Nash equilibrium of the inelastic electricity market game.*

Proof. For convenience, we write (9.2b) and (9.2c) as

$$J_1 z - J_2 x + y = 0 \quad \text{and} \quad J_3 z \leq \bar{z}_c,$$

respectively. Here, $J_1 \in \{0, 1, -1\}^{N_b \times N_b}$ defines the interconnection of buses in the digraph \mathcal{G} , specifically, (i, j) -th element of J_1 is 1 if $(i, j) \in \mathcal{E}$, is -1 if $(j, i) \in \mathcal{E}$, and 0 otherwise. The matrix $J_2 \in \{0, 1\}^{N_b \times N}$ defines the connectivity of generators to buses, that is, (i, j) -th element of J_2 is 1 if and only if j -th generator is connected to i -th bus. Lastly,

$$J_3 = \begin{bmatrix} I_{|\mathcal{E}|} \\ -I_{|\mathcal{E}|} \end{bmatrix} \quad \text{and} \quad \bar{z}_c = \begin{bmatrix} \bar{z} \\ \bar{z} \end{bmatrix}.$$

The Lagrangian of the optimization (9.2) is

$$\begin{aligned} L(x, z, \nu, \mu, \lambda) &= \sum_{n=1}^N f_n(x_n) + \nu^\top (J_1 z - J_2 x + y) \\ &\quad + \mu^\top (J_3 z - \bar{z}_c) - \lambda^\top x, \end{aligned}$$

where $\nu \in \mathbb{R}^{N_b}$, $\mu \in \mathbb{R}_{\geq 0}^{2|\mathcal{E}|}$, and $\lambda \in \mathbb{R}_{\geq 0}^N$ are Lagrange multipliers corresponding to constraints (9.2b), (9.2c), and (9.2d), respectively. Since constraints (9.2b)-(9.2c) are affine and the feasibility set is nonempty, the refined Slater condition is satisfied for (9.2) and hence, the duality gap between the primal and the dual optimization problems is zero [BV04]. Under this condition, a primal-dual optimizer $(x^*, z^*, \nu^*, \mu^*, \lambda^*)$ satisfies the following Karush-Kuhn-Tucker (KKT) conditions

$$\nabla f(x^*) - J_2^\top \nu^* - \lambda^* = 0, \quad (9.7a)$$

$$J_1^\top \nu^* - J_3^\top \mu^* = 0, \quad (9.7b)$$

$$J_1 z^* - J_2 x^* + y = 0, \quad (9.7c)$$

$$J_3 z^* \leq \bar{z}_c, \quad x^* \geq 0, \quad (9.7d)$$

$$\lambda^* \geq 0, \quad \mu^* \geq 0, \quad (9.7e)$$

$$(x^*)^\top \lambda^* = 0, \text{ and } (\mu^*)^\top (J_3 z^* - \bar{z}_c) = 0, \quad (9.7f)$$

where $\nabla f(x^*) = (\nabla f_1(x_1^*), \nabla f_2(x_2^*), \dots, \nabla f_N(x_N^*))^\top$. In the rest of the proof, we show that the following bid profile, constructed from a primal-dual optimizer, is an efficient Nash equilibrium of the inelastic electricity market game

$$b_n^* = \begin{cases} \nu_{i(n)}^*, & \text{if } \min\{x_m^* \mid m \in G_{i(n)}\} > 0, \\ \nabla f_n(0), & \text{otherwise,} \end{cases} \quad (9.8)$$

where $i(n) \in [N_b]$ denotes the bus of the network to which generator n is connected to. Given the form (9.1) of the cost functions, we deduce $b^* \geq 0$. Moreover, from the definition of J_2 , one can deduce that either all generators $n \in G_i$ have $b_n^* = \nu_i$ or all of them have $x_n^* = 0$. Next, to show that the bid b^* defined in (9.8) is efficient, we first establish

$$x_n^* = \operatorname{argmax}_{x \geq 0} b_n^* x - f_n(x), \quad (9.9)$$

for all $n \in [N]$. For each n , consider the optimization $\max_{x \geq 0} b_n^* x - f_n(x)$. Because zero duality holds for this optimization, a point $x_o \in \mathbb{R}_{\geq 0}$ is an optimizer if and

only if it satisfies the KKT conditions

$$\begin{aligned} b_n^* - \nabla f_n(x_o) - \mu_o &= 0, \\ \mu_o \geq 0, \quad x_o \geq 0, \quad \mu_o x_o &= 0, \end{aligned}$$

where μ_o is the dual optimizer. Since x_n^* satisfies the above conditions with $\mu_o = \lambda_n^*$, the expression (9.9) holds. To claim the efficiency of b^* , we next show that (x^*, z^*) is one of the optimizers of (9.3) given bids b^* . Note that the KKT conditions for (9.3) are given by (9.7) with the term $\nabla f(x^*)$ in (9.7a) replaced with b^* . Also, one can show using the KKT conditions (9.7) and the definition of b^* that $b^* - J_2^\top \nu^* \geq 0$. Using these facts, we deduce that $(x^*, z^*, \nu^*, \mu^*, b^* - J_2^\top \nu^*)$ satisfies the KKT conditions for (9.3) and hence, (x^*, z^*) is an optimizer of (9.3).

Our final step is to show the Nash equilibrium condition (9.5) for the bid profile b^* . Note that for each n , the payoff at the bid profile-optimizer pair $(b^*, x^{\text{opt}}(b^*)) = (b^*, x^*)$ is nonnegative. Specifically, if $x_n^* = 0$, then $u_n(b_n^*, x_n^{\text{opt}}(b^*)) = 0$. If $x_n^* > 0$, using the fact that $\nabla f_n(x) \leq b_n^*$ for all $x \in [0, x_n^*]$, we get

$$\begin{aligned} u_n(b_n^*, x_n^{\text{opt}}(b^*)) &= b_n^* x_n^* - f_n(x_n^*) \\ &= \int_0^{x_n^*} \nabla(b_n^* x - f_n(x)) dx \\ &= \int_0^{x_n^*} (b_n^* - \nabla f_n(x)) dx \geq 0. \end{aligned}$$

Now pick any generator $n \in [N]$. For bid $b_n \neq b_n^*$ we have two cases, first, $b_n > b_n^*$ and second, $b_n \leq b_n^*$. For the first case, either (i) $x_n^* = 0$ which implies that $x^{\text{opt}}(b_n, b_{-n}^*) = 0$ and so $u_n(b_n, x_n^{\text{opt}}(b_n, b_{-n}^*)) = u_n(b_n^*, x_n^*) = 0$; or (ii) $x_n^* > 0$, so all bids at bus $i(n)$ are equal, implying that n increasing its bid yields $x_n^{\text{opt}}(b_n, b_{-n}^*) = 0$. That is, $u_n(b_n, x_n^{\text{opt}}(b_n, b_{-n}^*)) = 0 \leq u_n(b_n^*, x_n^*)$. For the second case,

$$\begin{aligned} u_n(b_n, x_n^{\text{opt}}(b_n, b_{-n}^*)) &= b_n x_n^{\text{opt}}(b_n, b_{-n}^*) - f_n(x_n^{\text{opt}}(b_n, b_{-n}^*)) \\ &\leq b_n^* x_n^{\text{opt}}(b_n, b_{-n}^*) - f_n(x_n^{\text{opt}}(b_n, b_{-n}^*)) \end{aligned}$$

$$\leq b_n^* x_n^* - f_n(x_n^*) = u_n(b_n^*, x_n^*),$$

where in the first inequality we use $b_n \leq b_n^*$ and in the second we use (9.9). This shows (9.5), concluding the proof. \square

Note that the condition in Proposition 9.2.1 of having zero or at least two generators at each bus is reasonable. If this is not the case, i.e., there is a bus with a single generator, and the line capacities are such that the load at that bus can only be met by that generator, then there is possibility of market manipulation. The generator at the bus can set its bid arbitrarily high as no other generator can meet that load and consequently, there does not exist a Nash equilibrium. Next we provide a sufficient condition that ensures uniqueness of the efficient bid.

Lemma 9.2.2. *(Uniqueness of the efficient bid): Assume that the optimizer x^* of (9.2) satisfies $x_n^* > 0$ for all $n \in [N]$. Then, there exists a unique efficient bid $b^* \in \mathbb{R}_{\geq 0}^N$ of the inelastic electricity market game given by*

$$b_n^* = \nabla f_n(x_n^*) = 2a_n x_n^* + c_n, \quad \text{for all } n \quad (9.10)$$

Proof. By definition, an efficient bid $b \in \mathbb{R}_{\geq 0}^N$ satisfies

$$x_n^* = \operatorname{argmax}_{x \geq 0} b_n x - f_n(x)$$

for all n . Since $x_n^* > 0$, first-order optimality condition of the above optimization yields $b_n = \nabla f_n(x_n^*)$. This establishes (9.10) and hence, the uniqueness. \square

From Proposition 9.2.1 and Lemma 9.2.2, we conclude the following result.

Corollary 9.2.3. *(Uniqueness of the efficient Nash equilibrium): Assume that at each bus of the network either there is more than one generator or there is none. Further assume that the optimizer x^* of (9.2) satisfies $x_n^* > 0$ for all $n \in [N]$. Then, there exists a unique efficient Nash equilibrium of the inelastic electricity market game given by (9.10) for all n .*

In the rest of the paper, we assume that the sufficient conditions in Corollary 9.2.3 hold unless otherwise stated. Note that the definition of the unique efficient Nash equilibrium given in (9.10) is consistent with the one provided in (9.8). This is so because if $x_n^* > 0$ for all n , then $\nabla f_{\tilde{n}}(x_{\tilde{n}}^*) = \nu_i^*$ for each bus $i \in [N_b]$ and every generator $\tilde{n} \in G_i$.

9.3 The BID ADJUSTMENT ALGORITHM and its convergence properties

In this section, we introduce a decentralized Nash equilibrium seeking algorithm, termed BID ADJUSTMENT ALGORITHM. We show that its executions lead the generators to the unique efficient Nash equilibrium, and consequently, to the optimizer of the DC-OPF problem (9.2).

9.3.1 BID ADJUSTMENT ALGORITHM

We start with an informal description of the BID ADJUSTMENT ALGORITHM. The algorithm is iterative and can be interpreted as “learning via repeated play” of the inelastic electricity market game by the generators. Both ISO and generators have bounded rationality, with each generator trying to maximize its own profit and the ISO trying to maximize the welfare of the entities.

[Informal description]: At each iteration k , generators decide on a bid and send it to the ISO. Once the ISO has obtained the bids, it computes an optimizer of the S-DC-OPF problem (9.3), denoted $(x^{\text{opt}}(k), z^{\text{opt}}(k))$ for convenience, and sends the corresponding production level at the optimizer to each generator. At the $(k + 1)$ -th iteration, generators adjust their bid based on their previous bid, the amount of produced power that maximizes their payoff for the previous bid, and the allocation of generation assigned by the ISO. The iterative process starts with the generators arbitrarily selecting initial bids that yield a positive profit.

The BID ADJUSTMENT ALGORITHM is formally presented in Algorithm 3.

Algorithm 3: BID ADJUSTMENT ALGORITHM

Executed by: generators $n \in [N]$ and ISO

Data : cost f_n and stepsizes $\{\beta_k\}_{k \in \mathbb{Z}_{\geq 1}}$ for each generator n , and load y for ISO

Initialize : Each generator n selects arbitrarily $b_n(1) \geq c_n$, sets $k = 1$, and jumps to step 4; ISO sets $k = 1$ and waits for step 6

```

1 while  $k > 0$  do
    /* For each generator  $n$ : */
2   Receive  $x_n^{\text{opt}}(k-1)$  from ISO
3   Set  $b_n(k) = [b_n(k-1) + \beta_k(x_n^{\text{opt}}(k-1) - q_n(k-1))]^+$ 
4   Set  $q_n(k) = \operatorname{argmax}_{q \geq 0} b_n(k)q - f_n(q)$ 
5   Send  $b_n(k)$  to the ISO; set  $k = k + 1$ 
    /* For ISO: */
6   Receive  $b_n(k)$  from each  $n \in [N]$ 
7   Find a solution  $(x^{\text{opt}}(k), z^{\text{opt}}(k))$  to (9.3) given  $b(k)$ 
8   Send  $x_n^{\text{opt}}(k)$  to each  $n \in [N]$ ; set  $k = k + 1$ 
9 end

```

In the BID ADJUSTMENT ALGORITHM, the role of the ISO is to compute an optimizer of the S-DC-OPF problem after the bids are submitted. Generators adjust their bids at each iteration in a “myopically selfish” and rational fashion, with the sole aim of maximizing their payoff. Intuitively,

- **if n gets $x_n^{\text{opt}}(k) = 0$:** two things can happen: (i) n was willing to produce a positive quantity $q_n(k) > 0$ at bid $b_n(k)$ but the demand from the ISO is $x_n^{\text{opt}}(k) = 0$. Thus, the rational choice for n is to decrease the bid in the next iteration and increase its chances of getting a positive payoff; (ii) n was willing to produce nothing $q_n(k) = 0$ at $b_n(k)$ and got $x_n^{\text{opt}}(k) = 0$. At this point, reducing the bid will not increase the payoff as it will not be willing to produce more at a lower bid. Alternatively, increasing the bid will not make the amount that the ISO wants the generator to produce positive. Hence, the bid stays put.
- **if n gets $x_n^{\text{opt}}(k) > 0$:** then it would want to move the bid in the direction that makes its payoff higher in the next iteration, assuming that n gets a positive generation signal from the ISO in the next round. If $q_n(k) < x_n^{\text{opt}}(k)$,

then the demand from the ISO is more than what the generator is willing to produce, so n increases its cost, i.e., the bid. If $q_n(k) > x_n^{\text{opt}}(k)$, then the demand is less than what the generator is willing to supply so n decreases its bid.

Remark 9.3.1. (*Information structure and other learning approaches*): Generators have no knowledge of the number of other players, their actions, or their payoffs. The only information they have at each iteration is their own bid and the generation that the ISO requests from them. This information structure rules out the applicability of a number of Nash equilibrium learning methods, including best-response dynamics [BGJ10], fictitious play [FL98], or other gradient-based adjustments [BCKS10], all requiring some kind of information about other players. Methods that relax this requirement, such as extremum seeking used in [FKB12, SJS12], rely on the payoff functions being continuous in the actions of the players, which is not the case for the inelastic electricity market game. •

Remark 9.3.2. (*Stopping criteria and justification of “myopically selfish” strategies*): Algorithm 3 consists of an infinite number of iterations. To make it implementable, later we identify stopping criteria, see Remark 9.3.9, based on a parameter that the ISO selects. Since this is not known to the generators, they cannot predict when the algorithm will terminate and, hence, they do not have an incentive to play strategically to maximize their payoff in the long term. Given this, they should focus on maximizing the payoff in the next iteration, which justifies the myopically selfish perspective adopted here. •

9.3.2 Convergence analysis

In this section, we show that the generator bids along any execution of the BID ADJUSTMENT ALGORITHM converge to a neighborhood of the unique efficient Nash equilibrium. The size of the neighborhood is a decreasing function of the stepsize and can be made arbitrarily small.

We first present a series of results that highlight certain geometric properties of the bid update done in Step 3 of Algorithm 3. These results form the basis for

establishing later the convergence guarantee. The following result states that one could neglect the projection operator in Step 3 of Algorithm 3.

Lemma 9.3.3. (*Generator bids are lower bounded*): *In Algorithm 3, let $0 < \beta_k < 2a_n$ for all $n \in [N]$ and $k \in \mathbb{Z}_{\geq 1}$. Then, $b_n(k) \geq c_n$ and for all $n \in [N]$ and $k \in \mathbb{Z}_{\geq 1}$,*

$$q_n(k) = \frac{b_n(k) - c_n}{2a_n}. \quad (9.11)$$

Proof. Equation (9.11) follows directly from $b_n(k) \geq c_n$, so we focus on proving the latter. We proceed by induction. Note that $b_n(1) \geq c_n$ for all $n \in [N]$. Assume that $b_n(k) \geq c_n$ for some $k \in \mathbb{Z}_{\geq 1}$ and let us show $b_n(k+1) \geq c_n$. We have

$$\begin{aligned} b_n(k+1) &= [b_n(k) + \beta_k(x_n^{\text{opt}}(k) - q_n(k))]^+ \\ &\stackrel{(a)}{\geq} [b_n(k) - \beta_k q_n(k)]^+ \stackrel{(b)}{=} \left[b_n(k) - \beta_k \left(\frac{b_n(k) - c_n}{2a_n} \right) \right]^+ \\ &= \left[\left(1 - \frac{\beta_k}{2a_n} \right) b_n(k) + \beta_k \frac{c_n}{2a_n} \right]^+ \\ &\stackrel{(c)}{=} \left(1 - \frac{\beta_k}{2a_n} \right) b_n(k) + \beta_k \frac{c_n}{2a_n}, \end{aligned}$$

where (a) is due to the fact that $x_n^{\text{opt}}(k) \geq 0$, (b) follows from the definition of $q_n(k)$ given the fact that $b_n(k) \geq c_n$, and (c) follows from the assumption that $\beta_k < 2a_n$ for all n (which makes both terms in the expression positive). By contradiction, assume $b_n(k+1) < c_n$. Then,

$$\left(1 - \frac{\beta_k}{2a_n} \right) b_n(k) + \beta_k \frac{c_n}{2a_n} < c_n,$$

which implies that $b_n(k) < c_n$, a contradiction. \square

Our next result gives a different expression for the bid update step (cf. Step 3) presenting a geometric perspective of the direction along which the bids are moving. Specifically, we write the $k+1$ -th bid as the addition of two vectors. The first one is a convex combination of the k -th bid and the efficient Nash equilibrium b^* . Hence, the first vector is closer to b^* as compared to the k -th bid. The second

one depends on the difference between what the ISO requests from the generators and the optimizer of (9.2). If the second term is small enough, then we are assured that the bids move towards b^* .

Lemma 9.3.4. *(Geometric characterization of the bid update): In Algorithm 3, let $0 < \beta_k < 2a_n$ for all $n \in [N]$ and $k \in \mathbb{Z}_{\geq 1}$. Then, we have*

$$b(k+1) = b^{\text{coc}}(k+1) + \beta_k(x^{\text{opt}}(k) - x^*),$$

for all $k \in \mathbb{Z}_{\geq 1}$, where for each $n \in [N]$,

$$b_n^{\text{coc}}(k+1) = \left(1 - \frac{\beta_k}{2a_n}\right)b_n(k) + \frac{\beta_k}{2a_n}b_n^*.$$

Proof. In the proof of Lemma 9.3.3, we have shown that for all n and k , the term inside the projection operator $[\cdot]^+$ in Step 3 of Algorithm 3 is nonnegative. Hence, the projection can be dropped and we can write

$$\begin{aligned} b_n(k+1) &= b_n(k) + \beta_k(x_n^{\text{opt}}(k) - q_n(k)) \\ &\stackrel{(a)}{=} b_n(k) + \beta_k(x_n^{\text{opt}}(k)) - \beta_k\left(\frac{b_n(k) - c_n}{2a_n}\right) \\ &= \left(1 - \frac{\beta_k}{2a_n}\right)b_n(k) + \beta_k\left(x_n^{\text{opt}}(k) + \frac{c_n}{2a_n}\right) \\ &= \left(1 - \frac{\beta_k}{2a_n}\right)b_n(k) + \beta_k(x_n^{\text{opt}}(k) - x_n^*) + \beta_k\left(x_n^* + \frac{c_n}{2a_n}\right) \\ &\stackrel{(b)}{=} \left(1 - \frac{\beta_k}{2a_n}\right)b_n(k) + \frac{\beta_k}{2a_n}b_n^* + \beta_k(x_n^{\text{opt}}(k) - x_n^*). \end{aligned}$$

In the above expression, we have used (9.11) in the equality (a) and (9.10) in the equality (b). \square

The next result gives a lower bound on the inner product between the direction in which the bids move and the direction towards the efficient Nash equilibrium.

Lemma 9.3.5. *(Bids move in the direction of the efficient Nash equilibrium): In Algorithm 3, let $0 < \beta_k < 2a_n$ for all $n \in [N]$ and $k \in \mathbb{Z}_{\geq 1}$. Let $a_{\max} = \max_n \{a_n\}$.*

Then, for all $k \in \mathbb{Z}_{\geq 1}$,

$$\langle b(k+1) - b(k), b^* - b(k) \rangle \geq \frac{\beta_k}{2a_{\max}} \|b(k) - b^*\|^2. \quad (9.12)$$

Proof. Using Lemma 9.3.4, we write

$$\begin{aligned} & \langle b(k+1) - b(k), b^* - b(k) \rangle \\ &= \langle b(k+1) - b^{\text{coc}}(k+1), b^* - b(k) \rangle + \langle b^{\text{coc}}(k+1) - b(k), b^* - b(k) \rangle \\ &= \beta_k \langle x^{\text{opt}}(k) - x^*, b^* - b(k) \rangle + \sum_{n=1}^N \frac{\beta_k}{2a_n} (b_n^* - b_n(k))^2 \\ &\stackrel{(a)}{\geq} \sum_{n=1}^N \frac{\beta_k}{2a_n} (b_n^* - b_n(k))^2 \geq \frac{\beta_k}{2a_{\max}} \|b(k) - b^*\|^2. \end{aligned}$$

For the inequality (a), we have used the fact that

$$\begin{aligned} \langle x^{\text{opt}}(k) - x^*, b^* - b(k) \rangle &= (\langle x^{\text{opt}}(k), b^* \rangle - \langle x^*, b^* \rangle) \\ &\quad + (\langle x^*, b(k) \rangle - \langle x^{\text{opt}}(k), b(k) \rangle) \geq 0. \end{aligned}$$

The last inequality follows from the fact that x^* and $x^{\text{opt}}(k)$ are the optimizers of (9.3) given b^* and $b(k)$, resp., making both expressions on the right-hand side nonnegative. \square

The next result states that the distance between consecutive bids decreases as the bids get closer to b^* . In combination with Lemma 9.3.5, one can see intuitively that the bids get closer to b^* and, as they get closer to it, the bid update step behaves as if the bids are reaching an equilibrium of the update scheme. These two facts lead to convergence.

Lemma 9.3.6. (*Distance between consecutive bids is upper bounded*): *In Algorithm 3, let $0 < \beta_k < 2a_n$ for all $n \in [N]$ and $k \in \mathbb{Z}_{\geq 1}$. Let $a_{\min} = \min_n \{a_n\}$. Then, for all $k \in \mathbb{Z}_{\geq 1}$,*

$$\|b(k+1) - b(k)\|^2 \leq \frac{\beta_k^2}{2a_{\min}^2} \|b(k) - b^*\|^2 + 8\beta_k^2 \bar{y}^2. \quad (9.13)$$

Proof. Consider the following

$$\begin{aligned}
\|b(k+1) - b(k)\|^2 &\stackrel{(a)}{=} \sum_{n=1}^N \left(\frac{\beta_k}{2a_n} (b_n^* - b_n(k)) + \beta_k (x_n^{\text{opt}}(k) - x_n^*) \right)^2 \\
&\stackrel{(b)}{\leq} \sum_{n=1}^N 2 \left(\frac{\beta_k}{2a_n} (b_n^* - b_n(k)) \right)^2 + \sum_{n=1}^N 2\beta_k^2 (x_n^{\text{opt}}(k) - x_n^*)^2 \\
&\stackrel{(c)}{\leq} \frac{\beta_k^2}{2a_{\min}^2} \|b(k) - b^*\|^2 + 2\beta_k^2 \|x^{\text{opt}}(k) - x^*\|^2. \tag{9.14}
\end{aligned}$$

In the above expression, (a) follows from the expression of $b_n(k+1)$ from Lemma 9.3.4, (b) follows from the inequality $(x+y)^2 \leq 2(x^2+y^2)$ for $x, y \in \mathbb{R}$, and (c) follows from the definition of a_{\min} . Note that

$$\begin{aligned}
\|x^{\text{opt}}(k) - x^*\| &\leq \sum_{n=1}^N |x_n^{\text{opt}}(k) - x_n^*| \leq \sum_{n=1}^N |x_n^{\text{opt}}(k)| + |x_n^*| \\
&= \sum_{n=1}^N (x_n^{\text{opt}}(k) + x_n^*) = 2\bar{y}.
\end{aligned}$$

The proof concludes by using the above bound in (9.14). \square

We are ready to present the main convergence result.

Theorem 9.3.7. (*Convergence of the BID ADJUSTMENT ALGORITHM*): *In Algorithm 3, let $0 < \beta_k < 2a_n$ for all $n \in [N]$ and $k \in \mathbb{Z}_{\geq 1}$. Further, let $0 < r < \|b(1) - b^*\|$ and for all $k \in \mathbb{Z}_{\geq 1}$ assume*

$$\alpha \leq \beta_k \leq B(r) := \frac{1}{2a_{\max}} \left(\frac{1}{2a_{\min}^2} + \frac{16\bar{y}^2}{r^2} \right)^{-1}, \tag{9.15}$$

for some $\alpha > 0$. Then, the following holds

(i) *there exists $l \in \mathbb{Z}_{\geq 1}$ such that $\|b(l) - b^*\| < r$ and for all $k \in [l-1]$, we have $\|b(k) - b^*\| \geq r$ with*

$$\|b(k+1) - b^*\| \leq \left(1 - \frac{\alpha}{2a_{\max}} \right)^{k/2} \|b(1) - b^*\|, \tag{9.16}$$

(ii) for all $k \geq l$,

$$\|b(k) - b^*\| \leq \left(1 + \frac{B(r)}{2a_{\max}}\right)^{1/2} r. \quad (9.17)$$

Proof. Assume that $\|b(k) - b^*\| \geq r$ for some $k \in \mathbb{Z}_{\geq 1}$. Then, the upper bound on the stepsizes in the inequality (9.15) holds when r is replaced with $\|b(k) - b^*\|$, that is, $\beta_k \leq B(\|b(k) - b^*\|)$ for all $k \in \mathbb{Z}_{\geq 1}$. This is because $r \mapsto B(r)$ is strictly increasing in the domain $r > 0$. Proceeding with this replacement and reordering (9.15), we obtain

$$\beta_k \left(\frac{\|b(k) - b^*\|^2}{2a_{\min}^2} + 16\bar{y}^2 \right) \leq \frac{1}{2a_{\max}} \|b(k) - b^*\|^2,$$

or equivalently,

$$\frac{\beta_k}{2a_{\min}^2} \|b(k) - b^*\|^2 + 16\beta_k \bar{y}^2 - \frac{1}{a_{\max}} \|b(k) - b^*\|^2 \leq -\frac{1}{2a_{\max}} \|b(k) - b^*\|^2. \quad (9.18)$$

Now consider the following inequalities

$$\begin{aligned} \|b(k+1) - b^*\|^2 &= \|b(k+1) - b(k) + b(k) - b^*\|^2 \\ &= \|b(k+1) - b(k)\|^2 + \|b(k) - b^*\|^2 \end{aligned} \quad (9.19a)$$

$$+ 2\langle b(k+1) - b(k), b(k) - b^* \rangle$$

$$\stackrel{(a)}{\leq} \frac{\beta_k^2}{2a_{\min}^2} \|b(k) - b^*\|^2 + 8\beta_k^2 \bar{y}^2 + \|b(k) - b^*\|^2$$

$$- \frac{\beta_k}{a_{\max}} \|b(k) - b^*\|^2 \quad (9.19b)$$

$$\stackrel{(b)}{\leq} \left(1 - \frac{\beta_k}{2a_{\max}}\right) \|b(k) - b^*\|^2, \quad (9.19c)$$

where in (a) we have used the bounds (9.12) and (9.13) from Lemmas 9.3.5 and 9.3.6, respectively, and the inequality (b) is implied by that in (9.18). Note that the inequality (9.18) is conservative in the sense that the term $16\beta_k \bar{y}^2$ could be replaced with $8\beta_k \bar{y}^2$ and the inequality (9.19c) would still follow. However, we opt for this conservativeness while defining the map $r \mapsto B(r)$ in (9.15) because it

results into robustness guarantees for the algorithm as discussed in the forthcoming section. Therefore, (9.19c) holds whenever $\|b(k) - b^*\| \geq r$. By assumption, we have $0 < \left(1 - \frac{\beta_k}{2a_{\max}}\right) < 1$, $\|b(1) - b^*\| > r$, and $\beta_k \geq \alpha$ for all $k \in \mathbb{Z}_{\geq 1}$. Using these facts and applying (9.19c) recursively, we conclude part (i).

For part (ii), note that if $\|b(k) - b^*\| \geq r$ for some $k \geq l$, then $\|b(k+1) - b^*\| < \|b(k) - b^*\|$ by (9.19c). Therefore, to find an upper bound on $\|b(k) - b^*\|$ for all $k \geq l$, we only need to consider the case when $\|b(k) - b^*\| < r$. Plugging this bound in (9.19b) and neglecting the negative term, we get

$$\|b(k+1) - b^*\|^2 \leq \frac{\beta_k^2 r^2}{2a_{\min}^2} + 8\beta_k^2 \bar{y}^2 + r^2. \quad (9.20)$$

From (9.15), we have

$$\frac{\beta_k^2 r^2}{2a_{\min}^2} + 16\beta_k^2 \bar{y}^2 \leq \frac{\beta_k r^2}{2a_{\max}}.$$

The result now follows by upper bounding the right-hand side of (9.20) with the left-hand side of the above expression and then employing the bound on the stepsizes give in (9.15). \square

Remark 9.3.8. (*Convergence properties from Theorem 9.3.7*): The assertion (i) of Theorem 9.3.7 implies that for any choice of $r > 0$, one can select stepsizes according to (9.15) so that bids reach the set $\mathcal{B}_r(b^*)$ in a finite number of steps and at a linear rate. Further, once bids reach the set $\mathcal{B}_r(b^*)$, we are assured from assertion (ii) that they remain in a neighborhood of b^* , where the size of the neighborhood is proportional to r (cf. (9.17)). In combination, the above facts mean that bids converge to any neighborhood of the efficient Nash equilibrium at a linear rate provided the stepsizes are selected appropriately. Note that as r becomes small, $B(r)$ gets small and so does α . Thus, from (9.16), the rate of convergence decreases as r becomes small. This presents a trade-off between the desired precision and the rate of convergence. \bullet

Remark 9.3.9. (*Stopping criteria for the ISO*): From the proof of Theorem 9.3.7(i) note that, as long as $\|b(k) - b^*\| > r$, the distance to the efficient Nash equilibrium

decreases. Therefore, if $\|b(k) - b^*\| > r$ and $k < l$, then one can write

$$\begin{aligned}
\|b(k+1) - b(k)\| &= \|b(k+1) - b^* + b^* - b(k)\| \\
&\geq \|b(k) - b^*\| - \|b(k+1) - b^*\| \\
&\stackrel{(a)}{\geq} \|b(k) - b^*\| - \left(1 - \frac{\alpha}{2a_{\max}}\right)^{1/2} \|b(k) - b^*\| \\
&= \left(1 - \left(1 - \frac{\alpha}{2a_{\max}}\right)^{1/2}\right) \|b(k) - b^*\|, \tag{9.21}
\end{aligned}$$

where in (a) we have used (9.19c) and $\beta_k \geq \alpha$. Given this observation, if the ISO has an estimate of α and a_{\max} , then it can design a stopping criteria based on the distance between consecutive bids. In fact, if the ISO decides selects $\epsilon > 0$ and stops the iteration whenever $\|b(k+1) - b(k)\| \leq \epsilon$, then it has the guarantee that either of the following is satisfied

(i) the condition $\|b(k) - b^*\| > r$ and $k < l$ is met and from (9.21) we get

$$\|b(k) - b^*\| \leq \epsilon \left(1 - \left(1 - \frac{\alpha}{2a_{\max}}\right)^{1/2}\right)^{-1}; \tag{9.22}$$

(ii) $\|b(k) - b^*\| \leq r$; or

(iii) $k > l$ in which case from (9.17) we get

$$\|b(k) - b^*\| \leq \left(1 + \frac{B(r)}{2a_{\max}}\right)^{1/2} r.$$

The ISO does not know the value of r ; its value depends on the stepsizes that the generators select. Assuming that stepsizes are small, the ISO can adjust ϵ depending on the desired accuracy level to get the guarantee (9.22) for the k -th bid. For small ϵ , the stopping criteria might never be met if stepsizes are too big. •

9.4 Robustness of the BID ADJUSTMENT ALGORITHM

Here we study the robustness properties of the BID ADJUSTMENT ALGORITHM in a variety of scenarios. We first show that the introduction of disturbances in the bid update mechanism does not destroy the algorithm convergence properties. We then study robustness against either an individual agent or colluding agents changing their strategy to get a higher payoff.

9.4.1 Robustness to disturbances

Here we establish the robustness properties of the BID ADJUSTMENT ALGORITHM in the presence of disturbances by characterizing its input-to-state stability (ISS) properties [JW01]. Let $d : \mathbb{Z}_{\geq 1} \rightarrow \mathbb{R}^N$ model the disturbance to the bid update mechanism. Such disturbances might arise from agents using different stepsizes than the prescribed one or other disruption to the prescribed bid update scheme. The resulting perturbed version of the BID ADJUSTMENT ALGORITHM can be written as the following discrete-time dynamical system

$$b(k+1) = [b(k) + \beta_k(x^{\text{opt}}(k) - q(k)) + d(k)]^+, \quad (9.23a)$$

$$x^{\text{opt}}(k+1) \in \text{Sol}_{\text{sopf}}(b(k+1)), \quad (9.23b)$$

$$q(k+1) = \text{Sol}_{\text{eff}}(b(k+1)), \quad (9.23c)$$

where $\text{Sol}_{\text{sopf}} : \mathbb{R}_{\geq 0}^N \rightrightarrows \mathbb{R}_{\geq 0}^N$ and $\text{Sol}_{\text{eff}} : \mathbb{R}_{\geq 0}^N \rightarrow \mathbb{R}_{\geq 0}^N$ map a bid profile to the set of optimizers of problem (9.3) and (9.6), respectively. Note that Sol_{sopf} is a set-valued map since (9.3) is a linear program. If $d \equiv 0$, then the dynamics (9.23) represents the k -th iteration of the BID ADJUSTMENT ALGORITHM.

The next result shows that the perturbed version of the algorithm (9.23) retains the convergence properties of the unperturbed version provided the magnitude of the disturbance satisfies an upper bound dependent on the state of the bid.

Proposition 9.4.1. *(The BID ADJUSTMENT ALGORITHM is robust to pertur-*

bations in the bid update): For dynamics (9.23), let the hypotheses of Theorem 9.3.7 hold and assume that $b_n(k) \geq c_n$ for all $n \in [N]$ and $k \in \mathbb{Z}_{\geq 1}$. Let $0 < \theta < \frac{1}{6} \left(1 - \frac{\alpha}{2a_{\max}}\right)$ and assume $\|d(k)\| \leq \theta \|b(k) - b^*\|$ for all $k \in \mathbb{Z}_{\geq 1}$. Then, the following holds

(i) there exists $l \in \mathbb{Z}_{\geq 1}$ such that $\|b(l) - b^*\| < r$ and, for all $k \in [l-1]$, we have $\|b(k) - b^*\| \geq r$ with

$$\|b(k+1) - b^*\| \leq \left(1 - \frac{\alpha}{2a_{\max}} + 2\theta + 4\theta^2\right)^{k/2} \|b(1) - b^*\|, \quad (9.24)$$

(ii) for all $k \geq l$,

$$\|b(k) - b^*\| \leq \left(1 + \frac{B(r)}{2a_{\max}} + 2\theta + 4\theta^2\right)^{1/2} r. \quad (9.25)$$

Proof. Since $b_n(k) \geq c_n$, we obtain for dynamics (9.23), $q_n(k) = \frac{b_n(k) - c_n}{2a_n}$, for all $n \in [N]$ and $k \in \mathbb{Z}_{\geq 1}$. Moreover, mimicking Lemma 9.3.4, we rewrite the bid update (9.23a) as

$$b(k+1) = b^{\text{coc}}(k+1) + \beta_k(x^{\text{opt}}(k) - x^*) + d(k), \quad (9.26)$$

for all $k \in \mathbb{Z}_{\geq 1}$. Using (9.26) and following the steps of Lemma 9.3.5 for dynamics (9.23a) we get,

$$\langle b(k+1) - b(k), b(k) - b^* \rangle \leq \langle d(k), b(k) - b^* \rangle - \frac{\beta_k}{2a_{\max}} \|b(k) - b^*\|^2, \quad (9.27)$$

for all $n \in [N]$ and $k \in \mathbb{Z}_{\geq 1}$. Similarly, from the reasoning of Lemma 9.3.6 we obtain

$$\begin{aligned} \|b(k+1) - b(k)\|^2 &\leq \frac{\beta_k^2}{2a_{\min}^2} \|b(k) - b^*\|^2 + 2 \left(\|\beta_k(x^{\text{opt}}(k) - x^*) + d(k)\| \right)^2 \\ &\leq \frac{\beta_k^2}{2a_{\min}^2} \|b(k) - b^*\|^2 + 4\beta_k^2 \|x^{\text{opt}}(k) - x^*\|^2 + 4\|d(k)\|^2 \\ &\leq \frac{\beta_k^2}{2a_{\min}^2} \|b(k) - b^*\|^2 + 16\beta_k^2 \bar{y}^2 + 4\|d(k)\|^2 \end{aligned} \quad (9.28)$$

for all $k \in \mathbb{Z}_{\geq 1}$ for dynamics (9.23a). Employing (9.27) and (9.28), assuming $\|b(k) - b^*\| \geq r$, and writing the set of inequalities (9.19) with $\alpha \leq \beta_k$, we deduce the following

$$\begin{aligned} \|b(k+1) - b^*\|^2 &\leq \left(1 - \frac{\alpha}{2a_{\max}}\right) \|b(k) - b^*\|^2 + 4\|d(k)\|^2 \\ &\quad + 2\langle d(k), b(k) - b^* \rangle. \end{aligned} \quad (9.29)$$

Finally, using $\|d(k)\| \leq \theta \|b(k) - b^*\|$ we get

$$\|b(k+1) - b^*\|^2 \leq \left(1 - \frac{\alpha}{2a_{\max}} + 2\theta + 4\theta^2\right) \|b(k) - b^*\|^2. \quad (9.30)$$

Iteratively, we obtain (9.24). The bound (9.25) can be computed in a similar way as done in the proof of Theorem 9.3.7. \square

Similar to the convergence guarantees of Theorem 9.3.7, the above result establishes that the perturbed version of the algorithm (9.23) converges to a neighborhood of the efficient Nash equilibrium provided the stepsizes and the disturbance satisfy appropriate bounds, and that the size of this neighborhood is tunable as a function of these.

The next result complements Proposition 9.4.1 by giving an alternative representation of robustness of (9.23). It establishes two properties: first, when the disturbance is bounded (not necessarily satisfying the bound of Proposition 9.4.1), the bids remain bounded; second, if the disturbance goes to zero, then the bids satisfy the bound (9.17) asymptotically. Notice that both these results do not follow directly from Proposition 9.4.1, justifying the need for a formal proof.

Proposition 9.4.2. *(Bounded disturbance implies bounded bids for BID ADJUSTMENT ALGORITHM): For dynamics (9.23), let the hypotheses of Theorem 9.3.7 hold and assume that $b_n(k) \geq c_n$ for all $n \in [N]$ and $k \in \mathbb{Z}_{\geq 1}$. Let $\|d(k)\| \leq d_{\max}$ for all $k \in \mathbb{Z}_{\geq 1}$ and let $\theta \in \left(0, \frac{1}{6} \left(1 - \frac{\alpha}{2a_{\max}}\right)\right)$. Then, the following holds for all $k \in \mathbb{Z}_{\geq 1}$,*

$$\|b(k) - b^*\| \leq \left(1 - \frac{\alpha}{2a_{\max}} + 2\theta + 4\theta^2\right)^{k/2} \|b(1) - b^*\| + G(r, \theta, d_{\max}), \quad (9.31)$$

where $G(r, \theta, d_{\max}) := \max\{G_1(r, d_{\max}), G_2(\theta, d_{\max})\}$ and

$$G_1(r, d_{\max}) := \left(\frac{B(r)r^2}{2a_{\max}} + (2d_{\max} + r)^2 \right)^{1/2},$$

$$G_2(\theta, d_{\max}) := \left(2 + \frac{1}{\theta} \right) d_{\max}.$$

As a consequence, as $k \rightarrow \infty$, if $\|d(k)\| \rightarrow 0$, then

$$\max\left\{ \|b(k) - b^*\|, \left(1 + \frac{B(r)}{2a_{\max}} \right)^{1/2} r \right\} \rightarrow 0. \quad (9.32)$$

Proof. We first show that if for some $k \in \mathbb{Z}_{\geq 1}$, $\|b(k) - b^*\| \leq G(r, \theta, d_{\max})$, then $\|b(l) - b^*\| \leq G(r, \theta, d_{\max})$ for all $l \geq k$. To this end, as a first case, assume that $r \leq \|b(k) - b^*\| \leq G(r, \theta, d_{\max})$. Then, following the steps of the proof of Proposition 9.4.1, we arrive at (9.29). If $\|d(k)\| \leq \theta \|b(k) - b^*\|$, then we get the inequality (9.30) which implies that $\|b(k+1) - b^*\| \leq \|b(k) - b^*\| \leq G(r, \theta, d_{\max})$. On the other hand, if $\|d(k)\| > \theta \|b(k) - b^*\|$, then using this bound in (9.29), we get

$$\begin{aligned} \|b(k+1) - b^*\|^2 &< \left(1 - \frac{\alpha}{2a_{\max}} \right) \frac{\|d(k)\|^2}{\theta^2} + 4\|d(k)\|^2 + 2\frac{\|d(k)\|^2}{\theta} \\ &< \left(\frac{1}{\theta^2} + \frac{4}{\theta} + 4 \right) \|d(k)\|^2. \end{aligned}$$

Thus, using $\|d(k)\| \leq d_{\max}$, we get $\|b(k+1) - b^*\| < G_2(\theta, d_{\max}) \leq G(r, \theta, d_{\max})$. As a second case, assume $\|b(k) - b^*\| < r$. Note that $r < G(r, \theta, d_{\max})$, and so $\|b(k) - b^*\| < G(r, \theta, d_{\max})$. For this case, using $\|b(k) - b^*\| < r$ and inequalities (9.27) and (9.28), we get as in (9.19b) that

$$\|b(k+1) - b^*\|^2 \leq \frac{\beta_k^2 r^2}{2a_{\min}^2} + 16\beta_k^2 \bar{y}^2 + 4\|d(k)\|^2 + r^2 + 2r\|d(k)\|.$$

Now applying bounds $\|d(k)\| \leq d_{\max}$ and $\beta_k \leq B(r)$, we obtain $\|b(k+1) - b^*\| \leq G_1(r, d_{\max})$. Hence, we arrive at the conclusion that if $\|b(k) - b^*\| \leq G(r, \theta, d_{\max})$, then $\|b(l) - b^*\| \leq G(r, \theta, d_{\max})$ for all $l \geq k$.

Consider now the case when for some $k \in \mathbb{Z}_{\geq 1}$, $\|b(k) - b^*\| > G(r, \theta, d_{\max})$.

By definition of $G(r, \theta, d_{\max})$, this implies that $\|b(k) - b^*\| > r$ and $\|b(k) - b^*\| > \frac{d(k)}{\theta}$. Therefore, from the proof of Proposition 9.4.1, we arrive at (9.30). Finally, combining the reasoning of the two cases when $\|b(k) - b^*\|$ is greater than or less than equal to $G(r, \theta, d_{\max})$, we obtain the inequality (9.31). The limit (9.32) follows from that fact that as $k \rightarrow \infty$, the first term of (9.31) converges to zero and as d_{\max} tends to zero, $G(r, \theta, d_{\max})$ tends to $\left(1 + \frac{B(r)}{2\alpha_{\max}}\right)^{1/2} r$. \square

One can observe from (9.31) that the limiting behavior of the bids depend on the magnitude of r and d_{\max} : if r is designed to be small enough and if d_{\max} is small enough, or this bound becomes small as the algorithm iterates, then the bids do converge to a small neighborhood of b^* .

As an aside, in the theory of ISS for discrete-time dynamical systems [JW01], one typically would conclude Proposition 9.4.2 from Proposition 9.4.1. However, the traditional ISS results require asymptotic convergence of the unperturbed dynamics, (i.e., dynamics (9.23) with $d \equiv 0$) to a point. This is not the case here and hence, we provide a formal proof.

Remark 9.4.3. (*BID ADJUSTMENT ALGORITHM is robust to variation in step-sizes*): In practice, given that generators are competing and do not share information with each other, it is conceivable that they do not agree on a common stepsize. Propositions 9.4.1 and 9.4.2 provide a way to quantify the performance of the algorithm when the stepsizes are different. Specifically, let β_k , $k \in \mathbb{Z}_{\geq 1}$, denote a common set of stepsizes for all generators that satisfies the hypotheses of Theorem 9.3.7 and hence, guarantees the convergence properties outlined therein. Assume that each generator selects a different stepsize at each iteration, denoted as $\beta_{k,n}$, $k \in \mathbb{Z}_{\geq 1}$, for generator n . Then, the bid iteration in Step 3 of the BID ADJUSTMENT ALGORITHM can be written as (9.23) where now

$$d_n(k) = (\beta_{k,n} - \beta_k)(x_n^{\text{opt}}(k) - q_n(k))$$

for all $n \in [N]$ and $k \in \mathbb{Z}_{\geq 1}$. Now if the variation in stepsizes, i.e., the quantity $\beta_{k,n} - \beta_k$, is bounded above by a particular function of the distance of the bid-state to the efficient Nash equilibrium, then the linear convergence and the ultimate

bound is guaranteed following Proposition 9.4.1. On the other hand, if the variation in stepsizes do not depend on the state but are bounded then, then the bids still converge asymptotically to a neighborhood of the efficient Nash equilibrium, as concluded in Proposition 9.4.2. Note that the assumption of $b_n(k) \geq c_n$ for all n and k holds whenever the stepsizes are positive for all agents at all times (cf. Lemma 9.3.3). •

9.4.2 Robustness to deviation in bid update

We illustrate here another aspect of robustness of the BID ADJUSTMENT ALGORITHM by establishing that, if all generators follow the bid update scheme, then there is no incentive for any generator to deviate from it. We next formalize these notions. Assume that all generators, except $\tilde{n} \in [N]$, follow the BID ADJUSTMENT ALGORITHM, and that \tilde{n} follows an arbitrary strategy to update its bids. Then, one can write the BID ADJUSTMENT ALGORITHM under this deviation as

$$b_{-\tilde{n}}(k+1) = [b_{-\tilde{n}}(k) + \beta_k(x_{-\tilde{n}}^{\text{opt}}(k) - q_{-\tilde{n}}(k))]^+, \quad (9.33a)$$

$$b_{\tilde{n}}(k+1) = \mathcal{H}_{\tilde{n}}^{(k)}\left(\{b_{\tilde{n}}(t), x_{\tilde{n}}^{\text{opt}}(t), q_{\tilde{n}}(t)\}_{t=1}^k\right), \quad (9.33b)$$

$$x^{\text{opt}}(k+1) \in \text{Sol}_{\text{sopf}}(b(k+1)), \quad (9.33c)$$

$$q(k+1) \in \text{Sol}_{\text{eff}}(b(k+1)), \quad (9.33d)$$

where the maps $\{\mathcal{H}_{\tilde{n}}^{(k)} : \mathbb{R}_{\geq 0}^{3k} \rightarrow \mathbb{R}_{\geq 0}^{\infty}\}_{k=1}^{\infty}$ represent the update scheme of \tilde{n} at iterations $1, 2, \dots$. Recall that the subscript $-\tilde{n}$ denotes the vector without the component corresponding to the generator \tilde{n} . Note that (9.33b) implies that at each iteration k , the generator \tilde{n} only knows the bids it made and the quantities the ISO demanded from it up until iteration k .

We next introduce the notion of “incentive to deviate” from the BID ADJUSTMENT ALGORITHM for the generator \tilde{n} . A natural way to quantify incentives for a generator is in terms of the payoff (9.4): a generator has an incentive to deviate if this would bring in a higher payoff, when the ISO stops the iteration, than not deviating. This is formalized below.

Definition 9.4.4. (*Incentive to deviate from BID ADJUSTMENT ALGORITHM*): Let $r > 0$ and assume that the stepsizes for any execution of (9.33) satisfy the hypotheses of Theorem 9.3.7. Then, the generator $\tilde{n} \in [N]$ has an *incentive to deviate* from the BID ADJUSTMENT ALGORITHM if there exists an execution of (9.33) and $l \in \mathbb{Z}_{\geq 1}$ such that

$$u_{\tilde{n}}(b_{\tilde{n}}(k), x_{\tilde{n}}^{\text{opt}}(k)) > u_{\tilde{n}}^{\text{max}}, \quad (9.34)$$

for all $k \geq l$, where

$$u_{\tilde{n}}^{\text{max}} := \max \left\{ u_{\tilde{n}}(b_{\tilde{n}}, x_{\tilde{n}}^{\text{opt}}(b)) \mid \|b - b^*\| \leq \left(1 + \frac{B(r)}{2a_{\text{max}}}\right)r \right. \\ \left. \text{and } x^{\text{opt}}(b) \in \text{Sol}_{\text{sopf}}(b) \right\}. \quad (9.35)$$

In the above definition, recall the short-hand notation $x^{\text{opt}}(k)$ for $x^{\text{opt}}(b(k))$. Equation (9.34) implies that the generator \tilde{n} has an incentive to deviate if, after a finite number of iterations, it is guaranteed a higher payoff than what it might eventually get if it follows the BID ADJUSTMENT ALGORITHM. This captures the fact that the generator does not know when the ISO might stop the bid and hence it would deviate only when it is guaranteed to get a higher payoff after a finite number of steps. The next result shows that there is no incentive to deviate from the BID ADJUSTMENT ALGORITHM.

Proposition 9.4.5. (*Robustness to deviation from BID ADJUSTMENT ALGORITHM*): For dynamics (9.33), let the hypotheses of Theorem 9.3.7 hold and assume that $b_n(k) \geq c_n$ for all $n \in [N]$ and $k \in \mathbb{Z}_{\geq 1}$. Also, assume that the ISO selects a vertex solution $x^{\text{opt}}(k) \in \text{Sol}_{\text{sopf}}(b(k))$ at each iteration $k \in \mathbb{Z}_{\geq 1}$. Then, no generator has an incentive to deviate from the BID ADJUSTMENT ALGORITHM.

Proof. We reason by contradiction. Assume that a generator \tilde{n} has an incentive to deviate from the BID ADJUSTMENT ALGORITHM. That is, there exists an execution of (9.33) and $l \in \mathbb{Z}_{\geq 1}$ such that (9.34) holds for all $k \geq l$. By definition,

$$u_{\tilde{n}}^{\text{max}} > b_{\tilde{n}}^* x_{\tilde{n}}^* - f_{\tilde{n}}(x_{\tilde{n}}^*). \quad (9.36)$$

Now consider the map

$$\mathbb{R}_{\geq 0} \ni b \mapsto g_{\bar{n}}(b) := \max\{bq - f_{\bar{n}}(q) \mid q \geq 0\}.$$

From (9.6), we get $g_{\bar{n}}(b_{\bar{n}}^*) = b_{\bar{n}}^* x_{\bar{n}}^* - f_{\bar{n}}(x_{\bar{n}}^*)$. Further, using (9.1), one can show that this map is continuous, strictly increasing in the domain $b \geq c_{\bar{n}}$, and $g_{\bar{n}}(b) \rightarrow \infty$ as $b \rightarrow \infty$. These facts along with (9.36) imply that there exists a unique $b_{\bar{n}}^{\max} > b_{\bar{n}}^*$ such that $g_{\bar{n}}(b_{\bar{n}}^{\max}) = u_{\bar{n}}^{\max}$, $g_{\bar{n}}(b) > u_{\bar{n}}^{\max}$ for all $b > b_{\bar{n}}^{\max}$, and $g_{\bar{n}}(b) < u_{\bar{n}}^{\max}$ for all $c_{\bar{n}} \leq b < b_{\bar{n}}^{\max}$. Then, (9.34) reads as

$$u_{\bar{n}}(b_{\bar{n}}(k), x_{\bar{n}}^{\text{opt}}(k)) > g_{\bar{n}}(b_{\bar{n}}^{\max}), \quad (9.37)$$

for all $k \geq l$. From the above expression, we deduce that $b_{\bar{n}}(k) \geq b_{\bar{n}}^{\max}$ for all $k \geq l$. Indeed otherwise, there exists $\tilde{k} \geq l$ such that $b_{\bar{n}}(\tilde{k}) < b_{\bar{n}}^{\max}$. This further implies that

$$\begin{aligned} u_{\bar{n}}(b_{\bar{n}}(\tilde{k}), x_{\bar{n}}^{\text{opt}}(\tilde{k})) &= b_{\bar{n}}(\tilde{k})x_{\bar{n}}^{\text{opt}}(\tilde{k}) - f_{\bar{n}}(x_{\bar{n}}^{\text{opt}}(\tilde{k})) \\ &\leq g_{\bar{n}}(b_{\bar{n}}(\tilde{k})) < g_{\bar{n}}(b_{\bar{n}}^{\max}), \end{aligned}$$

contradicting (9.37). In the above expression, the first inequality follows from the definition of $g_{\bar{n}}$ and the second follows from the fact that $g_{\bar{n}}$ is strictly increasing.

The above reasoning has helped us establish that $b_{\bar{n}}(k) \geq b_{\bar{n}}^{\max} > b_{\bar{n}}^*$ for all $k \geq l$. Note that $x_{\bar{n}}^{\text{opt}}(k) > 0$ for all $k \geq l$ because otherwise $u_{\bar{n}}(b_{\bar{n}}(k), x_{\bar{n}}^{\text{opt}}(k)) = 0$ and (9.37) gets violated. By assumption, there exists at least one more generator connected to the bus $i(\tilde{n})$ to which \tilde{n} is connected to. For now assume that there is only one other generator $\bar{n} \in [N]$ connected to $i(\tilde{n})$. Since for all $k \geq l$, $x^{\text{opt}}(k)$ is a solution of (9.3), from the fact that $x_{\bar{n}}^{\text{opt}}(k) > 0$, we deduce

$$b_{\bar{n}}(k) \geq b_{\bar{n}}(k) \geq b_{\bar{n}}^{\max},$$

for all $k \geq l$. Now let

$$q_{\bar{n}}^{\max} := \inf_{b \geq b_{\bar{n}}^{\max}} \operatorname{argmax}\{bq - f_{\bar{n}}(q) \mid q \geq 0\}.$$

Note that $q_{\bar{n}}^{\max} > 0$ because of the facts: (i) $b_{\bar{n}}^* = b_{\bar{n}}^* < b_{\bar{n}}^{\max}$; (ii) $\operatorname{argmax}\{b_{\bar{n}}^*q - f_{\bar{n}}(q) \mid q \geq 0\} = x_{\bar{n}}^* > 0$; and (iii) $b \mapsto \operatorname{argmax}\{bq - f_{\bar{n}}(q) \mid q \geq 0\}$ is nondecreasing. Since $b_{\bar{n}}(k) \geq b_{\bar{n}}^{\max}$ for all $k \geq l$, we obtain $q_{\bar{n}}(k) \geq q_{\bar{n}}^{\max}$ for all $k \geq l$ (see Step 4 of the BID ADJUSTMENT ALGORITHM for the definition of $q_{\bar{n}}(k)$). Thus, if $b_{\bar{n}}(k) > b_{\bar{n}}(k)$ for some $k \geq l$, then $x_{\bar{n}}^{\operatorname{opt}}(k) = 0$ (because $x^{\operatorname{opt}}(k)$ is an optimizer of (9.3) given bids $b(k)$) and $b_{\bar{n}}(k) > b_{\bar{n}}^{\max}$. As a consequence,

$$b_{\bar{n}}(k+1) = b_{\bar{n}}(k) - \beta_k q_{\bar{n}}(k) \leq b_{\bar{n}}(k) - \alpha q_{\bar{n}}^{\max}. \quad (9.38)$$

Therefore, if $b_{\bar{n}}(k) > b_{\bar{n}}(k)$ for some $k \geq l$, then from (9.38) we deduce that there exists a finite $\tilde{k} > k$ such that, either $b_{\bar{n}}(\tilde{k}) < b_{\bar{n}}(\tilde{k})$ or $b_{\bar{n}}(\tilde{k}) = b_{\bar{n}}(\tilde{k})$. In the former case, $u_{\bar{n}}(b_{\bar{n}}(\tilde{k}), x_{\bar{n}}^{\operatorname{opt}}(\tilde{k})) = 0$ as $x_{\bar{n}}^{\operatorname{opt}}(\tilde{k}) = 0$. This contradicts (9.34). In the latter case, two further cases can arise. In the first one, we get $x_{\bar{n}}^{\operatorname{opt}}(\tilde{k}) = 0$ implying $u_{\bar{n}}(b_{\bar{n}}(\tilde{k}), x_{\bar{n}}^{\operatorname{opt}}(\tilde{k})) = 0$ and contradicting (9.34). In the second one, we obtain $x_{\bar{n}}^{\operatorname{opt}}(\tilde{k}) = 0$, implying $b_{\bar{n}}(\tilde{k}+1) < b_{\bar{n}}(\tilde{k}+1)$. This further yields $u_{\bar{n}}(b_{\bar{n}}(\tilde{k}+1), x_{\bar{n}}^{\operatorname{opt}}(\tilde{k}+1)) = 0$, thereby, contradicting (9.34). Finally, if there are other generators connected to $i(\bar{n})$ that follow the BID ADJUSTMENT ALGORITHM, then one can carry out the same reasoning as done above and show that we contradict (9.34). This completes the proof. \square

Remark 9.4.6. (*Generalization of Proposition 9.4.5*): It is interesting to observe that in the proof of Proposition 9.4.5, we have not used at any point that the generators connected at buses other than the one that \tilde{n} is connected follow the BID ADJUSTMENT ALGORITHM. In fact, independently of how such generators update their bids, the BID ADJUSTMENT ALGORITHM ensures that \tilde{n} does not have any incentive to deviate. This is a useful property which we use later when studying robustness to collusion. \bullet

Remark 9.4.7. (*Other notions of “incentive to deviate”*): In Definition 9.4.4, one can impose the condition of higher payoff (9.34) to hold for all executions of (9.33).

If this condition holds, then the generator has an even stronger incentive to deviate from the BID ADJUSTMENT ALGORITHM. However, by Proposition 9.4.5, we are ensured that there does not exist such strong incentive to deviate. This is because the result shows that there does not exist any execution of (9.33) for which (9.34) holds. If, on the other hand, we replace the condition (9.34) in Definition 9.4.4 with the requirement that there exists an execution of (9.33) along which

$$\limsup_{k \rightarrow \infty} u_{\tilde{n}}(b_{\tilde{n}}(k), x_{\tilde{n}}^{\text{opt}}(k)) > u_{\tilde{n}}^{\text{max}} \quad (9.39)$$

holds. This inequality means that there exists an execution of (9.33) in which the generator \tilde{n} gets a higher payoff than $u_{\tilde{n}}^{\text{max}}$ infinitely often. Since the ISO can stop the iterations at any time, the generator is not guaranteed a higher payoff, but the possibility is still there. We conjecture that the BID ADJUSTMENT ALGORITHM is not robust to this notion of weak incentive to deviate. However, the obfuscation of the stopping criteria by the ISO makes such a weak incentive not enough for a rational generator to deviate. •

9.4.3 Robustness to collusion

Here we study the robustness of the BID ADJUSTMENT ALGORITHM against collusion. Collusion refers to the action of a set of generators to share among themselves information about their bids and generation demands by the ISO, with the goal of getting a higher profit, possibly by deviating from the bid update scheme. The following makes this notion formal.

Definition 9.4.8. (*Collusion between generators*): A group of generators $\mathcal{J} \subset [N]$ form a collusion if at each iteration $k \in \mathbb{Z}_{\geq 1}$ of the algorithm, each generator $n \in \mathcal{J}$,

- (i) has the information

$$\mathcal{I}_k := \{(b_r(t), x_r^{\text{opt}}(t)) \mid r \in \mathcal{J}, t \in [k]\}, \text{ and}$$

- (ii) determines its next bid $b_n(k+1)$ based on the information \mathcal{I}_k , not necessarily following the update scheme (Step 3) of the BID ADJUSTMENT ALGORITHM.

An iteration of the BID ADJUSTMENT ALGORITHM under a collusion between a group of generators $\mathcal{J} \subset [N]$ is given by the following dynamics

$$b_n(k+1) = [b_n(k) + \beta_k(x_n^{\text{opt}}(k) - q_n(k))]^+, \forall n \notin \mathcal{J}, \quad (9.40a)$$

$$b_n(k+1) = \mathcal{H}_n^{(k)}\left(\mathcal{I}_k, \{q_n(t)\}_{t=1}^k\right), \forall n \in \mathcal{J} \quad (9.40b)$$

$$x^{\text{opt}}(k+1) \in \text{Sol}_{\text{sopf}}(b(k+1)), \quad (9.40c)$$

$$q(k+1) = \text{Sol}_{\text{eff}}(b(k+1)), \quad (9.40d)$$

where maps $\{\mathcal{H}_n^{(k)} : \mathbb{R}_{\geq 0}^{(2|\mathcal{J}|+1)k} \rightarrow \mathbb{R}_{\geq 0}\}_{n \in \mathcal{J}, k=1,2,\dots}$ represent the update scheme of generators in collusion. Notice that for each generator n , the quantity $q_n(k)$, for all $k \in \mathbb{Z}_{\geq 1}$, is part of its private information, irrespective of the fact that n belongs to \mathcal{J} or not. Next, we define what it means for the group of generators \mathcal{J} to have an incentive to collude.

Definition 9.4.9. (*Incentive to collude*): Let $r > 0$ and assume that the stepsizes for any execution of (9.40) satisfy the hypotheses of Theorem 9.3.7. Then, the group of generators \mathcal{J} has an *incentive to collude* under the BID ADJUSTMENT ALGORITHM if there exists an execution of (9.40), a generator $\tilde{n} \in \mathcal{J}$, and $l \in \mathbb{Z}_{\geq 1}$ such that

$$u_{\tilde{n}}(b_{\tilde{n}}(k), x_{\tilde{n}}^{\text{opt}}(k)) > u_{\tilde{n}}^{\max}, \quad (9.41)$$

for all $k \geq l$, where $u_{\tilde{n}}^{\max}$ is defined in (9.35).

This notion essentially says that there is an incentive to collude for the generators in \mathcal{J} if there exists at least one execution of (9.40) along which at least one generator in \mathcal{J} gets a higher payoff after finite number of steps. The next result shows that no group of generators has an incentive to collude provided there is at least one generator at each bus with generation that follows the BID ADJUSTMENT ALGORITHM.

Proposition 9.4.10. (*Robustness to collusion under the BID ADJUSTMENT ALGORITHM*): For dynamics (9.40), let the hypotheses of Theorem 9.3.7 hold and

assume that $b_n(k) \geq c_n$ for all $n \in [N]$ and $k \in \mathbb{Z}_{\geq 1}$. Assume that the ISO selects a vertex solution $x^{\text{opt}}(k) \in \text{Sol}_{\text{sopf}}(b(k))$ at each iteration $k \in \mathbb{Z}_{\geq 1}$. Assume that at each bus that has generators connected to it, there exists at least one generator that follows the update scheme of the BID ADJUSTMENT ALGORITHM. Denote these generators by $\mathcal{K} \subset [N]$. Then, there is no incentive to collude for any group of generators contained in $[N] \setminus \mathcal{K}$.

Proof. Let $\mathcal{J} \subset [N] \setminus \mathcal{K}$ be a group of generators that form a collusion. Assume first Scenario 1 where each generator in \mathcal{J} is connected to a different bus. By hypotheses, there exists at least one other generator following the BID ADJUSTMENT ALGORITHM at the bus where a generator in \mathcal{J} is connected to. Thus, mimicking the proof of Proposition 9.4.5 (cf. Remark 9.4.6), at each bus, no generator has an incentive to deviate from the BID ADJUSTMENT ALGORITHM. By Definition 9.4.4, this implies that there does not exist any execution of (9.40) for which (9.41) holds for any generator in \mathcal{J} . Hence, for Scenario 1, generators in \mathcal{J} do not have an incentive to collude.

Next, consider Scenario 2, where at least a bus, say $i \in [N_b]$, has more than one generator from \mathcal{J} , that is, $\mathcal{J}_i := G_i \cap \mathcal{J}$ has cardinality larger than or equal to 2. Let $\bar{n} \in G_i$ be the generator at i that follows BID ADJUSTMENT ALGORITHM. For the sake of contradiction, assume the existence of a generator $\tilde{n} \in \mathcal{J}_i$ for which (9.41) holds for some execution of (9.40). Since the ISO selects a vertex solution at each iteration $k \in \mathbb{Z}_{\geq 1}$, we deduce that for all $k \geq l$, all other generators in \mathcal{J}_i get zero production signal from the ISO, i.e., $x_n^{\text{opt}}(k) = 0$ for all $n \in \mathcal{J}_i \setminus \{\tilde{n}\}$ and $k \geq l$. Therefore, for the purpose of analysis, one can neglect the generators in $\mathcal{J}_i \setminus \{\tilde{n}\}$ and assume that only \tilde{n} and \bar{n} are connected to i . Again, mimicking the proof of Proposition 9.4.5, we deduce that \tilde{n} does not have an incentive to deviate and so (9.41) does not hold, a contradiction. Since i is arbitrary, we conclude that for Scenario 2, generators in \mathcal{J} do not have an incentive to collude either. \square

An alternative definition of an incentive to collude could be where every generator in the collusion gets a higher payoff after a finite number of steps. Proposition 9.4.10 however shows that, under the assumed hypotheses, such a scenario

does not occur as there is not even a single generator that gets a higher payoff after a finite number of iterations. Note that the assumptions of the above result is tight in the sense that if all generators at a bus collude, then based on the load and the line limits, generators at that bus can increase their bid to an arbitrarily high value, thus creating an incentive to collude.

Remark 9.4.11. (*Limitations on robustness under generator bounds*): The robustness of the BID ADJUSTMENT ALGORITHM against deviation and collusion relies heavily on the fact that we have not considered upper bounds on the generation capacities. In the presence of such bounds, the generators might be able to push the bids and their individual utilities to a higher value based on the load at the respective bus and the capacity constraints on the lines connected to the bus. To avoid such behavior of market manipulation, either one can modify network capacities or investigate alternative allocation mechanisms that disincentivizes such behavior. •

9.5 Simulations

We illustrate the convergence and robustness properties of the BID ADJUSTMENT ALGORITHM using a modified IEEE 9-bus test case [ZMST11]. The traditional IEEE 9-bus system has 3 generators, at buses v_1 , v_2 , and v_3 and three loads at buses v_5 , v_7 , and v_9 . In our modified test case, we have added one generator each at buses v_1 , v_2 and v_3 . The interconnection topology is given in Figure 9.1. The line flow limit between any two buses (v_i, v_j) is 2.5 except for three lines, (v_5, v_6) , (v_3, v_6) , and (v_6, v_7) , for which the limits are 1.5, 3.0, and 1.5, respectively. The loads are $y_5 = 2$, $y_7 = 3$, and $y_9 = 1$, where y_i denotes the load at bus v_i . The cost function for each generator i is $f_i(x_i) = a_i x_i^2 + c_i x_i$, where the coefficients for all the generators are given by the vectors

$$\begin{aligned} a &= (0.1100, 0.0950, 0.0850, 0.1000, 0.1225, 0.0750), \\ c &= (3.5, 3.8, 1.2, 0.8, 1.0, 1.3). \end{aligned} \tag{9.42}$$

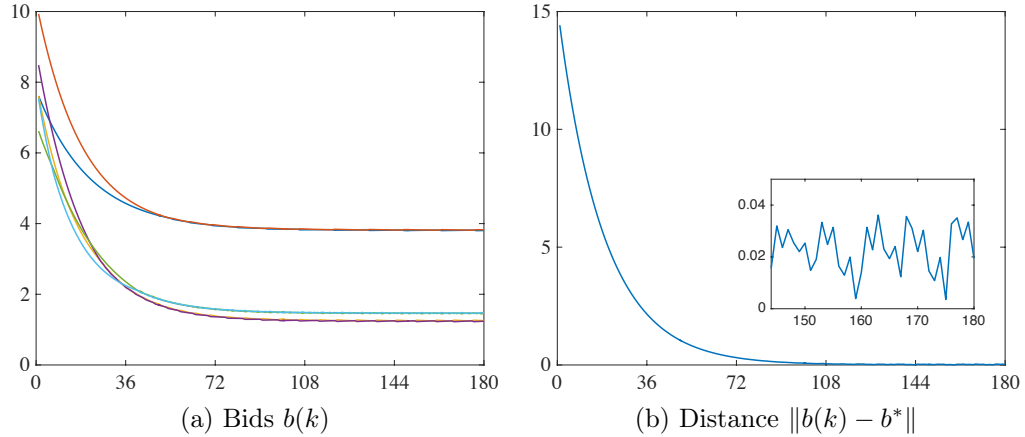


Figure 9.2: Execution of the BID ADJUSTMENT ALGORITHM for the modified IEEE 9-bus test case in Figure 9.1. The cost function for each generator i is $f_i(x_i) = a_i x_i^2 + c_i x_i$, with coefficients given in (9.42). The load is $y_5 = 2$, $y_7 = 3$, and $y_9 = 1$. The efficient Nash equilibrium b^* is given in (9.43). Plots (a) and (b) show, respectively, the evolution of the bids and their distance to b^* . The stepsizes are $\beta_k = 0.01$ for all k and the initial bids are $b(1) = (7.6096, 9.9313, 7.6087, 8.4827, 6.6175, 7.5254)$. Bids converge to and then remain in a neighborhood of the efficient Nash equilibrium.

we conclude that bids eventually remain in the neighborhood centered at b^* with radius 1.3775. Figure 9.2(b) validates this claim and, in fact, shows that the bound is conservative since bids actually remain in a neighborhood of radius 0.05.

We next illustrate the robustness properties of the BID ADJUSTMENT ALGORITHM against disturbances (cf. Section 9.4.1). Figure 9.3 considers the same setup as above but now with generators choosing a different stepsize at each iteration. These differences in stepsizes can be interpreted as a disturbance to the BID ADJUSTMENT ALGORITHM, as discussed in Remark 9.4.3. In Figure 9.3(a)-(b), the interval from which stepsizes are selected is constant, whereas in Figure 9.3(c)-(d) the size of this interval decays with time. In both cases, the bids converge to a neighborhood of b^* (in the latter case of decaying interval, the bids converge to a smaller neighborhood), as established in Proposition 9.4.2. Observe that the convergence rate in Figure 9.3(a)-(b) is higher than in Figure 9.2(a)-(b). This is because stepsizes are allowed to be large in the former. However, this higher convergence rate comes with the pitfall of loss in accuracy, cf. Remark 9.3.8. Hence, to retain both properties, stepsizes should be large initially and decay as iterations

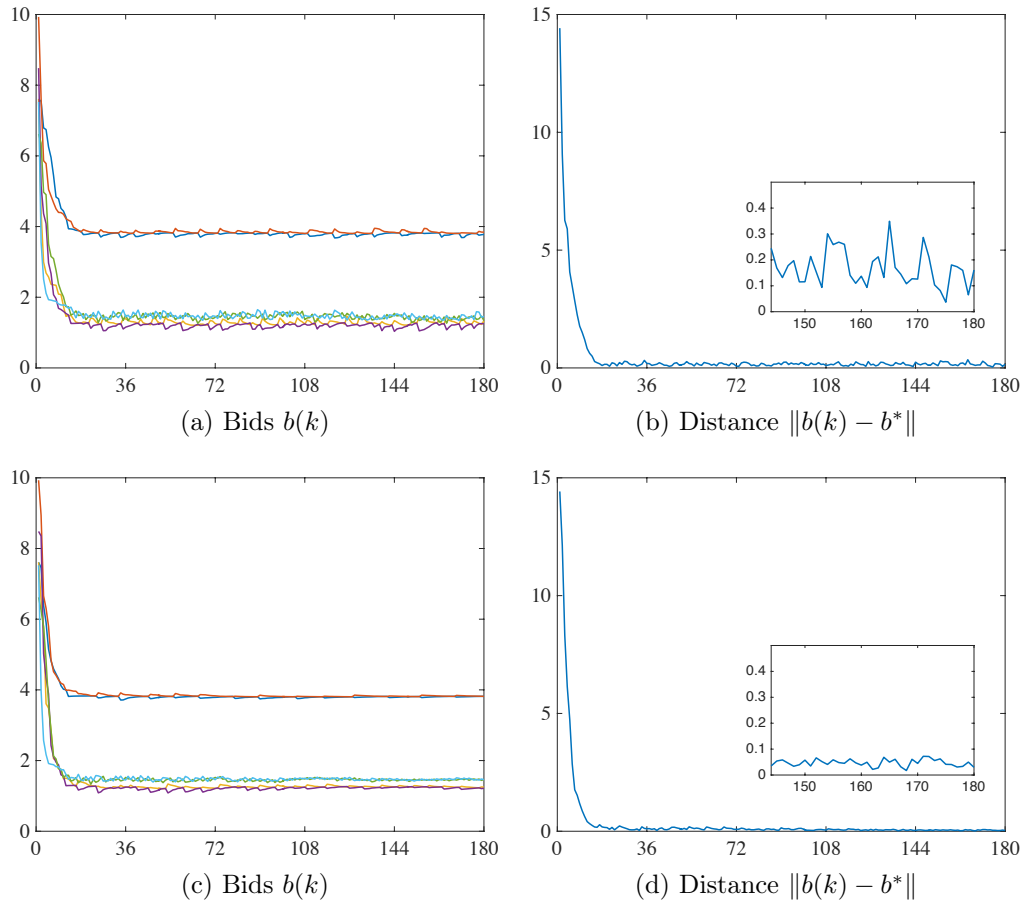


Figure 9.3: Execution of the BID ADJUSTMENT ALGORITHM under different stepsize selection for the example of Figure 9.2. All data is the same except for the stepsizes. In plots (a) and (b), each generator at each iteration randomly selects the stepsize from the set $[0.001, 0.1]$ with uniform probability distribution. We observe that the bids still converge to a neighborhood of the efficient Nash equilibrium, but the size of the neighborhood is bigger than that achieved in Figure 9.2. In plots (c) and (d), the interval of stepsize selection decays with time to a single point 0.01. The bids now converge to the efficient Nash equilibrium with greater accuracy. These observations validate the robustness guarantees of Proposition 9.4.2.

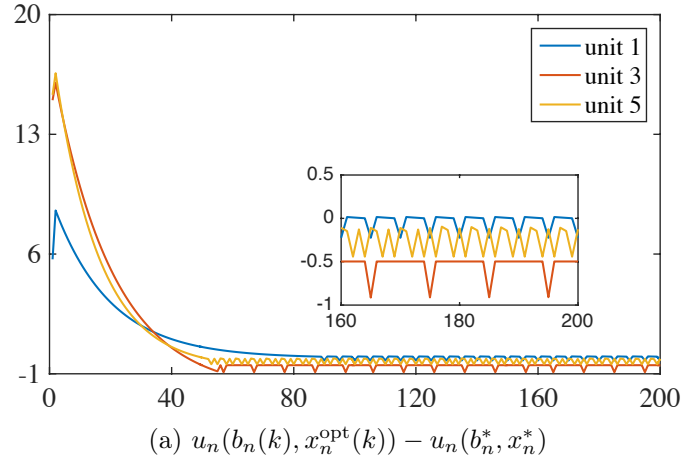


Figure 9.4: Execution of the BID ADJUSTMENT ALGORITHM for the example considered in Figure 9.2 with generators 1, 3, and 5 forming a collusion. The initial condition is the same and the stepsize is 0.01 at each iteration for generators 2, 4, and 6. For each $n \in \{1, 3, 5\}$, at each iteration k , $b_n(k) = 0.99 * b_{n+1}(k)$ if this value is bigger than or equal to b_n^* . Otherwise, $b_n(k)$ is selected randomly from the interval $[b_n^*, b_n^* + 1]$, with uniform probability distribution. With this choice of bid, the colluding generators aim to get a positive production signal and at the same time bid high enough so as to obtain a high utility. The plot shows the evolution of the difference between the utility obtained at each iteration, $u_n(b_n(k), x_n^{\text{opt}}(k))$, and the utility at the optimal bid and generation, $u_n(b_n^*, x_n^{\text{opt}}(b_n^*))$ for each $n \in \{1, 3, 5\}$. This value becomes negative for all generators after a finite number of iterations. Since $u_n^{\text{max}} > u_n(b_n^*, x_n^*)$, the example shows that (9.41) does not hold.

proceed. This is seen in Figure 9.3(c)-(d), where stepsizes decay over time (in expectation), yielding both high convergence rate and accuracy. Finally, Figure 9.4 demonstrates the robustness against collusion of the BID ADJUSTMENT ALGORITHM (cf. Section 9.4.3), where generators 1, 3, and 5 form a collusion. These generators may select their bids in any fashion they want: for this example, we assume a particular strategy of bid selection, explained in Figure 9.4. The plot shows that the utility of the colluding generators eventually becomes lower than u_n^{max} (defined in (9.35)). Hence, there is no incentive for collusion, as ensured by Proposition 9.4.10.

Acknowledgments

This chapter is taken, in part, from the work [CC17b] submitted as “Iterative bidding in electricity markets: rationality and robustness” by A. Cherukuri and J. Cortés, to the IEEE Transactions on Control of Network Systems, as well as [CC16a] where it appears as “Decentralized Nash equilibrium learning by strategic generators for economic dispatch” by A. Cherukuri and J. Cortés in the proceedings of the 2016 American Control Conference and as [CC17a] where it is going to appear as “Decentralized Nash equilibrium seeking by strategic generators for DC optimal power flow” by A. Cherukuri and J. Cortés in the proceedings of the 2017 Conference on Information Sciences and Systems. The dissertation author was the primary investigator and author of these papers. This research was partly supported by the ARPA-e Cooperative Agreement DE-AR0000695.

Chapter 10

Conclusions

In this thesis we have mainly focussed on designing coordination algorithms and analyzing market dynamics in the event of optimal dispatch of distributed energy resources. For the former part, we first designed a class of “Laplacian-gradient” dynamics that are anytime and distributed in nature and that solve the economic dispatch problem for a group of generators. These dynamics require a feasible initial condition to start with. To address this problem, we designed the DETERMINE FEASIBLE ALLOCATION strategy to allow a group of generators with box constraints communicating over an undirected graph to find a feasible power allocation in finite time. This initialization method is also useful in tackling cases where the load condition is violated by the addition and/or deletion of generators. However, the proposed initialization+“Laplacian-gradient” dynamics cannot track a time-varying load signal. Motivated by this, we interconnected the “Laplacian-gradient” dynamics with a dynamic average consensus block. The net result was a distributed dynamics that allows the group of generators to solve the economic dispatch problem starting from any initial power allocation. Our analysis has also shown that for this solution strategy, the mismatch dynamics between total generation and load are input-to-state stable and, as a consequence, the coordination algorithm is robust to initialization errors, time-varying load signals, and intermittent power generation. The class of “Laplacian-gradient”+dynamic average consensus dynamics has a general structural advantage. That is, it can be used as a building block to address more general problems. We have leveraged

on this aspect when dealing with the DEDS problem for a group of generators with storage capabilities. We have provided a distributed dynamics that provably converges to the set of solutions of this problem from any initial condition.

Motivated by the fact that saddle-point dynamics play a major role in designing distributed algorithms for network optimization problem, we have studied in detail the asymptotic stability and robustness of this dynamics. First, we have identified a set of complementary conditions under which the trajectories of the dynamics are proved to converge to the set of saddle points of the saddle function and, wherever feasible, we have also established global stability guarantees and convergence to a point in the set. These results include both cases: when the function is convex-concave in its argument and when it is nonconvex. Next, we considered the primal-dual dynamics (that has a projection operator on top of the saddle-point dynamics) for a constrained concave optimization problem and established the asymptotic convergence of its Caratheodory solutions to a primal-dual optimizer using notions of projected dynamical systems and invariance principle for discontinuous Caratheodory systems. Finally, we have studied the global convergence and robustness properties of the projected saddle-point dynamics. We have established global asymptotic convergence assuming only local strong convexity-concavity of the saddle function. For the case when this strong convexity-concavity property is global, we have identified a Lyapunov function for the dynamics. In addition, when the saddle function takes the form of a Lagrangian of an equality constrained optimization problem, we have established the input-to-state stability of the saddle-point dynamics by identifying an ISS Lyapunov function, which we have used to design a self-triggered discrete-time implementation.

For the competition between aggregators, we have formulated an inelastic electricity market game capturing the strategic interaction between them in a bid-based energy dispatch setting. For this game, we have established the existence and uniqueness of the efficient Nash equilibria. We have also designed the BID ADJUSTMENT ALGORITHM, which is an iterative strategy amenable to decentralized implementation that provably converges to a neighborhood of the efficient Nash equilibrium at a linear rate. We have characterized the robustness properties of

the algorithm against disturbances, deviation in bid updates, and collusions among generators.

10.1 Future research directions

10.1.1 Short-term plan

Robustness and energy-efficiency in distributed optimization: Distributed solution algorithms for network optimization problems have garnered much attention lately. While many recent developments have occurred in this field, there is still a gap between the theoretical analysis and the practical implementation of these algorithms. Two properties (among others) that determine the practicality of these algorithms are robustness to perturbations and efficiency in terms of the communication burden. Robustness concerns in distributed methods arise due to asynchronous communication, noisy channels, and packet drops. Often times, algorithms work in theory (and simulations) but fail in real-life implementation due to these drawbacks. This highlights the need for rigorous robustness analysis of the proposed algorithms. System-theoretic tools, such as Lyapunov functions, provide an elegant way of studying robustness. Conducting such analysis for the state-of-the-art distributed algorithms and designing algorithms that achieve robustness guarantees (while possibly compromising a bit on the rate of convergence) are important future research endeavors. Communication burden of distributed algorithms is a lesser studied topic. Relatively, communication requires far more energy than computation. Fast algorithms might require a lot of communication, directly impacting the energy requirement. Moreover, for certain problems, one might not desire speed or accuracy but require long-term energy-efficiency. Therefore, there is a need to propose communication-efficient algorithms. One possible way of doing so is to employ triggered communication strategies to design such algorithms. In this framework, agents run an optimization routine on their local variables and communicate with their neighbors only when a certain criteria is met. This criteria is designed so as to ensure monotonic evolution of a Lyapunov-like function.

Learning in multi-agent games: In relation to the competition in electricity

market, the overall outlook for future research is to pursue the “dynamic analysis of competition” in multiagent setting. The approach needs both the theoretical analysis and validation from the available data. Some theoretical questions are what other learning strategies can occur in competitive settings. Do these learning strategies converge to some equilibrium, is that equilibrium a maximizer of social welfare. If that is not the case, how can one change the incentives so as to align the selfish equilibrium to the global welfare maximizing equilibrium. Pertinent to validation, the central question to address is is there empirical evidence that agents follow certain behavior in certain competitions, for example, bidding in electricity markets. Some of these ideas have been explored in the are of behavioral economics.

10.1.2 Long-term plan

Delay in transportation due to traffic congestion is commonplace in modern cities. This causes inconvenience to commuters and leads to suboptimal usage of our much valued natural resources. One way of mitigating this problem is by designing efficient coordination and competition among the entities interacting in this network. For example, coordinating the infrastructure entities such as traffic lights is expected to ease the congestion. Various coordination algorithms have been designed for this problem and there is a continued effort in improving them. In addition to the infrastructure units, users of this network (humans and autonomous vehicles) immensely affect the efficiency (throughput of vehicles in this case) of the network. The actions of users are predominantly selfish, driven by their intention of maximizing their own welfare (that is, minimizing their travel time). Therefore, researchers have looked into designing incentives for users such that their selfish actions align to maximize the efficiency. An example of such a mechanism is the real-time traffic information available to the drivers through interactive maps. Given this context, an interesting research direction is to explore the possibility of co-design of coordination and incentive schemes in order to realize an efficient, agile, and resilient transportation management system. The answers to these questions lie at the intersection of distributed algorithms, mechanism design, and network science.

Bibliography

- [AC84] J. P. Aubin and A. Cellina. *Differential Inclusions*, volume 264 of *Grundlehren der mathematischen Wissenschaften*. Springer, New York, 1984.
- [ACK08] B. Awerbuch, I. Cidon, and S. Kutten. Optimal maintenance of a spanning tree. *Journal of the Association for Computing Machinery*, 55(4):1–45, 2008.
- [AE10] A. Arsie and C. Ebenbauer. Locating omega-limit sets using height functions. *Journal of Differential Equations*, 248(10):2458–2469, 2010.
- [AHU58] K. Arrow, L Hurwitz, and H. Uzawa. *Studies in Linear and Non-Linear Programming*. Stanford University Press, Stanford, California, 1958.
- [AK06] P.-A. Absil and K. Kurdyka. On the stable equilibrium points of gradient systems. *Systems & Control Letters*, 55:573–577, 2006.
- [BB03] S. P. Bhat and D. S. Bernstein. Nontangency-based Lyapunov tests for convergence and stability in systems having a continuum of equilibria. *SIAM Journal on Control and Optimization*, 42(5):1745–1775, 2003.
- [BC06] A. Bacciotti and F. Ceragioli. Nonpathological Lyapunov functions and discontinuous Caratheodory systems. *Automatica*, 42(3):453–458, 2006.
- [BCKS10] G. I. Bischi, C. Chiarella, M. Kopel, and F. Szidarovszky. *Nonlinear oligopolies: stability and bifurcations*. Springer, New York, 2010.
- [BCM09] F. Bullo, J. Cortés, and S. Martínez. *Distributed Control of Robotic Networks*. Applied Mathematics Series. Princeton University Press, 2009. Electronically available at <http://coordinationbook.info>.

- [BDL⁺14] G. Binetti, A. Davoudi, F. L. Lewis, D. Naso, and B. Turchiano. Distributed consensus-based economic dispatch with transmission losses. *IEEE Transactions on Power Systems*, 29(4):1711–1720, 2014.
- [BDN⁺14] G. Binetti, A. Davoudi, D. Naso, B. Turchiano, and F. L. Lewis. A distributed auction-based algorithm for the nonconvex economic dispatch problem. *IEEE Transaction on Industrial Informatics*, 10(2):1124–1132, 2014.
- [Ber75] D. P. Bertsekas. Necessary and sufficient conditions for a penalty method to be exact. *Mathematical Programming*, 9(1):87–99, 1975.
- [Ber05] D. S. Bernstein. *Matrix Mathematics*. Princeton University Press, Princeton, NJ, 2005.
- [BG05] B. Brogliato and D. Goeleven. The Krakovskii-LaSalle invariance principle for a class of unilateral dynamical systems. *Mathematics of Control, Signals and Systems*, 17(1):57–76, 2005.
- [BGJ10] E. N. Barron, R. Goebel, and R. R. Jensen. Best response dynamics for continuous games. *Proceeding of the American Mathematical Society*, 138(3):1069–1083, 2010.
- [BO82] T. Başar and G.J. Oldser. *Dynamic Noncooperative Game Theory*. Academic Press, 1982.
- [Bra98] M. S. Branicky. Multiple Lyapunov functions and other analysis tools for switched and hybrid systems. *IEEE Transactions on Automatic Control*, 43(4):475–482, 1998.
- [BV04] S. Boyd and L. Vandenberghe. *Convex Optimization*. Cambridge University Press, 2004.
- [BV09] S. Boyd and L. Vandenberghe. *Convex Optimization*. Cambridge University Press, 2009.
- [CAI15] CAISO. Expanded metering and telemetry options phase 2 - distributed energy resource provider, 2015. Draft proposal electronically available at https://www.caiso.com/Documents/DraftFinalProposal_ExpandedMetering_TelemetryOptionsPhase2_DistributedEnergyResourceProvider.pdf.
- [Car82] J. Carr. *Applications of Centre Manifold Theory*. Springer, New York, 1982.

- [CBW16] D. Cai, S. Bose, and A. Wierman. On the role of a market maker in networked Cournot competition. 2016. Preprint available at <http://boeses.ece.illinois.edu>.
- [CC14] A. Cherukuri and J. Cortés. Distributed coordination for economic dispatch with varying load and generator commitment. In *Allerton Conf. on Communications, Control and Computing*, pages 475–482, Monticello, IL, October 2014.
- [CC15a] A. Cherukuri and J. Cortés. Asymptotic stability of saddle points under the saddle-point dynamics. In *American Control Conference*, pages 2020–2025, Chicago, IL, July 2015.
- [CC15b] A. Cherukuri and J. Cortés. Distributed dynamic economic dispatch of power generators with storage. In *IEEE Conf. on Decision and Control*, pages 2365–2370, Osaka, Japan, 2015.
- [CC15c] A. Cherukuri and J. Cortés. Distributed generator coordination for initialization and anytime optimization in economic dispatch. *IEEE Transactions on Control of Network Systems*, 2(3):226–237, 2015.
- [CC16a] A. Cherukuri and J. Cortés. Decentralized Nash equilibrium learning by strategic generators for economic dispatch. In *American Control Conference*, pages 1082–1087, Boston, MA, July 2016.
- [CC16b] A. Cherukuri and J. Cortés. Distributed algorithms for convex network optimization under non-sparse equality constraints. In *Allerton Conf. on Communications, Control and Computing*, pages 452–459, Monticello, IL, September 2016.
- [CC16c] A. Cherukuri and J. Cortés. Distributed coordination of DERs with storage for dynamic economic dispatch. 2016. Available at arxiv.org/abs/1605.00721.
- [CC16d] A. Cherukuri and J. Cortés. Initialization-free distributed coordination for economic dispatch under varying loads and generator commitment. *Automatica*, 74:183–193, 2016.
- [CC17a] A. Cherukuri and J. Cortés. Decentralized Nash equilibrium seeking by strategic generators for DC optimal power flow. In *Annual Conference on Information Systems and Sciences*, Baltimore, MD, March 2017. Electronic proceedings.
- [CC17b] A. Cherukuri and J. Cortés. Iterative bidding in electricity markets: rationality and robustness. *IEEE Transactions on Control of Network Systems*, 2017. Submitted.

- [CC18] A. Cherukuri and J. Cortés. Distributed coordination of DERs with storage for dynamic economic dispatch. *IEEE Transactions on Automatic Control*, 63(3), 2018. To appear.
- [CCHL11] A. Cherukuri, D. Chatterjee, P. Hokayem, and J. Lygeros. Stochastic receding horizon control: stability results. In *IFAC World Congress*, pages 150–155, Milan, Italy, July 2011.
- [CDGC17] A. Cherukuri, A. D. Domínguez-García, and J. Cortés. Distributed coordination of power generators for a linearized optimal power flow problem. In *American Control Conference*, pages 3962–3967, Seattle, WA, May 2017.
- [CGC17] A. Cherukuri, B. Gharesifard, and J. Cortés. Saddle-point dynamics: conditions for asymptotic stability of saddle points. *SIAM Journal on Control and Optimization*, 55(1):486–511, 2017.
- [CL12] J. Chen and V. K. N. Lau. Convergence analysis of saddle point problems in time varying wireless systems – control theoretical approach. *IEEE Transactions on Signal Processing*, 60(1):443–452, 2012.
- [Cla83] F. H. Clarke. *Optimization and Nonsmooth Analysis*. Canadian Mathematical Society Series of Monographs and Advanced Texts. Wiley, 1983.
- [CLCD07] M. Chiang, S. H. Low, A. R. Calderbank, and J. C. Doyle. Layering as optimization decomposition: A mathematical theory of network architectures. *Proceedings of the IEEE*, 95(1):255–312, 2007.
- [CLSW98] F. H. Clarke, Y.S. Ledyaev, R. J. Stern, and P. R. Wolenski. *Nonsmooth Analysis and Control Theory*, volume 178 of *Graduate Texts in Mathematics*. Springer, 1998.
- [CMC14] A. Cherukuri, S. Martínez, and J. Cortés. Distributed, anytime optimization in power-generator networks for economic dispatch. In *American Control Conference*, pages 172–177, Portland, OR, 2014.
- [CMC15] A. Cherukuri, E. Mallada, and J. Cortés. Convergence of Caratheodory solutions for primal-dual dynamics in constrained concave optimization. *SIAM Conference on Control and Its Applications*, pages 290–296, July 2015.
- [CMC16] A. Cherukuri, E. Mallada, and J. Cortés. Asymptotic convergence of primal-dual dynamics. *Systems & Control Letters*, 87:10–15, 2016.

- [CMLC16a] A. Cherukuri, E. Mallada, S. Low, and J. Cortés. The role of convexity in saddle-point dynamics: Lyapunov function and robustness. *IEEE Transactions on Automatic Control*, 2016. Submitted.
- [CMLC16b] A. Cherukuri, E. Mallada, S. Low, and J. Cortés. The role of strong convexity-concavity in the convergence and robustness of the saddle-point dynamics. In *Allerton Conf. on Communications, Control and Computing*, pages 504–510, Monticello, IL, September 2016.
- [Cor08] J. Cortés. Discontinuous dynamical systems - a tutorial on solutions, nonsmooth analysis, and stability. *IEEE Control Systems Magazine*, 28(3):36–73, 2008.
- [CR90] B. H. Chowdhury and S. Rahman. A review of recent advances in economic dispatch. *IEEE Transactions on Power Systems*, 5(4):1248–1259, November 1990.
- [DE14] G. Droge and M. Egerstedt. Proportional integral distributed optimization for dynamic network topologies. In *American Control Conference*, pages 3621–3626, Portland, OR, June 2014.
- [DGCH12] A. D. Domínguez-García, S. T. Cady, and C. N. Hadjicostis. Decentralized optimal dispatch of distributed energy resources. In *IEEE Conf. on Decision and Control*, pages 3688–3693, Hawaii, USA, 2012.
- [DGH11] A. D. Dominguez-Garcia and C. N. Hadjicostis. Distributed algorithms for control of demand response and distributed energy resources. In *IEEE Conf. on Decision and Control*, pages 27–32, Orlando, Florida, December 2011.
- [DGH12] L. Du, S. Grijalva, and R. G. Harley. Potential-game theoretical formulation of optimal power flow problems. In *IEEE Power and Energy Society General Meeting*, San Diego, CA, July 2012. Electronic Proceedings.
- [DSS58] R. Dorfman, P. A. Samuelson, and R. Solow. *Linear programming in economic analysis*. McGraw Hill, New York, Toronto, and London, 1958.
- [Dug66] J. Dugundji. *Topology*. Allyn and Bacon, Inc., Boston, MA, 1966.
- [Far10] H. Farhangi. The path of the smart grid. *IEEE Power and Energy Magazine*, 8(1):18–28, 2010.
- [FD16] M. N. Faqiry and S. Das. Double-sided energy auction in microgrid: equilibrium under price anticipation. *IEEE Access*, 4:3794–3805, 2016.

- [FDM05] M. C. Ferris, S. P. Dirkse, and A. Meeraus. Mathematical programs with equilibrium constraints: automatic reformulation and solution via constrained optimization. In *Frontiers in Applied General Equilibrium Modeling*, pages 67–94. Cambridge University Press, Cambridge, UK, 2005.
- [FKB12] P. Frihauf, M. Krstić, and T. Başar. Nash equilibrium seeking in noncooperative games. *IEEE Transactions on Automatic Control*, 57(5):1192–1207, 2012.
- [FL98] D. Fudenberg and D. K. Levine. *The Theory of Learning in Games*. MIT Press, Cambridge, MA, 1998.
- [FP10] D. Feijer and F. Paganini. Stability of primal-dual gradient dynamics and applications to network optimization. *Automatica*, 46:1974–1981, 2010.
- [FP14] A. Ferragut and F. Paganini. Network resource allocation for users with multiple connections: fairness and stability. *IEEE/ACM Transactions on Networking*, 22(2):349–362, 2014.
- [FT91] D. Fudenberg and J. Tirole. *Game Theory*. MIT Press, Cambridge, MA, 1991.
- [FYL06] R. A. Freeman, P. Yang, and K. M. Lynch. Stability and convergence properties of dynamic average consensus estimators. In *IEEE Conf. on Decision and Control*, pages 398–403, San Diego, CA, 2006.
- [Gai03] Z.-L. Gaing. Particle swarm optimization to solving the economic dispatch considering the generator constraints. *IEEE Transactions on Power Systems*, 18(3):1187–1195, 2003.
- [GC13] B. Gharesifard and J. Cortés. Distributed convergence to Nash equilibria in two-network zero-sum games. *Automatica*, 49(6):1683–1692, 2013.
- [GC14] B. Gharesifard and J. Cortés. Distributed continuous-time convex optimization on weight-balanced digraphs. *IEEE Transactions on Automatic Control*, 59(3):781–786, 2014.
- [Hen81] D. Henry. *Geometric Theory of Semilinear Parabolic Equations*, volume 840 of *Lecture Notes in Mathematics*. Springer, New York, 1981.
- [HJT12] W. P. M. H. Heemels, K. H. Johansson, and P. Tabuada. An introduction to event-triggered and self-triggered control. In *IEEE Conf. on Decision and Control*, pages 3270–3285, Maui, HI, 2012.

- [HL14] T. Holding and I. Lestas. On the convergence of saddle points of concave-convex functions, the gradient method and emergence of oscillations. In *IEEE Conf. on Decision and Control*, pages 1143–1148, Los Angeles, CA, 2014.
- [HMC15] S. Hart and A. Mas-Colell. Markets, correlation, and regret-matching. *Games and Economic Behavior*, 93:42–58, 2015.
- [HMMD13] A. Hooshmand, J. Mohammadpour, H. Malki, and H. Daneshi. Power system dynamic scheduling scheduling with high penetration of renewable sources. In *American Control Conference*, pages 5847–5852, Washington, D.C., June 2013.
- [HR07] X. Hu and D. Ralph. Using EPECs to model bilevel games in restructured electricity markets with locational prices. *Operations Research*, 55(5):809–827, 2007.
- [HS74] W. M. Hirsch and S. Smale. *Differential Equations, Dynamical Systems and Linear Algebra*. Academic Press, 1974.
- [HUL93] J.-B. Hiriart-Urruty and C. Lemaréchal. *Convex Analysis and Minimization Algorithms I*. Grundlehren Text Editions. Springer, New York, 1993.
- [IEE] http://motor.ece.iit.edu/data/JEAS_IEEE118.doc.
- [IXJ11] M. D. Ilić, L. Xie, and J. Joo. Efficient coordination of wind power and price-responsive demand – part 1: theoretical foundations. *IEEE Transactions on Power Systems*, 26(4):1875–1884, 2011.
- [JJ09] B. Johansson and M. Johansson. Distributed non-smooth resource allocation over a network. In *IEEE Conf. on Decision and Control*, pages 1678–1683, Shanghai, China, December 2009.
- [Jov96] M. V. Jovanovic. A note on strongly convex and quasiconvex functions. *Mathematical Notes*, 60(5):584–585, 1996.
- [JRJ09] B. Johansson, M. Rabi, and M. Johansson. A randomized incremental subgradient method for distributed optimization in networked systems. *SIAM Journal on Control and Optimization*, 20(3):1157–1170, 2009.
- [JT11] R. Johari and J. N. Tsitsiklis. Parameterized supply function bidding: Equilibrium and efficiency. *Operations Research*, 59(5):1079–1089, 2011.

- [JW01] Z.-P. Jiang and Y. Wang. Input-to-state stability for discrete-time nonlinear systems. *Automatica*, 37(6):857–869, 2001.
- [KCLB13] M. Kraning, E. Chu, J. Lavaei, and S. Boyd. Dynamic network energy management via proximal message passing. *Foundations and Trends in Optimization*, 1(2):70–122, 2013.
- [KCM15a] S. S. Kia, J. Cortés, and S. Martínez. Distributed convex optimization via continuous-time coordination algorithms with discrete-time communication. *Automatica*, 55:254–264, 2015.
- [KCM15b] S. S. Kia, J. Cortés, and S. Martínez. Dynamic average consensus under limited control authority and privacy requirements. *International Journal on Robust and Nonlinear Control*, 25(13):1941–1966, 2015.
- [KH12] S. Kar and G. Hug. Distributed robust economic dispatch in power systems: A consensus + innovations approach. In *IEEE Power and Energy Society General Meeting*, San Diego, CA, July 2012. Electronic proceedings.
- [Kha02] H. K. Khalil. *Nonlinear Systems*. Prentice Hall, 3 edition, 2002.
- [Kos56] T. Kose. Solutions of saddle value problems by differential equations. *Econometrica*, 24(1):59–70, 1956.
- [KP87] V. A. Kamenetskiy and Y. S. Pyatnitskiy. An iterative method of Lyapunov function construction for differential inclusions. *Systems & Control Letters*, 8(5):445–451, 1987.
- [KS04] F. Kirschen and G. Strbac. *Fundamentals of power system economics*. John Wiley & Sons, Sussex, England, 2004.
- [Lan93] S. Lang. *Real and Functional Analysis*. Springer, New York, 3 edition, 1993.
- [LCA⁺12] H. Liang, B. J. Choi, A. Abdrabou, W. Zhuang, and X. Shen. Decentralized economic dispatch in microgrids via heterogeneous wireless networks. *IEEE Journal on Selected Areas in Communications*, 30(6):1061–1074, 2012.
- [Lib03] D. Liberzon. *Switching in Systems and Control*. Systems & Control: Foundations & Applications. Birkhäuser, 2003.
- [LJS⁺03] J. Lygeros, K. H. Johansson, S. N. Simić, J. Zhang, and S. S. Sastry. Dynamical properties of hybrid automata. *IEEE Transactions on Automatic Control*, 48(1):2–17, 2003.

- [LM10] S. Leyffer and T. Munson. Solving multi-leader-common-follower games. *Optimization Methods and Software*, 25(4):601–623, 2010.
- [LP04] R. H. Lasseter and P. Paigi. Microgrid: a conceptual solution. In *IEEE Power Electronics Specialists Conference*, volume 6, pages 4285–4290, Aachen, Germany, June 2004.
- [LPD02] S. H. Low, F. Paganini, and J. C. Doyle. Internet congestion control. *IEEE Control Systems Magazine*, 22(1):28–43, 2002.
- [LPR96] Z-Q. Luo, J-S. Pang, and D. Ralph. *Mathematical programs with equilibrium constraints*. Cambridge University Press, Cambridge, UK, 1996.
- [LS05] T. Li and M. Shahidehpour. Strategic bidding of transmission-constrained GENCO’s with incomplete information. *IEEE Transactions on Power Systems*, 20(1):437–447, 2005.
- [LSET16] T. Lykouris, V. Syrgkanis, and Éva Tardos. Learning and efficiency in games with dynamic population. In *Annual ACM-SIAM Symposium on Discrete Algorithms*, pages 120–129, Arlington, VA, 2016.
- [LSW95] Y. Lin, E. Sontag, and Y. Wang. Various results concerning set input-to-state stability. In *IEEE Conf. on Decision and Control*, pages 1330–1335, New Orleans, LA, 1995.
- [LV14] V. Loia and A. Vaccaro. Decentralized economic dispatch in smart grids by self-organizing dynamic agents. *IEEE Transactions on Systems, Man & Cybernetics: Systems*, 44(4):397–408, 2014.
- [LWZ⁺13] Z. Li, W. Wu, B. Zhang, H. Sun, and Q. Guo. Dynamic economic dispatch using Lagrangian relaxation with multiplier updates based on Quasi-Newton method. *IEEE Transactions on Power Systems*, 28(4):4516–4527, 2013.
- [Lyn97] N. A. Lynch. *Distributed Algorithms*. Morgan Kaufmann, 1997.
- [LZC16] N. Li, C. Zhao, and L. Chen. Connecting automatic generation control and economic dispatch from an optimization view. *IEEE Transactions on Control of Network Systems*, 3(3):254–264, 2016.
- [MCWG95] A. Mas-Colell, M. Whinston, and J. Green. *Microeconomic Theory*. Oxford University Press, Oxford, UK, 1995.
- [MDC12] R. Mudumbai, S. Dasgupta, and B. B. Cho. Distributed control for optimal economic dispatch of a network of heterogeneous power generators. *IEEE Transactions on Power Systems*, 27(4):1750–1760, 2012.

- [ME13] X. Ma and N. Elia. A distributed continuous-time gradient dynamics approach for the active power loss minimizations. In *Allerton Conf. on Communications, Control and Computing*, pages 100–106, Monticello, IL, October 2013.
- [Moh91] B. Mohar. Eigenvalues, diameter, and mean distance in graphs. *Graphs and Combinatorics*, 7(1):53–64, 1991.
- [MZL] E. Mallada, C. Zhao, and S. H. Low. Optimal load-side control for frequency regulation in smart grids. *IEEE Transactions on Automatic Control*. To appear.
- [MZL14a] E. Mallada, C. Zhao, and S. H. Low. Optimal load-side control for frequency regulation in smart grids. In *Allerton Conf. on Communications, Control and Computing*, pages 731–738, Monticello, IL, October 2014.
- [MZL14b] E. Mallada, C. Zhao, and S. H. Low. Optimal load-side control for frequency regulation in smart grids. 2014. Available at <http://arxiv.org/abs/1410.2931>.
- [NC16] S. K. Niederländer and J. Cortés. Distributed coordination for nonsmooth convex optimization via saddle-point dynamics. *SIAM Journal on Control and Optimization*, 2016. Submitted.
- [NMM⁺09] Z. Nagy, S. Miyashita, S. Muntwyler, A. Cherukuri, J. J. Abbott, R. Pfeifer, and B. J. Nelson. Morphology detection for magnetically self-assembled modular robots. In *IEEE/RSJ Int. Conf. on Intelligent Robots & Systems*, pages 5281–5286, St. Louis, MO, USA, October 2009.
- [NOP10] A. Nedic, A. Ozdaglar, and P. A. Parrilo. Constrained consensus and optimization in multi-agent networks. *IEEE Transactions on Automatic Control*, 55(4):922–938, 2010.
- [NP10] U. Nadav and G. Piliouras. No regret learning in oligopolies: Cournot vs Bertrand. In S. Kontogiannis, E. Koutsoupias, and P. G. Spirakis, editors, *Algorithmic Game Theory*, volume 6386 of *Lecture Notes in Computer Science*, pages 300–311. Springer, New York, 2010.
- [NZ96] A. Nagurney and D. Zhang. *Projected Dynamical Systems and Variational Inequalities with Applications*, volume 2 of *International Series in Operations Research and Management Science*. Kluwer Academic Publishers, Dordrecht, The Netherlands, 1996.

- [PC07] D. P. Palomar and M. Chiang. Alternative distributed algorithms for network utility maximization: Framework and applications. *IEEE Transactions on Automatic Control*, 52(12):2254–2269, 2007.
- [PdM82] J. Palis, Jr. and W. de Melo. *Geometric Theory of Dynamical Systems*. Springer, New York, 1982.
- [PF05] J-S. Pang and M. Fukushima. Quasi-variational inequalities, generalized nash equilibria, and multi-leader-follower games. *Computational Management Science*, 2(1):21–56, 2005.
- [PG16] S. Pu and A. Garcia. Iterative mechanisms for electricity markets. 2016. Available at <https://arxiv.org/abs/1608.08987>.
- [PM09] F. Paganini and E. Mallada. A unified approach to congestion control and node-based multipath routing. *IEEE/ACM Transactions on Networking*, 15(5):1413–1426, 2009.
- [PQP14] A. Pantoja, N. Quijano, and K. M. Passino. Dispatch of distributed generators under local-information constraints. In *American Control Conference*, pages 2682–2687, Portland, OR, June 2014.
- [RB08] W. Ren and R. W. Beard. *Distributed Consensus in Multi-Vehicle Cooperative Control*. Communications and Control Engineering. Springer, 2008.
- [RBS13] L. J. Ratliff, S. A. Burden, and S. S. Sastry. Characterization and computation of local Nash equilibrium in continuous games. In *Allerton Conf. on Communications, Control and Computing*, Monticello, IL, October 2013.
- [RBS16] L. J. Ratliff, S. A. Burden, and S. S. Sastry. On the characterization of local Nash equilibria in continuous games. *IEEE Transactions on Automatic Control*, 61(8):2301–2307, 2016.
- [RC15] D. Richert and J. Cortés. Robust distributed linear programming. *IEEE Transactions on Automatic Control*, 60(10):2567–2582, 2015.
- [RC16] D. Richert and J. Cortés. Distributed bargaining in dyadic-exchange networks. *IEEE Transactions on Control of Network Systems*, 3(3):310–321, 2016.
- [SC12] M. D. Schuresko and J. Cortés. Distributed tree rearrangements for reachability and robust connectivity. *SIAM Journal on Control and Optimization*, 50(5):2588–2620, 2012.

- [SCA16] D. J. Shiltz, M. Cvetković, and A. M. Annaswamy. An integrated dynamic market mechanism for real-time markets and frequency regulation. *IEEE Transactions on Sustainable Energy*, 7(2):875–885, 2016.
- [SJS12] M. S. Stankovic, K. H. Johansson, and D. M. Stipanovic. Distributed seeking of Nash equilibria with applications to mobile sensor networks. *IEEE Transactions on Automatic Control*, 57(4):904–919, 2012.
- [SKJ12] A. Simonetto, T. Keviczky, and M. Johansson. A regularized saddle-point algorithm for networked optimization with resource allocation constraints. In *IEEE Conf. on Decision and Control*, pages 7476–7481, Hawaii, USA, December 2012.
- [Soh03] H. H. Sohrab. *Basic Real Analysis*. Birkhäuser, Boston, MA, 2003.
- [SPvdS17] T. Stegink, C. D. Persis, and A. J. van der Schaft. A unifying energy-based approach to stability of power grids with market dynamics. *IEEE Transactions on Automatic Control*, 62(6):2612–2622, 2017.
- [SRK15] A. Soroudi, A. Rabiee, and A. Keane. Stochastic real-time scheduling of wind-thermal generation units in an electric utility. *IEEE Systems Journal*, 2015. To appear.
- [Sto02] S. Stoft. *Power system economics: designing markets for electricity*. IEEE Press, Piscataway, NJ, 2002.
- [TJ13] W. Tang and R. Jain. Game-theoretic analysis of the nodal pricing mechanism for electricity markets. In *IEEE Conf. on Decision and Control*, pages 562–567, Florence, Italy, December 2013.
- [WA04] J. T. Wen and M. Arcak. A unifying passivity framework for network flow control. *IEEE Transactions on Automatic Control*, 49(2):162–174, 2004.
- [WE11] J. Wang and N. Elia. A control perspective for centralized and distributed convex optimization. In *IEEE Conf. on Decision and Control*, pages 3800–3805, Orlando, Florida, 2011.
- [WGMM12] J. Warrington, P. Goulart, S. Mariéthoz, and M. Morari. A market mechanism for solving multi-period optimal power flow exactly on ac networks with mixed participants. In *American Control Conference*, pages 3101–3107, Montréal, Canada, June 2012.
- [XB06] L. Xiao and S. Boyd. Optimal scaling of a gradient method for distributed resource allocation. *Journal of Optimization Theory & Applications*, 129(3):469–488, 2006.

- [XE10] X. Xia and A. M. Elaiw. Optimal dynamic economic dispatch of generation: A review. *Electric Power Systems Research*, 80(8):975–986, 2010.
- [XZE11] X. Xia, J. Zhang, and A. Elaiw. An application of model predictive control to the dynamic economic dispatch of power generation. *Control Engineering Practice*, 19(6):638–648, 2011.
- [ZC12] Z. Zhang and M. Chow. Convergence analysis of the incremental cost consensus algorithm under different communication network topologies. *IEEE Transactions on Power Systems*, 27(4):1761–1768, 2012.
- [ZGG13] Y. Zhang, N. Gatsis, and G. B. Giannakis. Robust energy management for microgrids with high-penetration renewables. *IEEE Transactions on Sustainable Energy*, 4(4):944–953, 2013.
- [ZH14] D. Zhu and G. Hug. Decomposed stochastic model predictive control for optimal dispatch of storage and generation. *IEEE Transactions on Smart Grid*, 5(4):2044–2053, 2014.
- [ZKG16] L. Zhang, V. Kekatos, and G. B. Giannakis. Scalable electric vehicle charging protocols. 2016. Available at <https://arxiv.org/abs/1510.00403v2>.
- [ZL14] D. Zhang and G-H. Lin. Bilevel direct search method for leader-follower problems and application in health insurance. *Computers & Operations Research*, 41:359–373, 2014.
- [ZLW⁺14] W. Zhang, W. Liu, X. Wang, L. Liu, and F. Ferrese. Online optimal generation control based on constrained distributed gradient algorithm. *IEEE Transactions on Power Systems*, 30(1):35–45, 2014.
- [ZM12] M. Zhu and S. Martínez. On distributed convex optimization under inequality and equality constraints. *IEEE Transactions on Automatic Control*, 57(1):151–164, 2012.
- [ZMST11] R. D. Zimmerman, C. E. Murillo-Sánchez, and R. J. Thomas. Matpower: Steady-state operations, planning and analysis tools for power systems research education. *IEEE Transactions on Power Systems*, 26(1):12–19, 2011.
- [ZP14] X. Zhang and A. Papachristodoulou. Distributed dynamic feedback control for smart power networks with tree topology. In *American Control Conference*, pages 1156–1161, Portland, OR, June 2014.

- [ZTLL14] C. Zhao, U. Topcu, N. Li, and S. H. Low. Design and stability of load-side primary frequency control in power systems. *IEEE Transactions on Automatic Control*, 59(5):1177–1189, 2014.
- [ZYC11] Z. Zhang, X. Ying, and M. Chow. Decentralizing the economic dispatch problem using a two-level incremental cost consensus algorithm in a smart grid environment. In *North American Power Symposium*, Boston, MA, August 2011. Electronic Proceedings.